Australian Rainfall & Runoff

# A GUIDE TO FLOOD ESTIMATION

## BOOK 6 - FLOOD HYDRAULICS

Version 4.2

Australian Government

ENGINEERS AUSTRALIA

**Acknowledgement of Country**
We acknowledge the Traditional Owners of Country throughout Australia and recognise their continuing connection to land, waters and culture. We pay our respects to their Elders past and present.

If you have any questions about the copyright of the ARR, please contact:
hazards@ga.gov.au or admin@arr-software.org
c/o 11 National Circuit,
Barton, ACT

ISBN 978-1-925848-36-6

How to reference:
Ball J, Babister M, Nathan R, Weeks W, Weinmann E, Retallick M, Testoni I, (Editors) Australian Rainfall and Runoff: A Guide to Flood Estimation, © Commonwealth of Australia (Geoscience Australia), Version 4.2, 2019.

How to reference Book 9: Runoff in Urban Areas:
Coombes, P., and Roso, S. (Editors), 2019 Runoff in Urban Areas, Book 9 in Australian Rainfall and Runoff - A Guide to Flood Estimation, Commonwealth of Australia, © Commonwealth of Australia (Geoscience Australia), Version 4.2, 2019.

# PREFACE

Since its first publication in 1958, Australian Rainfall and Runoff (ARR) has remained one of the most influential and widely used guidelines published by Engineers Australia (EA). The 3rd edition, published in 1987, retained the same level of national and international acclaim as its predecessors.

With nationwide applicability, balancing the varied climates of Australia, the information and the approaches presented in Australian Rainfall and Runoff are essential for policy decisions and projects involving:

- infrastructure such as roads, rail, airports, bridges, dams, stormwater and sewer systems;
- town planning;
- mining;
- developing flood management plans for urban and rural communities;
- flood warnings and flood emergency management;
- operation of regulated river systems; and
- prediction of extreme flood levels.

However, many of the practices recommended in the 1987 edition of ARR have become outdated, and no longer represent industry best practice. This fact, coupled with the greater understanding of climate and flood hydrology derived from the larger data sets now available to us, has provided the primary impetus for revising these guidelines. It is hoped that this revision will lead to improved design practice, which will allow better management, policy and planning decisions to be made.

One of the major responsibilities of the National Committee on Water Engineering of Engineers Australia is the periodic revision of ARR. While the NCWE had long identified the need to update ARR it had become apparent by 2002 that even with a piecemeal approach the task could not be carried out without significant financial support. In 2008 the revision of ARR was identified as a priority in the National Adaptation Framework for Climate Change which was endorsed by the Council of Australian Governments.

In addition to the update, 21 projects were identified with the aim of filling knowledge gaps. Funding for Stages 1 and 2 of the ARR revision projects were provided by the now Department of the Environment. Stage 3 was funded by Geoscience Australia. Funding for Stages 2 and 3 of Project 1 (Development of Intensity-Frequency-Duration information across Australia) has been provided by the Bureau of Meteorology. The outcomes of the projects assisted the ARR Editorial Team with the compiling and writing of chapters in the revised ARR. Steering and Technical Committees were established to assist the ARR Editorial Team in guiding the projects to achieve desired outcomes.

**Assoc Prof James Ball**
ARR Editor

**Mark Babister**
Chair Technical Committee for
ARR Revision Projects

**ARR Technical Committee:**

*Chair*: Mark Babister
*Members:*

Associate Professor James Ball
Professor George Kuczera
Professor Martin Lambert
Associate Professor Rory Nathan
Dr Bill Weeks
Associate Professor Ashish Sharma
Dr Bryson Bates
Steve Finlay

Related Appointments:

| | |
|---|---|
| ARR Project Engineer: | Monique Retallick |
| ARR Admin Support: | Isabelle Testoni |
| Assisting TC on Technical Matters: | Erwin Weinmann, Dr Michael Leonard |

**ARR Editorial Team:**

*Editors*: James Ball

Mark Babister
Rory Nathan
Bill Weeks
Erwin Weinmann
Monique Retallick
Isabelle Testoni

Associate Editors for Book 9 - Runoff in Urban Areas

Peter Coombes
Steve Roso

Editorial assistance: Mikayla Ward

# Status of this document

This document is a living document and will be regularly updated in the future.

In development of this guidance, and discussed in Book 1 of ARR 1987, it was recognised that knowledge and information availability is not fixed and that future research and applications will develop new techniques and information. This is particularly relevant in applications where techniques have been extrapolated from the region of their development to other regions and where efforts should be made to reduce large uncertainties in current estimates of design flood characteristics.

Therefore, where circumstances warrant, designers have a duty to use other procedures and design information more appropriate for their design flood problem. The Editorial team of this edition of Australian Rainfall and Runoff believe that the use of new or improved procedures should be encouraged, especially where these are more appropriate than the methods described in this publication.

Care should be taken when combining inputs derived using ARR 1987 and methods described in this document.

## Change Log

### Version 4.2 - Climate Change Chapter Update

In late 2022 the Australian Government Department of Climate Change, Energy, the Environment and Water in partnership with Engineers Australia commenced an 18 month project to update the climate change considerations chapter of the Australian Rainfall and Runoff guidelines (Chapter 6, Book 1) to incorporate the most recent and relevant climate science and projections. The project involved the undertaking of a rigorous literature review of hydroclimatology under climate change relevant to design flood estimation, which was peer reviewed and published in a leading international journal. The findings were used to draft practical flood guidance which was finalised after an extensive process of review and feedback by industry. Funding for this project was received from National Emergency Management Agency under the Disaster Risk Reduction Package. The project report was adapted to replace Book 1 chapter 6.

*Climate Change Update Project Control Group*:

Leanne Haupt
Simon Koger
Andrew Dyer
Karl Braganza
Duncan McLuckie
Monique Retallick
Euan Brown
Andrew Gissing
Martyn Hazelwood
Professor Rory Nathan

*Climate Change Update Technical Working Group*:

Dr Conrad Wasko
Professor Seth Westra
Dr Dörte Jakob
Chris Nielsen
Professor Jason Evans
Simon Rodgers
Mark Babister
Dr Andrew Dowdy
Dr Wendy Sharples
Dr Ramona Dalla Pozza
Dr Michelle Ho

This version updates Book 1 Chapter 6 to reflect updates in climate science as discussed above. While no other chapters have been updated some minor amendments were made to remove inconsistencies with the new chapter. FAQs relating to the update are available https://arr.ga.gov.au/contact-us.

## Key updates in Version 4.2

| Update | Version 4.2 |
|---|---|
| Book 1 | Book 1 Chapter 6 Climate change updated |
| Guideline formats | PDF<br>Web-based version<br>Epub version |
| User experience | FAQs added to Geoscience Australia Website |
| Climate change | Reflected best practice as of 2024 and IPCC 6 |
| Other Minor Changes | List the minor changes to the following chapters for consistency<br>Book 1 Chapter 4 Section 15.1<br>Book 1 Chapter 4 Section 16.1<br>Book 1 Chapter 5 Section 10.4<br>Book 2 Chapter 1 Section 3<br>Book 2 Chapter 3 Section 3<br>Book 6 Chapter 5 Section 5<br>Book 8 Chapter 7 Section 7<br>Book 9 Chapter 6 Section 4.2<br>Book 9 Chapter 6 Section 4.6 |

## ARR 2019 (now Version 4.1)

Geoscience Australia, on behalf of the Australian Government, asked the National Committee on Water Engineers (NCWE) - a specialist committee of Engineers Australia - to continue overseeing the technical direction of ARR. ARR's success comes from practitioners and researchers driving its development; and the NCWE is the appropriate organisation to oversee this work. The NCWE has formed a sub-committee to lead the ongoing management and development of ARR for the benefit of the Australian community and the profession. The current membership of the ARR management subcommittee includes Mark Babister, Robin Connolly, Rory Nathan and Bill Weeks.

The ARR team have been working hard on finalising ARR since it was released in 2016. The team has received a lot of feedback from industry and practitioners, ranging from substantial feedback to minor typographical errors. Much of this feedback has now been addressed. Where a decision has been made not to address the feedback, advice has been provided as to why this was the case.

A new version of ARR is now available. ARR 2019 is a result of extensive consultation and feedback from practitioners. Noteworthy updates include the completion of Book 9, reflection of current climate change practice and improvements to user experience, including the availability of the document as a PDF.

## Key updates in ARR 2019

| Update | ARR 2016 | ARR 2019 |
|---|---|---|
| Book 9 | Available as “rough” draft | Peer reviewed and completed |
| Guideline formats | Epub version<br>Web-based version | Following practitioner feedback, a pdf version of ARR 2019 is now available |
| User experience | Limited functionality in web-based version | Additional pdf format available |
| Climate change | Reflected best practice as of 2016 Climate Change policies | Updated to reflect current practice |
| PMF chapter | Updated from the guidance provided in 1998 to include current best practice | Minor edits and reflects differences required for use in dam studies and floodplain management |
| Examples | | Examples included for Book 9 |
| Figures | | Updated reflecting practitioner feedback |

As of May 2019, this version was considered to be final.

## ARR 2016 (now Version 4.0)

Released July 2016

BOOK 6

# Flood Hydraulics

# Flood Hydraulics

# Table of Contents

# List of Figures

# List of Tables

# Chapter 1. Introduction

Martin Lambert

| Chapter Status | Final |
|---|---|
| Date last updated | 14/5/2019 |

## 1.1. Objectives and Scope

Much of Australian Rainfall and Runoff is dedicated to the determination of peak discharge, discharge hydrographs and flood volumes. This chapter deals with translating these discharge estimates into flood levels, flow velocities and the extent of flood inundation needed to determine flood damage and flood hazard. The importance of the inter-relationship between hydrology and hydraulics should not be under-estimated and there is often a blurring of the boundaries between the two areas. For example, the flood routing used to obtain a flow hydrograph and shallow flow surface runoff expressions are both founded in hydraulic engineering principles. In recent approaches to urban flooding, rainfall is a direct input to the hydraulic numerical grid hence forcing the hydraulic model to deal with the hydrology and the hydraulics simultaneously.

The primary objective of this book is to provide a document which provides background information to assist practitioners to carry out calculations or hydraulic investigations related to free surface flows. The needs for such calculations or investigations may be related to floods (inundation levels, concentration of flows to endanger life, the power of flood flows to threaten or impair structural integrity or even wash away structures, and bed level scour), stormwater disposal, water supply distribution systems and sewerage collection systems (the installation of new systems or augmentation of existing systems).

The present document concentrates on free surface flows. Textbooks are available which cover the basics of open channel flow. The traditional texts in this area are Henderson (1966) and Chow (1959) but more modern books include Chaudhry (2007) and Sturm (2009). Pipe flow is covered in fluid mechanics textbooks like Streeter and Wylie (1981) and Elger et al. (2014). There are numerous journals which publish research dealing with open channel, pipe flow and river flood flows and these include the ASCE - Journal of Hydraulic Engineering, IAHR - Journal of Hydraulic Research and the Journal of Flood Risk Management. Those practicing and working in this area are encouraged to keep abreast of new developments as this is an area that is evolving with increases in computational power.

## 1.2. References

Chaudhry, M.H. (2007), Open Channel Flow, Springer Publishing Company.

Chow, V.T. (1959), Open-Channel Hydraulics. McGraw-Hill Book Company, New York.

Elger, D.F. Williams, B.C. Clayton T. Crowe, C.T. and Roberson, J.A. (2014), Engineering Fluid Mechanics, 10th Edition.

Henderson, F.M. (1966), Open Channel Flow, Macmillan Publishing Co., New York.

Streeter, V.L. and Wylie E.B. (1981), Fluid Mechanics. McGraw-Hill Ryerson Ltd., Singapore.

Sturm, T. (2009), Open Channel Hydraulics Sturm, McGraw-Hill Water Resources and Environmental Engineering Series, New York.

# Chapter 2. Open Channel Hydraulics

Martin Lambert, Bruce Cathers, Robert Keller

| Chapter Status | Final |
|---|---|
| Date last updated | 14/5/2019 |

## 2.1. Introduction

All hydraulic flows are three dimensional in nature and involve complex turbulent flow motion. This is not unlike hydrology where the three dimensional and turbulent nature of atmospheric flows create temporal and spatial variability in rainfall and runoff which must be dealt with. The type of hydraulic computations to be undertaken will depend on the problem to be examined and on the data that is available. As a result, some thought is needed to determine the appropriate analysis techniques. For example, an unsteady flow analysis will not be possible if only peak discharges are known.

Free surface flows are driven by gravity and resisted by shear forces on the channel bed and drag forces on objects such as vegetation and obstructions. The free surface that exists in open channel flow means that the flow depth and flow area will most likely change with distance and/or time. In contrast, closed conduits that are operating under pressure have a fixed cross-sectional area and are driven by the pressure gradient. A combination of free surface flow in conjunction with closed conduit flow is not uncommon. Hydraulic modelling for the purposes of flood estimation typically assumes that the flow is composed of water that is incompressible but the reality maybe that it is sediment or debris laden and in some cases multi-phase.

Hydraulic computations are usually carried out to determine flood characteristics such as:

- flow depths or water levels (e.g. for recorded floods or synthesised floods of a particular magnitude),
- flow velocities (including flow direction),
- flood or inundation extent,
- the timing of transport network disruptions,
- sediment scour, and sometimes also,
- energy losses, be they :

i. friction losses which are cumulative and can be significant over long distances or

ii. local losses such as those which occur due flow constrictions and expansions imposed by hydraulic structures or flow around bends).

Hydraulic computations can be undertaken using a range of analytical or numerical model approaches often involving spreadsheets or computer programs (freeware or proprietary software). The level of detail in which the calculations are completed will depend upon the nature of the hydraulic investigation (including the risks to life and property and the complexity of the flows) and the availability of time and data to undertake the investigation.

In some circumstances, it is desirable to make recourse to physical models rather than numerical models.

## 2.2. General Characteristics of Open Channels

Open channels can be natural or man-made. The cross-sections of natural channels are irregular, usually broader than they are deep and often consisting of a deeper in-bank channel as well as a shallower over-bank area (floodplain). These are often referred to as compound channels. During floods, the flow frequently leaves the in-bank channel and enters the over-bank area as shown in Figure 6.2.1. An illustration of a complex floodplain associated with the River Murray in South Australia is shown in Figure 6.2.2. The increase in roughness on the floodplain due to vegetation means that the floodplain flows are typically shallower and slower than the flow in the main channel. This can lead to a complex interaction between the two flows and in meandering channels the flow direction may be different from the main channel leading to additional interaction and momentum exchange.

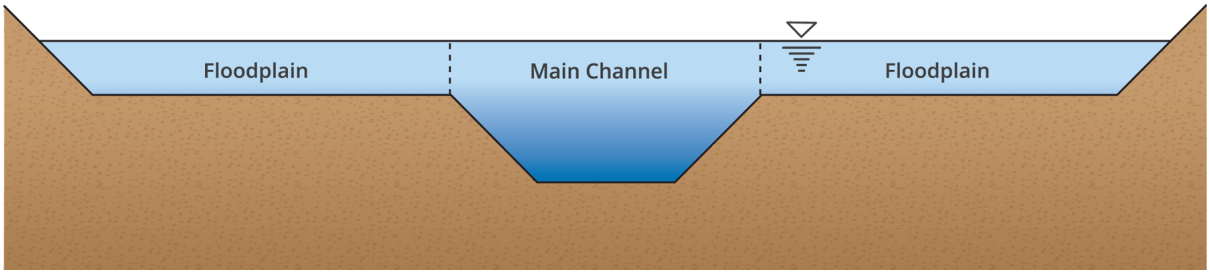


Figure 6.2.1. Illustration of the river main channel and floodplains

Figure 6.2.2. The River Murray and its floodplain near Waikerie in South Australia, Courtesy of Martin Lambert

At bends in the water course, natural cross-sections are asymmetrical; they tend to be deeper on the outside of the bend due to the effect of helicoidal secondary currents which tend to scour the outside of the bend and deposit sediment at the inside of the bend as illustrated in Figure 6.2.3.

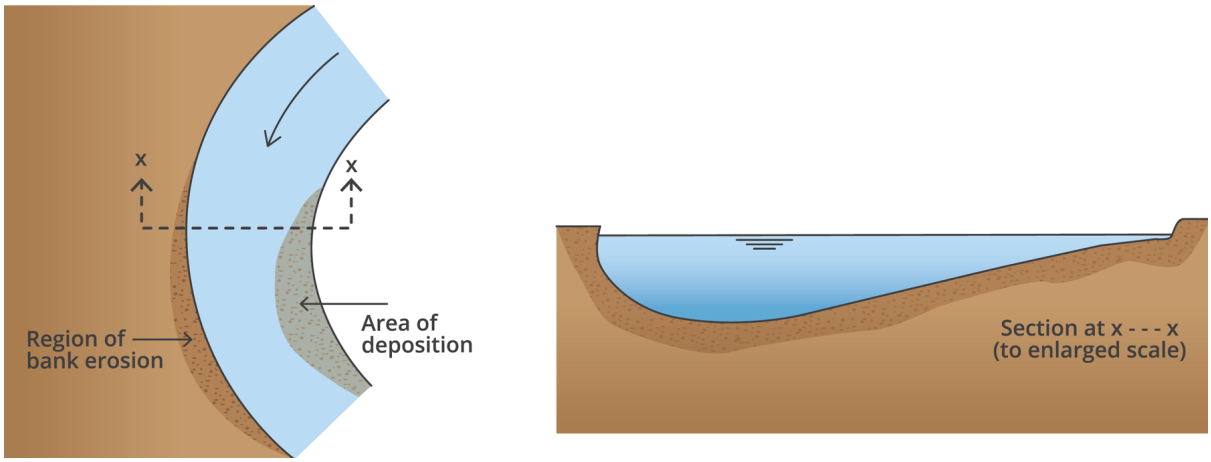


Figure 6.2.3. River bend showing areas of deposition and erosion and characteristic cross-section.

The cross-sections of man-made channels are usually rectangular, trapezoidal, triangular or circular. Stormwater channels often have a small deeper indentation along the centreline of the channel for easy cleaning and containing low flows.

Since the channel roughness affects the flow, it is important to be able to quantify the roughness. The roughness in channels is determined by the materials from which the channel is cut or made, including any vegetation which is growing (or lodged) in the channel. In man-made channels, the roughness must also include the effects of any jointing between panels, slabs or pipes. In channels with significant sediment transport, the roughness maybe changing with flow as the bedforms change in dimension. The challenge of determining the appropriate roughness to use in flood level computations should not be under-estimated and is often based on experience and should be validated or calibrated where possible.

Apart from channel roughness, the main parameters associated with the channels are:

i. the cross-sectional area (measured in a cross-section at right angles to the flow direction A),

ii. the depth y (especially for man-made channels),

iii. the top width B (sometimes also called the storage width),

iv. the wetted perimeter P,

v. the hydraulic radius R and

vi. the stage h.

Depth is usually measured vertically up from the bottom point in the cross-section (rather than at right angles to the bed), while the stage is measured vertically from a datum to the water surface. See Figure 6.2.4.

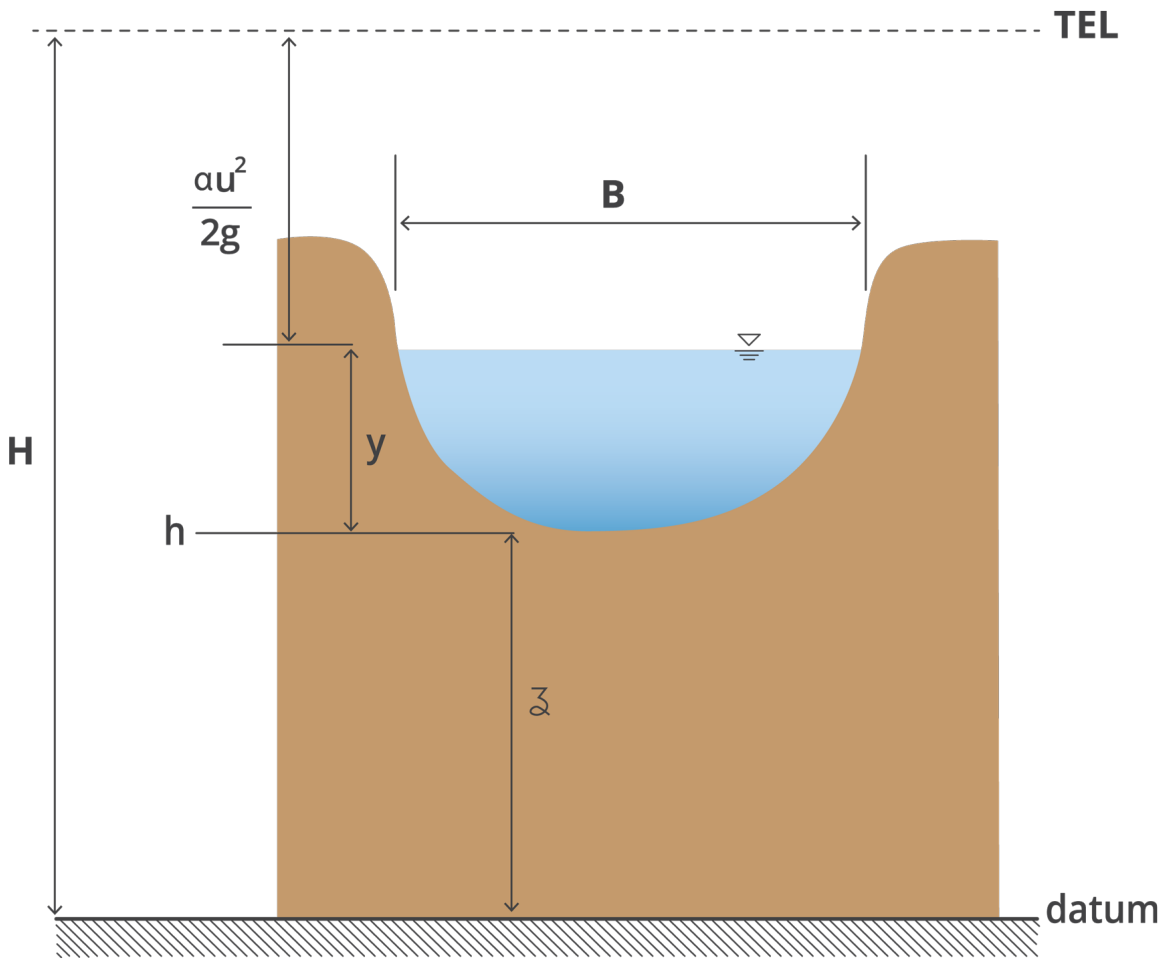


Figure 6.2.4. Parameters characterising flows in open channels

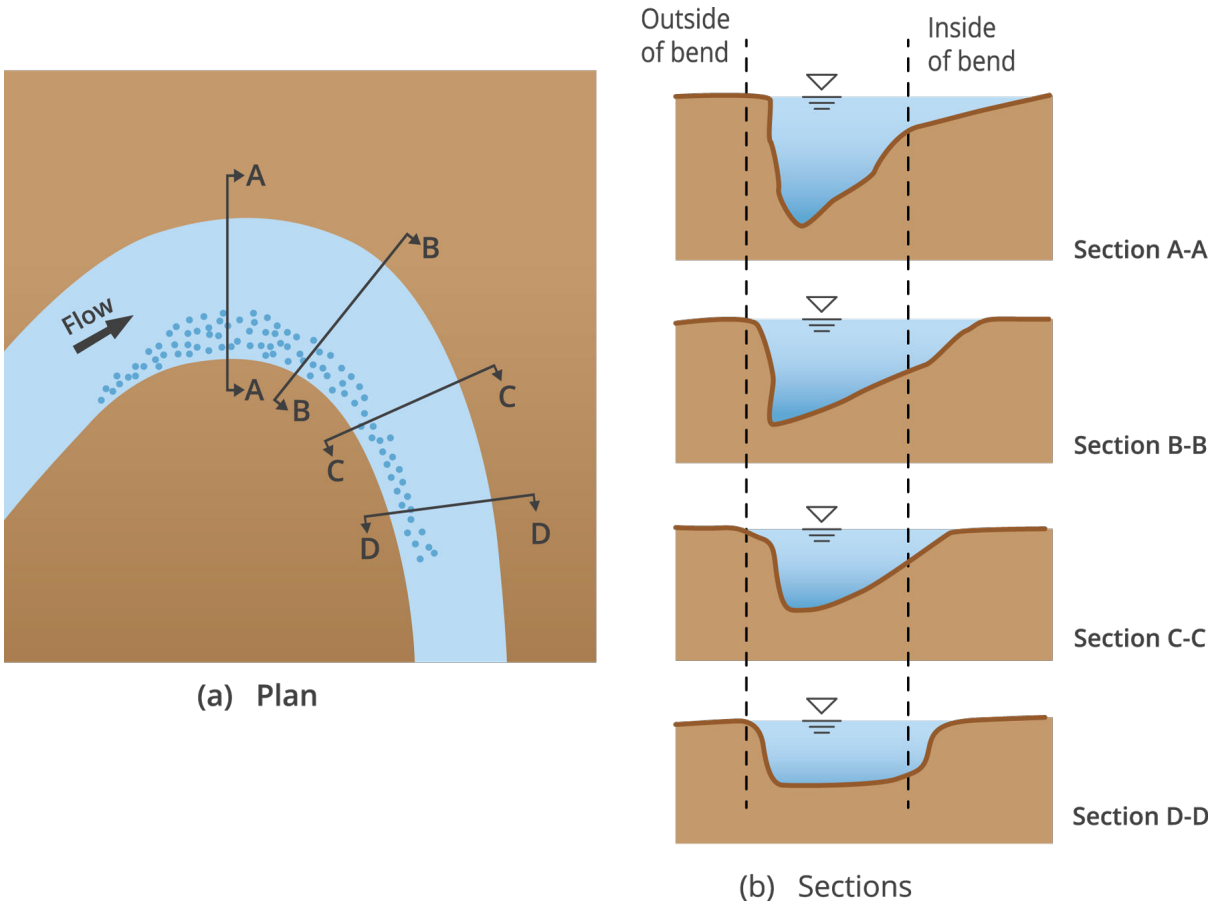


Figure 6.2.5. Variation of cross-sectional properties in natural channel

In natural channels the cross-sectional parameters vary with distance along the channel as shown in Figure 6.2.5.

***Open Channel Flows are three dimensional but often treated as one dimensional***

Open channel flows are three dimensional in nature and must satisfy the fundamental equations of fluid motion governed by the Navier-Stokes equations. A solution of these three-dimensional equations using direct numerical simulation, however, is not feasible for the spatial scales dealt with in flood estimation. Three-dimensional simulations using models which approximate the turbulence behaviour are feasible for small sections of a river reach and are seeing some use. Advances in computational power and numerical methods have allowed common usage of unsteady two-dimensional (2D) depth averaged models in flood hydraulics simulation. These approaches have largely replaced traditional one-dimensional (1D steady and unsteady) flow analysis for most flood studies even where the flood behaviour is essentially 1D due to ease that they produce flood inundation maps. While the treatment of river flows as a one-dimensional flow does make considerable assumptions about the flow field, this approach has served the engineering community well for over a century and is still a powerful tool provided the assumptions utilised are appropriate. The extent of some rivers are so large that even two dimensional models are infeasible, and methods have been developed which allow the 1D and 2D approaches to work together. When a fluid with a viscosity such as water flows in an open channel, boundary shear stresses resist the flow and prevent the unchecked acceleration of the water in the downhill direction. These resistive forces are transmitted throughout the main body of the flow by either viscous or turbulent shear stresses generated by velocity gradients over the cross-section. As a result, a uniform flow cannot have a uniform velocity distribution.

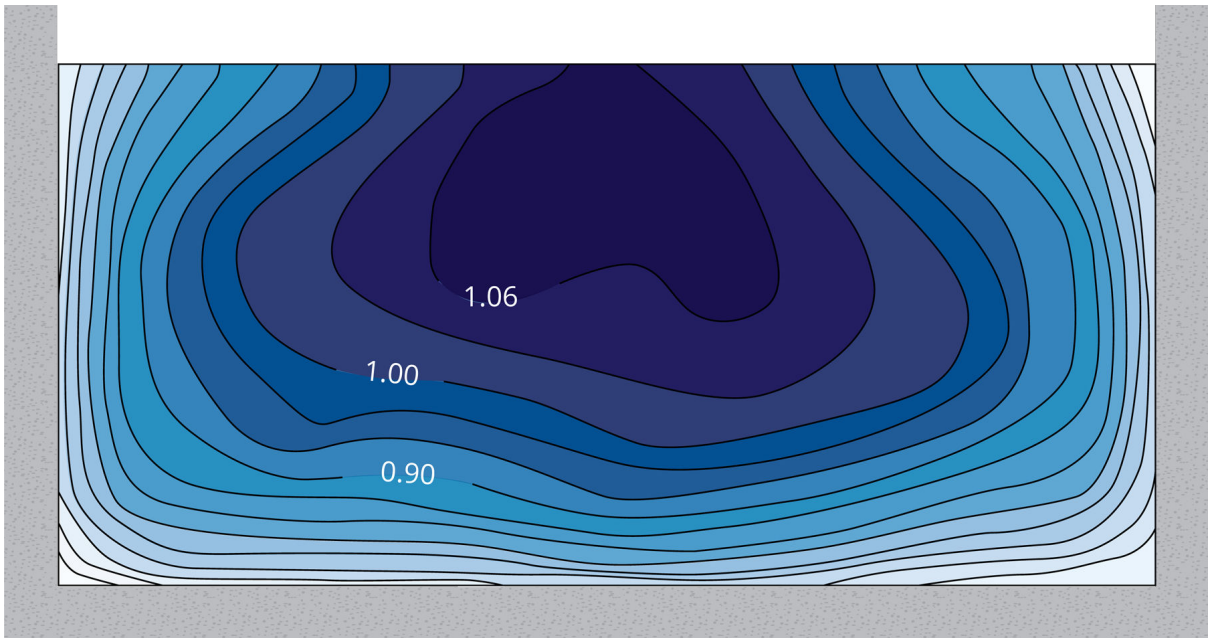


Figure 6.2.6. Cross-section velocity distribution in a small straight laboratory channel (velocities shown as a ratio of the mean)

The distribution of longitudinal velocity in a cross-section is controlled by the channel shape and the location of the free surface and boundary roughness. Figure 6.2.6 shows by lines of equal velocity the distribution of velocity in a straight laboratory channel. Figure 6.2.7 shows, for comparison, the velocity distribution in a typical river cross-section.

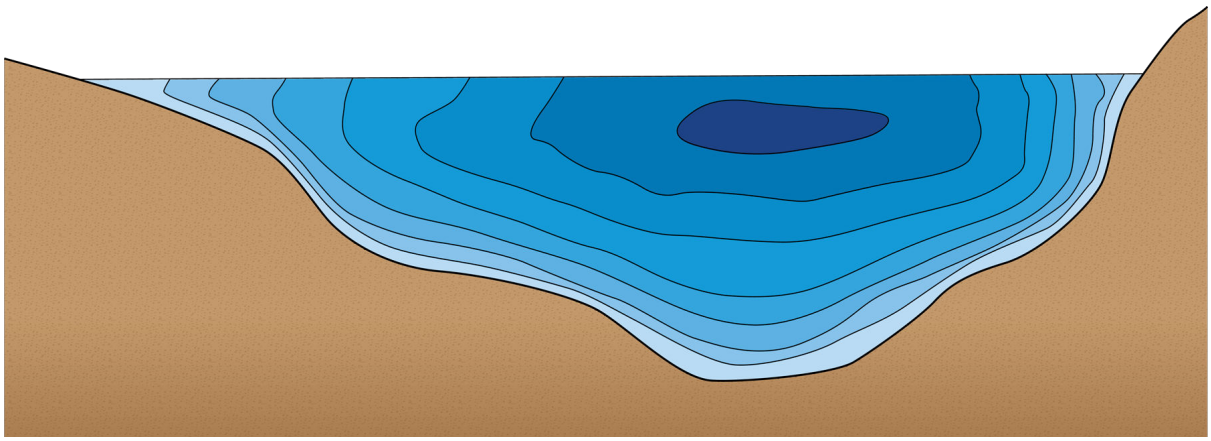

Figure 6.2.7. Typical velocity distribution in a natural channel cross-section

The velocity distribution is shown in Figure 6.2.8 where (a) shows the vertical velocity distribution on the centreline of a rectangular channel in which the depth is equal to one half of the breadth. In the same figure, curve (b) shows the vertical distribution of mean velocity; each point on this curve represents the average velocity in a horizontal line across the section at that level. Secondary currents in the plane of the cross-section produce circulation which account for both the depression of the maximum velocity filament and the observed movement of floating material towards the centre of the channel surface. This is another example of the three dimensional nature of the flows.

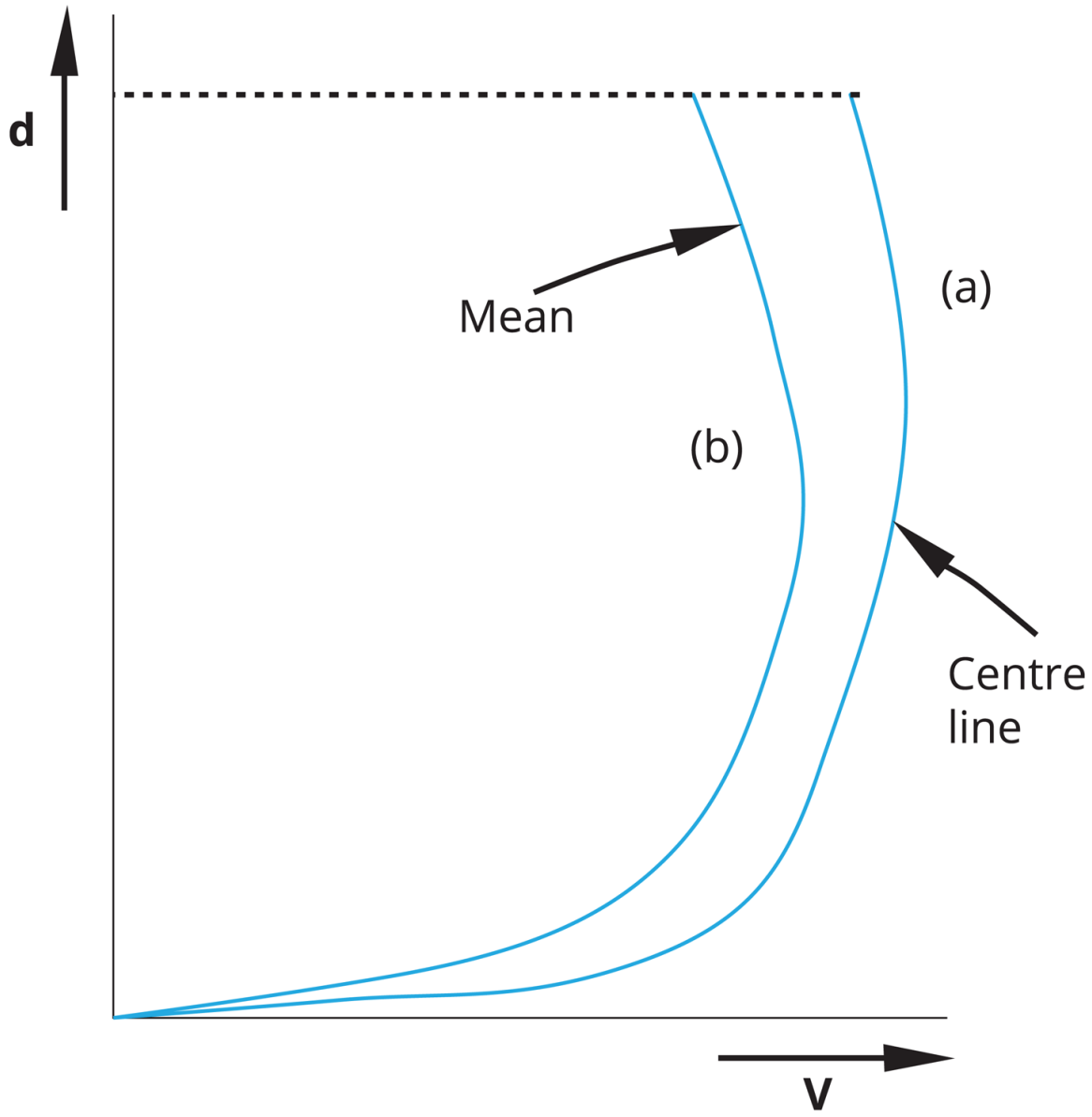


Figure 6.2.8. Typical vertical velocity distribution

A traditional one dimensional approach to open channel flow uses a single value to express the velocity at a cross-section. This is normally the average velocity V defined as the discharge divided by the cross-section area and forms the basis of the continuity equation.

$$V = \frac{Q}{A} \tag{6.2.1}$$

This simplification leads to an error in any calculations of kinetic energy head since the mean of the squares of individual values is always larger than the square of the mean value. To make allowance for this effect an energy coefficient a is normally introduced so that the kinetic energy head at a cross-section is then $\alpha\frac{V^2}{2g}$. For complex cross-sections, such as compound channels or close to constrictions like bridge piers and weirs, the value of $\alpha$ can be significant. Figure 6.2.9 shows the variation in the total energy line between the main channel and the floodplain if the water surface is horizontal in the channel cross-section.

Also shown is the average total energy line given by energy correction coefficient. For a detailed discussion of this and other velocity coefficients see Chow (1959).

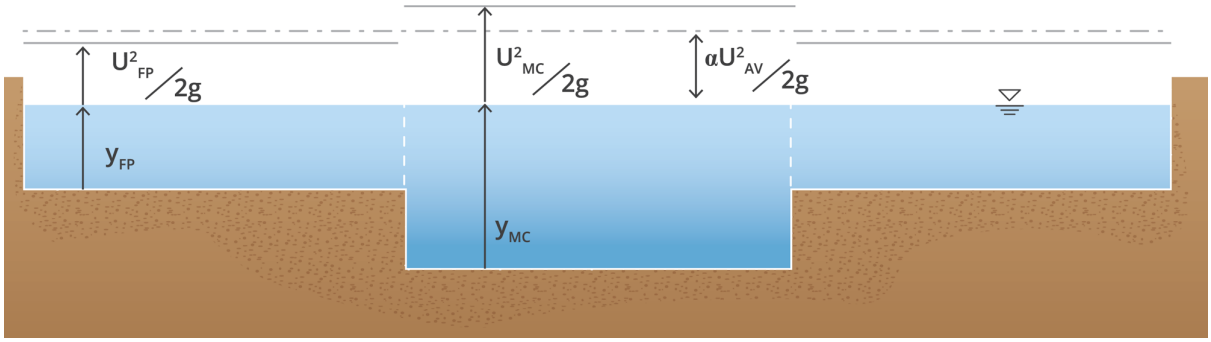


Figure 6.2.9. Variation of the total energy grade line across the compound channel section assuming a horizontal water surface.

It is frequently sufficient when analysing prismatic open channels, particularly man-made rectangular and trapezoidal channels, to assume a value of unity for the energy coefficient ($\alpha$). This can be justified by consideration of the error introduced in relation to the low order of accuracy inherent in many other factors involved with open channel flow characteristics.

## 2.2.1. The one dimensional energy equations

The total head (H) associated with a free surface flow has dimensions of energy per unit weight of fluid (i.e. length) and units of Joules per Newton (i.e. metres) and is given by:

$$H = z + y + \alpha\frac{u^2}{2g} \tag{6.2.2}$$

where... *z* = vertical distance from the datum to the channel invert or potential energy (*J* ) per unit weight of fluid (m), *y* = depth of flow (m), *u* = cross-sectionally averaged flow velocity (m/s), *g* = acceleration due to gravity =9.806m$^2$/*s*, $\alpha =$ dimensionless kinetic energy coefficient. The term

$$\alpha\frac{u^2}{2g} \tag{6.2.3}$$

represents the kinetic energy per unit weight of fluid (m).

The need for the kinetic energy coefficient (α) in Equation (6.2.2) and Equation (6.2.3) arises whenever the velocity is non-uniform over the cross-section. In the case of a uniform velocity over a cross-section, $\alpha = 1$. Departures from a uniform velocity over a cross-section, result in the cube of the mean velocity over the cross-section having a different value from the cube of the velocity (at each point in the cross-section) when averaged over the cross-section.

Because the cube of the cross-sectionally averaged velocity will be less that the average of the local velocity cubed, the parameter α is introduced as:

$$\alpha = \frac{\sum Q_i V_i^2}{QV^2} \tag{6.2.4}$$

$$\alpha = \frac{\sum A_i V_i^3}{AV^3} \tag{6.2.5}$$

where $V_i$ = velocity through cross-sectional area $A_i$, V = cross-section averaged velocity And A = total flow area.

In reality, the flow velocity varies over the cross-section and where measurements are available it is possible to evaluate the parameter $\alpha$. In practice, for turbulent flow in pipes, $\alpha = 1.03 - 1.06$ and is normally set to unity, but for open channels, particularly compound channels the value of $\alpha$ can depart significantly further from unity. However, it is not an uncommon practice to also adopt $\alpha = 1$ in computations for simple prismatic open channel flows.

The specific head or specific energy (*E*) is the total head with respect to the channel invert and is given by:

$$E = y + \alpha \frac{u^2}{2g} \tag{6.2.6}$$

Specific energy is a concept which is useful for determining the water surface profile through smooth transitions such as a channel narrowing, a smooth hump or smooth step in the channel or a combination of these channel transitions. This equation is often differentiated to give the minimum specific energy (critical flow) however the fact that $\alpha$ varies with depth is a complication. In a compound channel ($\alpha$) can be significantly greater than 1 and must be considered.

The equations defining total head Equation (6.2.2) and specific energy Equation (6.2.6) have two assumptions built into them:

i. The pressure distribution is hydrostatic since the streamlines are straight and parallel, and

ii. that depth measured vertically (*y*) which is a good approximation to the actual pressure head ($y\cos^2\theta$ ) in an open channel flow with a bed inclined at $\theta$ to the horizontal. For example, a bedslope (S = tan$\theta$) which is as steep as 1V:10H (or $\theta$ = 5.7°) only gives rise to an error which is close to 1% of the depth i.e. y. $\cos^2(5.7°) = 0.99y$.

# 2.3. Classification of Free Surface Flows

Free surface flows are flows in which the top water surface is subject to atmospheric pressure but is free from shear stresses exerted by any containing flow boundaries from the channel or pipe.

Free surface flows occur:

- as overland flows (across grasslands, bitumen surfaces or paved areas),
- in natural channels (as in-bank and overbank flows of rivers, streams, and creeks),
- in manmade channels (in stormwater and wastewater treatment plants, in urban drainage systems),
- other waterways (such as in estuaries or wetlands), and
- pipes and closed conduits (as in sewerage channels, pipelines and culverts).

Free surface flows can be classified:

- according to their time variation (as steady or unsteady),
- according to their spatial variation (as 1D, 2D or Three Dimensional (3D) - even though the small scale turbulent motions are always in 3D),
- as laminar or turbulent flows (depending upon the Reynolds number, *Re),*
- as subcritical or supercritical flows (depending upon the Froude number, *Fr*), or
- as gradually varying flow (as in backwater and drawdown longitudinal water surface profiles) or rapidly varying flows (as in hydraulic jumps). There is no sharp line of demarcation separating gradually varying flow and rapidly varying flow but the distinction between them can be put in terms of:

i. a comparison between the radius of curvature of the streamlines and the depth of flow, or

ii. whether the pressure distribution through the vertical can be approximated as being hydrostatic or not.

## 2.4. Uniform Flow and Critical Flow

There are two key flow conditions in steady state open channel flow calculations:

- uniform flow, and
- critical flow.

From a theoretical perspective, these form important bounding conditions to water surface profiles and allow the classification of the flow profiles. This water surface profile classification allows for a greater understanding of the flow, what controls it and how should it behave. For example, is the channel hydraulically mild or steep and where are the controls. In addition, it also gives insight into where a hydraulic jump might occur if the flow is constricted or controlled in some way downstream. A detailed discussion of flow profile classification is given in Henderson (1966). Detailed knowledge and understanding of these flow classifications and their implications is essential when interpreting outputs of water surface profile calculation numerical models. It is also good practice to verify and validate complex models with simpler water surface profile calculations before application to the more complex topologic problems often encountered in real flood studies. For example, can the model maintain a uniform flow, is the water surface profile correct in a variety of gradually varied flow situations, how does it handle controls, can it compute both sub-critical and super-critical flows in simple channels and can it locate hydraulic jumps correctly? These are good checks to ensure that 1) the model is working correctly and 2) that the user is using the model correctly.

### 2.4.1. Uniform Flow

Uniform flow is a useful reference condition in which the depth of flow (as well as the flow velocity) remains constant down a prismatic channel. The water is neither accelerating nor decelerating. Such a condition is brought about by the equilibration of two opposing forces,

- the weight or gravity force resolved down the channel ($W \sin\theta$ ) which tends to accelerate the flow, and

- the frictional shear force ($F\tau$) which opposes the motion of the water and acts in the longitudinal direction, tangential to the flow boundary of the channel in contact with the water (see Figure 6.2.10). The shear force acts around the wetted perimeter of the channel cross-section.

Figure 6.2.10 depicts the dominant forces acting on an elemental volume of water. For the flow condition of uniform flow, all the forces cancel out and there is no net force acting on the fluid element since *W*. sin *θ*= $F\tau$.

Because the hydrostatic pressure forces on the two ends of the control volume cancel each other out, they do not enter the picture here. In uniform flow, the bed slope $S_o$, the slope of the water surface $S_{ws}$ and the slope of the total head line or friction slope $S_f$ are all equal.

While uniform flow rarely (if ever) occurs in nature, it may be a reasonable approximation for the flow down a long, prismatic, manmade channel or as a first pass for estimating a flow depth in a natural channel given a discharge.

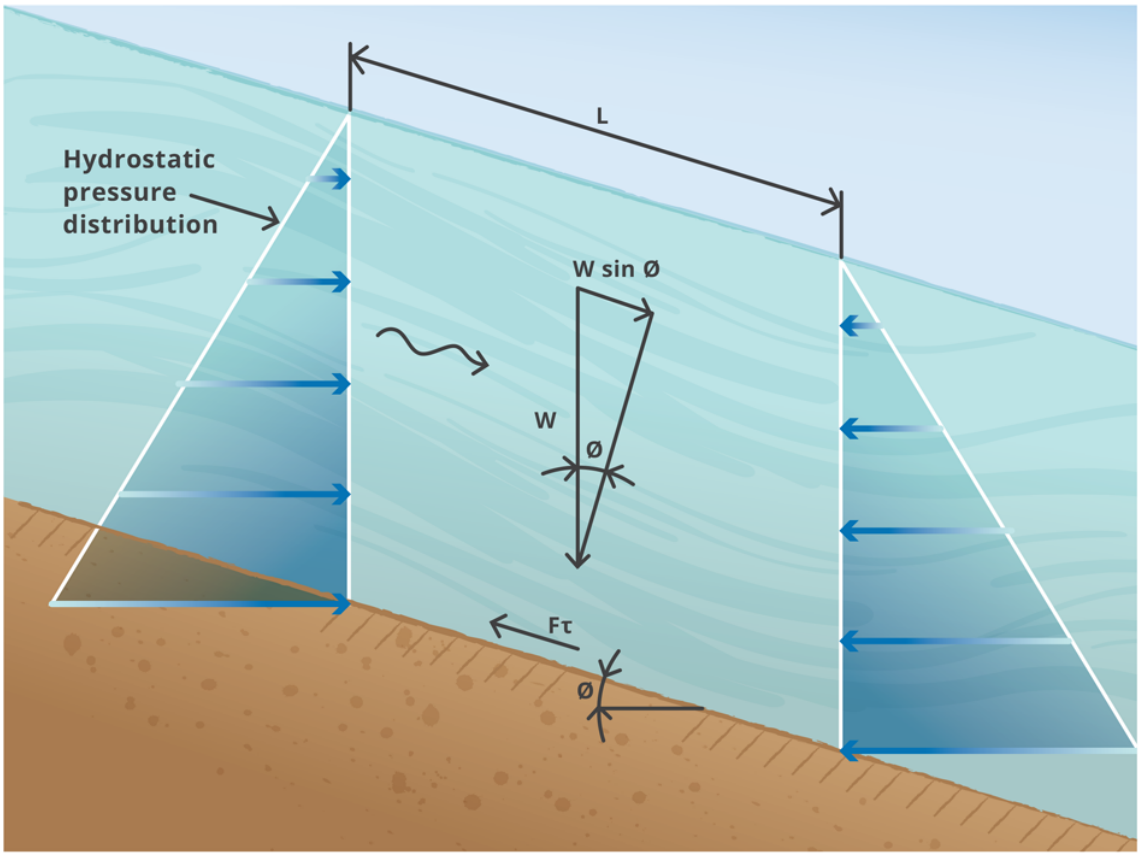


Figure 6.2.10. Opposing forces acting on a fluid element down the channel cancel thereby producing uniform flow.

## 2.4.2. Critical Flow

Critical flow occurs when the specific energy (*E*) at a cross-section is a minimum for a fixed flow, and this corresponds to the Froude number (*Fr*) having the value of unity at that cross-section. Here, we consider two cases:

i. channel with a general cross-section, and

ii. channel with a rectangular cross-section which is a particular but useful case.

## 2.4.2.1. Channel with a General Cross-Section

For a channel with a general (either natural or prismatic but not compound) cross-section as shown in Figure 6.2.7, critical flow is defined by setting the Froude number to unity.

$$Fr = \sqrt{\frac{Q^2 B}{gA^3}} = 1 \tag{6.2.7}$$

where. . . *B* = top width of the cross-section (*m*)

## 2.4.2.2. Channel with a Rectangular Cross-Section

Only for channels with a rectangular cross-section, is it convenient to work in terms of the flow per unit width of channel i.e. q = Q/b in units of ($m^2$/s).

At critical flow, the value of the Froude number is unity and the resulting expressions are:

$$Fr = \frac{q}{\sqrt{gy_c^3}} = \frac{V}{\sqrt{gy_c}} = 1 \tag{6.2.8}$$

$$y_c = \left(\frac{q^2}{g}\right)^{\frac{1}{3}} \tag{6.2.9}$$

where q = flow per unit width in channel with rectangular cross-section ($m^2$/s) $y_c$ = critical flow depth in channel with rectangular cross-section (m), V = flow velocity (m/s) when the depth is $y_c$.

Cross-sections at which the flow is critical are special in that there is a unique relation between velocity (or rate of flow) and depth, irrespective of the channel roughness or bedslope. Such cross-sections are technically known as controls and examples of locations where they occur might are:

i. a sudden steepening of the channel bedslope,

ii. a brink (or overflow),

iii. a hump of sufficient height,

iv. an upwards step of sufficient height,

v. a narrowing of the channel which is sufficiently constricting,

vi. flow from a reservoir or lake into a channel, or

vii. a hydraulic structure such as a broad crested weir. Some hydraulic structures that consist of control gates (such as sluice or radial gates) also provide a unique relationship between depth and discharge, but critical depth is not present.

In an open channel with various features such those listed above, it is possible that if the flow changes, so can the control(s). For a given flow, a channel can have more than one

control. The actual controls can only be identified through a trial and error process in which channel feature(s) is/are assumed to be control(s), and the computations on the backwater and drawdown curves completed. If the resulting water surface profile is compatible with the known boundary conditions at both ends of the channel, then the assumed control(s) are valid. If, on the other hand, an incompatibility is reached, it means that one of more of the assumptions regarding the controls needs to be changed and the solution process of calculating the water surface profiles is repeated until compatibility with all imposed boundary conditions is achieved. In a channel with some potential controls, the above solution process can be lengthy and require a number of trials.

## 2.4.2.3. Channels with a compound cross-section

While much research attention has been focused on uniform flow in compound channels in the past, little work has been done on predicting critical depth in such channel configurations. Critical depth in an open channel is most commonly defined as the point of minimum specific energy, the point of minimum specific force, or the transition between supercritical and subcritical flow, where the celerity of a surface wave is equal to the velocity of the flow.

Petryk and Grant (1978) were the first to propose an alternative Froude number for compound channels. This Froude number was based on a discharge weighted average of each subsections Froude number calculated from simple channel procedures. While this method was simple in its application, it was shown to have limitations (Blalock and Sturm, 1981).

Blalock and Sturm (1981) developed a method of calculating the critical depth in a compound channel based on the definition of minimum specific energy including the kinectic energy corrections coefficient.

$$E = \alpha\frac{V^2}{2g} + y \tag{6.2.10}$$

where, $\alpha$ is the kinetic energy correction factor, u is the average velocity within the cross section and y is the depth of flow.

The minimum specific energy is found by setting the derivative with respect to the depth of Equation (6.2.11) to zero. This yields the following general Froude number for open channel flow:

$$Fr_c = \left[\frac{\alpha Q^2 T}{gA^3} - \frac{Q^2}{2gA^2}\frac{d\alpha}{dy}\right]^{\frac{1}{2}} \tag{6.2.11}$$

where, Q is the total discharge, A is the total cross-sectional area and T is the channel top width.

Blalock and Sturm (1981) stated that early works on compound channel sections assumed a value of unity for the value of kinetic energy correction factor, $\alpha$, which gives:

$$Fr_c = \sqrt{\frac{Q^2 B}{gA^3}} \tag{6.2.12}$$

This is the equation that would be used in a prismatic channel where the average velocity is a good representation of the flow velocity distribution. Equation (6.2.12) considers the

compound channel as a single unit. There are some similarities here to the Single Channel Method (SCM) used to calculate uniform flow in compound channels (Lambert and Myers, 1998). Equation (6.2.12) would be appropriate in a compound channel if the velocities in the different sub-areas were of a similar magnitude (Lee et al., 2002)

Blalock and Sturm (1981) found that the value of a is not a constant value, but varies as a function of depth in compound channels. Blalock and Sturm (1981) evaluated the kinetic energy correction factor using the traditional divided channel method with vertical divisions (Chow, 1959). The channel was split into three independent sections, the main channel, and the two adjacent floodplains. The assumption was that the non-uniformity in the velocity profile occurs predominantly as a result of the difference in velocities between sections, and the variation within each section was seen to be negligible. The Manning formula was used to calculate the conveyance of each section and the boundary between the sub-sections was not included in the wetted perimeter of the sub-sections. Using this method, the value of $\alpha$ in a compound channel was derived to be:

$$\alpha = \frac{\sum_{i=1}^{3} \frac{K_i^3}{A_T^2}}{\frac{K_T^3}{A_T^2}} \tag{6.2.13}$$

where, $K_i$ is the conveyance of the i[th] subsection given by $\left(\frac{1}{n}A_i R_i^{\frac{2}{3}}\right)$, $A_i$ is the cross-sectional area, $n_i$ is the Manning surface roughness coefficient, $K_i$ is the hydraulic radius of the cross-section and $K_T$, $A_T$ are the total conveyance and cross-sectional area for the entire channel respectively.

Differentiating Equation (6.2.13) with respect to the depth *y* yields

$$\frac{\partial \alpha}{\partial y} = \left(\frac{A_T 2\sigma_1}{K_{T^3}} + \sigma_2\left(\frac{2A_T T}{K_{T^3}} - \frac{A_T 2\sigma_3}{K_{T^4}}\right)\right) \tag{6.2.14}$$

where $\sigma_n$ is the n[th] subsection property defined by Blalock and Sturm (1981) as:

$$\sigma_1 = \sum_{i=1}^{3}\left[\left(\frac{K_i}{A_i}\right)\left(3T_i - 2R_i\frac{\partial P_i}{\partial y}\right)\right] \tag{6.2.15}$$

$$\sigma_2 = \sum_{i=1}^{3}\frac{K_i^3}{A_i^2} \tag{6.2.16}$$

$$\sigma_3 = \sum_{i=1}^{3}\left[\left(\frac{K_i^3}{A_i^2}\right)\left(5T_i - 2R_i\frac{\partial P_i}{\partial y}\right)\right] \tag{6.2.17}$$

and, $T_i$ is the top width of flow and $P_i$ is the wetted perimeter for the i[th] subsection.

The Froude number for a compound channel, based on the definition of critical flow as the point of minimum specific energy is given by substituting Equation (6.2.13) and Equation (6.2.14) into Equation (6.2.11):

$$Fr_c = \frac{Q^2}{2gK_T^3}\left(\frac{\sigma_2\sigma_1}{K_T} - \sigma_1\right)^{\frac{1}{2}} \quad (6.2.18)$$

This approach can result in multiple values for critical depth in a compound channel. Typically, one crtitical depth is within the main channel and the other is above. Exactly which value should be used is somewhat unclear and is often found by a numerical minimisation method.

For any given overbank depth a discharge and velocity can be computed using the divided channel method with vertical divisions, and a subsection Froude number could be computed based on these values. This is consistent with treating these sub-sections as independent channels. Further discussion of this is given in Lee et al. (2002) who suggested that there may be a transition zone between subcritical and supercritical flow where a mixed flow regime is possible and that the concept of specific value of critical depth given above may not be meaningful.

## 2.4.3. Bed Shear Stress

As soon as there is movement of water through a channel or pipe with slope, $S = \tan\theta$, a resistive shear force is mobilised which opposes the motion of the water down the channel. This shear force (or friction force) is developed around the wetted perimeter or periphery (P) of the channel or conduit and has its origins in the (albeit small) viscosity of the water. The shear force arises from a combination of:

i. the viscous skin drag between the moving fluid and the flow boundary, and

ii. the form drag on the roughness projections of the flow boundary.

While a shear force is also developed at the air-water interface, is generally small (except for strong winds over large surface areas) in comparison to the shear force around the interface of the water and channel (or water and pipe wall).

An expression for the bed shear stress for uniform flow (t) can be determined by equating the two forces acting on the fluid element of length (L) in Figure 6.2.10.

$$W\sin\theta = F_T \quad (6.2.19)$$

$$\rho gLA\sin\theta = LP\tau_o \quad (6.2.20)$$

$$\tau_o = \rho g\left(\frac{A}{P}\right)\sin\theta \quad (6.2.21)$$

$$\approx \rho g R_h \tan\theta \quad (6.2.22)$$

$$= \rho g S R_h \quad (6.2.23)$$

$$where...R_h = \frac{A}{P} \quad (6.2.24)$$

$R_h$= hydraulic radius (m)

The approximation $\sin\theta \approx \tan\theta$ is only in error by 1% when the channel slope is as steep as about $8°$ or 7H:1V since $\left(\frac{\sin(8°)}{\tan(8°)}\right) = 0.99$.

Equation (6.2.21) applies to uniform flow, but it can be generalised to include gradually varying flow by replacing the slope, S by the friction slope, Sf. For gradually varying flow, the bed shear stress is given by:

$$\tau_o = \rho g R_h S_f \tag{6.2.25}$$

The bed shear stress is important when considering the flow velocities necessary for scour and deposition including:

i. the initiation of sediment motion,

ii. sediment motion in alluvial channels,

iii. avoiding deposition of sediment through suspension by fluid turbulence,

iv. scour at bridges, and

v. scouring conduits free of sediment.

# 2.5. Uniform Flow Resistance Formulas

In turbulent flow, there are three equations which are commonly used to quantify the effects of boundary resistance when a flow is passing down the channel:

- Manning equation
- Chezy equation, and
- Darcy-Weisbach equation in conjunction with the Colebrook-White equation to determine the Darcy friction factor, f.

While the Chezy and Manning formulas are more commonly applied to open channel flows, the Darcy-Weisbach and Colebrook-White equations are more commonly applied to pipe flows.

Both the Chezy and Manning formulas relate the cross-sectional averaged velocity to the channel slope, the hydraulic radius and an empirical parameter which is used to encapsulate the effects of the resistance to flow. The two formulas have a different form to each other. A discussion of the resistance equations is given in the American Society of Civil Engineers Task Force on Friction Factors in Open Channels (ASCE Task Force, 1963).

## 2.5.1. Manning Formula

The formula known as the Manning formula is the result of several modifications of a formula originally published by Manning in 1889. The Manning formula shown below is popular internationally and is the most used approach in practice in Australia:

$$V = \frac{R_h^{\frac{2}{3}} S^{\frac{1}{2}}}{n} \tag{6.2.26}$$

where V = cross-sectional averaged flow velocity ($m.s^{-1}$) = Q/A, Q = flow ($m^3/s$), $R_h$ = hydraulic radius of the cross-section (m) = A/P, S = longitudinal slope of the channel ($m.m^{-1}$)

The Manning's equation Equation (6.2.26) is not dimensionally homogeneous and this has led to confusion about the dimensions of the Manning roughness parameter n. There are three interpretations of the dimensions of Manning's n (See Section 5-6 in Chow (1959)):

- $L^{-\frac{1}{3}}T^{1}$ -These dimensions result directly from the Manning equation Equation (6.2.26),
- $L^{0}T^{0}$ - i.e. dimensionless. Consequently, the unstated coefficient of unity at the front of the right hand side of Equation (6.2.26) must have the dimensions of $L^{-1/3.T1}$ ,
- $L^{\frac{1}{6}}$ - In this case, the dimensions of n are independent of time, as would be expected of a roughness parameter and only involve length. As n is a measure of the absolute roughness of the channel surface. In this case, it is assumed that there is a coefficient of unity equal to $\sqrt{\frac{g}{9.81}}$ attached to the right hand side of the Manning equation Equation (6.2.26). In engineering practice, this is perhaps the most commonly adopted version for the units of Manning n.

## 2.5.2. Application of the Manning Equation

The Manning equation Equation (6.2.26) can be applied in two modes:

1. With Manning n being held constant for a particular channel, irrespective of the flows down the channel. This case corresponds to a direct relationship between the square of the flow velocity and the slope (i.e. S˜ v2) and is a characteristic of a fully rough turbulent flow.

2. With Manning n varying in some prescribed fashion according to the depth of flow (or stage or hydraulic radius). The actual variation of Manning n will normally have been determined from measurements and back-calculated through Manning equation. When used in numerical modelling of flood studies, the variation may be stored as a table of values for varying depth or stage.

Estimates for the values of Manning n can be found from various sources. An example of a table of Manning n is give in the table below.

Table 6.2.1. Values of Roughness Coefficient n for different channel conditions (Sellin 1961)

| *Description of channel* | Minimum | Normal | Maximum |
|---|---|---|---|
| Glass, plastic, machined metal | 0.009 | 0.010 | 0.013 |
| Fabricated steel channels | 0.011 | 0.012 | 0.017 |
| Planed timber, joints flush | 0.010 | 0.012 | 0.014 |
| Sawn timber, joints uneven | 0.011 | 0.013 | 0.015 |
| Concrete, trowel finished | 0.011 | 0.013 | 0.015 |
| Concrete, shuttering | 0.012 | 0.014 | 0.017 |

| *Description of channel* | Minimum | Normal | Maximum |
|---|---|---|---|
| Brickwork | 0.012 | 0.015 | 0.018 |
| ***Excavated channels:** | | | |
| earth, clean | 0.016 | 0.022 | 0.030 |
| gravel | 0.022 | 0.025 | 0.030 |
| rock cut, smooth | 0.025 | 0.035 | 0.040 |
| rock cut, jagged | 0.035 | 0.040 | 0.060 |
| ***Natural channels:** | | | |
| clean, regular section | 0.025 | 0.030 | 0.040 |
| some stones and weeds | 0.030 | 0.035 | 0.045 |
| some rocks and/or brushwood | 0.050 | 0.070 | 0.080 |
| very rocky or with standing timber | 0.075 | 0.100 | 0.150 |
| **Flood plains:** | | | |
| short grass pasture | 0.025 | 0.030 | 0.035 |
| mature crops | 0.025 | 0.035 | 0.045 |
| brushwood | 0.035 | 0.050 | 0.070 |
| heavy timber or other obstacles | 0.050 | 0.100 | 0.160 |

1. Tables of Manning n can be found in numerous references for different surfaces such as asbestos cement, concrete (centrifugally spun), ductile iron and steel (e.g. Table 2 in AS 2200 (2006) and Table 5-6 in Chow (1959)). References often give a range of values for minimum and maximum values corresponding to pipes in good to poor condition.

2. Twenty four black and white photographs of manmade and natural river channels can be found in Figure 5-5 of reference Chow (1959) with corresponding values of Manning roughness parameter ranging from n = 0.012 to n = 0.150. No information on the stream or river geometry (i.e. plan view or cross-sections) is given in this reference. The main difficulty with acquiring estimates of n from these photos is that one is relying on the brief caption for each photo and the view of the exposed part of the bank or channel to gauge the roughness (and hence the Manning's n) of the submerged part of the channel or of the channel under flood conditions.

3. Colour photos of fifty natural rivers, two to seven (but typically three or four) cross-sections of each river channel and a plan view can be found in Barnes (1967). This information was assembled by the U.S. Geological Survey over a 15 year period. Although this reference is old with its quantitative information in imperial units, it is perhaps the best known and complete compendium on Manning n for natural streams and rivers. The Manning n values range from n = 0.024 through to n = 0.075 and all measurements in this reference were made during the peaks of documented floods. The locations of the cross-sections are indicated on an accompanying plan view of the stream or river. It is clear from the plan views of all the channel reaches that where the Manning n values refer to are straight or gently curving. Other information which can be found in this

reference includes the river name, geographical location, date of the flood, the flow, a description of the bed material and condition of both river banks, and a table of cross-sectional flow area, top width, mean depth, hydraulic radius, mean flow velocity, length between cross-sections, and the slope between sections.

An example of the information contained in this reference is reproduced in Figure 6.2.11 to Figure 6.2.12 which refers to Esopus Creek. (Esopus Creek is one of three waterways with Manning n = 0.030 included in this reference.)

Interestingly, rivers and streams with sandy beds were not included in this reference because Manning n values for streams and rivers of this type, which depend upon the size of the bed material and bedforms, can be found elsewhere. The beds of the streams and rivers included in this reference ranged from boulder strewn mountain streams to heavily vegetated streams and rivers.

1. Other references with pictures of channels with varying channel roughness can be found from various web sites on the internet (Phillips and Ingersoll, 1998) or other references from the U.S. Geological Survey.

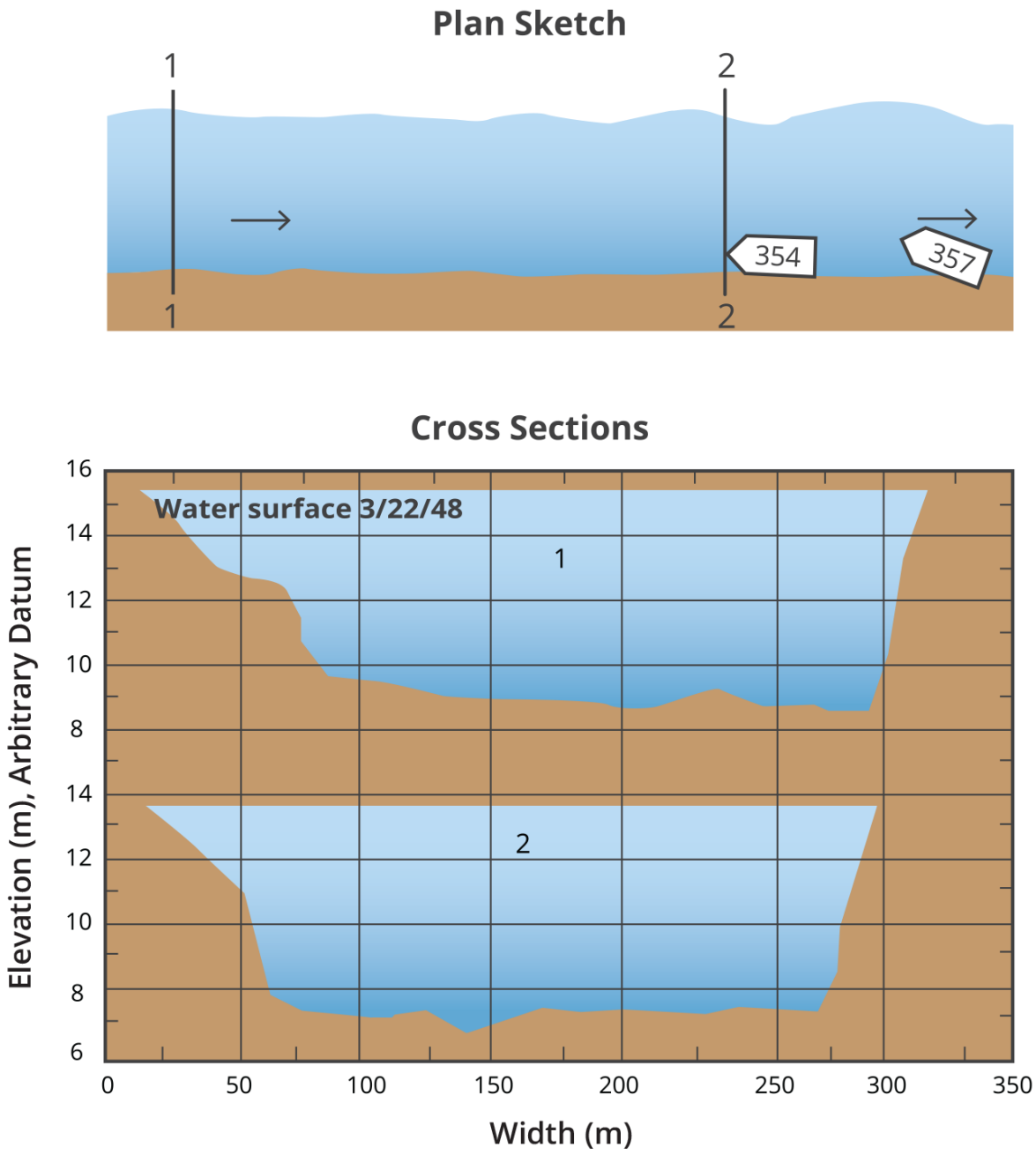


Figure 6.2.11. Roughness coefficient data for Esopus Creek with n = 0.030 (Page 34 in Barnes (1967)).

Figure 6.2.12. Esopus Creek

In a 1D model the roughness parameter can account for:

1. Friction losses associated with the bed material of a channel/floodplain,
2. Drag losses associated with vegetation or other obstructions in the channel/floodplain,
3. Losses due to turbulence in a channel/floodplain due to channel geometry,
4. Variations in geometry and associated form losses between cross-sections,
5. Bend losses in a channel.

**Developing Hydraulic Roughness**

As two dimensional models account for some non-boundary energy losses they often use slightly lower Manning roughness values than one dimensionalmodels listed above. In a 1D model roughness is typically assigned according to the cross-sections or along particular branches. For 2D models, roughness is generally specified as a spatially varying grid/mesh over the 2D model domain. It is important to note that the loss processes embedded in hydraulic roughness parameters for 1D and 2D models, whilst closely related, are not exactly the same.

In a 2D model, some of the above losses are to some degree accounted for by the numerical scheme. For example, some aspects of bend losses due to change in directional momentum are explicitly modelled in a full 2D solution. Similarly, part of the form loss due to variations in

geometry will be explicitly modelled in 2D scheme, depending on the grid/mesh resolution. Whilst the 2D roughness parameter nominally represents friction loss due to the ground surface material in each grid/mesh element, in practice there are still many sub-element loss processes that are not explicitly described, such as vegetation resistance (trees, shrubs), physical obstructions (fences, cars, poles etc) and local variability in topography. In effect, roughness parameters in a 2D domain also need to account for some losses in addition to the bed frictional losses, but less so than a 1D domain applied over the same area. In general, increasing grid/mesh resolution in the 2D domain can result in more of the additional losses being accounted for within that domain and less needing to be compensated for within the roughness parameter.

In urban areas, the way in which buildings are represented in the model has a significant bearing on the specification of roughness. In areas where buildings are explicitly represented as obstructions in the model topography, roughness in the surrounding areas should only account for the nature of the land-use (such as grass, paved, or vegetated areas). Alternatively, where buildings or other major obstructions are not explicitly modelled, the impact of these features on losses can be incorporated into the roughness parameter, using a significantly higher value than would otherwise be the case. Book 6, Chapter 4 contains further discussion on incorporating buildings, fences and other urban features within the 2D domain.

Applicable ranges for hydraulic roughness in 1D models have been well established and defined in numerous references over the last 50+ years, such as Chow et al. (1988). Values that represent average conditions within and between cross-sections are applied either at the cross-section or along a part or all of the branch.

Roughness for 2D models is generally specified as a map and based on land-use information that can be derived from aerial photography, satellite images, planning zone maps or field observations. Different areas can be digitised into land-use polygons representing zones of similar loss characteristics (e.g., vegetation or impervious surface type). This is typically conducted in a GIS environment and then transferred to the required format for a specific model package.

Roughness maps have also been generated from an auto image or LiDAR processing in some areas. However this is not a commonly adopted technique at present.

2D roughness is generally parameterised in terms of Manning ‘n’, or similar related parameterisation of bed friction. Typical ranges of 2D roughness parameters for various land-use types are listed in Table 6.2.2.

Table 6.2.2. Valid Manning ‘n’ Ranges for Different Land Use Types

| Land Use Type | Manning ‘n’ |
|---|---|
| Residential areas – high density | 0.2 – 0.5 |
| Residential areas – low density | 0.1 – 0.2 |
| Industrial/commercial | 0.2 – 0.5 |
| Open pervious areas, minimal vegetation (grassed) | 0.03 – 0.05 |
| Open pervious areas, moderate vegetation (shrubs) | 0.05 – 0.07 |
| Open pervious areas, thick vegetation (trees) | 0.07 – 0.12 |

| Land Use Type | Manning 'n' |
|---|---|
| Waterways/channels – minimal vegetation | 0.02 - 0.04 |
| Waterways/channels – vegetated | 0.04 – 0.1 |
| Concrete lined channels | 0.015 – 0.02 |
| Paved roads/car park/driveways | 0.02 – 0.03 |
| Lakes (no emergent vegetation) | 0.015 – 0.35 |
| Wetlands (emergent vegetation) | 0.05 – 0.08 |
| Estuaries/Oceans | 0.02 – 0.04 |

## 2.5.3. Factors Affecting the Manning Roughness Parameter

In practice, the Manning roughness coefficient n is used to encapsulate energy losses which may arise from several sources apart from boundary roughness. Other possible causes of energy losses are:

- flow expansions and contractions which may cause the flow to separate from the flow boundary and form a recirculation bubble in which energy is continuously dissipated in the eddy,
- vegetation (be it grasses, macrophytes or algae), and
- channel sinuosity which give rise to secondary currents. (No natural channel runs straight for more than ten times its width.)

If the flow expansion or contraction is sudden, it is more appropriate to formulate the resulting energy losses in any calculations or numerical model as a local loss. Chow (1959) and James and Wark (1992) discusses this in more detail.

## 2.5.4. Chezy Formula

The Chezy formula was proposed by Chezy in 1769 and is:

$$u = C\sqrt{SR_h} \tag{6.2.27}$$

where. . . u = cross-sectionally averaged velocity (m/s) = Q/A, Q = flow ($m^3.s^{-1}$) R = hydraulic radius of the cross-section (m) = A/P S = longitudinal slope of the channel ($m.m^{-1}$) A = flow area ($m^2$) P = wetted perimeter (m) C = Chezy coefficient ($m^{1/2}.s^{-1}$)

The Chezy coefficient is a measure of the smoothness of the channel since the smoother the channel, the greater is the value of the Chezy coefficient. However, in general, the resistance to flow depends on the viscosity of the water, as well as the roughness of the surface of the channel. The general semi-empirical expression for the Chezy coefficient is:

$$C = \sqrt{32g}\log\left(\frac{12R_h}{2\delta_s/7 + k_s}\right) \tag{6.2.28}$$

$$= 18\log\left(\frac{12R_h}{2\delta_s/7 + k_s}\right) \tag{6.2.29}$$

where. . . $\delta_s$ = viscous sublayer thickness (m) = 11.6 (v/ $v_* v_*$) = shear velocity ($m.s^{-1}$) = $\sqrt{g R_h S}$ = kinematic viscosity of water ($m^2.s^{-1}$) = $10^{-6}$ ($m^2.s^{-1}$) for water at $20°$ $k_s$ = boundary roughness projection height (m)

A few more words on $k_s$ as it relates to pipe wall roughness and to bedforms are in order.

- When $k_s$ refers to the roughness of a pipe or a manmade surface such as concrete, $k_s$ is also known as the equivalent sand grain roughness, after the definitive experimental work of Nikuradse (1933). Nikuradse conducted experiments aimed at measuring the head losses in pipes of varying roughness. In each experiment Nikuradse conducted, the inside wall of the pipe was coated with sand grains of approximately the same size. Nikuradse tested pipes with internal coatings of various discrete grain sizes, lengths and diameters and at various Reynolds numbers for the flow. In each case, the resulting head loss along the pipe was measured.

For commercial pipes (with their various pipe-to-pipe joints), the wall roughness will have a different geometry and distribution of roughness projection heights compared to Nikuradse's sand coated pipes.

The commercial pipe with an equivalent sand grain roughness is the pipe with the same size and length which yields the same head loss as a pipe coated with sand of a particular size. Data on commercial pipes (or other manmade surfaces) will include the equivalent sand grain roughness.

As pipes in service age, their walls become rougher through deterioration of the pipe wall and/or build-up of algal slimes. The equivalent sand grain roughness of pipes tends to increase with time and only through cleaning the pipes can the roughness (ks) be reduced.

1. In the case of bedforms on a mobile bed of sediment, it is recommended that $k_s$ be taken as half the height of the bedform. For example, for a river bed with dunes of height 10 cm engineering practice would be to set $k_s$ = 5 cm.

Retardation of the flow in an open channel is due to two forces which both oppose the flow:

1. the viscous force between the fluid and the boundary, and

2. the drag force due to the protuberances of the channel (or wall) roughness projections.

The effect of the roughness of the boundary surface on the value of the Chezy coefficient is quantified by the (wall) roughness (projection height) parameter ($k_s$) while the effect of the viscosity of the water is incorporated in the thickness of the viscous sublayer ($\delta_s$). The viscous sublayer is the very thin region of chaotic flow dominated by the viscous force and which separates the stationary fluid immediately in contact with the stationary flow boundary and the overlying turbulent boundary layer.

It is evident from the denominator in Equation (6.2.28) that there are two extremes of turbulent flow:

- the viscous force dominates i.e. $\delta_s$ $k_s$; the roughness projection elements are fully immersed in the viscous sublayer (see Figure 6.2.13) and the value of the Chezy coefficient is independent of the wall roughness projection height $k_s$. This extreme flow condition is known as hydraulically smooth turbulent flow and is unlikely in most practical situations.

- the drag forces on the roughness projection protuberances dominate i.e. $k_s >> \delta_s$; the roughness projection elements are sufficiently long to break down or protrude through and rupture the viscous sublayer and the value of the Chezy coefficient (and the uniform flow velocity) is independent of the fluid viscosity. This extreme flow condition is known as hydraulically rough turbulent flow and is normally the case when the Reynolds number Re > $10^6$ (approximately) and would commonly occur in earthen or natural channels. For hydraulically rough flow, Equation (6.2.29) can be simplified and the value of the Chezy coefficient can then be determined from:

$$C = 18\log\left(\frac{12R_h}{k_s}\right) \tag{6.2.30}$$

Values of the boundary roughness ($k_s$) vary according to the nature of the surface of the channel boundary. Three examples are earthen channels, brickwork, and concrete. Amongst other references, useful tabulations of the values for ks for various channel surfaces may be found in Table 5-6 of Chow (1959) or Table 4-1 in Henderson (1966). The values in Table 6.2.1 were extracted from Hydraulics Research Ltd. (1990) Table 3 in Charts for the Hydraulic Design of Channels and Pipes.

Table 6.2.3. Values of the roughness projection height $k_s$ and Manning n for straight, clean pipes concentrically jointed.

| Type of Pipe | Roughness Coefficient | |
|---|---|---|
| | Rouchness Projection Height $k_s$ (mm) | Manning n |
| Asbestos cement | 0.015 - 0.06 | 0.008 - 0.011 |
| Bitumen-lined concrete | 0.06 - 0.15 | 0.009 - 0.012 |
| Spun bitumen-lined steel | 0.03 - 0.06 | 0.009 - 0.010 |
| Brass | 0.003 - 0.015 | 0.008 - 0.009 |
| Cast iron (unlined) | 0.015 - 0.6 | 0.010 - 0.013 |
| Cement-mortar lined (in-situ) | 0.03 - 0.15 | 0.009 - 0.012 |
| Coal-tar enamel lined steel | 0.03 - 0.15 | 0.009 - 0.011 |
| Concrete, centrifugally spun | 0.03 - 0.15 | 0.009 - 0.012 |
| Copper | 0.003 - 0.15 | 0.008 - 0.009 |
| Zinc-coated (galvanised) steel | 0.03 - 0.15 | 0.009 - 0.011 |
| Thermoplastics | 0.003 - 0.15 | 0.008 - 0.009 |
| Thermosetting plastics | 0.003 - 0.15 | 0.008 - 0.009 |
| Vitrified clay | 0.15 - 0.6 | 0.010 - 0.013 |
| Fibre cement | 0.015 - 0.06 | 0.008 - 0.009 |
| Ductile iron, bitumen lined | 0.06 - 0.3 | 0.009 - 0.012 |
| Ductile iron and steel, cement mortar lined with or without seal coats | 0.01 - 0.06 | 0.006 - 0.011 |
| Ductile iron and steel | 0.01 - 0.03 | 0.006 - 0.009 |
| Steel, polyethylene lined | 0.003 - 0.15 | 0.008 - 0.009 |

## 2.5.5. Application of the Chezy Equation

In hydraulic investigations, the Chezy equation (Equation (6.2.27)) can be applied in two modes:

1. with the Chezy coefficient being held constant for a particular channel, irrespective of the flows down the channel. This case corresponds to a direct relationship between the square of the velocity and the slope (i.e. S ~ $u^2$)and is a characteristic of a fully rough turbulent flow.

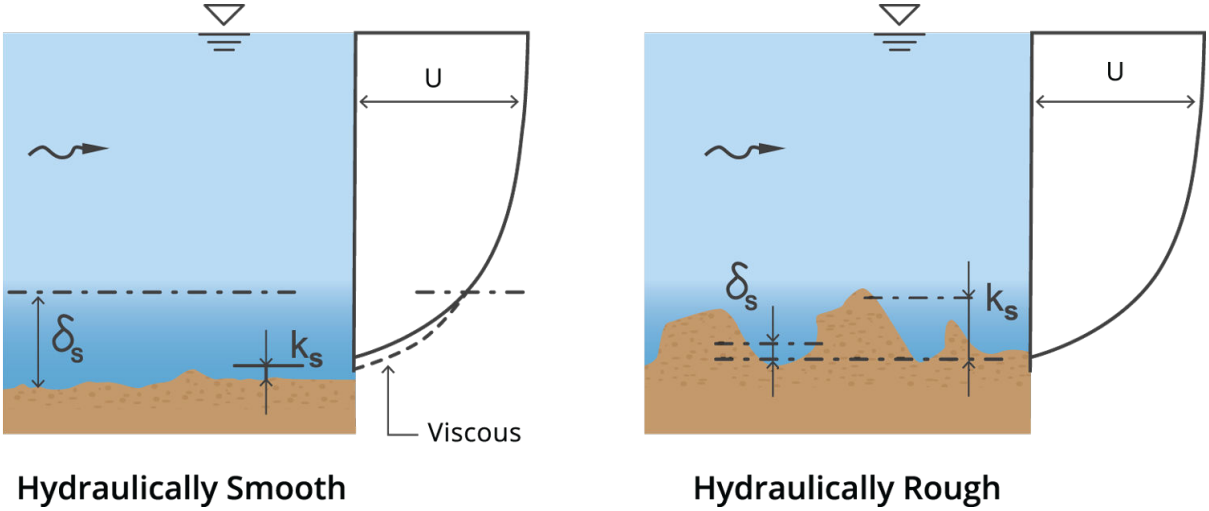


Figure 6.2.13. Relative height of the roughness projection elements and the thickness of the viscous sublayer.

1. with the Chezy coefficient varying according to Equation (6.2.28). In this case, the Chezy coefficient depends on the flow down the channel. Consequently, the flows capable of being simulated can range from hydraulically smooth turbulent flow to hydraulically rough turbulent flow. In effect, Equation (6.2.28) is closely related to the Colebrook-White equation of pipe flow.

## 2.5.6. The link between between the Manning Roughness coefficent and the roughness height

Some justification may be given for use of the Manning equation in terms of the dimensionally consistent Darcy-Weisbach friction factor. Figure 6.2.14 shows the logarithmic relationship for rough non-circular sections given in Equation (6.2.31) which is plotted against the power law approximation presented in Equation (6.2.32).

$$\frac{1}{\sqrt{f}} = 2\log\left(\frac{R}{ks}\right) + 2.34 \tag{6.2.31}$$

$$\frac{1}{\sqrt{f}} = 2.9\left(\frac{R}{k_s}\right)^{\frac{1}{6}} \tag{6.2.32}$$

Equation (6.2.32) provides an adequate description of Equation (6.2.31), giving an error of ± 5 %, within the range 5 < < 500. Given that the Manning roughness coefficient is related to

the Darcy-Weisbach friction factor by n = $\frac{1}{\sqrt{f}}R^{\frac{1}{6}}$ or $\frac{R^{\frac{1}{6}}}{C}$ Substitution of Equation (6.2.32) into this expression produces:

$$n = 0.039k_s^{\frac{1}{6}} \tag{6.2.33}$$

where $k_s$ is expressed in metres. Equation (6.2.33) relates the Manning n to the typical roughness height ($k_s$) used in Equation (6.2.31). The roughness height ks is often taken to be the $D_{75}$ value (diameter which more than 75% material passes through) of the gravel bed material. The Manning equation has also been applied to open channels which are not hydraulically rough with some success. Ackers (1991) discusses reasons for this by comparing the Manning equation to the Blasius equation (Streeter and Wylie, 1981) for the friction factor in smooth wall turbulent flow.

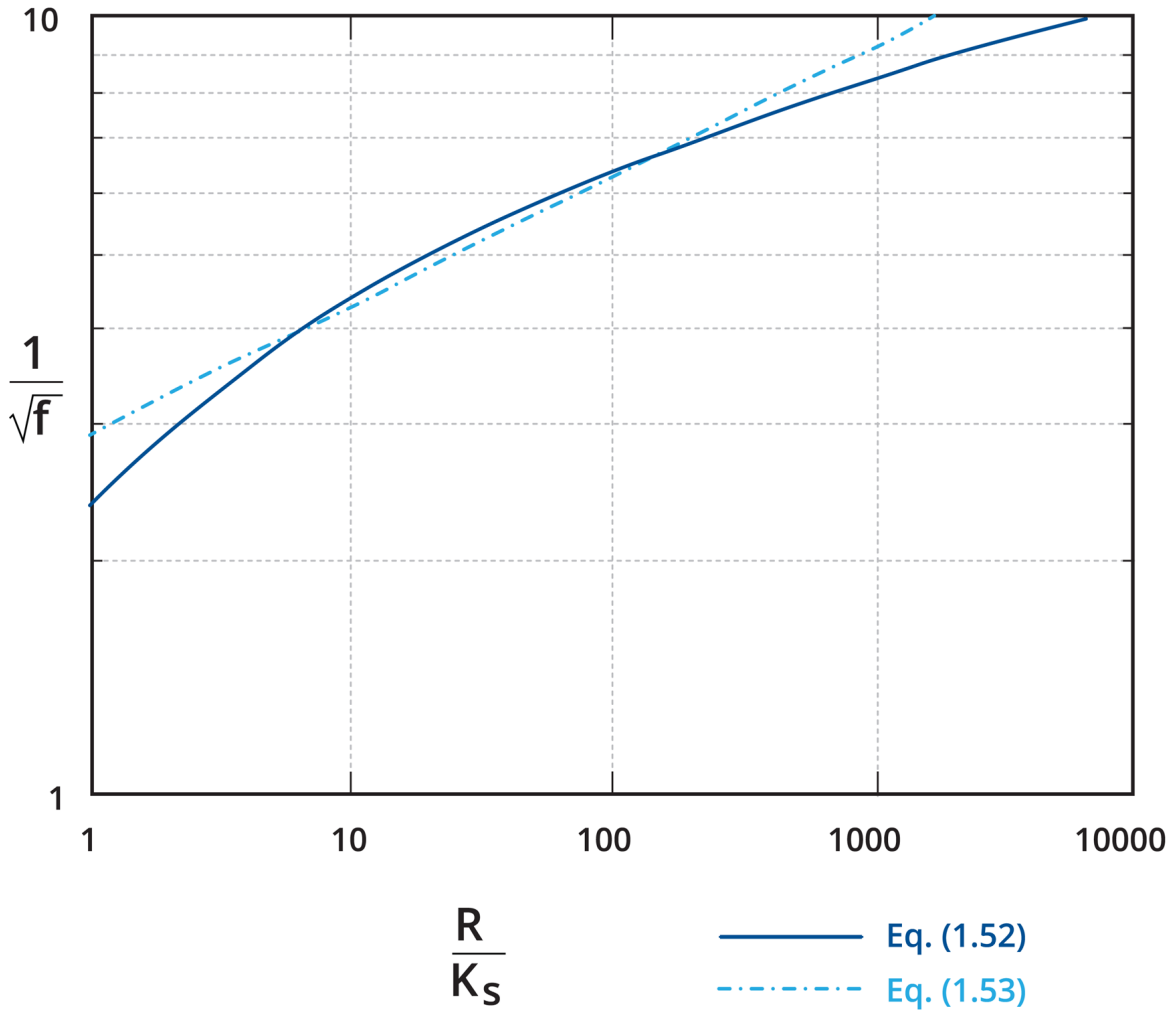


Figure 6.2.14. Comparison between Equation (6.2.31) and the power law approximation presented in Equation (6.2.32)

## 2.5.7. Uniform Flow in Channels of Compound Cross-Section

Compound channels are open channels with cross-sections which have berms or floodplains adjacent to a main channel that convey water at stages which exceed the bankfull depth as shown in Figure 6.2.15.

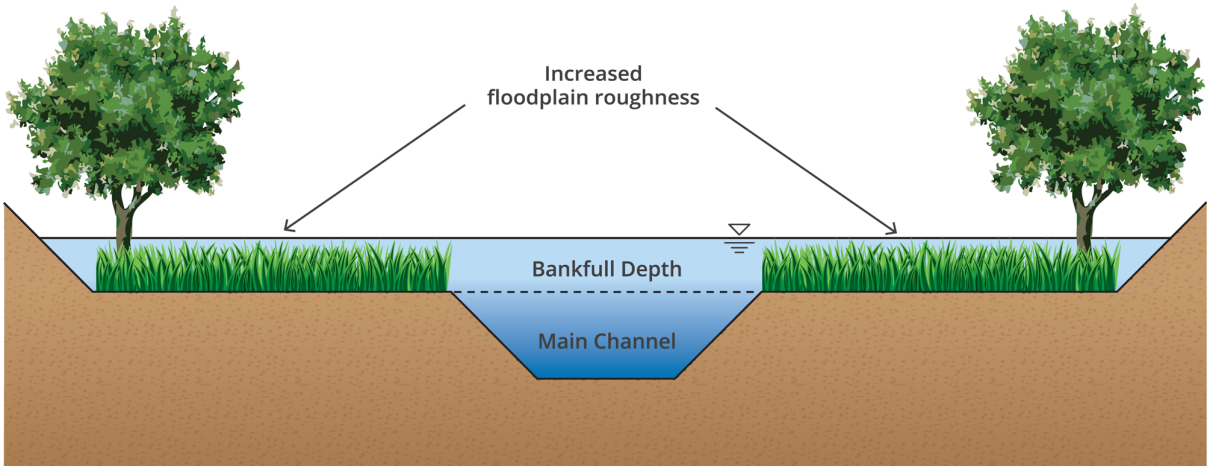


Figure 6.2.15. Typical compound channel with floodplains of greater roughness than the main channel

Typically the floodplains may be rougher than the main channel presenting the additional problem that the channel may have composite roughness as well as a complex or compound geometry. These features tend to set compound channels apart from simple prismatic channels for which the uniform flow depth can be predicted with some degree of accuracy.

Historically, compound channels were treated in the same manner as simple prismatic channels in which the overall hydraulic characteristics were used to calculate the discharge. This approach was formalised by Horton (1933) who gave the following relationship to calculate an equivalent Manning n ($n_e$) in simple channels where the roughness varied along the wetted perimeter. The same approach can be used for compound channels by employing Equation (6.2.34).

$$n_e = \left( \frac{\sum_{j=1}^{N} P_j n_j^{1.5}}{P} \right)^{\frac{2}{3}} \tag{6.2.34}$$

where P is the total wetted perimeter, $P_j$ is the length of wetted perimeter associated with $n_j$ and N is the number of different roughnesses. Both Horton (1933) and Einstein (1934) assumed that the water area is divided imaginatively into N parts (see Figure 6.2.16) for each different roughness. They then assumed that each part had the same velocity which is also equal to the average velocity of the whole section (ie. $u_1 = u_2 = u_3 = u$).

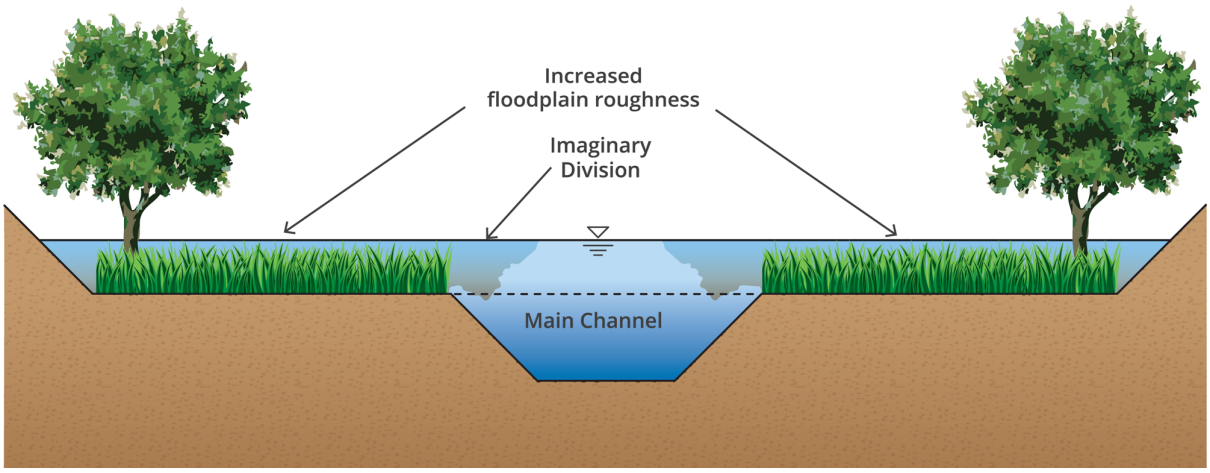


Figure 6.2.16. Imaginary division of a compound channel assumed by Horton (1933) to give the same average velocity on the floodplains and in the main channel.

While Horton's assumption is obviously invalid at low overbank depths when there is a large difference between the velocities of the two areas, work by Myers (1987) and Ackers (1991) shows that this approach produces satisfactory results for high overbank stages where the compound channel is once again tending to act as a single unit. This approach will be referred to as the Single Channel Method.

Lotter (1933) assumed that the total discharge is equal to the sum of the discharges in each sub-area. Lotter's approach, like Horton's, was developed to predict the discharge in a simple prismatic cross-section with varying roughness around the channel perimeter. In simple prismatic channels, but not in compound channels, it may be assumed that the hydraulic radius of each sub-area is equal. This however, does not restrict its application to compound channel flows. When the method suggested by Lotter (1933) is applied to compound channels some decisions need to be made regarding the subdivision of the channel cross-section. Typically for compound channels, a vertical division is used to separate the floodplain from the main channel as shown by the dashed lines in Figure 6.2.17.

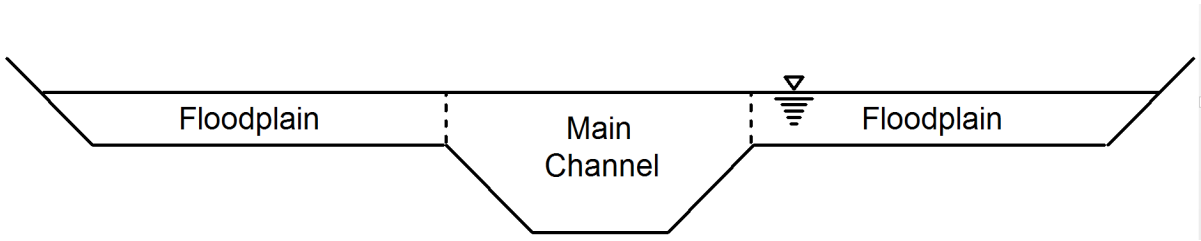


Figure 6.2.17. Vertical division of a compound channel into floodplain and main channel subsections

In compound channels, this leads to the assumption that the different sub-areas act independently of each other. As a result, the flood plain subsections and the main channel are treated as individual simple prismatic channels, and the discharge is obtained for each subsection by applying an appropriate resistance law, such as the Manning equation, to each subsection in turn. An expression for an equivalent Manning roughness coefficient ($n_e$) can also be obtained by this approach.

$$n_e = \frac{PR^{\frac{5}{3}}}{\sum_{j=1}^{N} \frac{P_j R_j^{\frac{5}{3}}}{n_j}} \tag{6.2.35}$$

where P and R are the overall wetted perimeter and hydraulic radius respectively and $P_j$, $R_j$ and $n_j$ are the wetted perimeter, hydraulic radius and Manning roughness coefficient of the $j^{th}$ sub-area. This approach, along with the use of vertical divisions at the edge of the main channel, has become the most popular method of dealing with compound channels. The methods used to divide the channel into the individual subsections is however, somewhat arbitrary. While it does seem logical to separate the floodplains (a lower average velocity typically) from the main channel, it does assume that they act independently of each other.

As a result of the need to subdivide a compound channel into different sub-areas, the following horizontal and diagonal divisions as illustrated below are equally valid.

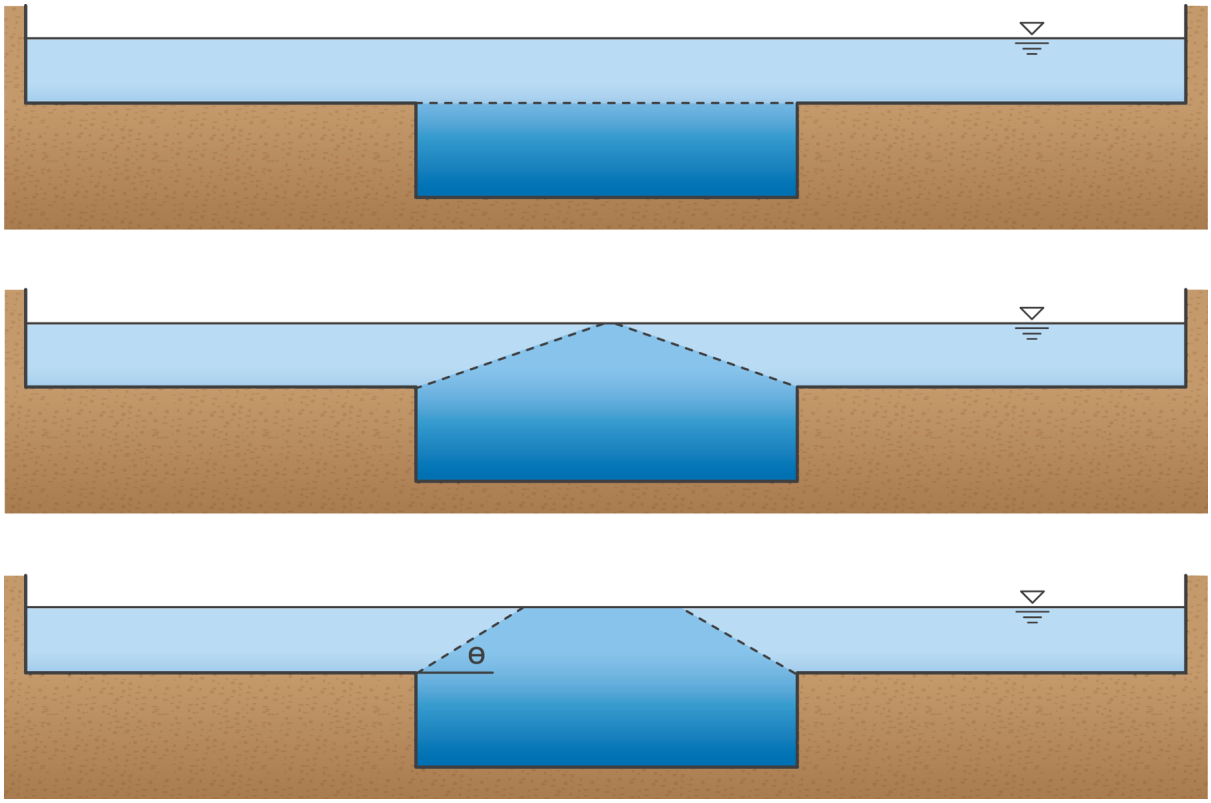


Figure 6.2.18. Alternative approaches to subdividing a compound channel cross-section.

Since 1964 evidence has been presented which demonstrates that flows in the different sub-areas do not act independently. The interaction between the faster moving water in the main channel and the slower moving water on the floodplain has the effect of reducing the overall discharge in the compound channel below the value that would be calculated assuming that they act independently. The first papers describing this phenomenon were Sellin (1964) and Zheleznyakov (1965).

Sellin (1964) provided photographic evidence of vortices which were believed to be the source of the interaction between the main channel and the floodplain. Sellin also provided experimental results which showed that the mean velocity in a channel with floodplains was approximately 30 % less than the same channel with the flood plains removed. Additionally,

Sellin showed that the discharge in the channel was over-predicted by approximately 10 - 12 %. Even though these experiments were carried out at a relatively small scale they did serve to illustrate that the prediction of the discharge capacity of a compound channel was not as straightforward as originally thought.

In the time since 1964, a great deal of experimental research has been carried out on this phenomenon in straight compound channels. A lot of the work has concentrated on discharge assessment, boundary shear stress distribution, velocity distribution, momentum transfer and apparent shear stress, as well as the structure of the turbulent flow.

Several other investigators have conducted field tests on compound channels including Bhowmik and Demissie (1982), Sellin and Giles (1988), Myers and Lyness (1989) and Martin and Myers (1991). Bhowmik and Demissie (1982) showed that above the bankfull level the floodplain velocity increased with stage, but the main channel velocity first reduces with increasing stage and later increases. Work carried out by Sellin and Giles (1988) on the River Roding in the United Kingdom and (Myers and Lyness, 1989) along with (Martin and Myers, 1991) on the River Main in Northern Ireland found similar reductions in discharge capacity above the bankfull level.

Many of the above authors have attempted to quantify, by various means, the effect of the interaction between the main channel and the floodplain on the overall discharge, component discharges and boundary shear stress distribution. The methods that have been used to date can be broadly classified as follows:

1. Using the single channel method with modified resistance coefficients or interaction factors.

2. Adjusting the subdivision boundaries between the main channel and the floodplain, sometimes coupled with the inclusion of the internal subdivision boundaries in the wetted perimeter.

3. Applying correction factors to the discharge which are determined from experimental research.

4. Using experimental research to assess the apparent shear force on the assumed subdivision boundary. The discharge is then estimated by incorporating the apparent shear stress in the external force balance required for uniform flow in the main channel and floodplain sub-areas.

5. Using turbulence models to predict the lateral spread of the interaction zone in the compound channel resulting in the determination of the lateral velocity profile.

In the absence of other information, the vertical divisions at the edge of the main channel are still the favoured technique because it is easy to apply and calculate and divides the zones in a practical way. It is used in many water surface profiles calculation packages. Lambert and Sellin (Lambert and Sellin, 1996a) illustrate the use of (Point no. 5 above) and an approach for determining the interactions between the different regions.

## 2.5.7.1. Flow in Non-Straight and Meandering Compound Channels

While this section has dealt primarily with the flow in straight and uniform channels not all natural channels can be modelled in this manner and additional parameters may become important in the determination of the stage-discharge relationship.

### 2.5.7.1.1. The Effect of Skewness on Flow in Compound Channels

Experimental work by Elliot and Sellin (1990) showed that skewing of the main channel relative to the floodplains by only 5° to 10° was enough to introduce some deviation in the stage-discharge relationship that would be expected for a similar straight channel. They also found that the region of maximum velocity is shifted in the direction of the cross-flow and that the secondary currents appeared to be stronger and more complex than in a straight compound channel. Additionally, a strong peak in the boundary shear stress distribution occurred where the cross-flow left the main channel and moved onto the floodplain. This situation common with meandering streams where the floodplain switches sides of the main channel.

### 2.5.7.1.2. Meandering Compound Channels

The earliest report on the effect of main channel sinuosity on the stage-discharge relationship in a compound channel appears to be by Lipscomb (1956). Lipscomb concluded that an increase in sinuosity results in a decrease in discharge.

Similar experiments by Toebes and Sooky (1966) concluded that energy losses in the model depended on both the Reynolds number and Froude number and that energy losses per unit length for the meandering channel were up to 2.5 times as large as those for a uniform channel of the same hydraulic radius and discharge. The work was extended by James and Brown (1977) who also found that with increasing sinuosity, the resistance to flow increases and the velocity profiles become more distorted.

Smith (1978) carried out an experimental investigation into the effect of channel meanders on flood stage. In this investigation, he compared the stage-discharge relationship of a meandering compound channel to the stage-discharge relationship of the floodplain alone where the main channel was filled in and sealed with cement mortar. In doing this Smith found that at high stages the floodplain without the main channel had a larger discharge capacity than the combined meandering main channel and floodplain system. This demonstrated, for this channel geometry, that at high stages (Dr > 0.41) the addition of a main channel did not contribute to the discharge capacity, on the contrary, it decreased the discharge capacity. At lower relative depths this was not the case but the meandering compound channel still showed evidence of the interaction between the main channel and the floodplain.

Rajaratnam and Ahmadi (1983) undertook experiments on a curved main channel constructed inside a tilting rectangular channel 1.2 m wide and 18 m long. Rajaratnam and Ahmadi (1983) considered two relative depths $\left(\frac{H-h}{H}\right)$, one equal to 0.37 and the other equal to 0.45. From this work Rajaratnam and Ahmadi (1983) concluded:

1. The main channel was not exclusively the location of the highest velocities in the section.

2. The maximum velocity filament (also observed by Toebes and Sooky (1966)) tended to roughly follow the inner side walls of the main channel.

3. For the floodplain flow the velocity varied continuously with distance above the floodplain whereas the main channel velocity remained almost constant with distance above the floodplain level.

More recently, interest in meandering compound channels has provided the impetus for more detailed experimental studies. One of these studies followed the Series A experiments (Knight and Sellin, 1987) on straight compound channels at the SERC-Flood Channel

Facility at HR Wallingford. Details of this experimental program (Series B) can be found in Greenhill (1992) and Sellin et al. (1993). A consequence of this experimental work was the commissioning of HR Wallingford to undertake the production of a hydraulic manual for discharge assessment in meandering compound channels. This manual (Wallingford, 1992) is intended to provide engineers with a more accurate method of estimating the stage-discharge relationships in meandering compound channels. The method is based mainly on the SERC-Flood Channel Facility data on meandering compound channels but also includes other suitable data sources.

Subsequently, a more detailed record of this study was published by James and Wark (1992) which considered both in-bank and overbank flows. For in-bank flow conditions, a modification of an existing method (U.S. Department of Agriculture, 1963) was found to give satisfactory results. For overbank flow, a new approach was adopted which quantified the loss mechanisms which occur in meandering compound channels. The new method splits the flow into four flow zones:

• the inner channel below the bankfull level (1)

• The floodplain within the meander belt (2).

• The floodplains either side of the inner channel and outside the meander belt (3-4).

and then adopts an empirical approach but using, where possible, parameter groups to represent the known flow mechanisms in each zone. The discharge is then calculated as the sum of the zonal discharges. It should be noted however that this approach is similar to that suggested by Ervine and Ellis (1987).

The increased use of 2D flood models now provides much more flexibility to capture the complex nature of these flows and how they vary across the cross-section than previously existed with 1D approaches. However, it should be remembered that meandering compound channels flow can be highly three-dimensional in nature, particularly at the cross-over if the floodplain switches sides of the main channel and water must flow across the main channel to get to the downstream floodplain as shown in Lambert and Sellin (Lambert and Sellin, 1996b). The assumptions that form the basis of the depth-averaged 2D approaches break down in this case and these assumptions need to be checked.

## 2.6. Classification of the 1D Backwater and Drawdown Water Surface Profiles

When the gradually varied flow equation is applied to a steady flow down a prismatic channel, it can be shown that there are 12 generic, gradually varying flow, water surface profiles (apart from uniform flow). These profiles can be classified according to (Fenton, 2007):

- 5 conditions which compare the normal depth ($y_o$) with the critical depth ($y_c$). This results in the classification of 5 bedslopes.

- 3 conditions which compare the actual depth (y) with the normal depth ($y_o$) and the critical depth ($y_c$). This results in 3 zones for the depth.

Table 6.2.4 contains the bedslope and depth classifications.

Table 6.2.4. Gradually varied flow classification system (modified from table on p35 of Fenton (2007))

| Bedslope Classification | | |
|---|---|---|
| S | steep | $y_o < y_c$ |
| C | critical | $y_o = y_c$ |
| M | mild | $y_o > y$ |
| H | horizontal ($S_o = 0$) | $y_o = y_c$ |
| A | adverse (($S_o < 0$) | $y_o$ does not exist |
| Depth Classification | | |
| Zone 1 | | $y > y_o$ and $y > y_c$ |
| Zone 2 | | y is between $y_o$ and $y_c$ |
| Zone 3 | | $y < y_o$ and $y < y_c$ |

The 12 gradually varied flow profiles are illustrated in Figure 6.2.19.

The 12 generic profiles are curves of increasing or decreasing curvature in either the downstream or upstream direction. When some simplifying assumptions are made ($IF^2$ <<1 and a linearisation about normal flow depth using a Taylor series has been employed), it has been shown that the departure of the actual depth (y) from the normal flow depth ($y_0$) follows an exponential variation in space (Samuels, 1989; Fenton, 2007); this is of the form $y - y_o \sim e^{-dS_f / d_x x}$ provided IF << 1 and where $S_r$ can be found from the Manning or Chezy equation.

A consequence of the nature of thewater surface profiles is that any errors introduced during a backwater computation tend to be systematic. As the computations proceed in one direction (be it downstream or upstream), the flow curvature continuously increases or decreases.

All the water surface profiles schematised in Figure 6.2.19 can be classified as a backwater curve or a drawdown curve:

- backwater curve - the flow depths continuously increase in the downstream direction; the flow is one of deceleration.
- drawdown curve - the flow depths continuously decrease in the downstream direction; the flow is one of acceleration.

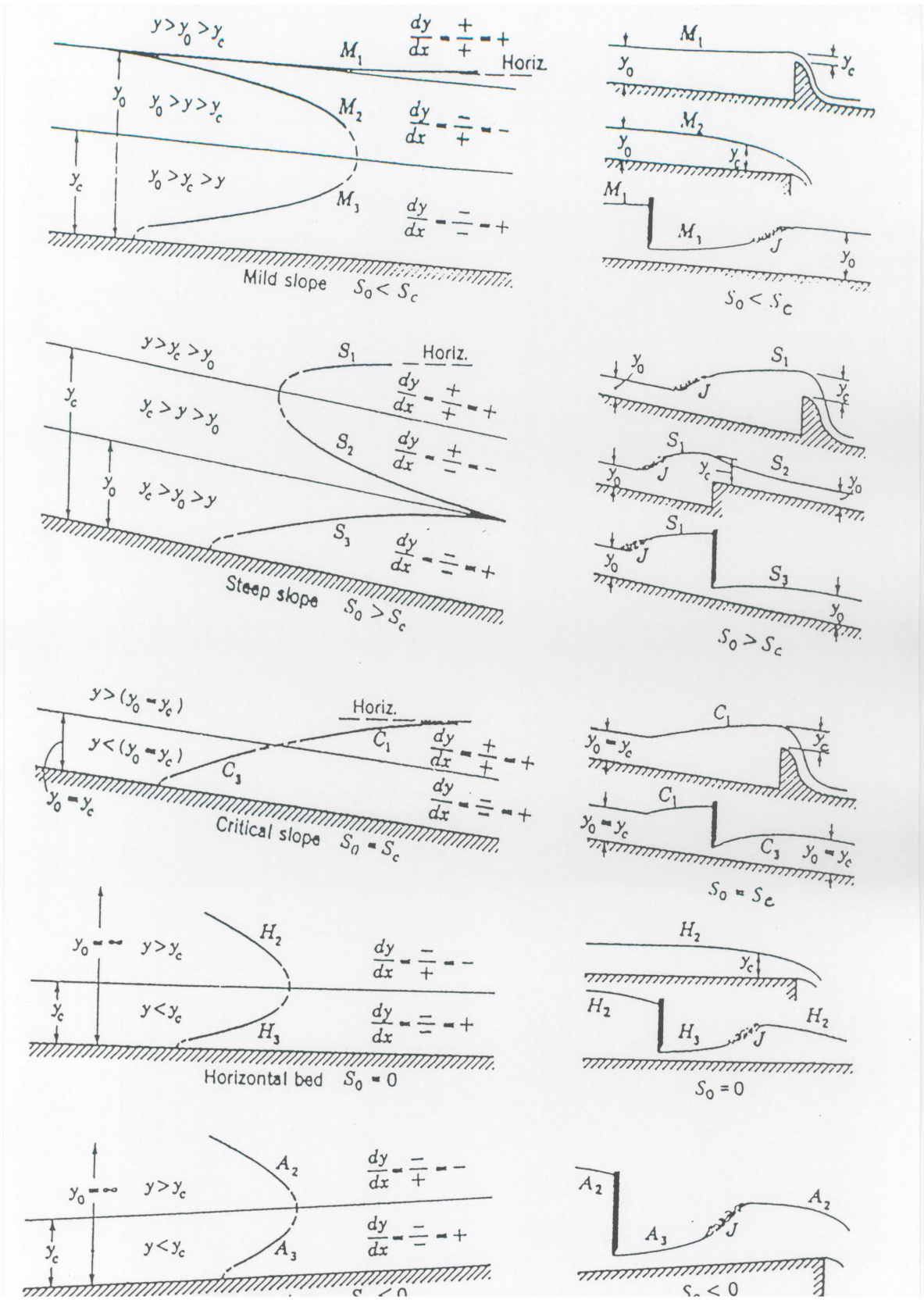




Figure 6.2.19. Drawdown Water Surfaces

## 2.7. Methods for Calculating Steady State Backwater and Drawdown Curves

Irrespective of whether steady-state flows are subcritical or supercritical, there are two well known methods for calculating the water surface profiles, be they (i) backwater curves or (ii) drawdown curves. In backwater profiles, the water surface deepens in the downstream direction and such flows are decelerating flows. In drawdown profiles, the water depths become shallower in the downstream direction and the flows are accelerating flows.

The two main numerical techniques for calculating steady water surface profiles are:

- the direct step method, and
- the standard step method.

A brief comparison of the two methods can be seen in Table 6.2.5.

Table 6.2.5. Comparison of the direct step and standard step methods

| | Direct Step Method | Standard Step Method |
|---|---|---|
| Governing Equation | $\frac{\delta E}{\delta x} = S_o - S_f$ | $\frac{\partial y}{\partial x} = \frac{S_o - S_f}{1 - Fr^2}$ |
| Unknowns | Find location x for a specified depth y | Find depth y at a specified location x |
| Solution | Explicit equation - no iteration needed | Implicit equation - iteration needed |
| Restrictions | • prismatic channels<br>• hydrostatic pressures<br>• calculate upstream for Fr < 1<br>• calculate downstream for Fr < 1 | • channels of general cross-section<br>• hydrostatic pressures<br>• calculate upstream for Fr < 1<br>• calculate downstream for Fr < 1 |

Since the direct step and other direct integration methods are based on a first order differential equation, a single boundary condition is required to initiate the computations. Suitable boundary conditions could be near (but not at) a control where the water level is known or can be approximated, or any location, reasonably well removed from any regions of rapidly varying flow, where the water level is known.

If the flow is subcritical, the flow is controlled from the downstream end and computations should advance in the upstream direction. On the other hand, for supercritical flows, the flow is controlled from the upstream end and computations should proceed in the downstream direction (McBean and Perkins, 1975; McBean and Perkins, 1970). If these guidelines regarding the direction of the solution procedure are not observed, it has been stated (McBean and Perkins, 1975; McBean and Perkins, 1970) that the calculations will eventually depart from the true solution. This rule-of-thumb is not without contention. There is some evidence which suggests that if an implicit finite difference method is employed to solve the governing equations, then the direction of computation is immaterial (Samuels and Chawdhary, 1992).

## 2.7.1. Direct Step Method for Calculating Backwater and Drawdown Curves

In the direct step method for calculating steady state, gradually varying flow profiles, the distance between two sections with specified depths is calculated.

The direct step method of calculating gradually varied flow profiles is only applicable to prismatic channels (which are more commonly manmade than natural). In this method, the flow depths at those sections where computations are to be carried out along the waterway are known (or specified) in advance. The (specified) depth increments or decrements between these sections need not be constant. With the depths (y) along the waterway known, the direct step method enables the distances between these sections (Δx) to be calculated directly without the need for iteration or trial and error. The governing equation is the first order ordinary differential equation:

$$\frac{\partial E}{\partial x} = S_o - S_f \tag{6.2.36}$$

$$E = y + \frac{v^2}{2g} \tag{6.2.37}$$

= specific head or specific energy (m) x = co-ordinate in downstream direction (m)

It is conventional to choose the x−coordinate such that it increases in the downstream direction, irrespective of whether the flow is subcritical or supercritical. When Equation (6.2.36) is recast in a finite difference form, Equation (6.2.36) becomes:

$$\frac{E_2 - E_1}{\Delta x} = S_o - S_f \tag{6.2.38}$$

$$\Rightarrow \Delta x = \frac{E_2 - E_1}{S_o - S_f} \tag{6.2.39}$$

where. . . 1, 2 = spatial indices which increase in the downstream direction

$$\Delta x = x_2 - x_1 \tag{6.2.40}$$

$$(\text{bedslope})\ S_0 = -\frac{\partial z}{\partial x} \tag{6.2.41}$$

$$(\text{friction slope})\ S_f = \frac{(nv)^2}{R_h^{4/3}} \tag{6.2.42}$$

n is the Manning roughness parameter

$S_f$ is the average friction slope over the elemental reach Δx

$$= \frac{\left(S_{f1} + S_{f2}\right)}{2} \tag{6.2.43}$$

$S_{f\,1}$ = friction slope at Section 1

$S_{f\,2}$ = friction slope at Section 2

The reason that the direct step method is only applicable to prismatic channels is that the unknown in Equation (6.2.39) is Δx. In the case of a subcritical flow, the computations proceed in the upstream direction; while $x_2$ will be known (or specified), $x_1$ will be unknown. Unless the section properties at $x_1$ are known, the computation of the specific energy and friction slope at this location cannot (in principle) proceed. The requirement imposed by the direct step method is therefore that the channel be prismatic.

Since the direct step method is explicit, no iteration is needed. The solution of Equation (6.2.39) is straightforward and easily executed in tabular form on a spreadsheet.

## 2.7.2. Standard Step Method for Calculating Backwater and Drawdown Curves

The standard step method is more versatile than the direct step method in that it can be applied to irregular (usually natural) channels i.e. channels with cross-sections which are changing along the length of the waterway. The relevant equations for the standard step method are based on the definition for the total head, the difference in head between two sections separated by a horizontal distance Δx, and an expression for the friction slope based on the Manning (or Chezy or Colebrook-White) equation.

Figure 6.2.20 contains a definition diagram for calculating the gradually varying flow water surface profile for a subcritical flow.

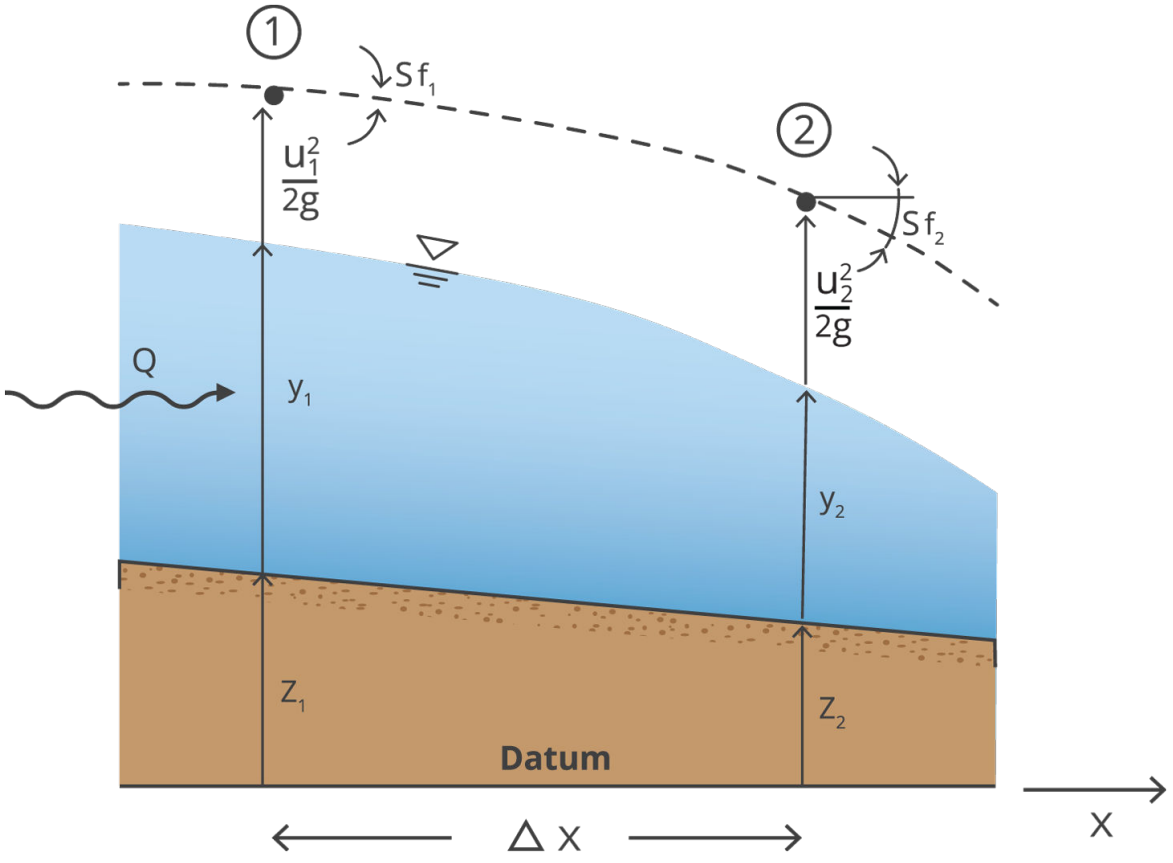


Figure 6.2.20. Lateral inflow

In the standard step method, the aim is to satisfy the two expressions below (Equation (6.2.44) and Equation (6.2.45)), and this will only happen when the correct unknown depth

$y_1$ has been determined. The depth $y_2$ is known for sub-critical flow (reversed for sueprcritical flow). Because the unknown depth $y_1$ is needed for the flow area $A_1$ and the friction slope $S_{f1}$, a trial and error process or some other iterative technique is needed to arrive at a solution.

$$H_1 = y_1 + z_1 + \frac{Q^2}{2gA_1^2} \tag{6.2.44}$$

$$H_1 = H_2 + \Delta x \frac{\left(S_{f1} + S_{f2}\right)^2}{2} \tag{6.2.45}$$

$$\text{where...}\ S_f = \frac{(nQ)^2}{A^2 R_h^{4/3}} \tag{6.2.46}$$

If the Newton-Raphson technique is applied to $H_E$ = the difference in $H_1$ as given by Equation (6.2.44) less that from Equation (6.2.45), the solution process can be speeded up:

$$(y_1)^{now} = (y_1)^{old} - \frac{H_E}{1 - IF_1^2 + \frac{\Delta x}{y_1}\left(1 + \frac{2Rh_1}{3y_1}\right)S_{f1}} \tag{6.2.47}$$

$$(\text{for a wide channel with } \mathrm{Rh}_1 \approx y_1) \approx (y_1)^{old} - \frac{H_E}{1 - IF_1^2 + \frac{5}{3}\left(1 + \frac{\Delta x}{y_1}\right)S_{f1}} \tag{6.2.48}$$

where. . . $H_E$ = error or difference between the two values of $H_1$ in Equation (6.2.44) and Equation (6.2.45)

$$= \left[y_1 + z_1 + \frac{Q^2}{2gA_1^2}\right] - \left[H_2 + \Delta x \frac{\left(S_{f1} + S_{f2}\right)}{2}\right] \tag{6.2.49}$$

$(y_1)^{old}$ = previous value of $y_1$

$(y_1)^{new}$ = new value of $y_1$ after iteration

In the case of a supercritical flow, the equations above would need to be modified with the unknown being $y_2$.

## 2.7.3. Averaging Required in Water Surface Profile Calculations

Because Equation (6.2.36) is an ordinary differential equation, they are a point relation which holds at all points in the 1D continuum. When these equations are discretised using (say) a finite difference method, the resulting equations span a small elemental reach of length Δx as shown in Equation (6.2.38) which contains non-linear terms that are discretised using a finite difference method, that in both cases, there are some non-linear terms which require representation over the length of the elemental reach Δx. Various methods have been adopted to provide these approximations, and four versions are identified below with respect to the friction slope $S_f$ at sections j and (j + 1).

$$(\text{average conveyance})\ \left(\overline{S_f}\right)_K = \left[\frac{Q}{K}\right]^2 \tag{6.2.50}$$

$$\text{(arithmetic mean)}\ \left(\overline{S_f}\right)_a = \frac{1}{2}\left[\left(S_f\right)_1 + \left(S_f\right)_2\right] \tag{6.2.51}$$

$$\text{(geometric mean)}\ \left(\overline{S_f}\right)_g = \sqrt{\left(S_f\right)_1\left(S_f\right)_2} \tag{6.2.52}$$

$$\text{(harmonic mean)}\ \left(\overline{S_f}\right)_h = \frac{1}{\frac{1}{2}\left[\left(S_f\right)_1 + \left(S_f\right)_2\right]} \tag{6.2.53}$$

$$\text{where...}\ \bar{v} = \frac{1}{2}\left(v_1 + v_2\right) \tag{6.2.54}$$

$Q = K.S^{1/2}$

K = conveyance

$K = 1/2\ (K_1 + K_2)$

The four averages listed above vary systematically (Laurenson (1986)) so that:

$\left(\overline{S_f}\right)_a > \left(\overline{S_f}\right)_g > \left(\overline{S_f}\right)_K > \left(\overline{S_f}\right)_h$

In addition to the above averages, there are many other equations which average reach-end parameters A, P, Rh by arithmetic, geometric or harmonic methods, but the averaged friction slope values have all been found to lie between the two extremes given by $\left(\overline{S_f}\right)_a$ and $\left(\overline{S_f}\right)_h$ (Cahdderton and Miller, 1980).

The effect of using the various estimates for the average friction slope have been explored by various investigators. Laurenson's conclusion (Laurenson, 1986) was that the best single method of averaging appears to be the arithmetic average of reach-end friction slopes, especially if this method is used in concert with the selection of representative cross-sections of the channel.

# 2.8. One Dimensional Unsteady Flow Equations

The governing equations for free surface flow are based on considerations of mass, momentum and energy. There are various combinations of dependent variables which are used, e.g. stage and flow; depth and flow; flow area and flow; depth and (cross-sectional averaged) velocity; and stage and velocity. Moreover, the equations can be expressed in conservation form or nonconservation form. The factors above give rise to different forms of the governing equations. Several of these forms are listed below.

It should be noted that the various forms of the equations below are not equivalent and some forms may be preferred over others due to:

- conservation vs non-conservation (i.e. divergent) form,
- choice of variables may be more accurate than others (Cunge et al., 1980), or
- if there are discontinuous solutions (Cunge et al., 1980).

By considering unsteady flow in an open channel through the following control volume shown in Figure 6.2.21 below:

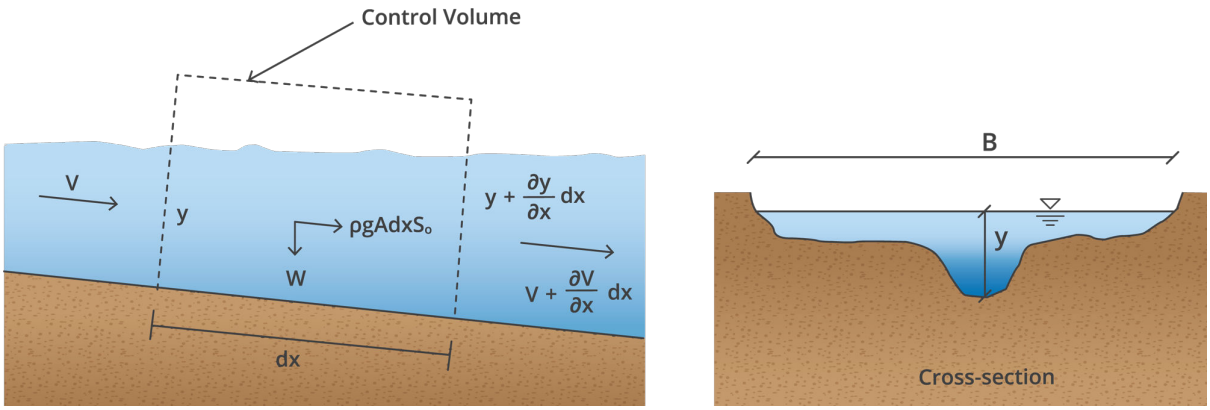


Figure 6.2.21. Control volume used to derive the gradually varying unsteady flow equations

In dealing with the control volume it has been assumed that the flow is incompressible, one dimensional and that the streamlines are straight and parallel. It has also been assumed that the slope of the channel is small, so that $\sin\theta \approx S_0$ and that there is no lateral inflow. Additionally, it has been assumed that the geometry of the channel does not change with time.

## 2.8.1. Derivation of the Continuity Equation for Gradually Varied Unsteady Flow in an Open Channel

For the control volume shown in Figure 6.2.21 the continuity equation can be derived using Equation (6.2.55) where *M* is the mass of the system of particles instantaneously occupying the control volume.

$$\frac{dM}{dt} = \frac{\partial}{\partial t}\int_{c\vartheta}\rho d\vartheta + \int_{c\vartheta}\rho\tilde{v}\tilde{d}A \tag{6.2.55}$$

where $\tilde{v}$ is the velocity vector, $\tilde{d}A$ is a vector with a magnitude equal to dA in a direction normal to the elemental area, $\rho$ is the fluid density, t is time. Applying the above equation to the control volume shown in Figure 6.2.21 and evaluating the integrals yields:

$$\frac{dM}{dt} = \frac{\partial}{\partial t}\rho dx + \rho\left(V + \frac{\partial V}{\partial x}\partial x\right)\left(A + \frac{\partial A}{\partial x}\partial x\right) - \rho VA \tag{6.2.56}$$

Expanding Equation (6.2.56), ignoring second order terms and dividing by $\rho$dx produces the Unsteady Continuity Equation.

$$\frac{\partial A}{\partial t} + u\frac{\partial A}{\partial x} + A\frac{\partial u}{\partial x} = 0 \tag{6.2.57}$$

where *A* is the cross-sectional area, *U* is the average velocity, *t* is time and *x* is the longitudinal distance along the channel.

## 2.8.2. Derivation of the Momentum Equation for Gradually Varied Unsteady Flow in an Open Channel

Application of Reynolds Transport Theorem to the control volume shown in Figure 6.2.21 for the momentum in the x-direction yields the one-dimensional unsteady momentum equation for open channel flow:

$$\sum F_x = \frac{\partial}{\partial t}\int_{c\vartheta} \rho v_x d\vartheta + \int_{c\vartheta} \rho v_x \tilde{v} \tilde{d}A = 0 \tag{6.2.58}$$

where $\sum F_x$ is the sum of the external forces acting in the x-direction on the control volume in Figure 6.2.21 and $v_x$ is the velocity in the x-direction. By considering all the external forces acting on the system and evaluating the volume and surface integral terms on the right side of Equation (6.2.58) yields:

$$\rho g A dx S_0 - \rho g \frac{\partial y}{\partial x} dx A - \tau_o P dx = \frac{\partial}{\partial t}(AV)\rho dx + \frac{\partial}{\partial t}\left(\beta \rho A V^2\right) dx \tag{6.2.59}$$

where $\beta$ is the momentum correction coefficient. By dividing by $\rho g A dx$ and expanding the derivative terms on the right-hand side, Equation (6.2.59) produces:

$$S_0 - \frac{\partial y}{\partial x} - \frac{\tau_o P}{\rho g A} = \frac{1}{gA}\left(A\frac{\partial V}{\partial t} + V\frac{\partial A}{\partial t} + \beta \frac{\partial}{\partial t}\left(AV^2\right) + AV^2 \frac{\partial \beta}{\partial t}\right) \tag{6.2.60}$$

However, many of the individual terms in Equation (6.2.60) can be replaced by more convenient forms. For example:

$$\frac{\partial y}{\partial x} = \frac{1}{T}\frac{\partial A}{\partial x} \tag{6.2.61}$$

$$\frac{\partial \beta}{\partial x} = \frac{\partial \beta}{\partial y}\frac{\partial y}{\partial x} = \frac{1}{T}\frac{\partial \beta}{\partial y}\frac{\partial A}{\partial x} \tag{6.2.62}$$

and

$$\frac{\partial}{\partial x}\left(AV^2\right) = V^2\frac{\partial A}{\partial x} + 2AV\frac{\partial V}{\partial x} = V\left(V\frac{\partial A}{\partial x} + A\frac{\partial V}{\partial x}\right) + AV\frac{\partial V}{\partial x} \tag{6.2.63}$$

$$V\frac{\partial A}{\partial x} = \beta V\frac{\partial A}{\partial t} + (1-\beta)V\frac{\partial A}{\partial t} \tag{6.2.64}$$

Equation (6.2.60) can be rearranged after substitution of Equation (6.2.61) to Equation (6.2.64) and $S_f$ for the friction slope to give Equation (6.2.65) below:

$$S_0 - \frac{1}{T}\frac{\partial A}{\partial t} - S_f = \frac{1}{gA}\left(A\frac{\partial V}{\partial t} + (1-\beta)V\frac{\partial A}{\partial t} + \beta V\left(\frac{\partial A}{\partial t} + V\frac{\partial A}{\partial x} + A\frac{\partial V}{\partial x}\right) + \beta AV\frac{\partial V}{\partial x} + \frac{AV^2}{T}\frac{\partial \beta}{\partial y}\frac{\partial A}{\partial x}\right) \tag{6.2.65}$$

The continuity equation (Equation (6.2.57)) can now be used to eliminate the third term on the right-hand side giving the Unsteady Momentum Equation.

$$S_0 - \frac{1}{T}\frac{\partial A}{\partial t} - S_f = \frac{1}{g}\frac{\partial V}{\partial t} + \frac{(1-\beta)}{gA}V\frac{\partial A}{\partial x} + \frac{\beta V}{g}\frac{\partial V}{\partial x} + \frac{V^2}{gT}\frac{\partial \beta}{\partial y}\frac{\partial A}{\partial x} \tag{6.2.66}$$

where $S_f$ is the friction slope, $S_o$ is the longitudinal bed slope, $V$ is the mean cross-sectional velocity, $A$ is the cross-sectional area, $T$ is the channel top width, $g$ is the gravitational acceleration, $t$ is time and $x$ is the distance in the direction of flow. This partial differential equation is the unsteady momentum equation for flow in open channels and includes the momentum correction factor (b) to account for a non-uniform distribution of velocity in the cross-section. Equation (6.2.66) is a more general form of the Saint-Venant equation. It was

Boussinesq in 1877 who first incorporated correction coefficients for the velocity distribution in the momentum equation. While he originally proposed three coefficients only one (b) is used in modern literature and is given by Chow (1959) as:

$$\beta = \frac{\int u^2 dA}{V^2 A} \tag{6.2.67}$$

where u is the local velocity through the elemental area *dA*, *A* is the cross-sectional area, and *V* is the mean velocity.

## 2.8.3. Why is the time step so important?

Often these equations are solved using finite difference, finite element or more commonly now finite volume methods. As these are a hyperbolic system of partial differential equations, very similar to the wave equations consideration must be given to the time step that is used in the computational scheme for both computational stability and more importantly for computational accuracy. While this is sometimes controlled automatically to maintain accuracy it is worth understanding the importance of the time step.

The unsteady momentum equation can be converted into a total differential equation using the method of characteristics. While the steady form of the momentum equation can be obtained from Equation (6.2.66) the transformation to a system of total differential equations will be carried out for later use.

The method of characteristics allows two partial differential equations to be combined using an unknown multiplier ($\lambda_m$) as shown below in Equation (6.2.68). For any two real and distinct values of $\lambda_m$ two equations in *V* and *A* are obtained that contain the properties of the original two equations $L_1$ and $L_2$ and may replace them in any solution.

$$L = L_1 + \lambda_m L_2 = 0 \tag{6.2.68}$$

where $L_1$ and $L_2$ are equal to the unsteady momentum function (Equation (6.2.66)) and continuity relation (Equation (6.2.57)) respectively as shown below:

$$L_1 = \frac{1}{g}\frac{\partial V}{\partial t} + \frac{(1-\beta)}{gA}V\frac{\partial A}{\partial t} + \frac{\beta V}{g}\frac{\partial V}{\partial x} + \frac{1}{T}\left(1 + \frac{V^2}{g}\frac{\partial \beta}{\partial y}\right)\frac{\partial A}{\partial x} + S_f - S_0 \tag{6.2.69}$$

$$L_2 = \frac{\partial A}{\partial t} + V\frac{\partial A}{\partial x} + A\frac{\partial V}{\partial x} \tag{6.2.70}$$

Substituting Equation (6.2.69) and Equation (6.2.70) into Equation (6.2.68) yields:

$$\frac{1}{g}\frac{\partial V}{\partial t} + \frac{(1-\beta)}{gA}V\frac{\partial A}{\partial t} + \frac{\beta V}{g}\frac{\partial V}{\partial x} + \frac{1}{T}\left(1 + \frac{V^2}{g}\frac{\partial \beta}{\partial y}\right)\frac{\partial A}{\partial x} + S_f - S_0 + \lambda_m\frac{\partial A}{\partial t} + \lambda_m V\frac{\partial A}{\partial x} + \lambda_m A\frac{\partial V}{\partial x} \tag{6.2.71}$$

If Equation (6.2.71) is rearranged by collecting separately the derivatives of velocity and area then:

$$\frac{1}{g}\left[(\beta V+\lambda_m gA)\frac{\partial V}{\partial x}+\frac{\partial V}{\partial t}\right]+\lambda_m\left[V+\frac{1}{\lambda_m T}\left(1+\frac{V^2}{g}\frac{\partial \beta}{\partial y}\right)\frac{\partial A}{\partial x}+\left(\frac{(1-\beta)V}{\lambda_m gA}\right)\frac{\partial A}{\partial t}\right]+S_f - S_0=0 \tag{6.2.72}$$

The total derivatives of *V*, *A* with respect to *t* are:

$$\frac{dV}{dt}=\frac{\partial V}{\partial t}+\frac{\partial V}{\partial x}\frac{dx}{dt}\ and\ \frac{dA}{dt}=\frac{\partial A}{\partial t}+\frac{\partial A}{\partial x}\frac{dx}{dt} \tag{6.2.73}$$

Equation (6.2.72) is therefore modified to:

$$\frac{1}{g}\left[(\beta V+\lambda_m gA)\frac{\partial V}{\partial x}+\frac{\partial V}{\partial t}\right]+\left(\lambda_m+\frac{(1-\beta)V}{gA}\right)\left[\left(V+\frac{1}{\lambda_m T}\left(1+\frac{V^2}{g}\frac{\partial \beta}{\partial y}\right)\right)\left(\frac{\lambda_m gA}{\lambda_m gA+(1-\beta)V}\right)\frac{\partial A}{\partial x}+\frac{\partial A}{\partial t}\right]+S_f-S_0=0 \tag{6.2.74}$$

This leads to the following total differential equations by equating Equation (6.2.73) with Equation (6.2.74).

$$\frac{1}{g}\frac{dV}{dt}+\left(\lambda_m+\frac{(1-\beta)V}{gA}\right)\frac{dA}{t}+S_f-S_0=0 \tag{6.2.75}$$

$$\frac{dx}{dt}=(\beta V+\lambda_m gA)=\frac{\lambda_m gA\left(V+\frac{1}{\lambda_m T}\left(1+\frac{v^2}{g}\frac{\partial \beta}{\partial y}\right)\right)}{\lambda_m gA+(1-\beta)V} \tag{6.2.76}$$

Now solving for $\lambda_m$ in Equation (6.2.76) to produce equal values of the term associated with both the velocity and area derivatives produces:

$$(\lambda_m gA+(1-\beta)V)(\beta V+\lambda_m gA)=\lambda_m gA\left(V+\frac{1}{\lambda_m T}+\frac{V^2}{g}\frac{\partial \beta}{\partial y}\right) \tag{6.2.77}$$

Expanding Equation (6.2.77) yields a quadratic equation in $\lambda_m$:

$$\lambda_m \beta A+\lambda_m^2 g^2 A^2+(1-\beta)\beta V^2+\lambda_m gA(1-\beta)V=\lambda_m gAV+\frac{gA}{T}+V^2\frac{A}{T}\frac{\partial \beta}{\partial y} \tag{6.2.78}$$

Collecting and cancelling terms in Equation (6.2.78) results in the following solution for $\lambda_m$ given in Equation (6.2.79):

$$(\lambda_m gA)^2=\frac{gA}{T}-\beta(1-\beta)V^2+\frac{V^2A}{T}\frac{\partial \beta}{\partial y} \tag{6.2.79}$$

$$\lambda_m gA=\pm\sqrt{\frac{gA}{T}-\beta(1-\beta)V^2+\frac{V^2A}{T}\frac{\partial \beta}{\partial y}} \tag{6.2.80}$$

$$\lambda_m gA=\pm\sqrt{\frac{gA}{T}+\beta V^2-V^2\beta+V^2\frac{A}{T}\frac{\partial \beta}{\partial y}} \tag{6.2.81}$$

$$\lambda_m gA=\pm\sqrt{\frac{gA}{T}+\beta^2 V^2-V^2\beta+V^2\frac{A}{T}\frac{\partial \beta}{\partial y}} \tag{6.2.82}$$

The method of characteristics when applied to Equation (6.2.57) and Equation (6.2.66) transform these two partial differential equations into the following system of total differential equations.

$$\frac{1}{g}\frac{dV}{dt}+\frac{1}{gA}\left[(1-\beta)V\pm\sqrt{\frac{gA}{T}+\beta^2V^2-V^2\beta+V^2\frac{A}{T}\frac{\partial\beta}{\partial y}}\right]\frac{dA}{dt}+S_f-S_0 \tag{6.2.83}$$

and

$$\frac{dx}{dt}=\beta V\pm\sqrt{\frac{gA}{T}+\beta^2V^2-V^2\left(\beta-\frac{A}{T}\frac{\partial\beta}{\partial y}\right)}=\beta V\pm c_\beta \tag{6.2.84}$$

Or

$$\frac{1}{g}\frac{dV}{dt}+\frac{(1-\beta)V\pm c_\beta}{gA}\frac{dA}{dt}+S_f-S_0=0 \tag{6.2.85}$$

$$\frac{dx}{dt}=\beta V\pm c_\beta \tag{6.2.86}$$

where $c_\beta$ is the celerity of a small disturbance. When $\beta$ is set equal to unity (a common assumption) then $c_\beta=\sqrt{\frac{gA}{T}}$ for a non-rectangular section or for rectangular sections. The characteristic direction represents the direction along which a small disturbance travels is equal to the absolute wave velocity of a disturbance. The positive sign is used for the downstream direction, and the negative sign is used for the upstream direction. Referring to the Equation (6.2.84), *dx/dt* is positive for both alternatives of Equation (6.2.84) when the first term ( $\beta V$) on the right hand side of Equation (6.2.84) is greater than the square root term. This represents supercritical flow and the disturbances can only travel in the downstream direction. Similarly, *dx/dt*is negative for the upstream direction and positive for the downstream direction when the first term ($\beta V$) on the right hand side of Equation (6.2.84) is smaller than the square root term. This case represents subcritical flow and the disturbances travel in both upstream and downstream directions. For critical flow, both terms of Equation (6.2.84) are equal. This physically based criterion may be used to determine the occurrence of critical flow, since it shows whether the flow control is located at an upstream or downstream location. The Froude number, which is so important in determining the flow type (subcritical, supercritical, and critical) is the ratio of the first term on the right hand side of Equation (6.2.84) to the second term on the right hand side. In a rectangular open channel flow (where $\beta$ is usually set to unity) the Froude number becomes:

$$F=\frac{V}{\sqrt{gy}} \tag{6.2.87}$$

This relationship between space (dx) and time (dt) that results is termed the Courant number, and it seeks to ensure that the various disturbances or changes at one time level are captured appropriately at the next advanced time level. While some numerical schemes do not require this for stability, they will require it for accuracy. This is made even more important in 2D and 3D flow computations where the disturbances now need to be captured moving in the plane of the channel cross-section and not just along the channel.

## 2.8.4. Steady Flow Equations

The unsteady momentum equation (see Equation (6.2.66)) can be reduced to the steady form of the equation by eliminating the time derivative terms from Equation (6.2.88) as shown:

$$\frac{1}{g}\frac{V}{dt}+\frac{(1-\beta)}{gA}V\frac{\partial A}{\partial t}+\frac{\beta V}{g}\frac{\partial V}{\partial x}+\frac{V^2}{gT}\frac{d\beta}{dy}\frac{\partial A}{\partial x}+\frac{1}{T}\frac{\partial A}{\partial x}+S_f-S_0=0 \tag{6.2.88}$$

$$\frac{\beta V}{g}\frac{\partial V}{\partial x}\left[\frac{1}{T}+\frac{V^2}{gT}\frac{d\beta}{dy}\right]\frac{\partial A}{\partial x}+S_f-S_0=0 \tag{6.2.89}$$

Substituting $\frac{dV}{dx}$ for using the equation of continuity for steady flow:

$$\frac{dV}{dx}=\frac{-V}{A}\frac{dA}{dx} \tag{6.2.90}$$

and by letting:

$$\frac{dA}{dx}=\frac{dA}{dy}\frac{dy}{dx}=T\frac{dy}{dx} \tag{6.2.91}$$

an equation $\frac{dy}{dx}$ determining for steady gradually varied flow using the momentum approach (Equation (6.2.93)) is obtained by the substitution of Equation (6.2.90) and Equation (6.2.91) into Equation (6.2.88) and rearranging to give:

$$\frac{-\beta V^2T}{gA}\frac{dy}{dx}+\left(\frac{1}{T}+\frac{V^2}{gT}\frac{d\beta}{dy}\right)T\frac{dy}{dx}+S_f-S_0=0 \tag{6.2.92}$$

$$\frac{dy}{dx}=\frac{S_0-S_f}{1-\frac{V^2}{gT}\left(\beta-\frac{A}{T}\frac{d\beta}{dy}\right)} \tag{6.2.93}$$

Taking the momentum correction coefficient as being equal to unity then:

$$\frac{dy}{dx}=\frac{S_0-S_f}{1-\frac{V^2}{gT}}=\frac{S_0-S_f}{1-F^2} \tag{6.2.94}$$

Note Equation (6.2.93) includes the derivative of the momentum flux correction coefficient. Similarly for the unsteady energy equation (Equation (6.2.95)):

$$\frac{\beta}{g}\frac{\partial V}{\partial t}=\frac{V}{2g}\left(3\alpha+\beta-\frac{\beta' A}{T}\right)\frac{\partial V}{\partial x}+\frac{V^2}{2gA}\left(\alpha-\beta-\frac{\beta A'}{T}-\frac{A\alpha'}{T}\right)\frac{\partial A}{\partial x}+\frac{1}{T}\frac{\partial A}{\partial x}-S_0+S_e=0 \tag{6.2.95}$$

Eliminating the time derivative terms and substituting Equation (6.2.90) and Equation (6.2.91) provides an equation determining $\frac{dy}{dx}$ for steady gradually varied flow (Equation (6.2.98)) after some rearrangement as shown in Equation (6.2.96) and Equation (6.2.97).

$$\frac{3}{2}\frac{\alpha V}{g}\frac{dV}{dx}+\frac{1}{T}\frac{dA}{dx}+\left[\frac{\alpha V^2}{gA}+\frac{V^2}{gT}\frac{\partial A}{\partial y}\right]\frac{dA}{dx}+S_e-S_0=0 \tag{6.2.96}$$

$$\frac{dy}{dx}\left[1-\frac{V^2T}{gA}\left(\alpha-\frac{A}{2T}\frac{\partial A}{\partial y}\right)\right]=S_0-S_e \tag{6.2.97}$$

$$\frac{dy}{dx} = \frac{S_o - S_e}{1 - \frac{V^2 T}{gA}\left(\alpha - \frac{A}{2T}\frac{\partial \alpha}{\partial y}\right)} \tag{6.2.98}$$

Again taking the energy correction factor as unity :

$$\frac{dy}{dx} = \frac{S_0 - S_e}{1 - \frac{V^2 T}{gA}} = \frac{S_0 - S_e}{1 - F^2} \tag{6.2.99}$$

It should be noted that Equation (6.2.98) includes an additional term for the derivative of the kinetic energy correction coefficient, which is commonly neglected.

## 2.8.5. Simplifying from Gradually Varied to Steady Uniform Flow

In the case of steady uniform flow the depth and velocity are not changing with distance along the channel hence, $\frac{dy}{dx} = 0$. From Equation (6.2.94) and Equation (6.2.98) it can be seen that this only occurs when $S_0 = S_f = S_e$.

# 2.9. Numerical Modelling - Two Dimensional Models of Flood Flows

Fully 2D hydrodynamic models are based on the numerical solution of depth-averaged equations describing the conservation of mass and momentum in two horizontal dimensions *x* and *y*. In a form used by many of the commonly used 2D models, these equations can expressed in terms of three main dependent variables; ς*, u and v*, as shown in Figure 6.2.22.

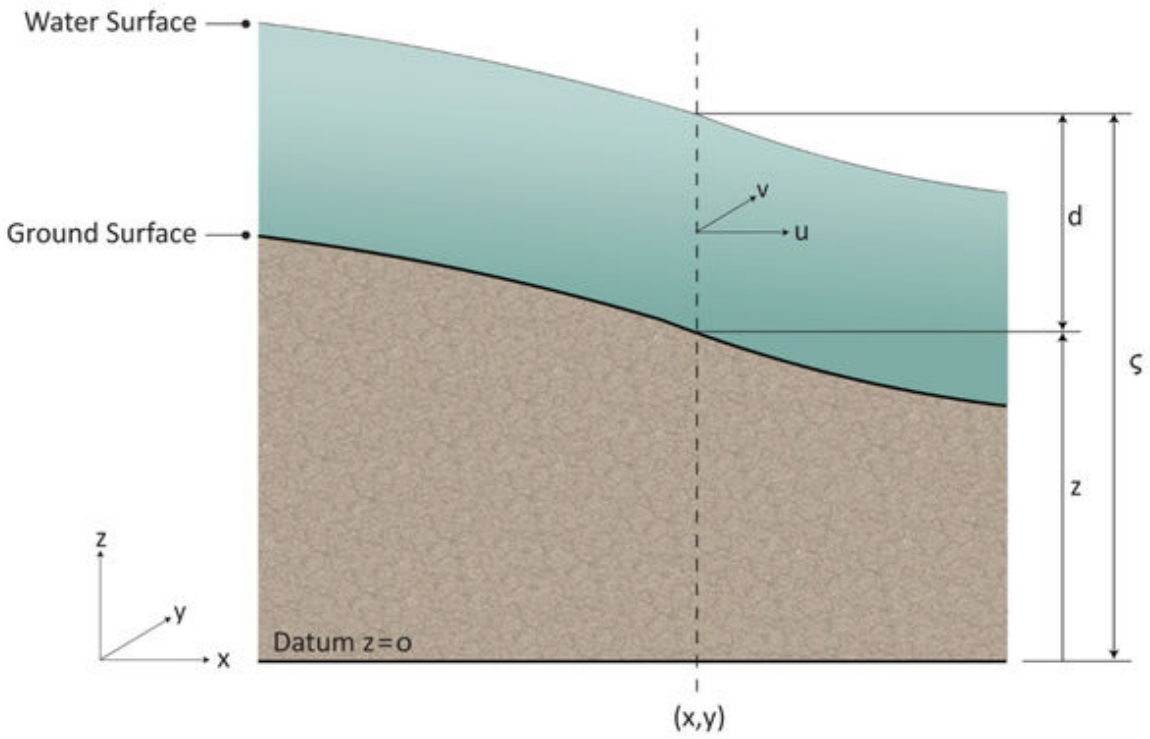


Figure 6.2.22. Definition of symbols

Where:

ς: is the water surface elevation relative to a fixed datum *(m).*

*u*: is the depth-averaged velocity in the *x* direction *(m/s)*

*v*: is the depth-averaged velocity in the *y* direction *(m/s)*

These are described as a function of the three main independent variables:

*x:* the horizontal distance in the x direction (*m*)

*y:* the horizontal distance in the y direction (*m*)

*t:* the time (*s*)

Additionally, the time varying water depth at any location *d(x,y),* can be expressed as:

where:

$$d = \varsigma - z \tag{6.2.100}$$

*z*: is the bed surface elevation relative to a fixed datum *(m).*

## 2.9.1. The Mass Equation

For flooding applications, water can be considered to be incompressible. As such, water volume can be used to represent the water mass. In terms of the variables described above, the depth-averaged equation describing the conservation of volume (and therefore mass) in two horizontal directions can be expressed as:

$$\frac{\partial \varsigma}{\partial t} + \frac{\partial (d.u)}{\partial x} + \frac{\partial (d.v)}{\partial y} = 0 \tag{6.2.101}$$

Where:

$\frac{\partial \varsigma}{\partial t}$ is the rate of increase (or decrease) in water level, which for a fixed cell size is representative of the rate of change of volume of water contained in the cell, and

$\frac{\partial (d.u)}{\partial x} + \frac{\partial (d.v)}{\partial y}$ is the spatial variation in inflow (or outflow) across the cell in the *x* and *y* directions.

Simply put, any increase (or decrease) in volume, must be balanced by a net inflow (or outflow) of water.

## 2.9.2. The Momentum Equations

In a similar form, the equations for describing the conservation of momentum in the *x* and *y* directions can be expressed as:

$$\frac{\partial u}{\partial t} + u\frac{\partial u}{\partial x} + v\frac{\partial u}{\partial y} + g\frac{\partial \varsigma}{\partial x} = 0 \tag{6.2.102}$$

$$\frac{\partial v}{\partial t} + v\frac{\partial v}{\partial y} + u\frac{\partial v}{\partial x} + g\frac{\partial \varsigma}{\partial y} = 0 \quad (6.2.103)$$

where:

*g:* is the acceleration due to gravity (m/s$^2$)

The equations presented above are in the primitive, Eulerian form. The same equations can exist in other forms; e.g. the conservation law form (Abbott, 1979) and the conservative-integral form (LeVeque, 2002).

Due to the symmetry between the two *x* and *y* momentum equations, further discussion will be focused on the x-momentum equation only.

$$\frac{\partial u}{\partial t} + u\frac{\partial u}{\partial x} + v\frac{\partial u}{\partial y} + g\frac{\partial \varsigma}{\partial x} = 0 \quad (6.2.104)$$

where:

$\frac{\partial u}{\partial t} + u\frac{\partial u}{\partial x} + v\frac{\partial u}{\partial y}$ is the partial differential form of the flow acceleration *du/dt*

$g\frac{\partial \varsigma}{\partial x}$ is the hydrostatic pressure gradient

It can be shown that the momentum equation is effectively an impulse/momentum equation, where the flow acceleration, that is, the rate of increase (or decrease) in momentum is balanced by the impulse of the hydrostatic pressure gradient.

## 2.9.3. Assumptions

In the derivation of these equations, it has been assumed that:

- The flow is incompressible,
- The pressure is hydrostatic (i.e. vertical accelerations can be neglected and the local pressure is dependent only on the local depth),
- The flow can be described by continuous (differentiable) functions of ς, *u* and *v* (that is, it does not include step changes in ς, *u* and *v),*The flow is two-dimensional (that is, the effects of vertical variations in the flow velocity can be neglected),
- The flow is nearly horizontal (that is, the average channel bed slope is small), and
- The effects of bed friction can be included through resistance laws (e.g., Manning equation) that have been derived for steady flow conditions.

Problems associated with accurate modelling of transport equations have been highlighted by Leonard (1979a). Simple first order schemes are inaccurate and diffusive, while second order schemes (that are good for solving wave propagation) tend to be oscillatory and unstable. This has lead to the use of more innovative approaches to modelling the convective momentum terms (Abbott and Rasmussen, 1977), and the use of higher third order solution schemes (Leonard, 1979b; Stelling, 1984).

# 2.10. Extension of the Equations for Modelling Applications

The 2D mass and momentum equations described in Book 6, Chapter 2, Section 9 and Book 6, Chapter 2, Section 9 are sometimes referred to as the 2D “long wave” equations. These equations can be used to describe the behaviour of waves, including flood waves, which are long relative to the water depth.

For practical modelling applications, these equations need to be expanded to include the additional effects of other phenomena of interest. The most important of these is probably the inclusion of the dissipative effects of bed-friction in the momentum equation. The inclusion of additional terms to form extended modelling equations is considered below.

## 2.10.1. Extension of the Mass Equation

For modelling applications, the mass equation can be expanded to include additional source and/or sink terms to allow for localised and/or distributed inflows and outflows, as follows:

$$\frac{\partial \varsigma}{\partial t} + \frac{\partial (d.u)}{\partial x} + \frac{\partial (d.v)}{\partial y} = \text{Sources-Sinks} \tag{6.2.105}$$

Where the Source terms can represent localised inflows such as may occur at stormwater or pump outlets, or distributed inflows associated with rainfall, and the Sink terms can represent localised outflows at drainage pits or pump intakes or distributed losses due to infiltration or, in long-term simulations the evaporation.

## 2.10.2. Extension of the Momentum Equations

For modelling applications, the extension of the momentum equations to include the effects of bed-friction, eddy viscosity and other source and sink terms is discussed below.

**Bed Friction**

For flood modelling applications, the momentum equation must be coupled with a suitable friction formulation. This is typically achieved by adding a Chezy-type friction term to the momentum equation, which then becomes:

$$\frac{\partial u}{\partial t} + u\frac{\partial u}{\partial x} + v\frac{\partial u}{\partial y} + g\frac{\partial \varsigma}{\partial x} = -\frac{gu\sqrt{u^2+v^2}}{C^2 d} \tag{6.2.106}$$

where:

*C:* is a Chezy roughness coefficient ($m^{1/2}s^{-1}$)

For practical modelling applications, the Chezy coefficient can be related to the more usual (for Australian applications) Manning ‘n’ *roughness coefficient* by the Strickler relation, where:

$$n = \frac{d^{\frac{1}{6}}}{C} \tag{6.2.107}$$

In some European models, the friction coefficient is sometimes specified in terms of Manning ‘M’, where:

$$n = \frac{1}{M} \tag{6.2.108}$$

**Eddy Viscosity**

Most commercially available 2D models also include an “eddy viscosity” type term to allow for the effects of sub-grid scale mixing processes. This can be important when modelling flow separations and eddies, or in situations where it is necessary to model channel/ overbank interactions.

Introducing a typical eddy viscosity formulation, the *x* momentum equation becomes:

$$\frac{\partial u}{\partial t} + u\frac{\partial u}{\partial x} + v\frac{\partial u}{\partial y} + g\frac{\partial \varsigma}{\partial x} = -\frac{gu\sqrt{u^2+v^2}}{C^2 d} + E\left(\frac{\partial^2 u}{\partial x^2} + \frac{\partial^2 u}{\partial y^2}\right) \tag{6.2.109}$$

where:

*E:* is an “eddy viscosity” coefficient ($m^2s^{-1}$)

If, for illustration purposes only, the hydrostatic pressure and friction terms are neglected, the *x* momentum equation can be rearranged to the form:

$$\frac{\partial u}{\partial t} + u\frac{\partial u}{\partial x} + v\frac{\partial u}{\partial y} - E\left(\frac{\partial^2 u}{\partial x^2} + \frac{\partial^2 u}{\partial y^2}\right) = 0 \tag{6.2.110}$$

This is analogous to a two-dimensional advection-diffusion equation describing the transport and diffusion of *u*, the *x* velocity component. Continuing the analogy, the eddy viscosity coefficient *E* becomes equivalent to the diffusion coefficient used in advection-diffusion modelling. Thus, as well as having wave propagation and transport properties the momentum equation can also have diffusion properties.

Eddy viscosity and its application to 2D flood models is discussed in more detail in Book 6, Chapter 4. It is noted, however, that for eddy viscosity calculations to be meaningful, the $u\frac{\partial u}{\partial x}$ and $v\frac{\partial u}{\partial y}$convective momentum terms must be modelled with sufficient accuracy.

**Other Terms**

The early 2D flood models were originally derived from 2D coastal and estuarine models. These models typically included additional terms to represent wind shear and Coriolis effects. When these terms are included, along with additional source/sink terms to allow for the addition or loss of momentum associated with any sources or sinks of mass, discussed above, the *x* momentum equation becomes:

$$\frac{\partial u}{\partial t} + u\frac{\partial u}{\partial x} + v\frac{\partial u}{\partial y} + g\frac{\partial \varsigma}{\partial x} = -\frac{gu\sqrt{u^2+v^2}}{C^2 d} + E\left(\frac{\partial^2 u}{\partial x^2} + \frac{\partial^2 u}{\partial y^2}\right) + fVV_x - \Omega u + \text{Source/Sink} \tag{6.2.111}$$

where:

*f* is a wind shear stress coefficient

*V* is the wind speed (m/s)

*Vx* is the component of the wind speed in the *x* direction (m/s)

*Ω* is a latitude dependent Coriolis parameter

The wind and Coriolis terms are only likely to become important in wide open floodplains or in lake or estuarine systems, and are not considered further in the present discussion.

## 2.10.3. Final Forms of the Equations

As developed above, the final forms of the mass and momentum equations used in many 2D flood models can be expressed as:

**Mass**

$$\frac{\partial \varsigma}{\partial t} + \frac{\partial (du)}{\partial x} + \frac{\partial (dy)}{\partial y} = \text{Sources - Sinks} \tag{6.2.112}$$

**x-Momentum**

$$\frac{\partial u}{\partial t} + u\frac{\partial u}{\partial x} + v\frac{\partial u}{\partial y} + g\frac{\partial \varsigma}{\partial x} = -\frac{gu\sqrt{u^2+v^2}}{C^2 d} + E\left(\frac{\partial^2 u}{\partial x^2} + \frac{\partial^2 u}{\partial y^2}\right) + \text{Source/Sink} \tag{6.2.113}$$

**y-Momentum**

$$\frac{\partial v}{\partial t} + V\frac{\partial v}{\partial y} + u\frac{\partial v}{\partial x} + g\frac{\partial \varsigma}{\partial y} = -\frac{gv\sqrt{u^2+v^2}}{C^2 d} + E\left(\frac{\partial^2 u}{\partial x^2} + \frac{\partial^2 u}{\partial y^2}\right) + \text{Source/Sink} \tag{6.2.114}$$

This coupled system of equations provides the three equations necessary to solve for the three dependent variables; ς the free surface elevation, *u* the velocity in the *x* direction and *v* the velocity in the *y* direction.

## 2.10.4. Modelling Requirements and Simplifications

The previous sections show that the combination of the mass and momentum equations can describe the wave propagation properties associated with a flood, and how the momentum equations include terms for describing the effects that advection and dispersion of momentum can have on the flow. The relative importance of these properties can vary significantly depending on the flow conditions. This has little impact on how the mass equation is treated, but in some cases can allow simplifying assumptions to be made in the treatment of the momentum equations.

### 2.10.4.1. The Mass Equation

For flood modelling applications, it is important that the solution procedure used in the model does not generate or destroy mass numerically. It is therefore essential that all the terms in the mass equation are described accurately in the numerical solution procedure.

With the staggered grids used by most finite difference models, there can be issues with achieving time and space centring of the non-linear spatial derivative terms. In this respect, it is noted that Stelling et al. (1998) presented a numerical scheme that conserves mass and maintains non-negative water levels. Nevertheless, modellers should be aware that any errors in the mass equation, however small, can accumulate with time as the computation progresses. If the mass equation is not modelled correctly, the error accumulation can continue to the extent that the final solution may be compromised.

## 2.10.4.2. The Momentum Equation

For the momentum equations, the relative importance of the different terms can vary quite significantly depending on the flow conditions. In some conditions it may be possible for simplifying assumptions to be made either to the equations themselves, or to the way in which individual terms are treated numerically. The types of simplifications used tend to be made for numerical expediency, or to avoid numerical problems with particular types of flow (e.g., supercritical flow). The extent to which they can be used is dependent upon the level of detail and/or accuracy required.

Ignoring wind, Coriolis and source/sink terms, the x-momentum equation developed above can be expressed as:

$$\frac{\partial u}{\partial t} + u\frac{\partial u}{\partial x} + v\frac{\partial u}{\partial y} + g\frac{\partial \varsigma}{\partial x} = -\frac{gu\sqrt{u^2+v^2}}{C^2 d} + E\left(\frac{\partial^2 u}{\partial x^2} + \frac{\partial^2 u}{\partial y^2}\right) \quad (6.2.115)$$

Using this as a base, some of the more commonly used approximations to the momentum equation are discussed below.

**The Linearised Momentum Equation**

With this approximation, the convective momentum (momentum transport) terms are neglected. When these terms are neglected, the eddy viscosity (momentum dispersion) terms have little physical meaning and can also be neglected. With this approach, the *x*-momentum equation reduces to:

$$\frac{\partial u}{\partial t} + g\frac{\partial \varsigma}{\partial x} = -\frac{gu\sqrt{u^2+v^2}}{C^2 d} \quad (6.2.116)$$

This approach should only be used in areas where the velocities are small, and the wave propagation properties of the flow are dominant. This rarely happens in most practical flood flow simulations. However, it is noted that the linearised momentum equation is sometimes used for numerical expediency in order to maintain stability in high velocity flow areas, including regions of supercritical flow. Although this approximation maintains the wave propagation properties of the full momentum equation, it cannot model momentum dominated effects, including flow separations and eddies, and main channel/overbank momentum transfers.

**The Steady State Momentum Equation**

With this approximation, the local acceleration term *δu/δt* is neglected and the *x*-momentum equation reduces to:

$$u\frac{\partial u}{\partial x} + v\frac{\partial u}{\partial y} + g\frac{\partial \varsigma}{\partial x} = -\frac{gu\sqrt{u^2+v^2}}{C^2 d} + E\left(\frac{\partial^2 u}{\partial x^2} + \frac{\partial^2 u}{\partial y^2}\right) \quad (6.2.117)$$

This approximation neglects the wave propagation properties of the momentum equation. It can be used in reaches with moderate to steep slopes, where the flow is dominated by friction. However, it should not be used for rapidly varying flows, such as in dam-breaks, or in reaches with flat slopes and/or deep water where the local acceleration term (and wave propagation properties of the equation) becomes more important.

**The Diffusive Wave Approximation**

With this approximation, the convective momentum and eddy viscosity terms are also neglected and the *x*-momentum equation reduces to:

$$\frac{\partial \varsigma}{\partial x} = -\frac{u\sqrt{u^2+v^2}}{C^2 d} \tag{6.2.118}$$

That is, the water surface slope is balanced by the friction slope.

As for the steady state momentum equation, this approximation can be used to describe gradually varied flows in reaches with moderate to steep slopes. It includes backwater effects, but has the added limitation that it cannot be used to simulate flow separations and eddies, or main channel/overbank momentum transfers.

**The Kinematic Wave Approximation**

With this approximation, the surface slope of the water is assumed to be the same as the bed slope the *x*-momentum equation further reduces to:

$$\frac{\partial z}{\partial x} = -\frac{u\sqrt{u^2+v^2}}{C^2 d} \tag{6.2.119}$$

That is, the friction slope is equal to the bed slope.

This approximation is effectively the same as solving for the flow properties using a steady state friction law (such as the Manning equation). Backwater effects are not included, and water can only flow downstream. As such, the kinematic wave approximation can only be used to describe gradually varied flows in reaches with moderate to steep slopes where backwater effects can be neglected.

# 2.11. Three Dimensional Flow Equations

Regardless of the nature of flow, all flow situations must satisfy the following relationships:

1. The continuity equation (law of conservation of mass).

2. Newton's law of motion, which must hold for every particle at every instant.

3. Boundary conditions, for example a real fluid has zero velocity relative to an adjacent boundary.

4. The first and second laws of thermodynamics.

Other relations such as Newton's law of viscosity or the Boussinesq eddy viscosity concept are also necessary so that solutions can be obtained for the equations developed from these relations.

An approach to 3D modelling of flows is achieved by integrating the point form (or more precisely, infinitesimal unit volume) equations of continuity, momentum and energy over the cross-section. This leads to the continuity equation and Navier-Stokes equations expressed in tensor notation below (Rodi, 1980).

Mass Conservation: Continuity equation

$$\frac{\partial u_i}{\partial x_i} = 0 \tag{6.2.120}$$

Momentum conservation: Navier-Stokes equations

$$\frac{\partial u_i}{\partial t} + u_j \frac{\partial u_i}{\partial x_j} = \frac{-1}{\rho}\frac{\partial P}{\partial x_j} + \upsilon \frac{\partial^2 u_i}{\partial x_j \partial x_j} \tag{6.2.121}$$

where $u_i$ is the instantaneous velocity component in the direction $x_i$, $P$ is the instantaneous static pressure and u is the molecular kinematic viscosity. The Navier-Stokes equations are exact equations describing the turbulent motion, and numerical procedures are available to solve these equations. However, the storage capacity and speed of present-day computers are still not sufficient to allow a solution for practically relevant turbulent flow. The reason for this is that turbulent motion contains elements which are much smaller than the extent of the flow domain (typically of the order of $10^{-3}$ times smaller). Thus to resolve the motion of these elements in a numerical procedure at least $10^9$ grid points would be necessary to cover the flow domain in three dimensions.

A statistical approach to turbulence suggested by Reynolds (1894) may be used to solve the Navier-Stokes equations for mean values of velocity and pressure when the turbulence correlations $u'v'$ which result can be determined in some way. The determination of these correlations is the main problem in calculating turbulent flows and a turbulence model must be introduced which approximates the correlations and simulates the average character of real turbulence. The instantaneous values of velocity $u_i$ and pressure $P$ are separated into mean and fluctuating components, as shown in Equation (6.2.123).

$$u_i = \overline{u_i} + u_i' \text{ and } P = \bar{P} + P' \tag{6.2.122}$$

where the mean quantities are defined as:

$$u_i = \frac{1}{t_2 - t_1}\int_{t_1}^{t_2} u_i dt \text{ and } \bar{P} = \frac{1}{t_2 - t_1}\int_{t_1}^{t_2} P dt \tag{6.2.123}$$

and the averaging time $t_2$-$t_1$ is long compared with the time scale of the turbulent fluctuations. This results in the following equations:

Continuity equation:

$$\frac{\partial \overline{u_i}}{\partial x_i} = 0 \tag{6.2.124}$$

Momentum equation written in terms of the cartesian coordinates for the *x*-direction, Equation (6.2.121) becomes:

$$\begin{aligned}\frac{\partial \bar{u}}{\partial t} + \bar{u}\frac{\partial \bar{u}}{\partial x} + \bar{v}\frac{\partial \bar{u}}{\partial y} + \bar{w}\frac{\partial \bar{u}}{\partial z} = \frac{-1}{\rho}\frac{\partial \bar{P}}{\partial x} - \left(\frac{\partial \overline{u'v'}}{\partial y} + \frac{\partial \overline{u'u'}}{\partial x} + \frac{\partial \overline{u'w'}}{\partial z}\right) \\ + \upsilon\left(\frac{\partial^2 \bar{u}}{\partial x^2} + \frac{\partial^2 \bar{u}}{\partial y^2} + \frac{\partial^2 \bar{u}}{\partial z^2}\right)\end{aligned} \tag{6.2.125}$$

where $\bar{u}$,$\bar{v}$and $\bar{w}$ ,and are the local time-averaged velocity values in the *x,y* and *z* directions and *u', v'* and *w'* are their fluctuating components. The terms on the left-hand side of the

equation represent the momentum flux through an element dx, dy, dz. The three terms on the right-hand side are the external forces acting on the element.

The three components of the external forces are:

1. The body force of the element (due to its weight).

2. The resulting turbulent shear forces on all surfaces (resulting from Reynolds stress distributions).

3. The viscous forces causing shear stresses at the molecular level.

Physically, the correlations when multiplied by the density represent the transport of momentum due to the fluctuating motion as shown below:

$$\tau_{xy} = -\rho\overline{u'v'} \tag{6.2.126}$$

The equation above represents the transport of x-direction momentum in the y-direction and may be considered as a shear stress on the fluid called the turbulent or Reynolds stress.

Strelkoff (1969) integrated the equation of continuity and the Navier-Stokes equation to obtain the one-dimensional open channel flow equations for an incompressible homogeneous fluid. Further work was presented by Yen (1973) providing a more detailed and unified view of the general open channel flow equations.

Often 3D models are applied to steady flows. One approach was described by Olsen (2003) and Olsen (2004). He solves the three-dimensional Reynolds Averaged Navier-Stokes equations (RANS) for each cell. The equations can be written in Cartesian form as:

$$\frac{\partial V_i}{\partial x_i} = 0 \tag{6.2.127}$$

for continuity, and

$$\frac{\partial V_i}{\partial t} + V_j\frac{\partial V_i}{\partial x_j} = \frac{1}{\rho}\frac{\partial}{\partial x_j}\left(-p\delta_{ij} - \rho\overline{u_i u_j}\right) \tag{6.2.128}$$

for momentum, where *i* and *j* represent standard tensor notation indicating the *x, y* and *z* coordinate directions, $V_i$ is the mean velocity component in the $x_i$ direction, *p* is the pressure, *ρ* is the fluid density, $\delta_{ij}$ is the Kronecker delta and is the turbulent Reynolds stress, where $u_i$ and $u_j$ are fluctuating velocities, and is Reynolds averaged value of $u_i u_j$. The first term is the transient term which is neglected and the second term is the convective term. The third term is the pressure term and the final term is the Reynolds stress term which requires a turbulence model to be evaluated. The standard *k-ε* model was used for turbulence closure. The model calculates the eddy-viscosity as:

$$v_T = c_\mu\frac{k^2}{\varepsilon} \tag{6.2.129}$$

where *cμ* is a constant, $k = \frac{1}{2}\overline{u_i u_j}$ and is the turbulent kinetic energy and *ε* is the dissipation rate of turbulent kinetic energy. The turbulent kinetic energy *k* is modelled as:

$$\frac{\partial k}{\partial t} + V_j \frac{\partial k}{\partial x_j} = \frac{\partial}{\partial x_j}\left(\frac{V_T}{\sigma_k}\frac{\partial k}{\partial x_j}\right) + P_k - \varepsilon \quad (6.2.130)$$

where $\sigma k$ is a constant and $P_k = v_T \frac{\partial V_j}{\partial x_i}\left(\frac{\partial V_j}{\partial x_i} + \frac{\partial V_i}{\partial x_j}\right)$ which is a term for the production of turbulence. The dissipation of turbulent kinetic energy $\varepsilon$ is modelled as:

$$\frac{\partial k}{\partial t} + V_j \frac{\partial k}{\partial x_j} = \frac{\partial}{\partial x_j}\left(\frac{V_T}{\sigma_k}\frac{\partial k}{\partial x_j}\right) + C_{\varepsilon 1}\frac{\varepsilon}{k}P_k - C_{\varepsilon 2}\frac{\varepsilon^2}{k} \quad (6.2.131)$$

where $C_{\varepsilon 1}$, $C_{\varepsilon 2}$ and $\sigma\varepsilon$ are constants. Recommended values for the five constants in the $k$-$\varepsilon$ model given by Rodi (1980). The SIMPLE method (Patankar, 1980) can be used for the pressure and velocity coupling, and an implicit solver was used to produce the velocity field across the geometry. Model convergence was assumed when all residuals of the RANS and turbulence equations between consecutive iterations were of the order of $10^{-4}$. An approach for the application of these equations in compound open channels is given in Conway et al. (2013).

# 2.12. Physical Modelling

The first designed physical model pre-dates the routine use of numerical models in hydraulic engineering practice by approximately a century. Prior to the advent of digital computers, physical models offered the most practical means for the investigation of problems involving complex bathymetry, sediment transport, unsteady flow and 2D or 3D flow.

Since the advent of numerical models, the domain of application of physical models has been shrinking. However, certain problems remain which are still more appropriately investigated through the use of physical models, and this is likely to remain the case for some time yet.

Physical models have been around for hundreds of years, however, it was only in 1885 when the first physical model study based on scientific principles, was undertaken. This model study was conducted by Osborne Reynolds for investigating the tidal currents in the Mersey Estuary near Liverpool, England. Reynolds is reputedly the first person to introduce the time scale into physical modelling (Lawson and O'Neill, 1980; Allen, 1970). His first model was distorted with the vertical and horizontal length scales differing by a factor of 33.1. The model sides were vertical and initially, the bed of sand was flat. After a period of model operation however, Reynolds observed that the bed was reshaped with the principal features of the natural estuary. This early success provided the impetus for Reynolds to follow up on this work with another bigger model, again of the Mersey Estuary.

## 2.12.1. The Basis for Physical Model Design

Physical models are scaled (usually reduced) representations of the real life or prototype flows and their boundaries. The flow boundaries may be:

- *fixed bed* - often made out of cement mortar. Such models yield information about the flow patterns and velocity field in, for example, estuaries, river channels or tidal inlets.
- *mobile bed* - with the model bed typically consisting of one of the following: sand, particles of coal or a granulated plastic. Mobile bed models yield (qualitative) information about the sediment movement as well as the water motion; they are of interest for investigating scour holes, or regions of sediment accretion or erosion.

The flow boundaries of a modelled region of interest can be:

- *natural* - where the floodplains and river channels of fixed bed models are constructed by first locating a series of templates made out of metal or plywood into position. Vertically, these sections are positioned using a theodolite. The channel bed and land form between the templates is interpolated. Sand is used as a fill material between the templates, and then a cement mortar capping is applied and frequently painted.
- *manmade* - in which case, physical models often incorporate a hydraulic structure such as a culvert, pipe, drainage channel, basin, levee, spillway or outlet works. In the model, hydraulic structures could be made out of (painted) timber, marine plywood, PVC pipes and also Perspex when visibility is a consideration e.g. for tracing the flow patterns through a structure with the use of a dye.

Accurate simulation of the flows in a physical model requires three kinds of similitude (or similarity) and it will be noticed that the word geometry enters the description of each kind of similitude:

- *Geometric similitude*- requires the geometry or shapes of the flow boundaries to be similar in model and prototype. Lengths in the model are scaled versions of the corresponding prototype lengths. Geometric similitude is secured by ensuring that the model is a scaled reproduction of the prototype.
- *dynamic similitude*- requires that all forces (be they pressure forces, weight, boundary friction forces, drag forces, surface tension forces, centripetal forces) at each point in the flow domain are each scaled by the same factor between model and prototype. If this were to be achieved, the force polygon acting on each elemental fluid parcel in the flow field, would have the same geometry in model and prototype; this is referred to as complete similitude. Complete similitude is the ideal situation, but in practice, is impossible to achieve. The reasons for this are twofold.

Firstly, the scaling requirements of the various forces are incompatible because some forces act through volumes (e.g. gravity and centripetal forces), other forces act over areas (e.g. pressure, drag and viscous forces) and another force acts over lengths (the surface tension force). The scales associated with volumes, areas and lengths are different. Consequently, the forces associated with volumes, areas and lengths will, in general, scale differently. If a model was built full scale, all forces would scale correctly. However, the smaller the model compared to the prototype, the larger the length scale and the greater the discrepancy between the scalings of the various forces which act through volumes or over areas or lengths.

Secondly, the limited fluids available for use in models (in terms of their fluid properties of density and viscosity, and cost and safety) restrict the range of length scales which can be used in physical models. In nearly all cases in engineering practice, the fluids used in hydraulic models are water (and occasionally air). Consequently, a compromise has to be reached in which only the dominant forces are correctly scaled by the same factor, and the incorrect scalings of the smaller forces are of negligible consequence in a well designed model. This is termed incomplete similitude.

The task of the modeller is to identify the dominant forces, ensure that these forces are scaled correctly, and disregard any insignificant forces. The effects (i.e. errors) due to those incorrectly scaled, insignificant forces are known as scale effects. In current engineering practice, most hydraulic investigations involve free surface flows and to a much lesser extent, pressurised or closed conduit flows. These two types of problems require different scaling criteria:

In free surface flows, the dominant forces are usually gravity, the associated pressure force, and boundary friction. By asserting equality of the Froude number between model and prototype at all points in the flow field, the gravity and pressure forces are scaled by the same (desired) factor. By adjusting the model boundary roughness, consistent scaling of the boundary friction force is then achieved. Dynamic similitude is achieved provided the scale effects are negligible. A model which is based on point-to-point equality of the Froude number between model and prototype is known as a Froude model. Effectively, what the modeller is doing here is to ensure that gravity, pressure and boundary friction forces are scaled consistently. All other forces are insignificant and so the momentum equation (or equations if in 2D or 3D) for any elemental parcel of fluid in the model mimics (i.e. is a scaled version of) the momentum equation(s) for the corresponding elemental parcel of fluid in the prototype. Dynamic similitude means that the corresponding terms in the model and prototype momentum equations for each of the dominant forces are all related by a constant factor. In models of closed conduit or pressurised flows, such as flows through pipes, the dynamic scaling requirement is that there is point-to-point equality of the Reynolds number in model and prototype. The dominant forces are the viscous and pressure forces which are correctly scaled in a Reynolds model.

Kinematic similitude requires the flow patterns in the model and prototype to be geometrically similar. In other words, the velocities at all points in the model, bear the same ratio between model and prototype. If this is achieved, then the model is in similitude with the prototype.

If any two of the above three kinds of similitude are satisfied, then the remaining similitude is inferred. In normal modelling practice, models are designed to satisfy both geometric and dynamic similitude. It then follows that kinematic similitude is also satisfied. The usual approach to model design is to satisfy geometric similitude through careful model construction and dynamic similitude by adopting the appropriate modelling criterion. In general, there are various modelling criteria involving various dimensionless numbers, but in practice, the most common criterion which has been mentioned above, is based on the Froude number (for free surface flows). The next most common criterion is based on the Reynolds number (for closed conduit or pressurised flows).

The Froude number may be regarded as the ratio of the inertial (or resultant) force to the gravity force, and the Reynolds number as the ratio of the inertial force to the viscous force. In models based on the Froude criterion or the Reynolds criterion, the correct scaling of the ubiquitous pressure forces is also achieved and the question arises as to how this comes about. The reason is that if the dominant forces (including the resultant force) are all correctly scaled, then the force polygon in model and prototype will also be correctly scaled. Consequently, one of these forces is a dependent force and this is taken to be the pressure force in Froude and Reynolds type models (Warnock, 1949).

Considering any small parcel of fluid in the prototype, what is required of the model is that the corresponding parcel of fluid in the model moves along the corresponding path at a scaled velocity of the prototype velocity. For this to happen, all forces (weight, pressure, drag, viscous, surface tension, elastic) acting on that parcel of fluid in the prototype must be in the same proportions to each other in the model. If this is the case, then there would be complete similitude between model and prototype. However, the various forces scale in different ways: some forces scale as the length cubed (e.g. weight, centripetal forces), other forces scale as length squared (e.g. pressure) and one other scales as length (i.e. surface tension). Therefore, as soon as the length scale departs from unity (i.e. full scale model), it is impossible or very difficult for all these forces to scale together in the same proportion.

Fortunately, however, it is frequently the case, that there are one or two dominant forces present in the flow field and it is therefore of no consequence if the minor forces are not scaled correctly, so long as the dominant forces are. This is termed incomplete similitude.

## 2.12.2. Model Scales

The design of a physical model requires the selection of a modelling criterion and following on from this, the scales to be used in the model.

In general, it is desirable that the model be as large as possible because:

- scale effects will be reduced,
- the accuracy of model construction will be less critical, and
- the results derived from the model will be less sensitive to errors in measurements.

On the other hand, there are a number of factors which tend to limit the size of the physical model:

- model construction costs. Construction costs depend on the complexity of the bathymetry and topography, and the detail in any hydraulic structures.
- the extent of the available floor area to accommodate the model. Models are preferably housed under cover so that the model testing is weather independent i.e. free of wind and rain and the model itself is sheltered. Moreover, to fit a model into a given area, a river channel can be 'folded' into a more compact form. If additional bends are introduced into the model which do not exist in the prototype, it may be necessary to take the additional head losses into consideration. Also, channel areas which in the prototype provide storage, can have their effects simulated by having areas of different shape but equivalent plan area.
- flows available from the water supply. The bigger the model, the larger the flow needed.

The length scales for most (undistorted) physical models are generally in the range of 1: 5 to 1: 2000.

## 2.12.3. Distorted Models

It is often useful to be able to distort a physical model by asserting different length scales in the horizontal and vertical directions. While undistorted models should be used whenever there is significant vertical and horizontal fluid motion, distorted models can be used whenever the fluid motion is mainly in the horizontal plain. As a rule of thumb, care should be taken whenever the horizontal to vertical length scales differ by more than a factor of about 5. (Recall that the first model of Reynolds had a distortion of 33.1.)

The advantage of distorting a free surface flow model is that for the same plan area of model, the depths of flow will be deeper in the distorted model. In nearly all prototype free surface flows, the flow is turbulent; and prototype turbulent flows can only be simulated in a model with turbulent flows. For example, if a model is distorted by a factor of 5, for the same (available) plan area, the model depths would be deeper by a factor of 5 and the model velocities would be greater by a factor of $\sqrt{5}$ when compared to an undistorted model. Consequently, the Reynolds numbers in the distorted model will be greater by a factor of $5^{3/2}$ = 11.2 compared to the corresponding undistorted model (with the same plan area) and turbulent flow is more likely to be guaranteed.

## 2.12.4. Model Scales in Froude Models

In a Froude model, the Froude number in model and prototype at corresponding locations is unity i.e Fr = $Fr_p/Fr_m$ = 1 where ( )$_r$ stands for the ratio of prototype value divided by the corresponding model value.

There are various scales of interest in a physical model and the main ones in a distorted Froude model are:

- length scales in the horizontal ($x_r$) and vertical directions ($z_r$),
- velocity scale (Fr = $v_r /g_r y_r$ = 1 )$\Rightarrow$ $v_r = y_r^{1/2} = z_r^{1/2}$ since $g_r$ = 1),
- time scale for essentially horizontal motion ($t_r = x_r/v_r = x_r/z_r^{1/2}$ ),
- discharge scale for flow through a vertical plane ($Q_r = A_r v_r = (x_r y_r) z_r^{1/2}$),
- pressure scale ($p_r = \rho_r v_r^2 = z_r$ if $\rho_r$ = 1 implying that the fluid in the model is the same as the fluid in the prototype), and
- dynamic pressure force scale (($F_{press}$)$_r = p_r A_r = (\rho_r z_r)(x_r z_r) = x_r z_r^2$), and
- hydrostatic pressure force scale (($F_{press}$)$_r = \rho_r g_r y_r A_r = x_r z_r^2$ )

If the model is undistorted, the various scales above can be determined by setting the length scale $L_r = x_r = z_r$ in the expressions above. For example, the flow scale would be $Q_r = L_R^{5/2}$ and the velocity and time scales both become $v_r = t_r = L_R^{1/2}$ .

## 2.12.5. Model Roughness in Froude Models

One scale which has not been discussed above is the roughness scale, and to determine this, recourse is made to the Manning equation (refer to Book 6, Chapter 2, Section 5) to determine the scale for Manning's n ($n_r$).

$$v_r = \frac{(R_h) r^{\frac{2}{3}} S_r^{\frac{1}{2}}}{n_r} \tag{6.2.132}$$

$$z_r^{\frac{1}{2}} = \frac{(R_h) r^{\frac{2}{3}} \left(\frac{z_r}{x_r}\right)^{\frac{1}{2}}}{n_r} \tag{6.2.133}$$

$$n_r = \frac{(R_h)_r^{2/3}}{x_r^{1/2}} \tag{6.2.134}$$

It is evident from Equation (6.2.134) that $n_r$ depends upon the hydraulic radius scale (($R_h$)$_r$) and for a distorted model, this in turn depends upon both $x_r$ and $z_r$. One consequence of distortion is that the friction forces at the model bed are under-represented. Equation (6.2.134) indicates that usually, the Manning n in the model should be greater than the Manning's n in the prototype. For a model made out of cement mortar, the model roughness will be too smooth and additional artificial roughness has to be applied to the surface of the model. This can take the form of coarse sand, pebbles or other roughness elements glued to

the model surface; sometimes a light gauge wire mesh is attached to the model. Model roughness is adjusted empirically during the calibration phase of the model investigation.

Figure 16 is of a distorted physical flood model in which the model roughness was increased in two ways:

- the over-bank areas were artificially roughened with appropriately spaced and patterned, vertical dowels or roughness elements. The dowels exert a drag force on the water moving over the model floodplain; this additional force is designed to make up for the deficit of boundary friction at the overly smooth model bed.
- the in-bank areas were roughened with small pads of synthetic fibrous material. The spacing of these pads was adjusted by trial and error until the slope of the water surface matched the required slope.

If the roughness in the model is too smooth, not only will the magnitude of the velocities be too large, but also, the flow paths will tend to be too straight. The opposite trends tend to occur in a model which is too rough.

In the design of the distorted model depicted in Figure 16, it was found that while the model simulation of floods with a 50 year and 100 year Average Recurrence Interval (2% and 1% AEP) satisfied the requirement for turbulent flow in the model, the model flow corresponding to a smaller flood with a return period of 25 years was transitional between laminar and turbulent and therefore could not be tested in the model.

In an undistorted model with $n_r = L_r^{1/6}$ , the Manning n for the model surface is too high. Model spillways are usually constructed of timber and marine plywood and the usual approach is to try and achieve as smooth a surface as possible through sanding and painting, and to tolerate the mismatch. As the boundary friction forces in this flow scenario are not as important as the dominant gravity force, any scale effect in the model roughness is not usually significant.

## 2.12.6. Mobile Bed Models

Physical models can be classified as (i) fixed bed or (ii) mobile bed. Most studies by physical models are of the fixed bed variety. In fixed bed models, the bottom flow boundaries remain the same throughout model testing. In mobile bed models, the water movement and the sediment movement have to be reproduced at the same time. The model bed consists of a sediment which may be natural or artificial. A diverse range of materials have been used in mobile bed models to simulate non-cohesive prototype sediments; amongst other materials, they include sand, grains of coal, crushed walnut shells, granulated plastics. Mobile bed models are used to investigate erosion, accretion and localised scour holes.

Mobile bed models are considerably more complex than fixed bed models, and only some general considerations will be included here. With the introduction of a sediment, the specifications for the sediment particles in the model need to be decided. If the model sediment grain size was simply scaled down according to the length scale, the resulting model sediment particles would be so fine that they may well exhibit cohesive behaviour, and such a sediment could not be used to simulate the behaviour of a non-cohesive, prototype sediment. This problem is circumvented by using sediment grains in the model (which are oversized compared to the grain size which would be obtained from the length scale), but made out of a material which is less dense than sand, for example coal or a granulated plastic. By balancing sediment density and particle size for the model sediment particles, their fall velocity can be scaled according to the velocity scale according to the Froude criterion.

Mobile bed modelling of non-cohesive sediments is far from routine. The bed roughness of a mobile bed is a combination of grain roughness and bedforms. The size and type of the bedforms (ripples or dunes) cannot be specified a priori, but rather are determined by interactions between the near-bed fluid dynamics and morphodynamics; this includes the turbulence intensity and its distribution, the permeability of the bed and the shape of the deformable bed.

With the introduction of sediment into a model, there is the need to establish a morphological time scale which is best based on comparisons between the model and prototype bed evolution. This may require distortion of the flow scale in the model to achieve.

The motion of the sediment in the prototype is a mixture of suspended sediment and bed load. While the suspended sediment moves at approximately the flow velocity, the bed load travels much slower. The simulation of sediment movement which consists of nearly all suspended load or nearly all bed load is easier than the much more difficult problem of modelling the total sediment load which consists of comparable proportions of both suspended and bed load. It is possible also, that the proportions of bed load and suspended load vary with time, such as during a flood hydrograph. When this happens, the sedimentation time scale will also vary with time.

In connection to physical modelling, the comment or question is often raised in which physical modelling is referred to as an art or a science?

Some flow scenarios may involve a combination of free surface flow (which required a Froude model) and pressurised flow (which requires a Reynolds model). The resulting scales from applying the Froude and Reynolds criteria are in conflict. Therefore, some other solution, probably involving some compromises, must be sought in such a situation.

## 2.12.7. Stages of an Investigation by Physical Models

A summary of the main stages in a hydraulic investigation by physical modelling follow:

- *Model design* - the modeling criterion is selected ($IF_r = 1$), a decision on the model type is made (distorted or undistorted model, fixed bed or mobile bed), the length scale/s is/are selected taking cognisance of available space, flows and funding, drainage system and model boundaries, which should be well removed from the study area.

- *Model calibration* - the model is adjusted so as to reproduce a known event, such as a flood, to within an accepted tolerance. If the model fails to achieve this, the validity of the model geometry should be checked as a first response. Next, consideration should be given to the possibility of changes having taken place between the time of the recorded event and the time of the bathymetric survey. Following on from this, the roughness of the flow boundaries should be adjusted until the event has been successfully simulated in the model (Jenkins, 1987).

- *Model verification* - the performance of the model is further checked on another event, which is independent of the data used for calibration. While verification is a desirable stage of model testing to perform, it is not often carried out due to a lack of appropriate data or inadequate funding. In selecting the data for both the calibration and verification phases, it good practice to use the data from events which are of comparable magnitude to the scenarios to be tested. For example, it is not sound modelling practice to calibrate a model on a small and frequent event when the purpose of building the model is to undertake tests corresponding to rare events. The reason for this is that the reliability of extrapolating the model performance cannot be taken for granted and should be questioned.

- *Model testing* - the model is tested under one or more scenarios which may correspond to real or synthesised events.

- *Reporting of model results* - a technical report is prepared which includes the investigation methodology and the findings of the investigation. All results should be in terms of prototype values rather than model values.

## 2.12.8. Physical Models Development And Non-dimensional Analysis

In most cases of fluid motion in hydraulics, the complexity is such that the strict application of basic equations is possible in only relatively simple geometries. Analytical treatment requires the situation to be idealised to some extent and the effect of the consequent simplifications can only be tested by experiment.

As a result, the science of hydraulics has been marked by intense development of experimental methods. Experimental observation and measurements, and consequent conceptual deductions, have been at the heart of many of the great discoveries in fluid mechanics and hydraulics. Along with the experimental study of basic fluid phenomena, the science and art of physical hydraulic modelling have developed.

With the advent of widespread, powerful, and cheap computing facilities, numerical modelling has advanced significantly. Physical modelling, however, is by no means obsolete. Indeed, as discussed by Martins (1989)Martins (1989), the development of physical modelling has kept pace with numerical modelling. Often the two are intertwined through the concept of “hybrid modelling” where a physical model of a complex flow region provides the boundary conditions for a numerical model covering a much larger area.

This section examines the particular application of physical modelling to the design of hydraulic structures and identifies outstanding issues that remain to be solved. The field of physical modelling is vast, both with regard to the range of problems tackled and the breadth of literature in the field. Excellent reviews and texts include those of Martins (1989), Kobus (1980), and Novak and Cábelka (1981).

Firstly general modelling criteria are reviewed. In particular, the need to supplement pure dimensional analysis with process functions, based on sound analytical concepts, is emphasised. Attention is then focussed on the modelling of hydraulic structures and the potential implications of scale effects. Actual model studies are used to illustrate these issues. Finally some outstanding issues for further development are then identified.

## 2.12.9. Model Criteria - Dimensional Analysis and Process Functions

As an example of the use of dimensional analysis, and to illustrate its insufficiency on its own, the simple case of flow in a fixed-bed open channel is considered. Adopting the mantle of dimensional analysis, the controlling parameters and their dimensional units are identified as follows:

Flow velocity, $V$, L/T

Channel width, $W$, L

Channel depth, $y$, L

Fluid density, $\rho$, M/L$^3$

Fluid viscosity, $u$, M/(LT)

Fluid surface tension, $\sigma$, M/T$^2$

Surface roughness, $\varepsilon$, L

Gravitational acceleration, *g*, L/T$^2$

Dimensional analysis enables the grouping of these parameters in a number of ways. Adopting *V*, *y*, and $\rho$ as the repeating variables, we can develop a legitimate set of dimensionless variables as follows:

$$f\left(\frac{V^2}{gy}, \frac{V^2}{\frac{\sigma}{y\rho}}, \frac{Vy\rho}{\mu}, \frac{W}{y}, \frac{\varepsilon}{y}\right) = 0 \tag{6.2.135}$$

Strict similitude would only be possible if all five groups are identical in model and prototype. It can quickly be established, however, that this is not possible, especially if the same fluid is used in model and prototype. Using physical understanding and a process function the first term of Equation (6.2.135) represents the ratio of inertial forces to gravitational forces. Since open channel flow phenomena in general, and most hydraulic structure flows in particular, are gravity driven, this parameter must be retained. Requiring equality of the first term at homologous points in the model and the prototype leads to the well-known Froude law of modelling, appropriate to open channel flows, of:

$$\lambda V = \sqrt{\lambda y} \tag{6.2.136}$$

where $\lambda$ means “the scale of” (model to prototype).

The second term of Equation (6.2.135) is a Weber number, representing the ratio of inertial forces to surface tension forces. This ratio increases with model size because the inertial forces act on a volume whereas the surface tension forces act on an area. Thus the surface tension forces become negligible, provided the model is reasonably large, and the second term can be disregarded.

Turning now to the third term of Equation (6.2.135), we identify a Reynolds number, Re, representing the ratio of inertia forces to viscous forces. In the context of an open channel flow, viscous forces affect the surface resistance, apparently requiring Reynolds number equality between model and prototype for full similarity.

If the same fluid is used in model and prototype, Reynolds number equality at homologous points would require that:

$$\lambda V = \frac{1}{\lambda y} \tag{6.2.137}$$

and this condition is clearly incompatible with Equation (6.2.136). Indeed, it is readily shown that, if the velocity scale is based on Equation (6.2.136):

$$\lambda \mathrm{Re} = \lambda y^{\frac{3}{2}} \tag{6.2.138}$$

This can be resolved by making use of a process function for flow resistance which links the friction factor, Reynolds number, and relative roughness through the well-known Colebrook-

White equation. This function is conveniently plotted as a Moody diagram and is reproduced in Figure 6.2.23.

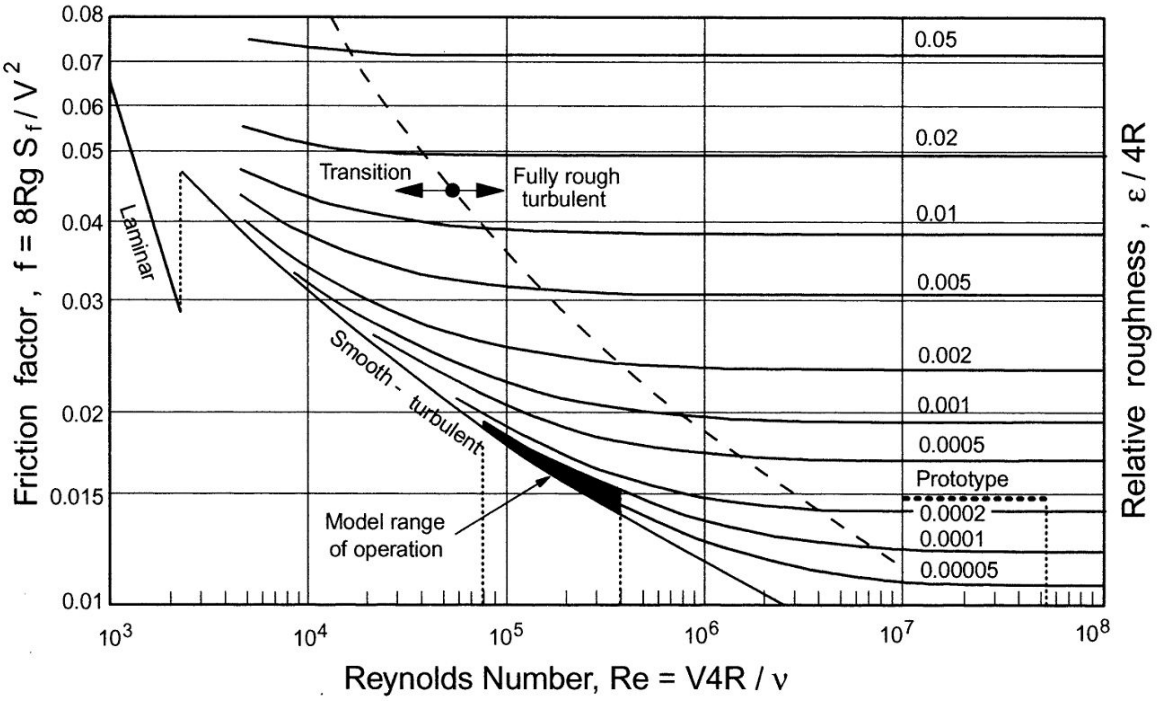


Figure 6.2.23. Process Function Diagram for Friction

The equation for friction factor, the ordinate of Figure 6.2.23, shows that the Froude criterion of Equation (6.2.136) can only be satisfied if the friction factor is the same in model and prototype. Superimposed on Figure 6.2.23 is a hypothetical range of prototype Reynolds numbers and a corresponding range of model operation, assuming a model scale of 1:25. For the example given, it is evident that equality of friction factor between model and prototype can only be obtained if the model is relatively smoother than the prototype. It is noted, further, that this equality is only possible for one particular operating condition (characterised by Reynolds number). For other operating conditions, the model friction factor will be different from that in the prototype, introducing a friction scale effect. The scale effect can be calculated, however, and model results adjusted when scaling up to prototype values.

Figure 6.2.23 also demonstrates that, if the prototype is relatively smooth, it may not be possible to build a model with a low enough friction factor to match that of the prototype. In this situation, the higher model friction factor may be accepted as at least conservative with respect to predicted flow depths, or, again, the scale effect can be calculated and used to adjust the predicted prototype values.

The discussion above has demonstrated that dimensional analysis is insufficient on its own to provide a basis for the modelling of open channel flow. Indeed, relying solely on dimensional analysis, it would be concluded that accurate modelling is not possible. It is only by using knowledge of flow resistance and its corresponding process function to dimensional analysis that an appropriate modelling procedure is possible.

Other examples of the necessity for process functions, in addition to dimensional analysis, for physical modelling of weir flows and vortex drop shafts have been discussed by Ackers (1987).

The discussion above applies to undistorted models only - ie those for which the horizontal and vertical scales are identical. Undistorted models are common in hydraulic structure investigations, but are often impractical for large rivers because of their typically large width:depth ratios. A typical river may have a width of 500 m and a depth of perhaps 2 m. The corresponding undistorted model of a scale of, say, 1:250 would be 2 m wide and 8 mm deep. The model flow is then likely to be totally different in character to the prototype flow due to surface tension effects and the likelihood of laminar model flow.

This situation is resolved by utilising a vertical scale that is larger than the horizontal. The Froude relationship is still expressed in the form of Equation (6.2.136), where, however, *ly* represents the vertical scale because it is vertical, rather than horizontal distances which measure the effect of gravity on velocity.

Given Figure 6.2.23 and the expression for head loss:

$$h_L = f\frac{L}{4R}\frac{V^2}{2g} \tag{6.2.139}$$

Rearrangement and expression in terms of scale ratio yields:

$$\lambda S = \frac{\lambda y}{\lambda x} = \lambda f \frac{\lambda R}{\lambda x} \tag{6.2.140}$$

or

$$\lambda f = \frac{\lambda R}{\lambda x} = \frac{\lambda y}{\lambda x} \tag{6.2.141}$$

if the channel is wide.

Because $\lambda y$ is always greater than $\lambda x$, Equation (6.2.141) shows that the model must be rougher than the prototype. Indeed, in direct contrast to undistorted models, significant effort is often required to make the model rough enough!

Mobile bed models introduce an additional degree of complexity because the roughness of the bed is largely dependent on the form losses associated with the bed features. Because the bed features are formed by the flow conditions, and hence cannot be directly established by the modeller, it is important that the model flow conditions are such that the model bed simulates closely the bed of the prototype.

Resolution of these complexities is beyond the scope of this chapter. Further details are provided in Keller (1998).

## 2.12.10. Scale Effects

The whole issue of scale effects is too broad to be effectively covered in this chapter. There is a large body of literature on the topic and several specialist symposia have been held eg Kobus (1984). Herein, attention is confined to scale effects in hydraulic structures, specifically flow measurement structures where scale effects can significantly affect the model determination of prototype rating curves.

An undistorted geometric scale model is normally built and operated under conditions of Froudian similarity. The model head (stage)-discharge data are then simply scaled up to prototype values, utilizing the equations:

$$\lambda h = \lambda L \tag{6.2.142}$$

$$\lambda Q = \lambda L^{\frac{5}{2}} \tag{6.2.143}$$

The characteristics of boundary layer growth are such that model scaling for reproduction of free surface effects (Froudian scale) will introduce dissimilarities. We illustrate this by considering the equations for turbulent boundary layer growth on a flat plate Streeter and Wylie (1979):

$$\delta = \frac{0.38x}{\mathrm{Re}^{0.2}} \tag{6.2.144}$$

$$\delta^* = \frac{1}{8}\delta \tag{6.2.145}$$

Equation (6.2.145) is developed from the one-seventh power law velocity distribution:

$$\frac{u}{U} = \left(\frac{y}{\delta}\right)^{\frac{1}{7}} \tag{6.2.146}$$

In the above equations, $\delta$ and $\delta^*$ are boundary layer thickness and boundary layer displacement thickness respectively, Re is the flow Reynolds number defined with respect to the length *x* of boundary layer development, *u* is the velocity at elevation *y* above the bed, and *U* is the free stream velocity.

Equation (6.2.144) and Equation (6.2.145) indicate that similarity of boundary layer growth will only be possible if the Reynolds numbers are the same in model and prototype. This criterion is not met in a Froudian model, for which $\lambda\mathrm{Re} = \lambda L^{1.5}$.

The measured water surface elevation upstream of the flume control is affected by the boundary layer growth on the flume floor in that the water surface is displaced by a distance equal to the boundary layer displacement thickness. Accordingly, any dissimilarities in the modelling of the boundary layer displacement thickness will reflect as a dissimilarity in the position of the water surface, and a consequent scale effect in the measurement of pressure head.

Keller (1984a) has developed a procedure for determining the magnitude of the scale effect and for adjusting the model data to correctly predict the prototype behaviour. For details, the reader is referred to the original paper. The procedure relies on the use of the process function for boundary layer growth embodied in Equation (6.2.144) to Equation (6.2.146).

Keller (1984b) has applied the procedure to undrowned cut-throat flumes and typical results are presented in Figure 6.2.24. These data were obtained from a study involving three geometrically similar flumes to scale ratios of 1:2:4. Flume 1 (x) is the smallest, Flume 2 (⊙) is twice as large as Flume 1, and Flume 3 (+) is four times as large as Flume 1. The ordinate is the piezometric head, *ha*, normalised with the throat width, *BT*. The abscissa is the non-dimensional discharge parameter.

The data in Figure 6.2.24(a) are uncorrected and show a tendency at values of *ha*/*BT* below about 0.8 to plot progressively to the right with flume size - ie for *ha* to be slightly less for the large flume than would be predicted from tests on the small flumes. Expressed in terms of more relevance to the practising engineer, an uncorrected model rating would result in an under-prediction in the discharge through a four times larger prototype structure by up to

10%. Figure 6.2.24(b) shows the data adjusted for dissimilar boundary layer growth. It is clear that the small trend with flume size has been completely eliminated.

The point of this example has been to demonstrate that scale effects arise in many model studies. However, with an understanding of the physical processes which govern the phenomena and with a knowledge of the appropriate process functions, the scale effects can be assessed and, in many cases, explicitly determined.

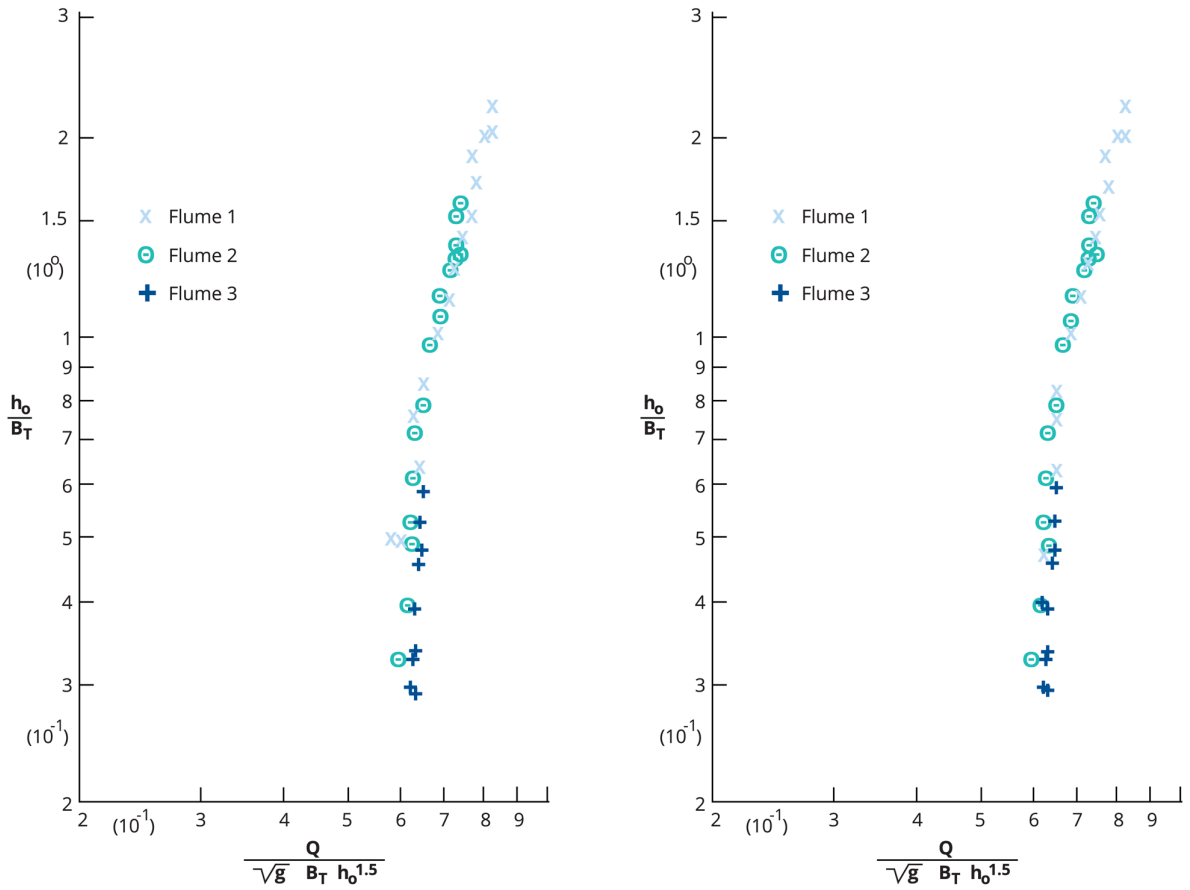


Figure 6.2.24. Data for Cut-throat flumes (a) Uncorrected, (b) Corrected for Scale Effects (after Keller (1984b))

## 2.12.11. Some Issues for the Future

It is fashionable in some quarters to predict the eventual demise of physical modelling as computing power becomes ever cheaper and more readily available, and as our ability to translate knowledge of the physics of a phenomenon into process equations for its quantitative solution develops. It is indeed true that some problems that were once routinely solved using physical models may now be solved using numerical models. Among these are simple spillway layouts, flow measurement structures, and far-field dispersion problems in rivers. It is equally true, however, that many problems remain the exclusive province of the physical modeller. Problems with complex boundary conditions and/or strongly three-dimensional characteristics remain extremely difficult to solve by numerical means. The same problems, however, are amenable to study by physical models because the model represents, within generally understood limits, an exact replica of the prototype.

Developments over the next few years are likely to concentrate on hybrid models – ie model approaches where physical modelling and numerical modelling are applied in tandem to the

solution of complex hydraulic problems. There is evidence of this already, and two examples are given in the following.

The mixing processes downstream of a pollutant outfall are often classified as “near field” and “far field”. Sometimes an additional “mid-field” may be introduced. Rutherford (1994) provides an excellent review of mixing processes.

In all but the most simple of cases, near-field mixing is extremely difficult to model numerically. The flow field is very strongly three-dimensional and the mixing processes may be dominated by vertical mixing, transverse mixing, or both. In the far-field region, full vertical mixing may well have been achieved, and a numerical two dimensional mixing model may be adequate to describe the continuing diffusion of the pollutant. In this situation, the most efficient modelling framework may be to build an undistorted physical model to simulate the near-field region and to use its measured downstream parameters as the upstream boundary conditions for the numerical model.

The second example has been described by Ackers (1987) and concerns prototype phenomena where air entrainment is a primary parameter. On spillways, self-aeration through floor slots is commonly permitted in order to control cavitation damage on the spillway. The amount of air that is entrained depends on the length of the trajectory of the nappe which springs from the upstream edge of the spillway slot. However, the length of the trajectory depends on the air pressure beneath the nappe. This depends on the rate of air entrainment, which, in turn, is a function of the resistance of the air supply ducts. Neither of these features can be properly simulated in an undistorted scale model. The trick is, in fact, to link the general spillway model with a separate computational study of the performance of the ducts with a design value of air demand. The aerodynamic resistance of the prototype supply duct determines the pressure to be expected beneath the nappe and this (sub-atmospheric) pressure must then be reproduced artificially in the model.

There are many other areas that will keep the physical modeller busy for many years to come. Some examples are:

- Interactions between hydrodynamic loads and structural loads and vibrations,
- Self-aeration in free surface spillway flows,
- Modelling of the scour potential of cohesive sediments and clays,
- Modelling of the influence of turbulence and flocculation on the performance of settling basins, and
- Modelling of the scour resistance of bank and bed vegetation.

# 2.13. References

AS Committee (2006), PL-045. Australian Standard AS 2200, Design Charts for Water Supply and Sewerage. Standards Australia, Sydney, January 2006. ISBN 0 7337 7084 3.

ASCE Task Force (1963), Friction Factors in Open Channels. Journal of Hydraulics Division, ASCE, 89(2), 97-143.

Abbott, M.B. (1979), Computational Hydraulics - 's of the Theory of Free Surface Flows, Pitman, London.

Abbott, M.B. and Rasmussen, C.H. (1977), On the Numerical Modelling of Rapid Contraction and Expansion in Models that are Two-dimensional in Plan, Proc. XV11 Congress, IAHR, Baden-Baden.

Ackers, P. (1991), Hydraulic Design of Straight Compound Channels. Report SR281, HR Wallingford, October 1991 (Volumes 1 and 2).

Ackers, P. (1992), Hydraulic design of two stage channels. Proc. of the Institution of Civil Engineers, Water, Maritime and Energy, Dec. 1992, 96: 247-257.

Ackers, P. (1987), 'Scale Models. Examples of how, why, and when - with some ifs and buts', Proceedings of XXII Congress, International Association for Hydraulic Research, Technical Session B, Lausanne, Switzerland, pp: 1-15

Allen, J. (1968), The life and work of Osborne Reynolds, chapter 1, pages 1-82. Manchester University Press and Barnes and Noble, Inc., Manchester and New York, 1970. Osborne Reynolds and Engineering Science Today, edited by McDowell, D.M. and Jackson, J.D. Papers presented at the Osborne Reynolds Centenary Symposium, University of Manchester, September 1968, ISBN 0 7190 0376 8.

Barnes, H.H.Jr. (1967), Roughness characteristics of natural channels. Geological Survey Water- Supply Paper 1849, U.S. Department of the Interior, Geological Survey, pages 1-213, 1967. Electronic full text available as 'Roughness characteristics of normal supply channels', available at web.utk.edu/btschant/manning%20n/two.htm.

Bhowmik, N.G. and Demissie, M. (1982), Carrying capacity of flood plains. Proc. ASCE, Journal of the Hydraulics Division, Mar. 1982, 108(3), 443-452.

Blalock, M.E. and Sturm, T.W. (1981), Minimum Specific Energy in Compound Open Channel. Journal of the Hydraulics Division, ASCE, Jun. 1981, 107(6), 699-717.

Cahdderton, R.A. and Miller, A.C. Friction slope models for M2 profiles. Water Resources Bulletin, American Water Resources Association, 16(2), 235-242, April 1980. Paper No. 79037.

Chow, V.T. (1959), Open-Channel Hydraulics. McGraw-Hill Book Company, New York.

Chow, V., Maidment, D. and Mays, L. (1988), Applied hydrology. New York: McGraw-Hill.

Conway, P., O'Sullivan, J.J., Lambert M.F. (2013), Stage-discharge prediction in straight compound channels using 3D numerical models, Proceedings of the Institution of Civil Engineers: Water Management, Vol.166, No.1, January, 3-15.

Cunge, J.A., Holly, F.M. and Verwey, A. (1980), Practical Aspects of Computational River Hydraulics, Pitman, London (Reprinted by University of Iowa).

Einstein, H.A. (1934), Der hydraulische oder profile-radius [The hydraulic or cross-section radius]. Schweizerische Bauzeitung, Zurich, 103(8), 89-91 (in German).

Elliot, S.C.A. and Sellin, R.H.J. (1990), SERC flood channel facility: skewed flow experiments. IAHR, Journal of Hydraulic Research, Feb. 1990, 28(2), 197-214.

Ervine, D.A. and Ellis, J. (1987), Experimental and computational aspects of overbank flood plain flow. Transactions of the Royal Society of Edinburgh: Earth Sciences, 1987, 78: 315-325.

Fenton, J. (2007), Lecture Notes on Open Channel Hydraulics. pp59, University of Karlsruhe, accessed on the web, 2007, April 2007.

Greenhill, R.K. (1992), An Investigation into the Mechanisms of Compound Meandering Channel Flow. PhD Thesis, Department of Civil Engineering, University of Bristol, U.K.

Henderson, F.M. (1966), Open Channel Flow, Macmillan Publishing Co., New York.

Horton, R.E. (1933), Separate roughness coefficients for channel bottom and sides. Engineering News-Record, Nov. 1933, III(22), 652-653.

Hydraulics Research Ltd, Wallingford, Thomas Telford, London. (1990), Charts for the Hydraulic Design of Channels and Pipes, sixth edition, 1990. ISBN 0 946466 02 5.

James, M. and Brown, R.J. (1977), Geometric parameters that influence flood plain flow. U.S. Army Engineer Waterways Experiment Station, Vicksburg, Miss., Jun. 1977, Research Report H-77-1.

James, C.S. and Wark, J.B. (1992), Conveyance Estimation for Meandering Channels, Report SR329, HR Wallingford, U.K., Dec. 1992.

Jenkins, B.S. (1987), Aspects of Hydraulic Calculations, volume 1 of Australian Rainfall and Runoff, A Guide to Estimation, D. H. Pilgrim (editor-in-chief ), chapter 4, pp. 53-91. The Institution of Engineers, Australia, Barton, ACT, revised edition, 1987. ISBN 085825 434 4.

Keller, R.J. (1998), The Continuing Application of Physical Models to Hydraulic Engineering, Keynote Address to 6th International Conference on Hydraulics in Civil Engineering, Proceedings of HYDRASTORM '98 combining 3rd International Symposium on Stormwater Management and 6th International Conference on Hydraulics in Civil Engineering, Adelaide, Australia, 27-30 September 1998, Institution of Engineers, Australia, pp: 11-21.

Keller, R.J. (1984a),'Boundary Layer Scale Effects in Hydraulic Model Studies of Discharge Measuring Flumes', in KOBUS, H. (ed),'Symposium on Scale Effects in Modelling Hydraulic Structures', International Association for Hydraulic Research, Esslingen, Germany, 1984, pp: 2.10-1 to 2.10-4.

Keller, R.J. (1984b)'Cut-throat Flume Characteristics', Journal of Hydraulic Engineering, American Society of Civil Engineers, 110(9), 1248-1263.

Knight, D.W. and Sellin, R.H.J. (1987), The SERC Flood Channel Facility. J. Inst. Water and Environmental Mgmt, 1(2), 198-204.

Kobus, H. (1980) (ed.),'Hydraulic Modelling', German Association for Water Resources and Land Improvement, Bonn.

Kobus, H. (1984) (ed),'Symposium on Scale Effects in Modelling Hydraulic Structures', International Association for Hydraulic Research, Esslingen, Germany.

Lambert, M.F. and Myers, W.R.C. (1998),'Estimating the discharge capacity in compound channels.'Water, Energy and Maritime, Journal of Institution of Civil Engineers, London, 130: 84-94.

Lambert, M.F. and Sellin, R.H.J. (1996a),'Velocity distribution in a doubly-sinuous compound channel.'Water, Energy and Maritime, Journal of Institution of Civil Engineers, London, 118: 10-20.

Lambert, M.F. and Sellin, R.H.J. (1996b),'Discharge prediction in compound channels using the mixing length concept.'Journal of Hydraulic Research, International Association of Hydraulic Research, 34(3), 381-394.

Laurenson, E. M. (1986), Friction slope averaging in backwater calculations. Journal of Hydraulic Engineering, ASCE, 112(12):1151-1163, December 1986. ISSN 0733 9429/86/0012 1151, Paper No.21083.

Lawson, J. D. and O'Neill, I. C. (1980), The role of physical and mathematical models in hydraulic engineering, June 1981. ACADS Publication no. U217, Presentation to the Association for Computer Aided Design Limited (ACADS), Water Engineering Technical (WET) Committee, Wednesday 12 November, 1980.

LeVeque, R.J (2002), Finite Volume Methods for Hyperbolic Problems, Cambridge University Press, Cambridge.

Lee P., Lambert M.F. and Simpson A.R. (2002),'Critical depth prediction in straight compound channels.'Water and Maritime Engineering, Journal of Institution of Civil Engineers, London, 154(4), 317 - 332.

Leonard, B.P. (1979a), A Survey of Finite Differences of Opinion on Numerical Muddling of the Incomprehensible Defective Confusion Equation, In: T.J.R. Hughes (ed.) Finite Element Methods for Convection Dominated Flows, AMSE, New York.

Leonard, B.P. (1979b), A Stable and Accurate Convective Modelling Procedure Based on Quadratic Upstream Interpolation. Computer Methods in Applied Mechanics and Engineering, 19(1), 59-98.

Lipscomb, E.B. (1956), Hydraulic capacity of Meandering Channels in Straight Floodways, Report T.M. No. 2-2429, Waterways Experiment Station, Vicksburg, Miss, U.S.A.

Lotter, G.K. (1933), Soobrazheniia k gidravlicheskomu raschetu rusel s razlichnoli sherokhovatostiiu stenok (Considerations on hydraulic design of channels with different roughness of walls). Izvestiia Vsesoiuznogo Nauchno-Issledovatel skogo Instituta Gidrotekhniki (Trans., All Union Scientific Research, Institute of Hydraulic Engineering, Leningrad), 9: 238-241. Cited from Chow (1959).

Martin, L.A. and Myers, W.R.C. (1991), Measurement of overbank flow in a compound river channel. Proc. of the Institution of Civil Engineers, London, Dec. 1991, Part 2, 91(9729), 645-657.

Martins, R. (1989),'Preface to Recent Advances in Hydraulic Physical Modelling', R. Martens (ed), Kluwer Academic Publishers, Dordrecht, The Netherlands.

McBean, E. and Perkins, F. (1975), Numerical errors in water profile computation. Journal of the Hydraulics Division, American Society of Civil Engineers, 101(HY11):1389-1403.

McBean, E. A. and Perkins, F. E. (1970), Error criteria in water surface profile computations. Technical Report 124, Massachusetts Institute of Technology Hydrodynamics Laboratory, Cambridge, Masachusetts, June 1970.

Myers, W.R.C. (1987). Velocity and discharge in compound channels. Proc. ASCE, Journal of Hydraulic Engineering, Jun. 1987, 113(6), 753-766.

Myers, W.R.C. and Lyness, J.F. (1989), Flow resistance in rivers with flood plains. Final Report on Research Grant GR5/D/45437, University of Ulster.

Nikuradse, J. (1933), Strömungsgestze in rauhen Rohren (Laws of Flow in Rough Pipes). Ver. Dtsh. Ing. Forschungsh, Vol.361.

Novak, P. and Cábelka, J. (1981),'Models in Hydraulic Engineering - Physical Principles and Design Applications', Pitman Publishing Limited, London.

Olsen, N.R.B. (2003), 3D CFD Modeling of a Self-Forming Meandering Channel, Journal of Hydraulic Engineering, No.5, May, pp:366-372, doi:10.1061/(ASCE)0733-9429(2003)129:5(366).

Olsen, N.R.B. (2004), Closure to 'Three-dimensional CFD modeling of self-forming meandering channel', Journal of Hydraulic Engineering, 130(8), 838-839, doi:10.1061/(ASCE)0733-9429(2004)130:8(838).

Patankar, Suhas. (1980), Numerical heat transfer and fluid flow. CRC Press.

Petryk, S. and Grant, E.U. (1978), Critical Flow in Rivers with Flood Plains, Journal of the Hydraulics Division, May, 1978, 104(5), 583-594.

Phillips, J.T. and Ingersoll, T.L. (1998) Verification of roughness coefficients for selected natural and constructed stream channels in Arizona. U.S. Geological Survey Professional Paper, (1584).

Rajaratnam, N. and Ahmadi, R.M. (1983), Meandering Channels with Flood plains. Unpublished Paper.

Reynolds, O. (1894), On the Dynamic Theory of Incompressible fluids and the Determination of Criterion. Phil. Trans., Roy. Soc., 186: 123-164.

Rodi, W. (1980), Turbulence models and their applications in hydraulics - a state of the art review. Delft: IAHR book publications.

Rutherford, J.C. (1994),'River Mixing', John Wiley and Sons, Inc., New York.

Samuels, P.G. (1989), Backwater lengths in rivers. Proceedings of the Institution of Civil Engineers, Part 2, 87: 571-582, December 1989. Paper 9479, Water Engineering Group.

Samuels, P.G. and Chawdhary, K.S. (1992), A backwater method for trans-critical flows. In R. A. Falconer, K. Shiono, and R. G. S. Matthew, editors, Proceedings of the Second International Conference on Hydraulic and Environmental Modelling of Coastal, Estuarine and River Waters, volume two, pp.79-89, Aldershot, U.K., 1992. Ashgate Publishing Limited. Conference organised and sponsored by Hydraulics Research Limited, ISBN 1 85742 085 3.

Sellin, R.H.J. (1964), A laboratory investigation into the interaction between flow in the channel of a river and that over its flood plain. La Houille Blanche, Nov. 1964, 19(7), 793-801.

Sellin, R.H.J. and Giles, A. (1988), Two Stage Channel Flow, Final Report for the Thames Water Authority, Department of Civil Engineering, University of Bristol.

Sellin, R.H.J., Ervine, D.A. and Willets, B.B. (1993), Behaviour of meandering two-stage channels. Proc. of the Institution of Civil Engineers, Water, Maritime and Energy, June 1993, 101(2), 99-111.

Smith, C.D. (1978), Effect of channel meanders on flood stage in valley. Proc. ASCE, Journal of the Hydraulics Division, Jan. 1978, 104(1), 49-58.

Stelling, G.S. (1984), On the Construction of Computational Methods for Shallow Water Flow Problems, Rijkswaterstaat Communications, No.35/1984, The Hague.

Stelling, G.S., Kernkamp, H.W.J and Laguzzi, M.M. (1998), Delft Flooding System: A Powerful Tool for Inundation Assessment based upon a Positive Flow Simulation, in V. Babovic and L.C. Larsen (eds) Hydroinformatics '98, A.A. Balkema, Brookfield.

Streeter, V.L. and Wylie E.B. (1981), Fluid Mechanics. McGraw-Hill Ryerson Ltd., Singapore.

Streeter, V. L. and Wylie, E. B. (1979),'Fluid Mechanics', (7th ed), McGraw-Hill Kogakusha Ltd., Japan.

Strelkoff, T. (1969), One dimensional Equations of Open-Channel Flow. Journal of the Hydraulics Division, ASCE, May 1969, 95(3), 861-876.

Toebes, G.H. and Sooky, A.A. (1966), Hydraulics of meandering rivers with flood plains. ASCE Water Resource Engineering Conference, Denver, Colorado.

U.S. Department of Agriculture. (1963), Guide for selecting roughness coefficient (n) values for channels, Soil Conservation Service, Washington D.C.

Wallingford, H.R. (1992), SERC Flood Channel Facility Experimental Data - Phase A, Report SR 314, Wallingford, United Kingdom, May 1992, Vol.1-14.

Warnock, J.E. (1950), Hydraulic Similitude, chapter II, pages 136-176. John Wiley and Sons, Inc. and Chapman and Hall, Ltd., New York, London, 1950. Engineering Hydraulics, H. Rouse (editor), Proceedings of the Fourth Hydraulics Conference, Iowa Institute of Hydraulic Research, June 12-15, 1949.

Yen, B.C. (1973), Open Channel Flow Equation Revisited. Journal of the Engineering Mechanics Division, ASCE, Oct. 1973, 99(EM5), 979-1009.

Zheleznyakov, G.V. (1965), Relative deficit of mean velocity of unstable river flow, kinematic effect in river beds with flood plains. Proc. of the 11th International Congress IAHR, Leningrad, USSR.

# Chapter 3. Hydraulic Structures

Robert Keller, William Weeks

| Chapter Status | Final |
|---|---|
| Date last updated | 14/5/2019 |

## 3.1. Introduction

Hydraulic structures are used to guide and control water flow velocities, directions and depths, elevation and slope of the streambed, general configuration of the waterway, and its stability and maintenance characteristics.

Careful and thorough hydraulic engineering is justified for hydraulic structures and consideration of environmental, ecological and public safety objectives should be integrated with hydraulic engineering design. The correct application of hydraulic structures can reduce maintenance costs by managing the character of the flow to fit the environmental and project needs.

Examples of hydraulic structures include flow measurement structures, transitions, constrictions, channel drops, low-flow checks, energy dissipators, bridges, bends, and confluences. Their shape, size, and other features vary widely for different projects, depending on discharge and the function to be accomplished. Hydraulic design procedures must govern the final design of all structures, including model testing for larger structures when the proposed design requires a configuration that differs significantly from known documented guidelines or when questions arise over the character of the structure being considered.

This review deliberately focusses on few the most important structures in urban and rural setting, as the general field of hydraulic structures is extremely vast. . Therefore, structures such as large dams are not considered. Hydraulic structures covered include flood bypass channels, control structures (gates, weirs and flumes, and spillways), levees, culverts, bridge waterways, floodways on roads, scour, rock chutes, rock riprap, and flow measurement structures.

## 3.2. Flood Bypass Channels

Diversion channels are used to divert waters from the main channel for many purposes including flood control, municipal water supply, and irrigation. The term *flood bypass channel* is typically used to describe a separate channel into which floodwaters are diverted to lessen the impact of flooding on the main river system. Such channels may bypass the flood flows into an adjacent waterway or return the flows back into the same stream a distance downstream from the point of the diversion.

On large river systems, flood bypass channels may simply comprise of adjacent low-lying areas or old river courses. Typically, control structures may be located at the head of the diversion channel to divert flows during periods of high water and return flows after the flood has passed. Flood bypass channels are often used in urban areas where it is not possible to widen the existing channel due to development.

Design considerations for flood bypass channels include:

- Determination of the percentage of the flood flow that should be carried by the bypass channel;
- Design of appropriate controls;
- Determination of the size of the channel to convey the design discharge; and
- Design the channel to reduce maintenance.

For effective reduction in the flood stage, the distance between the point of diversion and point of return to the main channel must be of sufficient length to prevent backwater effects. Additionally, it is essential to consider potential morphologic effects on both the main channel and receiving channel.

Flood bypass channels generally have steeper slopes than the main channel and this may lead to stability problems such as erosion of the channel bed and banks. The bed of tributary channels may be higher than that of the floodway channel, and bed degradation may migrate upstream of the tributary, resulting in excessive sediment transport and deposition in the floodway. Methods to mitigate channel instability such as grade control, channel lining and bank stabilisation may be required on diversion projects.

Additionally, diversion flows can adversely impact the main channel. If the flow rate is reduced in the main channel due to a diversion then, noting that the main channel slope and particle size remain constant, the sediment transport capacity of the main channel will decrease. This, in turn, could lead to aggradation in the main channel between the point of diversion and the point of re-entry. However, if excess bed material is diverted, the sediment transport capability of the stream may increase with the resultant rise in channel instability. Flow returning to the main channel from a diversion can also result in accelerated erosion of the channel and banks around the point of re-entry. Therefore, it is essential to conduct a detailed geomorphic and sediment transport analysis at the design stage of a diversion project, accounting for potential problems.

There are many environmental benefits of using a flood bypass channel as an alternative to modifying the main channel to convey flood flows. The original stream substrates and meanders are maintained, as well as in-stream cover and riparian vegetation. If designed only for occasional flood flows, the bypass channel can have multiple social and lifestyle benefits such as an urban greenbelt or sports and recreation areas.

One major application of flood bypass channels lies in reinstating meandering channels. Many previously meandering rivers in Australia are artificially straightened, thereby increasing the gradient of the river channel. The effect of this is to increase the conveyance of the river channel, thereby improving the drainage of the land and reducing the frequency and duration of overbank flooding. The consequences include deepening and widening and consequent instability of the main channel and a major decline of ecological function.

Where the original meanders are still available, there is a significant focus on redirecting the river channel flow back into the meanders, thereby *renaturalising* the river. Normally, however, the meanders have a significantly reduced flow capacity since they were filled up significantly during the years that the river has been straightened. For this reason, the straight alignment of the river can be treated as a flood bypass channel during the passage of large floods. This is achieved by introducing a weir into the straight bypass channel that overtops when the flow exceeds a predetermined value.

Figure 6.3.1 shows a schematic of the arrangement of a meander, floodway and weir.

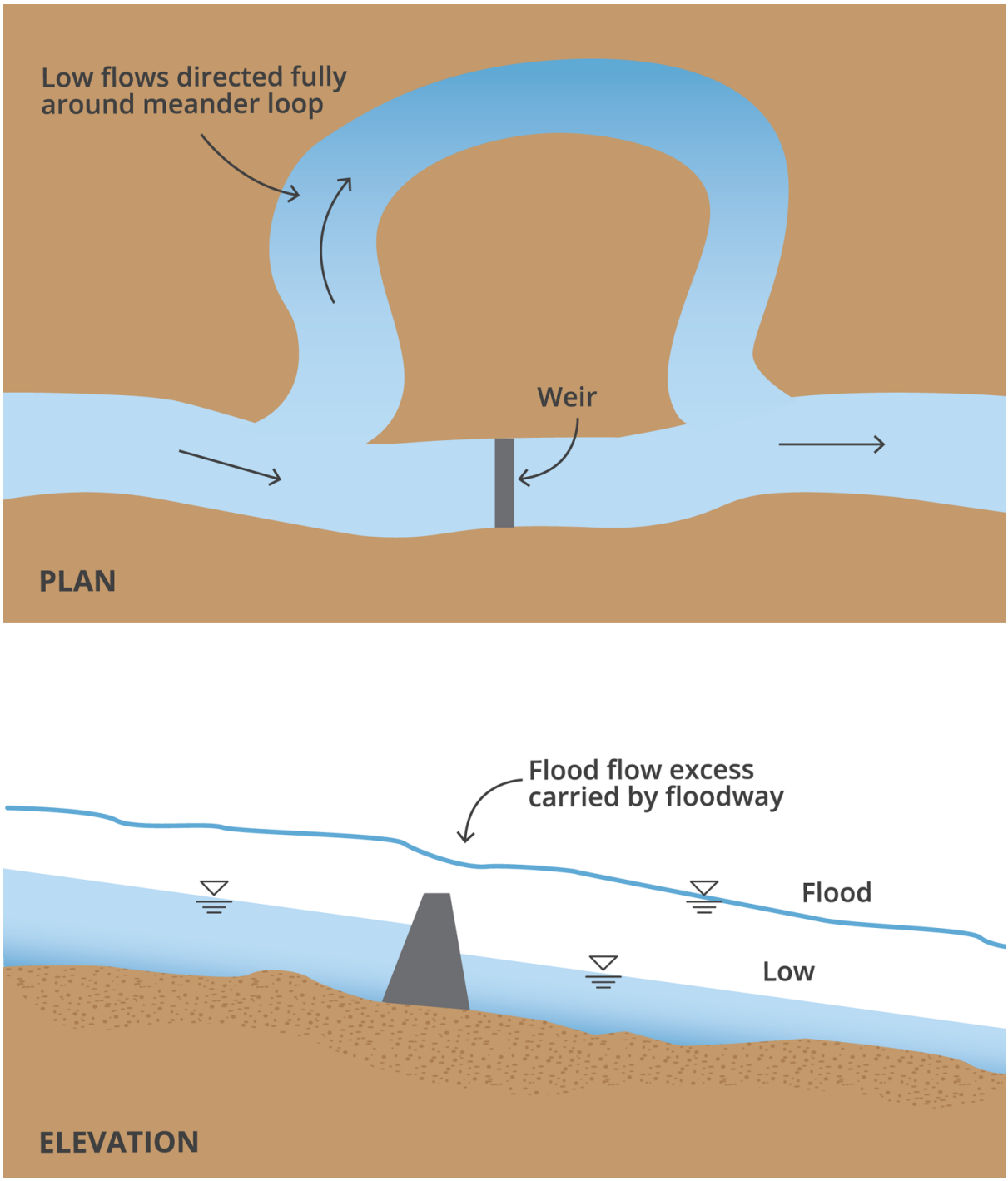


Figure 6.3.1. Schematic of Meander, Floodway, and weir

The design of this system requires careful consideration of the weir under drowned conditions. Under low flow conditions the weir directs all river flow around the meander. However, for a given design flood, the floodway and weir must pass all of the flow in excess of the capacity of the meander.

Keller (1995) has developed the theoretical analysis of the drowned weir. The analysis has been verified by experimental studies in the laboratory and with limited field data by Keller et al. (2012). The design process is assisted by the use of a spreadsheet based program described by Keller et al. (2012).

In summary, the design of a flood bypass channel must be aimed at preventing channel instability in the main channel and the diversion channel. Channel design must take into account the design flows and sediment transport to ensure bed and bank stability. The hydraulic design of flood bypass channels can be accomplished with standard hydrology and hydraulics analysis techniques, while determinations of sediment transport through the diversion are much more difficult.

# 3.3. Control structures – Gates, weirs and flumes and spillways

## 3.3.1. Sluice gates and other control gates

Sluice gates are used to control the river flow, artificial channels and are sometimes referred to as underflow gates because the flow passes under the gate and control is exercised by lowering the gate. In addition to controlling the flow rate, gates can be used for flow measurement if they are calibrated by field measurement or by model testing. Figure 6.3.2 shows three different types of underflow gates – the vertical sluice gate, the radial (or Tainter) gate, and the drum gate.

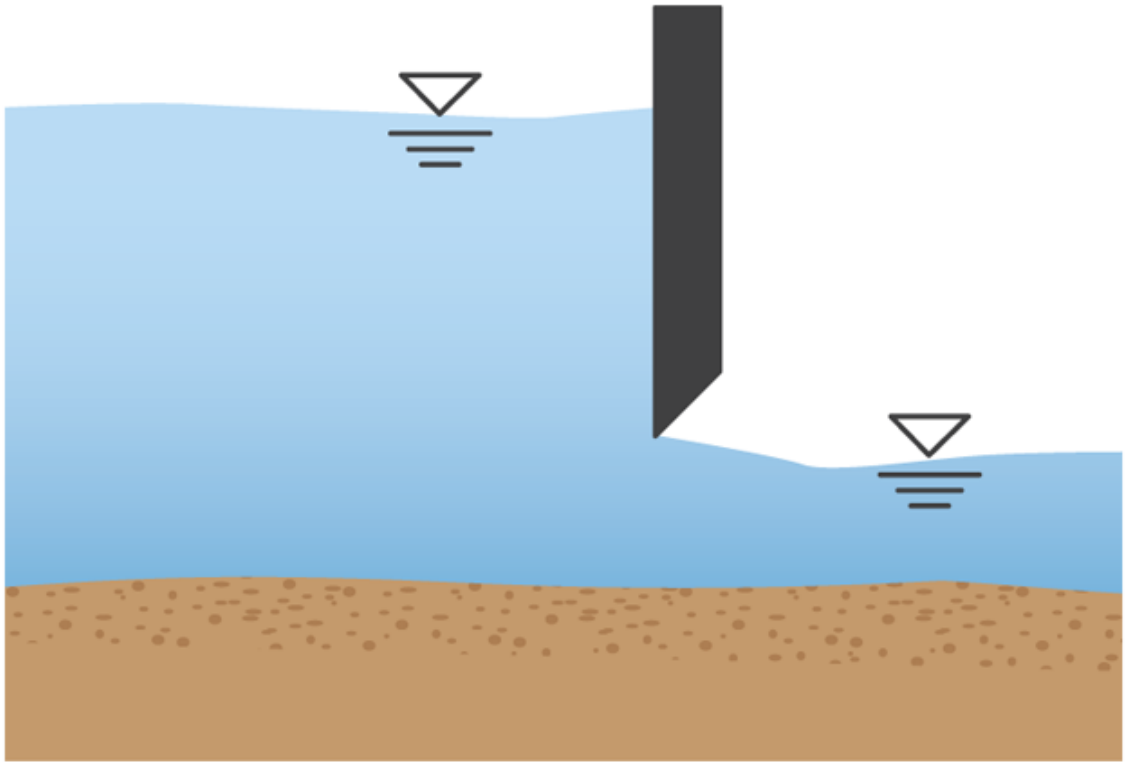

(a)

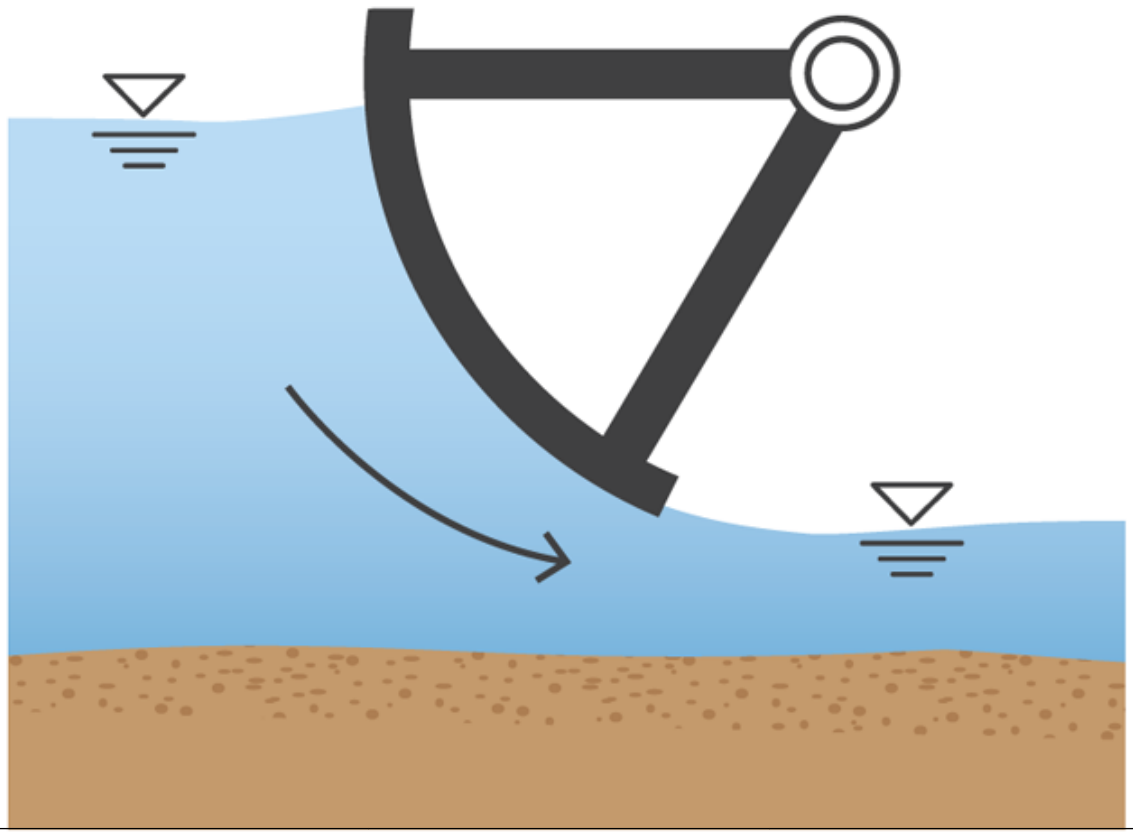



(b)

The choice of gate in a particular situation depends on a number of factors. The vertical sluice gate is the simplest to construct, but has the disadvantage of requiring an expensive guide system to transmit the hydraulic thrust to the side-walls. The radial gate is better in this case because the thrust is carried through the radial arms upto the hinge. Drum gates are hollow gate sections that float on water and are pinned to rotate up or down. Water is allowed into or out of the flotation chamber to allow the gate to, respectively, fall or rise.

Flow through an underflow gate may be classified as free outflow or submerged outflow and the analysis for each is different.

## 3.3.2. Free Outflow

Free outflow conditions occur when the issuing jet of supercritical flow is open to the atmosphere and this is shown schematically in Figure 6.3.3.

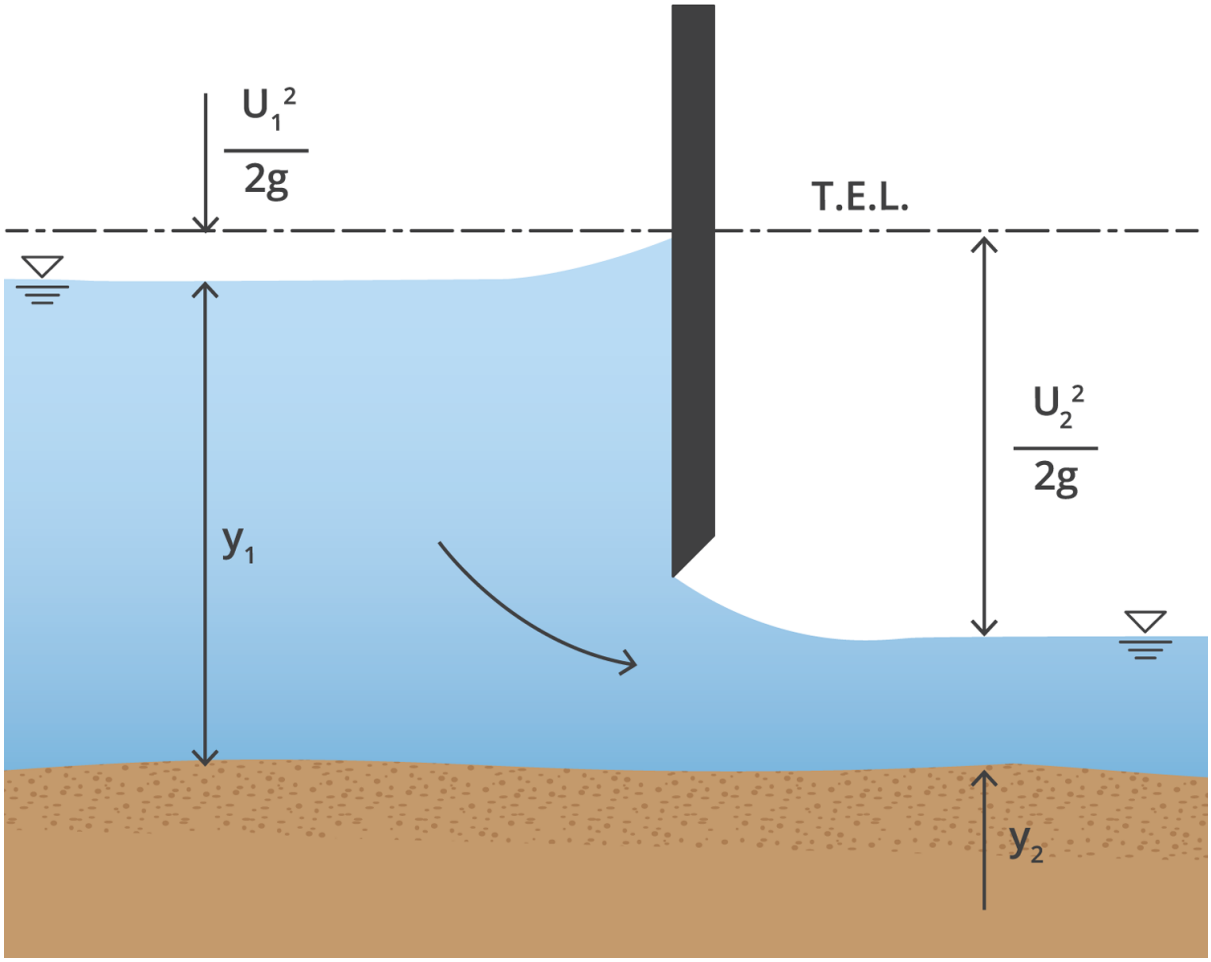


Figure 6.3.3. Schematic for flow under a Sluice Gate

The sluice gate is a case of rapidly varied flow in which large variations in depth and velocity occur over a short length of channel. Furthermore, because the flow contracts smoothly under the gate with a minimum of turbulence, energy losses are negligible and the energy level can be assumed to be the same on both sides of the gate.

For a rectangular channel with a horizontal bed and of uniform width, it can be shown – Henderson (1966) that:

$$Q = C_c wB\sqrt{2gy\frac{y_1}{y_1 + y_2}} \tag{6.3.1}$$

where $C_c = \frac{y_2}{w}$

Equation (6.3.1) is then written as:

$$Q = C_d wB\sqrt{2gy_1} \tag{6.3.2}$$

where $C_d = \sqrt{\frac{C_c}{1 + \frac{C_c w}{y_1}}}$

The contraction coefficient, $C_c$ typically has the value of 0.611. However, for increased values of the ratio $w/y_1$, the value decreases slightly.

The same analysis can be undertaken for the radial gate. In this case, however, the contraction coefficient, $C_c$, varies significantly depending on the angle that the gate lip makes with the horizontal. To an accuracy of 5%, the contraction coefficient is given by:

$$C_c = 1 - 0.75\theta + 0.36\theta^2 \tag{6.3.3}$$

where the unit of θ is 900.

Equation (6.3.3) shows that $C_c$ has the value of 0.61 for θ = 1 ($90^0$), which is the value used for the vertical sluice gate.

## 3.3.3. Drowned Outflow

A schematic of a drowned vertical sluice gate is shown in Figure 6.3.4. The depth $y_2$ is produced by the gate, and the depth $y_3$ is produced by some downstream control. It is clear that if $y_3$ is greater than the subcritical depth required to form a hydraulic jump with $y_2$, then the gate outlet must be drowned; a condition where subcritical flow impinges on the downstream side of the gate. The effect is that the jet of water issuing from beneath the gate is overlaid by a mass of water which, although strongly turbulent, has no net motion in the longitudinal direction.

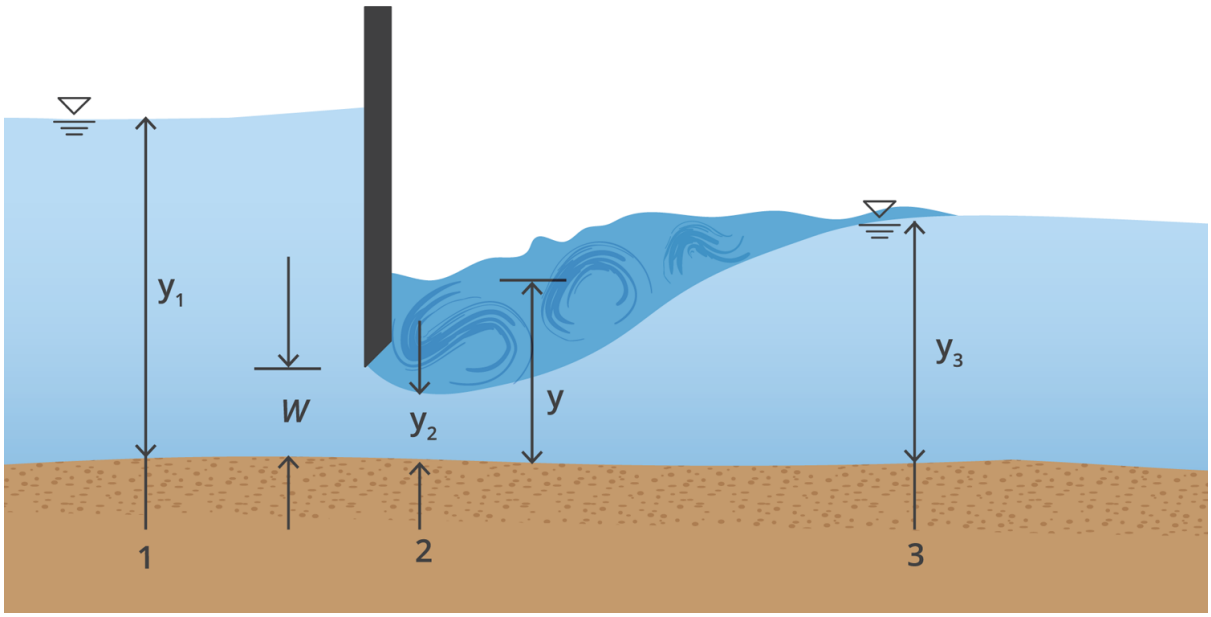


Figure 6.3.4. Schematic of Drowned Vertical Sluice Gate

An approximate analysis can be made by treating the case as one of *divided flow*, in which part of the flow section is occupied by moving water, and part by stagnant water. While there will be some energy loss between Sections 1 and 2, a much greater proportion of the total loss will occur in the expanding flow between Sections 2 and 3. The approximation enters when it is assumed that all of the energy loss occurs between Sections 2 and 3, where the momentum equation is utilised.

This procedure, developed in Henderson (1966), leads to two independent equations with two unknowns – q and y.

The solution for drowned gates in non-rectangular channels follows the same basic methodology although the computations are more complex.

The methodology has been tested experimentally and shown to predict the flow rate within 5%.

## 3.3.4. Weirs and flumes

Weirs and flumes are often used for flow measurement, as noted in the section of this chapter on Flow Measurement Structures. However, since the design of these structures involves application of a known relationship between flow rate and water surface elevation, they can also be employed as control structures – used to control the water level or water level range, for a given flow rate or flow rate range.

In this context, the structure design follows the same procedure as developed earlier. In particular, broad-crested weirs are robust structures that span the full width of the channel and are normally constructed of reinforced concrete. Especially for flow control in relatively large rivers, they are preferred over sharp-crested weirs, which can be easily damaged. Furthermore, because it is a critical depth meter, the broad-crested weir has the advantage that it operates effectively with higher downstream water levels than a sharp-crested weir.

For relatively small open channels, the long-throated flume is a better alternative than a weir and is capable of measuring relatively large flows. It is basically a width constriction that, in

plan, a rounded converging section, a parallel throat section, and a diverging downstream section. It is typically constructed of concrete.

The design of a long-throated flume requires some compromise between ensuring that the throat is narrow enough to control the flow without submergence, but not so narrow that it creates unacceptable afflux.

As noted in this chapter on Flow Measurement Structures, the analysis of both the broad-crested weir and the long-throated flume is identical as both rely on the relationship between the upstream water level (which may be measured) and critical depth within the constricted section, which is a known function of the flow rate. Thus, a unique relationship between flow rate and upstream water surface elevation can be determined.

## 3.3.5. Spillways

Flow behaviour on spillways has been investigated extensively by the US Army Corps of Engineers Waterways Experiment Station since the early 1950s (USACE: Water Ways Experiment Station, 1952). Hydraulic design charts and a Manual of Practice (USACE, 1995) have been prepared, enabling the design of a spillway profile and a water surface profile for a given design flood condition. However, the design charts are only applicable for certain types of spillway profiles and pier configurations and cover a limited range of flood levels.

In the past, this limitation was overcome by building scaled physical models to investigate the flow behaviour. These models tended to include both the spillway and any associated energy dissipation structure. Physical models are considered later in the chapter. More advanced mathematical models may also be appropriate, which are also discussed later in this Book.

A spillway is ideally designed so that, when operating at its design head, the pressure at the spillway surface is atmospheric. Consequentially, when the reservoir level is below or above the design flood level, the pressure over the spillway will be above or below atmospheric respectively. In the latter case, the negative pressures may create unstable conditions on the spillway surface and damage due to cavitation.

Existing dams and spillways in Australia were designed and constructed to handle estimated design floods. Since their construction, the increase to and reanalysis of, hydrological data have led in many cases to a revision upwards of the design floods, requiring major upgrades to spillway capacity.

To select optimum upgrade design, many dam owners have needed to consider the most cost-effective way to analyse the behaviour of the spillway flow under conditions of increased maximum flood. In many cases, as in the original design, use has been made of physical scale models.

With appropriate recognition of scale effects, physical models have been the upgrade design method of choice. However, the use of numerical methods is attractive in terms of lower cost and substantially reduced preparation time. Additionally, results can be obtained throughout the flow domain rather than at selected monitoring locations.

### 3.3.5.1. Design

A spillway is sized to provide the required capacity, usually the entire spillway design flood, at a specific reservoir elevation. This elevation is normally at the maximum operating level or at a surcharge elevation greater than the maximum operating level. Hydraulic design of a

spillway usually involves four conditions of flow, each occurring at a different location as follows:

1. Subcritical flow in the spillway approach, initially at a low velocity, accelerating, however, as it approaches the crest.

2. Critical flow as the water passes over the spillway crest.

3. Supercritical flow in the chute below the crest.

4. Transitional flow at or near the downstream end of the chute where the flow must transition back to subcritical, typically with the dissipation of large amounts of energy.

When a relatively large storage capacity can be obtained above the normal maximum reservoir elevation by increasing the dam height, a portion of the flood volume can be stored in this reservoir surcharge space and the size of the spillway can be reduced. The use of a surcharge pool for passing the spillway design flood involves an economic analysis that considers the added cost of a dam height compared to the cost of a wider and/or deeper spillway. When a gated spillway is considered, the added cost of higher and/or additional gates and piers must be compared to the cost of additional dam height.

When an un-gated spillway is considered, the cost of reduced flood-control benefits due to a reduction in reservoir storage must be compared to the cost of additional dam height.

Chute design and stilling basin design are considered in particular in the following sections.

## 3.3.5.2. Chute Design

The basic principle used to analyse steady incompressible flow on a chute spillway is the law of conservation of energy expressed by the Bernoulli equation. This equation has been developed elsewhere in this chapter. Herein, the issues consequent to the (generally) steep spillway slope are considered.

The elevation of the hydraulic grade line is typically given by:

$$HGL = z + y_1 \tag{6.3.4}$$

where z is the elevation of the bed above datum

$y_1$ is the depth of flow, normal to the channel bottom

Strictly speaking the second term on the right hand side should be replaced by $y_1\cos\theta$ where θ is the slope of the channel bottom. Additionally, the form of Equation (6.3.4) assumes that the pressure distribution at the point under consideration must be hydrostatic. This is a valid assumption if vertical accelerations are small and the bed slope is mild. A non-hydrostatic pressure distribution will occur whenever the value of cos2θ departs materially from unity, such as on a steep spillway slope. This does not mean that the energy equation cannot be used on a steep slope. It does mean, however, that the designer must recognise that the values derived from the energy equation become increasingly inaccurate as the value of cos2θ departs further from unity. This conditions describes one of the basic reasons that physical model studies may be required when designing a spillway.

When applying Equation (6.3.4) to spillway design, correct account should be taken of energy loss on the spillway surface. This has three components - boundary roughness (friction), turbulence resulting from boundary alignment changes (form loss), and boundary

layer development. Boundary roughness is normally dealt with using a standard friction loss equation such as Manning's equation. For information on the other two loss terms, reference should be made to (USACE, 1995).

## 3.3.5.3. Stilling Basin Design

The transition of flow from supercritical on the chute to subcritical usually involves considerable energy dissipation. Dissipation of hydraulic energy is accomplished by various methods such as the hydraulic jump, impact, dispersion, etc. The type of energy dissipator used is dependent upon factors that include site geology, the type of dam structure, and the magnitude of the energy to be dissipated. The design discharge for effective energy dissipation is frequently set at the standard project flood rate; however, each facility must be evaluated, and the design discharge used should be dependent upon the damage consequences when the design discharge is exceeded.

Hydraulic jump stilling basins are structures located downstream of chutes, gates and spillways to dissipate excess kinetic energy. The dimensions of these structures depend on the length of the hydraulic jump and the conjugate depth of the jump.

Peterka (1978) classified the hydraulic jump into five categories based on the value of the upstream Froude number. On the basis of extensive experimental studies, he developed four types of hydraulic jump stilling basins. These are now known as the USBR Type 1, 2, 3, and 4 Basins. A major focus of the development of these basins was to reduce the size of the structure by forcing the jump to occur using blocks and end sills within the basin. In addition to localising the hydraulic jump, the Type 4 basin is designed for the special purpose of wave suppression and is not considered herein.

The Type 1 Basin is a classic hydraulic jump basin without baffle blocks or an end sill. It is a relatively large structure and is suitable only for small upstream Froude numbers.

When the Froude number is greater than 4.5, Type 2 or Type 3 Stilling Basins are recommended. The Type 2 basin incorporates a series of chute blocks at the upstream end of the basin to stabilise the start of the jump and to feather the incoming jet into several jets. At the downstream end, a continuous or dentated sill is present, designed to force the jump to occur within the basin and to prevent it from moving downstream. Figure 6.3.5 shows a schematic of the Type 2 Basin. In this figure, $y_2$ is the required conjugate downstream depth.

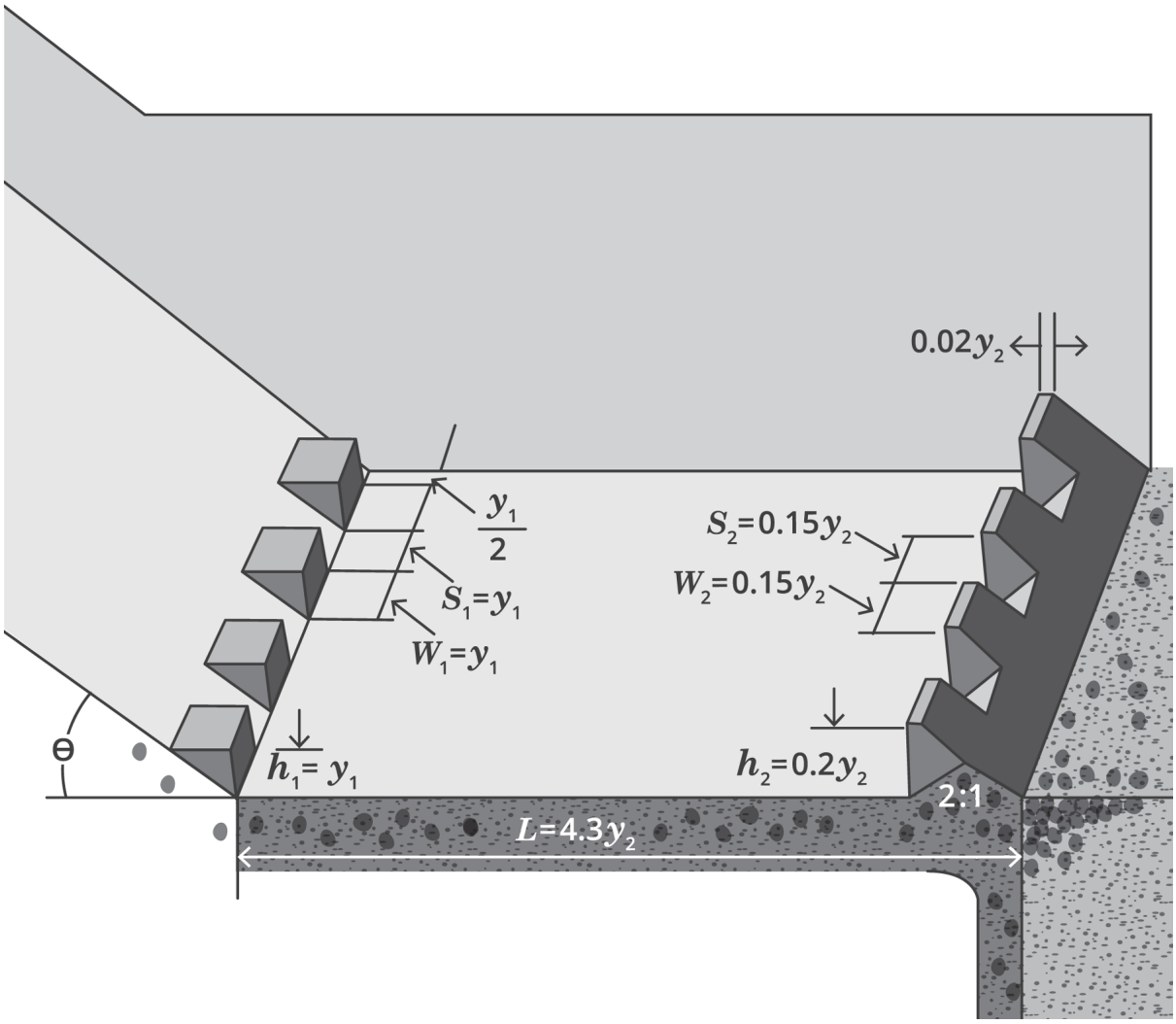


Figure 6.3.5. Schematic of USBR Type 2 Stilling Basin

The length of the Type 2 basin is less than the length for the Type 1 basin.

The Type 3 stilling basin is similar to the Type 2 basin but baffle blocks are included to provide additional energy dissipation by direct impact, increased turbulence and consequent mixing of the high velocity incoming jets into the water body of the basin. This results in a required basin length that is up to 60% shorter than a Type 1 basin for the same flow conditions. However, it should be noted that the presence of the baffle blocks can create conditions of cavitation in their vicinity with consequent severe structural damage. For this reason the Type 3 basin should not be used in conditions where the incoming velocity exceeds 16m/s. Figure 6.3.6 shows a schematic of a Type 3 Basin.

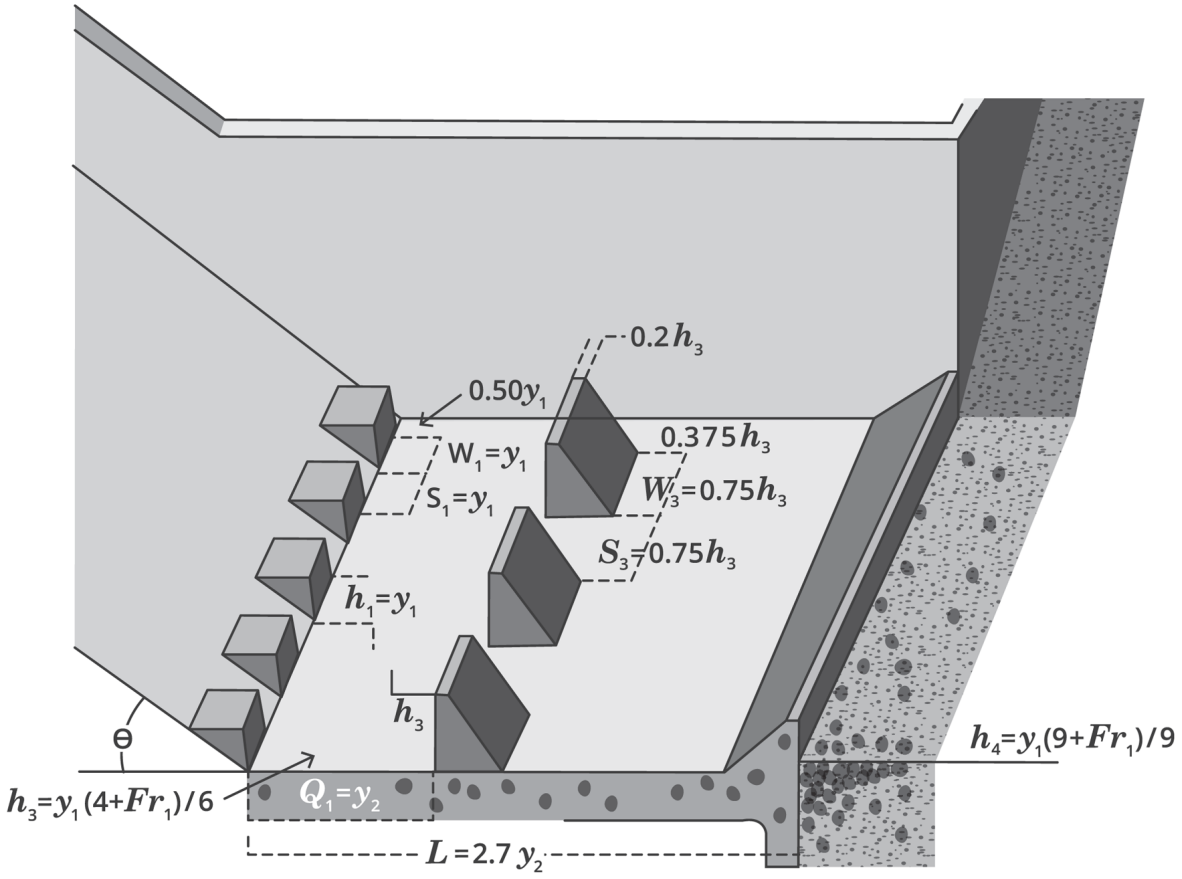


Figure 6.3.6. Schematic of USBR Type 3 Stilling Basin

## 3.4. Levees

Levees are embankments that are constructed to artificially increase the capacity of a channel, confining high flows that otherwise would overtop the banks and spread over the floodplain. Levees are key components of a flood control plan to protect communities and agricultural areas within the floodplain. Levees are used in conjunction with reservoirs, floodways, control structures and various channel modification activities to reduce and control the extent and duration of flooding.

The design elevation of levees is based on containing a design discharge, generally for a short period of time. The levee cross section is generally designed as a trapezoid, with an access road running along the levee crown. To control seepage, a long, tapering berm may be extended on the landside of the levee as subsequently discussed. Fill material for levees is generally obtained locally from borrow areas adjacent to the riverside of the embankment. Although the local materials may not be ideally suitable for construction, economic necessity normally dictates its use.

On streams without levees, flood flows spread out over the floodplain. The floodplain acts as storage for the additional flows, lowering the peak of the flood hydrograph. The construction of levees decreases the floodplain storage, resulting in an increase of the peak of the hydrograph. Furthermore, because levees typically confine river flows to a narrower cross section, water elevations are higher during flood flows. If levees are not set back from the main channel, the hydraulic connectivity between the river and the floodplain is lost, thus confining flows and putting more energy into the flow. The required levee height can be

determined using industry-standard analysis programs such as HEC-RAS. Frequently it is useful to compare the water surface elevations for a river without levees and with levees to evaluate the cost-benefit of levee construction.

Channel instabilities may arise from streams with levees because degradation of the bed and banks may occur. Sometimes, aggradation may occur due to the increased sediment load in the main channel and the lack of available floodplain sediment storage. The precise response is complex and is a function of the width of levees, the effects on duration of flows, and other factors.

Seepage is a major problem with levees during time of high water. When water is contained on one side with the other side being dry, a head differential exists across the levee. This tends to force water through the porous soil, eventually seeping out to the landward side of the levee. This seepage carries both fine and coarse particles through the levee. This internal erosion of the levees can lead to piping through the levee and catastrophic failure.

To prevent excessive seepage, impervious barrier materials such as clay can be built into the levee. Flows from tributaries that are cut off from the river system due to levees must be carefully assessed to prevent flooding on the landward side of the levee. Pumping stations can be applied to divert tributary flows.

On streams without levees, flows periodically flow onto the floodplain depositing sediment, flushing riparian aquatic environments, and generally providing valuable habitat for aquatic organisms and waterfowl. The flora and fauna are adapted to periodic flooding and the unique environment that it creates. As noted above, levees act as a barrier for overbank flows. Confining stream flows within a levee system creates a dryer environment on the landside of the levee system and a wetter environment on the streamside.

The dryer environment results in changes in both flora and fauna that occupy the floodplain. After a levee system is constructed, upland trees and vegetation colonise the floodplain. The lands between the levee and the stream bank will experience more prolonged flooding with more extreme fluctuations in water level. This may inhibit the growth of ground cover, thus reducing the available habitat for ground-dwelling mammals (Fredrickson, 1979). Frequently, for reasons of economy, material used to construct the levees is sourced from areas within the floodplain, resulting in vegetation removal and loss of habitat. The flat slopes used for levees in rural areas require large land requirements for the embankments and berms.

To offset changes in riparian habitat, consideration can be given to the habitat provided by the levees themselves and the adjacent borrow pits. Traditionally, the vegetation on levees is kept to a minimum. However, with proper maintenance, certain species of shrubs and plants can be allowed to grow without affecting the integrity of the levee. However, this vegetation may provide habitat for burrowing animals that must be controlled.

Borrow pits remaining from levee construction can serve as valuable aquatic habitat. Normally, the pits will fill with rainwater or groundwater after construction. Riverside borrow pits will exchange water with the river system, thus recharging the pit with fish and other aquatic organisms. In this way, borrow pits partially compensate for the loss of aquatic habitat in the floodplain. Additionally, siting levees further from the channel will conserve wetland environments between the levee and the river.

Levees must be periodically inspected and maintained to provide the designed degree of flood protection. Conditions affecting the integrity of the levee include erosion of the banks, seepage, and damage from burrowing animals. Vegetation planted on the levees for aesthetic reasons should be well maintained. Vegetation that may affect the integrity of the levee should be removed.

Seepage beneath the levee foundations is one of the principal causes of levee failure. Without control, this seepage may result in excessive hydrostatic pressures beneath an impervious top stratum on the landside, sand boils, and/or piping beneath the levee itself. Seepage problems tend to be most acute in situations where the levee is built above a pervious substratum, which extends both landward, and riverward of the levee and where a relatively thin top stratum exists on the landside of the levee.

Among seepage control measures are cutoffs, riverside blankets, and landside seepage berms.

## 3.4.1. Cutoffs

A cutoff beneath a levee to block seepage through pervious foundation strata is the most positive means of eliminating seepage problems. A cutoff may consist of an excavated trench backfilled with compacted earth or slurry. Trenches are usually located near the riverside toe.

To be effective, a cutoff must penetrate at least 95 percent of the thickness of the pervious strata to be effective. For this reason cutoffs are rarely economical where they must penetrate more than about 12 m. Steel sheet piling can significantly reduce the possibility of piping of sand strata in the foundation, but is not always entirely watertight due to leakage at the interlocks between individual sheet piles.

## 3.4.2. Riverside Blankets

Levees are frequently situated on foundations having natural covers of relatively fine-grained soils overlying pervious sands and gravels. These surface strata constitute impervious or semi-pervious blankets when considered in connection with seepage control. If these blankets are continuous and extend riverward for a considerable distance, they can effectively reduce seepage flow and seepage pressures on the landside of the levee.

Where seepage beneath the levee is expected to be a problem, riverside borrow operations should be limited in depth to prevent breaching the impervious blanket. If there are limited areas where the blanket becomes thin or disappears entirely, the blanket can be remediated by placing impervious materials in these areas. The effectiveness of the blanket depends on its thickness, length, distance to the levee riverside toe, and permeability and can be evaluated by flow-net or approximate mathematical solutions (USACE, 2000). Protection of the riverside blanket against erosion is important.

## 3.4.3. Landside Seepage Berms

If uplift pressures in pervious deposits underlying an impervious top stratum landward of a levee become greater than the effective weight of the top stratum, heaving and rupturing of the top stratum may occur, resulting in sand boils. The construction of landside berms (where space is available) can eliminate this hazard by providing the additional weight needed to counteract these upward seepage forces. Furthermore, the berm can provide the additional length required to reduce uplift pressures at the toe of the berm to acceptable values. Seepage berms may reinforce an existing impervious or semi-pervious top stratum, or, if none exists, be placed directly on pervious deposits. A berm also affords some protection against degradation of the landside levee slope.

Berms are relatively simple to construct and require very little maintenance. They frequently improve and reclaim land as areas requiring remediation treatment for seepage are often low

and wet. Because they require additional fill material and space, they are used primarily with agricultural levees where land use pressures are less severe than in urban areas.

Subsurface profiles must be carefully studied in selecting berm widths. For example, where a levee is founded on a thin top stratum and thicker clay deposits lie a short distance landward, as shown in Figure 6.3.7, the berm should extend far enough landward to lap the thick clay deposit, regardless of the computed required length. Otherwise, a concentration of seepage and high exit gradients may occur between the berm toe and the landward edge of the thick clay deposit.

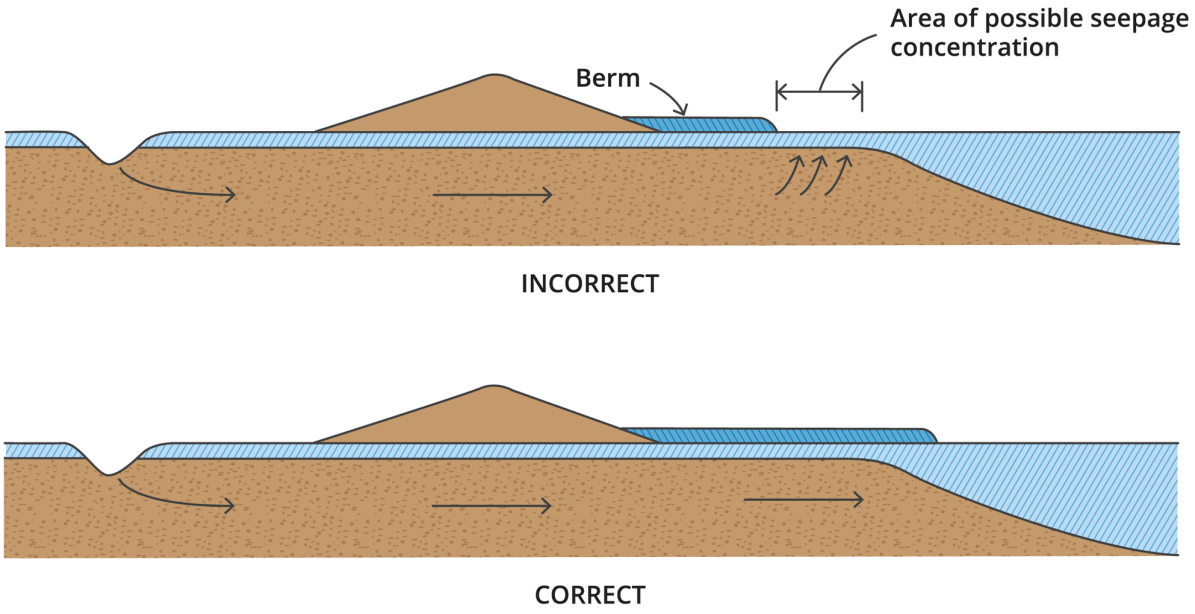


Figure 6.3.7. Example of incorrect and correct berm length according to existing foundation conditions (USACE, 2000)

In summary, levees are embankments that artificially increase the capacity of a channel, confining high flows that otherwise would overtop the banks and spread over the floodplain. They are key components of a flood control plan to protect communities and agricultural areas within the floodplain.

Seepage is a major problem with levees during high water and is one of the principal causes of levee failure. When water is contained on one side with the other side being dry, a head differential exists across the levee. Without control, this seepage may result in excessive hydrostatic pressures beneath an impervious top stratum on the landside, sand boils, and/or piping beneath the levee itself.

Among seepage control measures are cutoffs, riverside blankets, and landside seepage berms.

# 3.5. Culverts

## 3.5.1. Culvert Flow Principles

The term *culvert* is normally applied in engineering practice to any large underground pipe especially where used in relatively short lengths to convey streams or flood water under an embankment. The design of culverts has been the subject of considerable research and considerable misunderstanding. Despite this, the culvert is such a common structure that

analysis and design have become quite standardised. The hydraulic analysis and subsequent selection of the proper culvert size is aided by charts and nomographs prepared for the specific shape and type of culvert. These design procedures incorporate directly such factors as the entrance loss coefficient for a particular pipe shape and inlet configuration.

The emphasis herein is on the basic analysis of culverts and is, thus, more general than direct recourse to design charts. It is accepted, of course, that engineers will continue to use the available charts and nomographs. However, the material presented herein is aimed at giving a better understanding of culvert flow principles and will make the use of standard charts and nomographs clearer and more reliable.

Because a culvert is a closed conduit, it has a larger wetted perimeter than a channel. Accordingly, the average energy gradient through the culvert will be steeper than in the equivalent length of channel. In general, the only way that the steepening of the hydraulic gradient through the culvert can occur is by raising the water surface elevation at the upstream side of the embankment.

However, the headwater level cannot be increased indefinitely without severe consequences. The consequent backwater effect may cause water to overflow the channel banks and cause flooding of the surrounding land. This may have severe social and economic repercussions. There are, however other less obvious consequences of an increase in the upstream water level such as bank stability, scour of the earth embankment, and erosion of downstream channel.

It is apparent, then, that the culvert cross-sectional area and hydraulic properties are of great importance. It may be possible to evaluate economically the consequences of a headwater rise against the cost of the culvert and embankment height. Under these circumstances the system with the least total cost of structure and flooding should be selected.

The factor subject to most misunderstanding in culvert design is that arising from the determination of the point of control – either inlet or outlet control. In some cases, the operating control is not clear and careful calculations are necessary to determine both the type of control and the various hydraulic characteristics.

The hydraulic operation of culverts is complex and often difficult to predict. However, once the type of operation is established, the analysis may proceed according to well-defined principles. The factors affecting the discharge in a culvert are the following:

a. The geometry of the inlet.

b. The combined effect of entrance, length, slope and roughness of the culvert barrel.

c. The elevation of the outlet tailwater.

The flow characteristics and, hence, the discharge capacity of a culvert are determined by the location of the control section. In general, the discharge is controlled either at the culvert entrance or at the outlet and is designated inlet control and outlet control respectively. Inlet control will exist as long as the ability of the culvert barrel to carry the flow exceeds the ability of water to enter the culvert through the inlet. Outlet control will exist when the ability of the culvert barrel to carry water away from the entrance is less than the flow than can enter the inlet. The location of the control section may shift as the relative capacities of the entrance and barrel sections change with increasing or decreasing discharge.

**Inlet control:** With the inlet control operation, the discharge is independent of the pipe length, slope and roughness of the pipe wall. The discharge depends only upon the

headwater elevation above the invert at the entrance, the inlet size, and the inlet geometry. Although a variation in factors affecting the culvert barrel will affect flow characteristics within a barrel, they will normally have no effect on the total discharge. The only exception occurs if the variations in barrel design are sufficiently severe to cause the control section to shift to the outlet.

A culvert operating under inlet control will always flow part full for at least part of the culvert length. In many cases, particularly at high discharges, the headwater will submerge the entrance of the culvert. In these cases, flow contraction occurring at the entrance will limit the discharge. It should be noted that roughness, slope and length are not influential in determining the discharge capacity of a culvert operating with inlet control, but are important in determining outlet velocities and the discharge at which the operation mode changes from inlet control to outlet control.

**Outlet control:** Under outlet control, the total discharge is affected by all hydraulic factors upstream of the outlet. These factors include the headwater elevation, entrance geometry, barrel size, wall roughness, barrel length and slope. The tailwater elevation is a factor as long as it is above the pipe outlet.

Culverts flowing full throughout their length are always under outlet control. However, as will be shown, a culvert flowing part full may operate under either inlet control or outlet control.

**Hydraulic Analysis:** For computational convenience, flow through culverts is divided into size categories based on the relative heights of the head and tailwater and, for three of the categories, on barrel slope. The six types of flow are shown schematically in Figure 6.3.8 and their respective characteristics are summarised in Table 6.3.1. In the table, D is the maximum vertical dimension of the culvert, $y_1$ is the depth of flow in the approach section, $d_c$ is the critical depth of flow, and $y_4$ is the tailwater depth of flow.

The limit for $\frac{y_1}{D}$ of 1.5 recommended in Table 6.3.1 is not universally accepted and several texts suggest a limiting value of 1.2. This lower limit is probably more appropriate since it allows for effects of factors such as wave motion or transitory debris blockage for example.

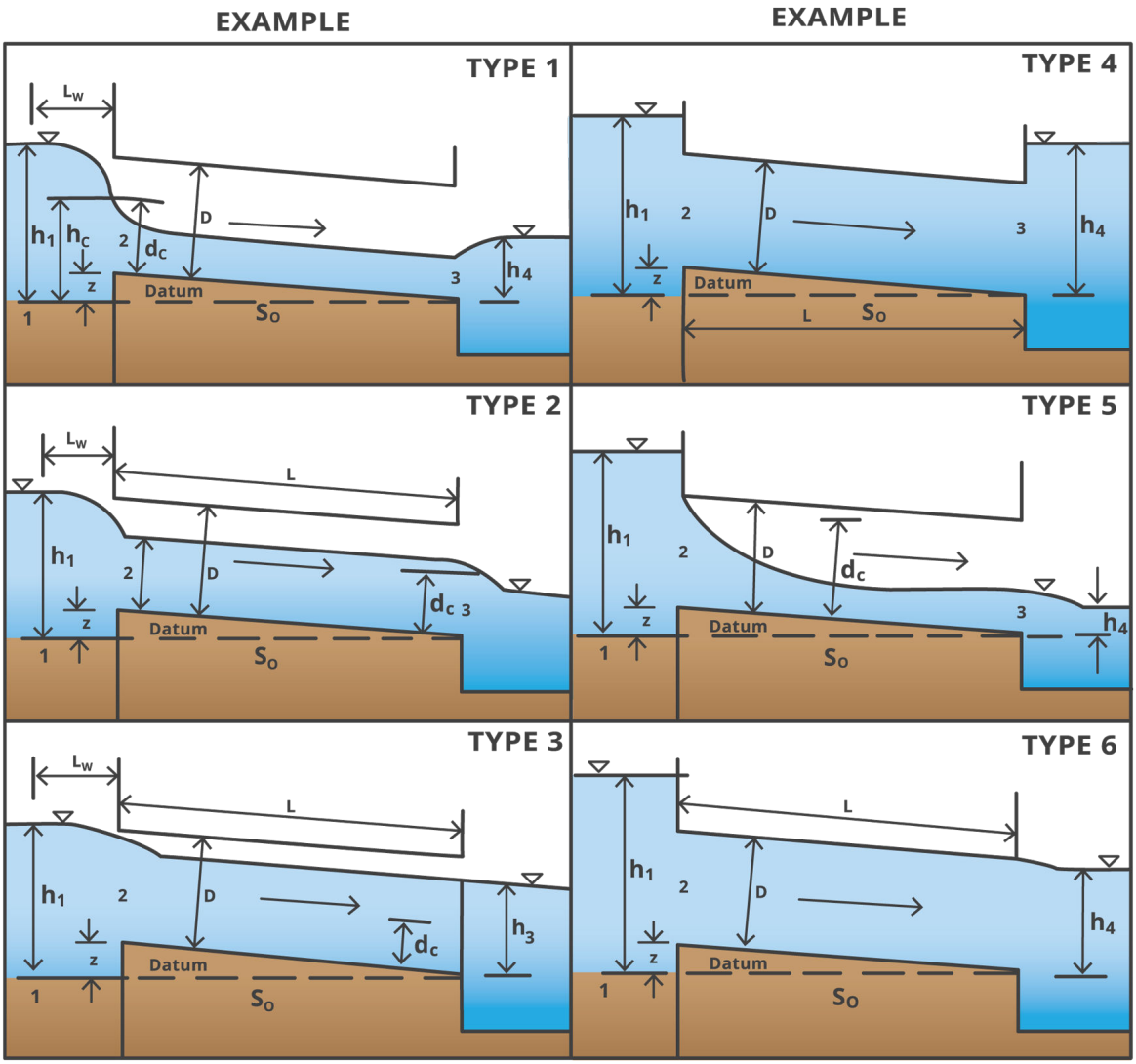


Figure 6.3.8. Culvert Flow Types

Table 6.3.1. Culvert Flow Characteristics

| Flow Type | Culvert barrel flow | Location of downstream section | Control type | Culvert slope | $\frac{y_1}{D}$ | $\frac{y_1}{d_c}$ | $\frac{y_4}{D}$ |
|---|---|---|---|---|---|---|---|
| 1 | Partly full | Inlet | Critical depth | Steep | <1.5 | <1.0 | ≤1.0 |
| 2 | Partly full | Outlet | Critical depth | Mild | <1.5 | <1.0 | ≤1.0 |
| 3 | Partly full | Outlet | Backwater | Mild | <1.5 | <1.0 | ≤1.0 |
| 4 | Full | Outlet | Backwater | Any | | | > 1.0 |

| | | | | | | | |
|---|---|---|---|---|---|---|---|
| 5 | Partly full | Inlet | Entrance geometry | Any | | | ≤1.0 |
| 6 | Full | Outlet | Entrance and barrel geometry | Any | | | ≤1.0 |

Full details of the analysis of each flow type are presented by French (1985).

There are several practical factors associated with culvert design which may be of equal importance as the hydraulic analysis. Some of these aspects are discussed in the following.

## 3.5.2. Inlet Design

Full utilisation of the culvert cross-sectional area requires that it should run full or nearly so. This may not be possible especially in the case of low tailwater levels or steep gradients, leading to flow Type 5. Careful attention is then necessary in the inlet design to ensure minimum contraction of the flow and, hence, a maximum discharge coefficient. The objective is to ensure that the flow traverses the inlet section with a minimum of separation.

A variety of methods are available for improving the inlet conditions and these include a steep throat, a drop inlet, wingwalls, a hood and bevelled edges. The shape of the soffit is the most important and of the invert, the least important, because the flow at the invert is horizontal.

Some of these inlet improvements are illustrated schematically in Figure 6.3.9. The simplest improvement is a vertical headwall above the culvert entrance, thereby eliminating the re-entrant angle in the case of a battered embankment. The soffit of the inlet can be bevelled as shown in Figure 6.3.9(a). It is recommended that the bevel be at least 10% of the culvert height and at between 33° and 45° to the culvert axis (Portland Cement Association, 1964). This can increase the flow by up to 20%.

Full details and design charts and tables for improved culverts inlets may be found in a number of publications (e.g. Portland Cement Association (1964), U.S. Department of Transportation (1972)).

## 3.5.3. Outlet Design

In practice, culvert outlets have little significance in efficient culvert operation.

However, outlet structures have two important practical purposes:

a. to retain the embankment and support the end of the culvert.

b. to prevent damage by scour to the culvert, embankment, stream bed, or adjacent property.

Despite the common practice of making inlet and outlet structures identical, it should be noted that the two structures serve different purposes and, therefore, logically should be treated separately.

A number of different types of culvert outlets are shown in Figure 6.3.10.

The simple projecting outlet is sufficient when flow velocities are low and the filldoes not require special protection. The endwall structure alone acts to support the end of the culvert

and as a retaining wall for the embankment. The wingwall helps to transition the culvert flow smoothly into the downstream channel and protects the endwall so that it may continue to function in its original capacity. A concrete apron serves to provide protection to the endwall structure by removing the point of potential erosion well away from the endwall foundation, thereby ensuring the stability of the structure.

Where wingwalls are used for bank protection and not merely as retaining walls, a concrete apron should always be provided. The absence of such an apron may encourage channelling and undercutting along the wingwall.

Where outlet velocities are particularly high, special energy dissipation structures may be required.

Scour at culvert outlets is not necessarily only due to concentrated flow issuing from the culvert barrel. Recirculating eddies, associated with a downstream channel which is significantly wider than the culvert, can cause potentially serious scour damage to the embankment fill.A further form of scour at culvert outlets is channel degradation which may occur if the culvert does not permit the passage of sediment from upstream.

Whatever the cause, the process of erosion may be associated with the excavated material being redeposited in the channel some distance downstream from the point of scour. It is entirely possible that with time, a shoal will form capable of causing excessively high tailwater depths during periods of high flow. Such a process should always be considered because high tailwater depths may not necessarily work to the advantage of culvert operation.

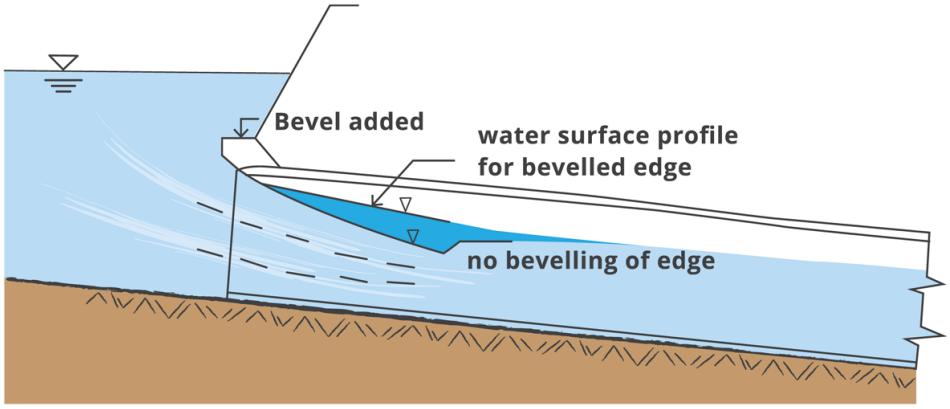


A. BEVELED TOP

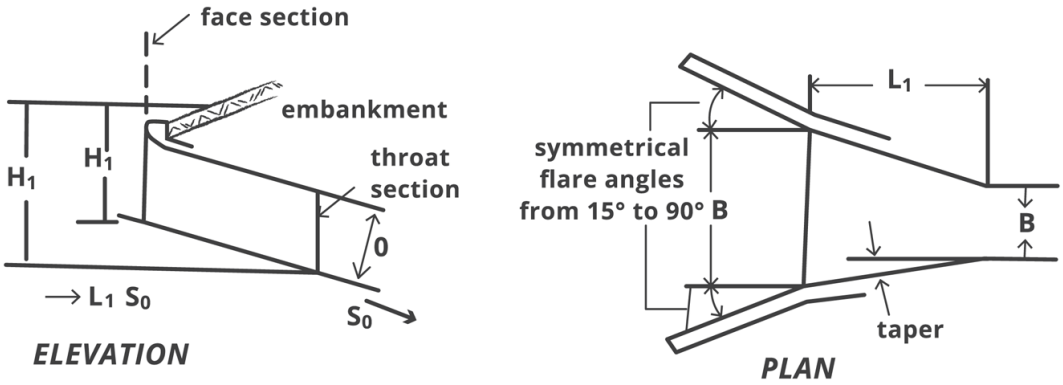


B. SIDE-TAPERED INLET

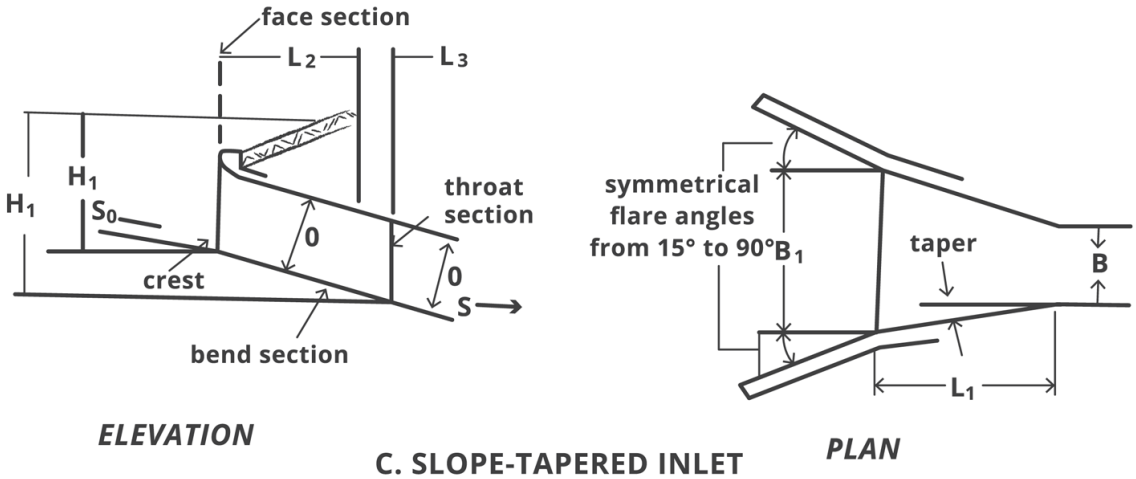


C. SLOPE-TAPERED INLET

Figure 6.3.9. Schematics of Improved Inlets

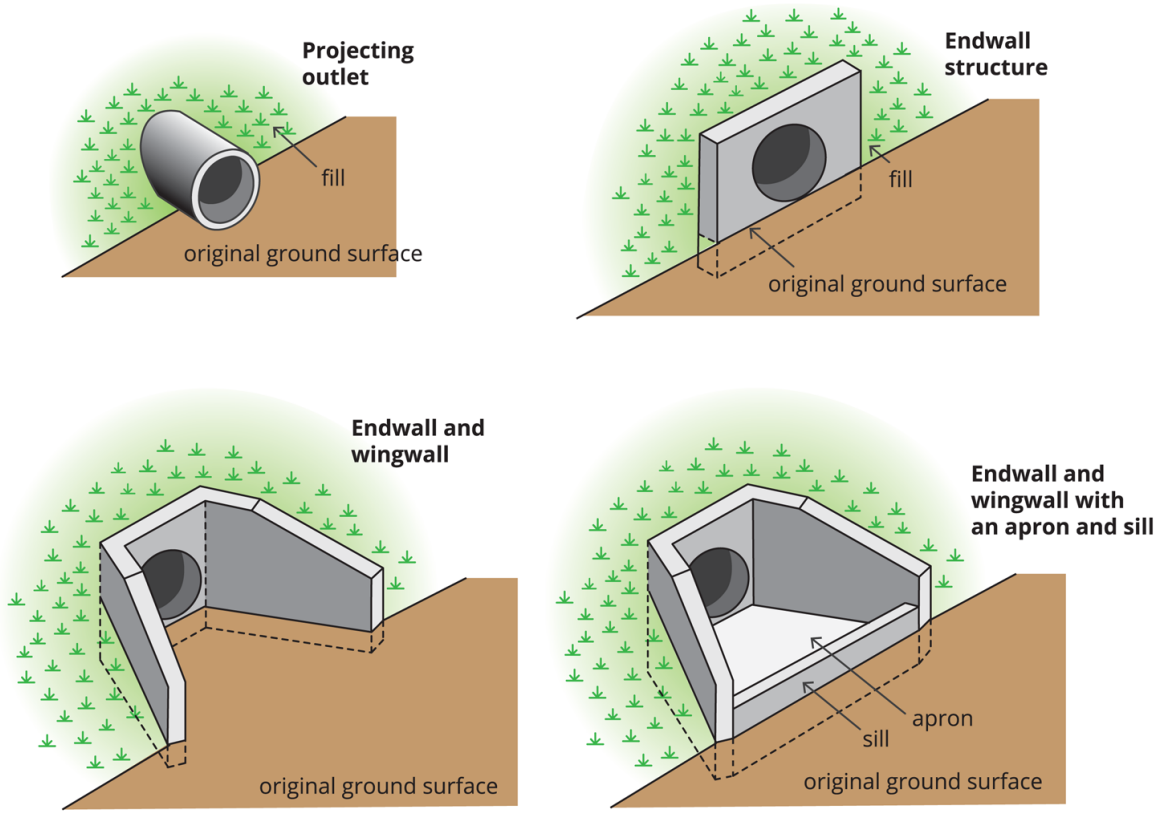


Figure 6.3.10. Examples of Culvert Outlets

Erosive velocities vary widely, depending upon the characteristics of the channel material, the depth of flow in the channel, and the velocity distribution. Erosive velocity limits for various types of soils are published in a number of texts (e.g. Portland Cement Association (1964)). Such published values should, however, be treated with caution because of the vast variations in naturally occurring materials.

Special problems occur in situations where relief culverts discharge directly on to an unchannelled flood plain. In this case, the tailwater level is likely to be significantly lower that the water level of the emerging supercritical jet. The erosive potential in this case is high and a schematic of the flow situation is shown in Figure 6.3.11.

It is apparent that the discharging jet will spread beyond the culvert and energy dissipation additional to bed friction will result from the interaction between the jet and the tailwater. The latter phenomenon is manifested in the zones of recirculation shown in Figure 6.3.11.

One method of analysis for this case has been proposed by Keller (1986). He drew a comparison between this phenomenon and that due to the interaction between shallow flood plain and deep main channel flows where the turbulent shear stresses are of the same order of magnitude as an equivalent wall shear stress if the interaction region were replaced by a solid wall. The present case can then be solved by assuming that the culvert outflow is contained within diverging vertical walls of roughness equal to that of the bed. A divergence angle of about 20° is indicated by the work of Rouse et al. (1951) and List and Imberger (1973). The modification of the outlet velocity with distance from the outlet can then be calculated using a water surface profile program such as HEC-RAS and appropriate invert protection determined.

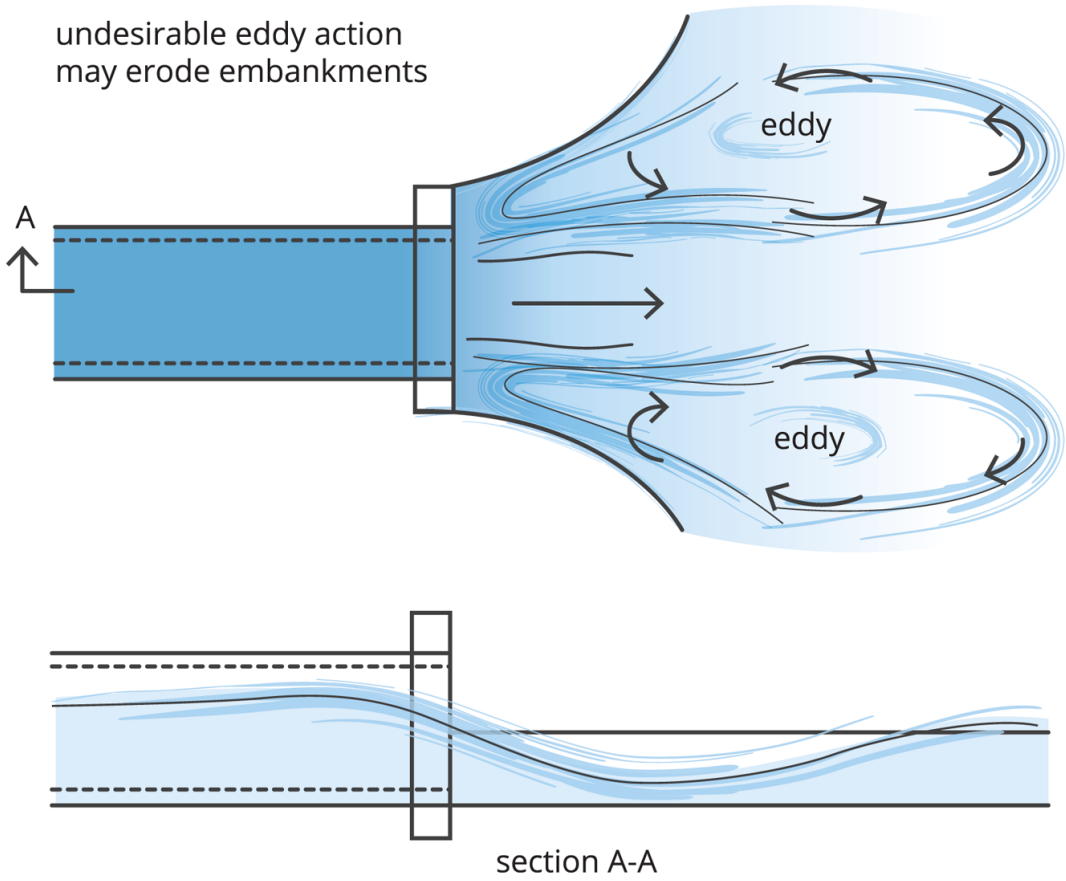


Figure 6.3.11. Schematic of Flow at Unsubmerged Outlet

**Culvert Modeling Using HEC-RAS**

HEC-RAS incorporates a module for the accurate design of culverts. Although the detail is outside the scope of this section, some comments are provided in the following.

Data for the culvert structure is simply entered on two templates in HEC-RAS – the Deck/ Roadway Editor for roadway information and the Culvert Data Editor for the physical data defining the culvert.

Although not required for culvert computations, the modeller may choose to enter embankment side slopes for the upstream and downstream embankment faces in the Deck/ Roadway Data Editor. The sloping embankment is used for graphical purposes only on the cross-section plots.

The primary information for inlet and outlet control analyses is entered in the Culvert Data Editor. For inlet control, these data are the inlet geometry with the corresponding chart and scale numbers. For outlet control computations, the entrance loss coefficient is required along with the Manning's n values for different portions of the culvert cross-section. A table is available to assist the modeller in choosing an appropriate entrance loss coefficient.

The exit loss coefficient defaults to the value 1, but the modeller has the option to adjust this parameter. A tail water elevation is not required because it is computed by HEC-RAS as part of the downstream water surface profile calculations.

# 3.6. Bridge Waterways

## 3.6.1. Introduction

Bridges are a necessary component of waterways that are crossed by roads and other embankment structures. For reasons of economy, bridges do not span the full width of a river, especially when it is in flood. The flow through bridges inevitably, then, involves energy losses that reflect in a higher water surface elevation upstream than would be the case if the waterway could flow freely.

Despite the simple appearance of a bridge, its hydraulics is by no means simple. In addition to the potential for the constricted flow through a bridge site to cause flooding, there is a second issue of importance in the assessment of bridges and this is the issue of scour. Bridges continue to fail through scour of piers and/or abutments and it is vital to be able to determine the magnitude of this scour. Both the energy loss at a bridge site and the potential for scour are complex topics and special techniques have been developed to cope with their difficulties.

It should be noted that conservatism in the design of bridge waterways for their flooding potential requires an under-estimate of the magnitude of scour since this will minimise the size of the bridge opening, maximise the velocity through the bridge, and maximise the energy loss across the bridge. Conversely, conservatism in assessing the structural integrity of the bridge requires an over-estimate of the magnitude of scour. Thus, it is important to keep in mind the reason for undertaking the hydraulic analysis of the bridge site when assessing the results of such an analysis.

In this chapter, the hydraulics of flow through bridges is discussed, with special emphasis on energy losses and scour. A brief discussion is also presented on the bridge analysis routines contained within the HEC-RAS computer program.

## 3.6.2. Energy Losses at Bridges

Energy losses at bridge sites have three components. The first consists of losses that occur in the reach immediately downstream from the structure where an expansion of flow takes place. The second component comprises the losses that occur at the structure itself. The third component comprises the losses that occur in the reach immediately upstream of the structure where the flow is contracting to pass through the bridge opening. These three components are illustrated in Figure 6.3.12.

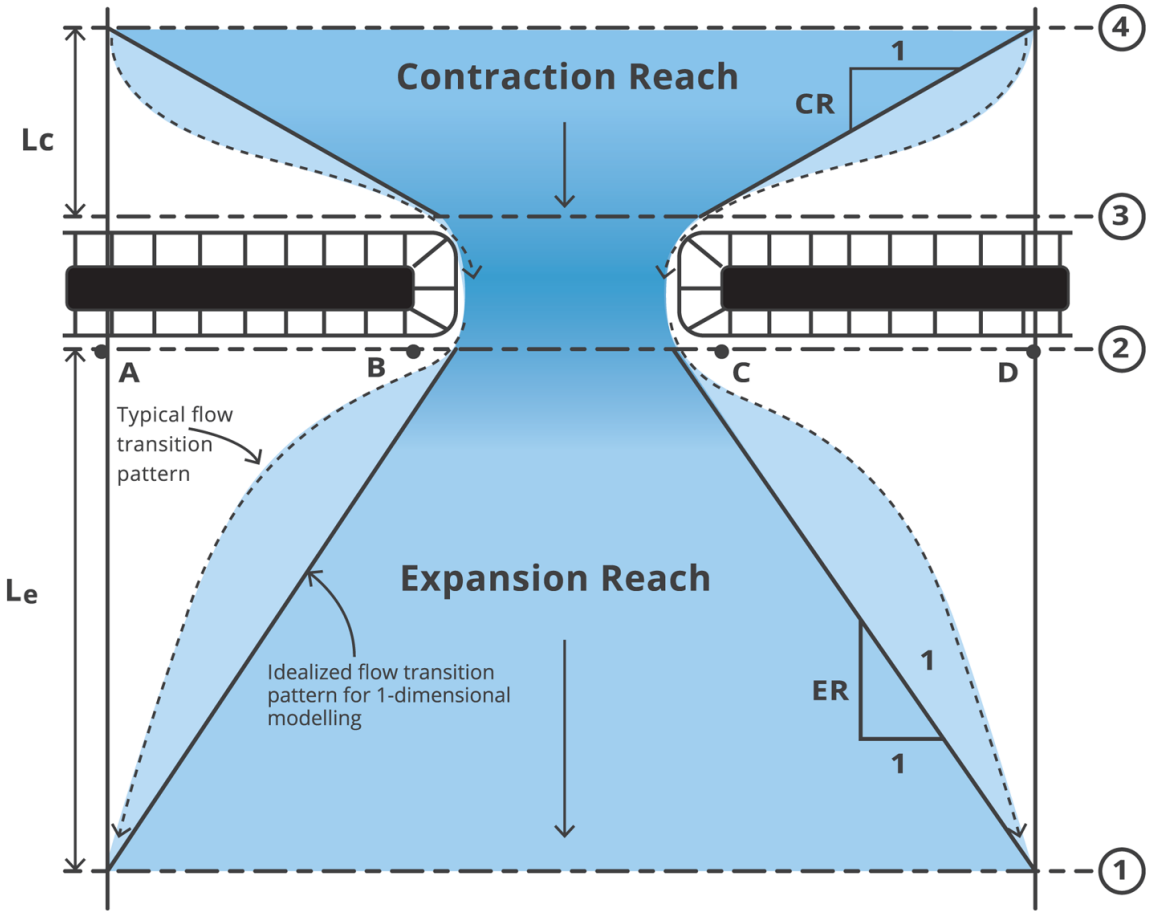


Bridge losses within the expansion reach downstream (sections 1 to 2) can be relatively large. The region is characterised by recirculation zones on either side that are maintained by extracting energy from the mean flow. Energy losses through the contraction (sections 3 to 4) are relatively smaller because the channel length over which the change in cross-section occurs is less and the recirculation zones are smaller.

Within each of these regions the energy loss is normally calculated as the sum of friction losses and expansion or contraction losses. Friction and contraction losses between sections 3 and 4 are calculated the same as friction and expansion losses between sections 1 and 2. Friction losses are typically determined using standard step profile equations. Contraction and expansion losses are described in terms of a coefficient times the absolute value of the change in velocity head between adjacent cross sections. For a detailed discussion on selecting contraction and expansion coefficients at bridges, the user is referred to Chapter 5 of the HEC-RAS Hydraulic Reference Manual.

Within the bridge structure itself (between sections 2 and 3) the computation of the energy loss can be simple or complex, depending on the flow characteristics. A low flow, where the water surface does not interact with the bottom chord of the bridge, may be analysed using a simple standard step procedure. On the other hand, interaction of the water surface with the bridge deck structure may lead to a combination of low flow and weir flow or pressure flow and weir flow. These cases require more complex modelling techniques that are outside the scope of this section. Modelling details may be found in the HEC-RAS Hydraulic Reference Manual.

In most cases of flow through bridge sites, the river flow downstream and upstream is sub-critical. Under these circumstances, the hydraulic effect of the bridge is to increase the water level upstream of the bridge, with no effect downstream. On the other hand, in the rare cases where the natural flow is characterised by super-critical conditions, the effect of the bridge manifests downstream. In such cases, upstream water levels are affected only if the bridge constriction is sufficiently severe to transform the supercritical flow to subcritical.

## 3.6.3. Modelling Approaches for Non-Standard Bridge Crossings

Non-standard bridge crossings include perched bridges, submerged bridges, skewed bridges, parallel bridges and multiple opening bridges. Notes on the modelling of each are presented in the following.

A perched bridge is one for which the road approaching the bridge is at the flood plain ground level, and only in the immediate area of the bridge does the road rise above ground level to span the water course. This condition is shown schematically in Figure 6.3.13.

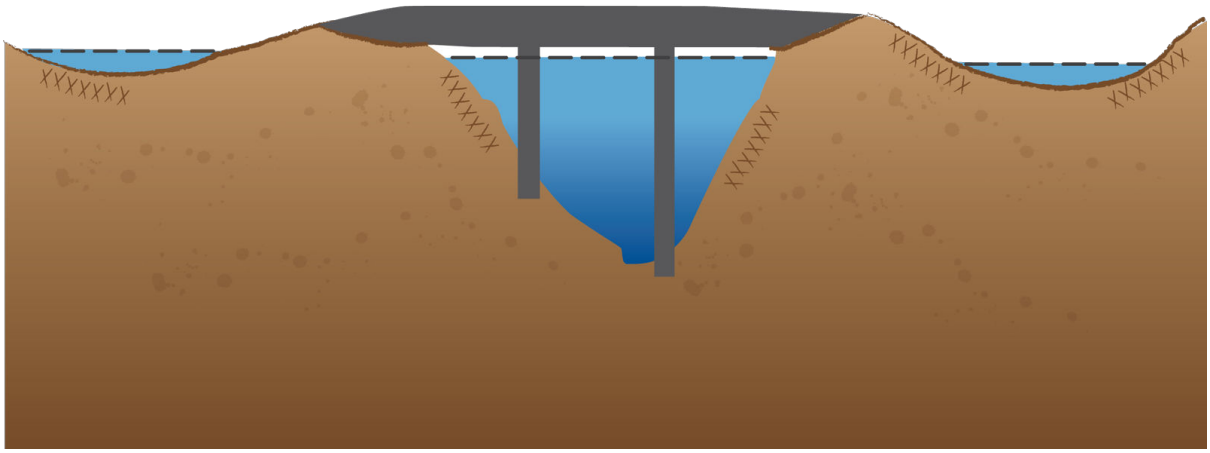

Figure 6.3.13. Schematic of a Perched Bridge

A typical flow situation with this type of bridge is low flow under the bridge and overbank flow around the bridge. Because the road approaching the bridge is usually not much higher than the surrounding ground, the assumption of weir flow is usually not justified.

For this reason, perched bridges should generally be modelled using the energy-based method, especially when a large percentage of the total flow rate is carried in the overbank areas.

A submerged bridge (or low water bridge) is designed to accommodate only low flows under the bridge. Flood flows are carried over the bridge and road. A typical example of a submerged bridge is shown in Figure 6.3.14.

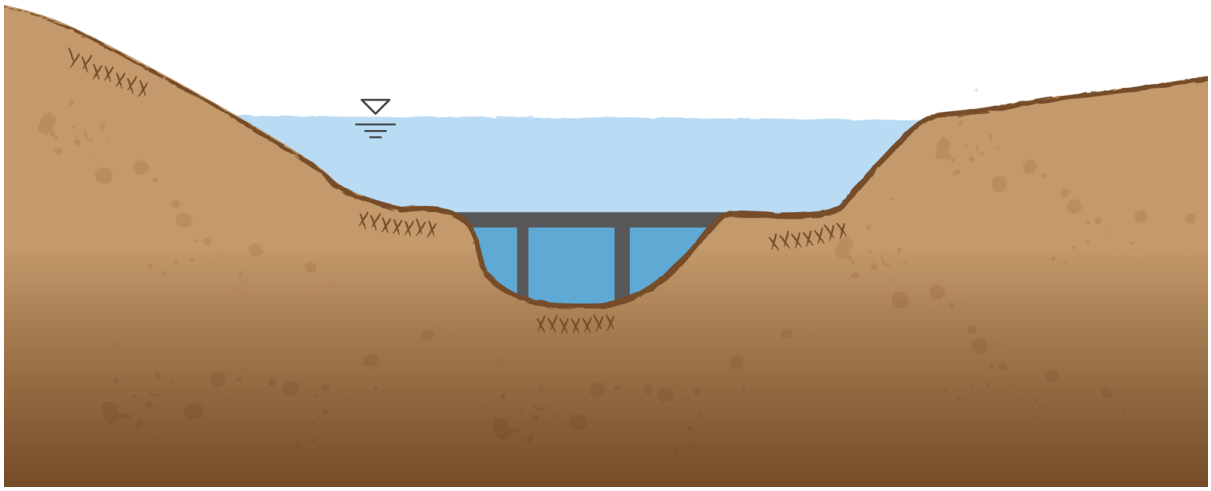

Figure 6.3.14. Schematic of a Submerged Bridge

When modelling this bridge for flood flows, the anticipated solution would be a combination of pressure and weir flow. However, with most of the flow passing over the top of the bridge, the correction for submergence can introduce considerable error. For this reason, if the tailwater level is likely to be relatively high, the energy based method of analysis is recommended.

A schematic of a skewed bridge is shown in Figure 6.3.15.

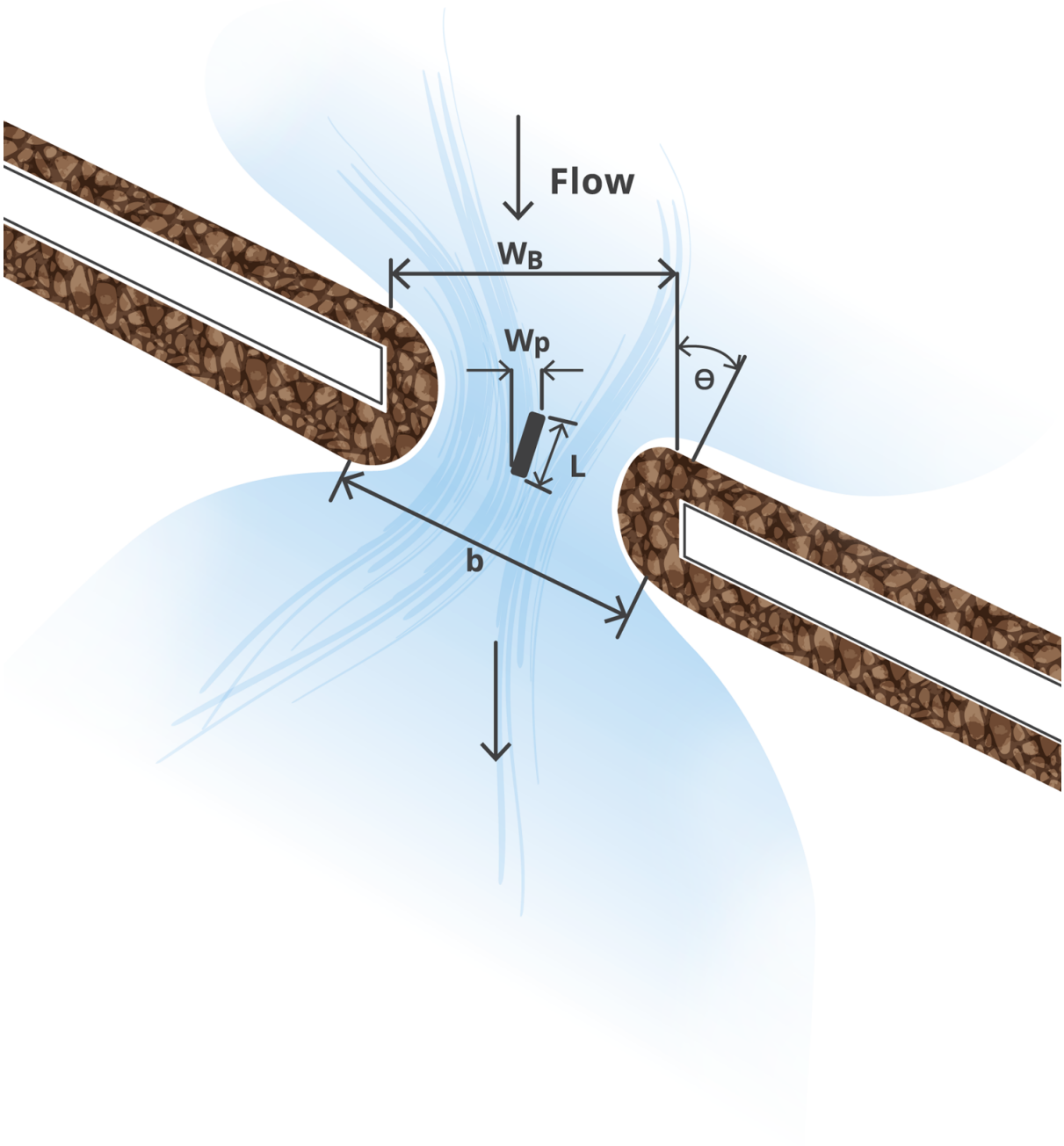


Figure 6.3.15. Schematic of a Skewed Bridge

A skewed bridge crossing is generally handled by making adjustments to the bridge dimensions to define an equivalent cross-section perpendicular to the flow lines.

For low flow, skewed crossings with angles up to 20 degrees show no objectionable flow patterns. However, for larger angles of skew, the flow efficiency decreases. For reasonably small flow contractions, the projected length is adequate for assessing the impact of skew up to skew angles of 30 degrees.

With reference to Figure 6.3.15, the projected width of the bridge opening, perpendicular to the flow lines, is given by:

$$W_B = b\cos\theta \tag{6.3.5}$$

The pier information must also be adjusted to account for the skew of the bridge. The program HEC-RAS assumes that the piers are continuous, as shown in Figure 6.3.15.

Thus, the projected width of the piers, perpendicular to the flow lines, is given by:

$$W_P = L\sin\theta + w_p\cos\theta \tag{6.3.6}$$

The construction of divided highways often leads to the common modelling problem of parallel bridges. The situation is shown schematically in Figure 6.3.16.

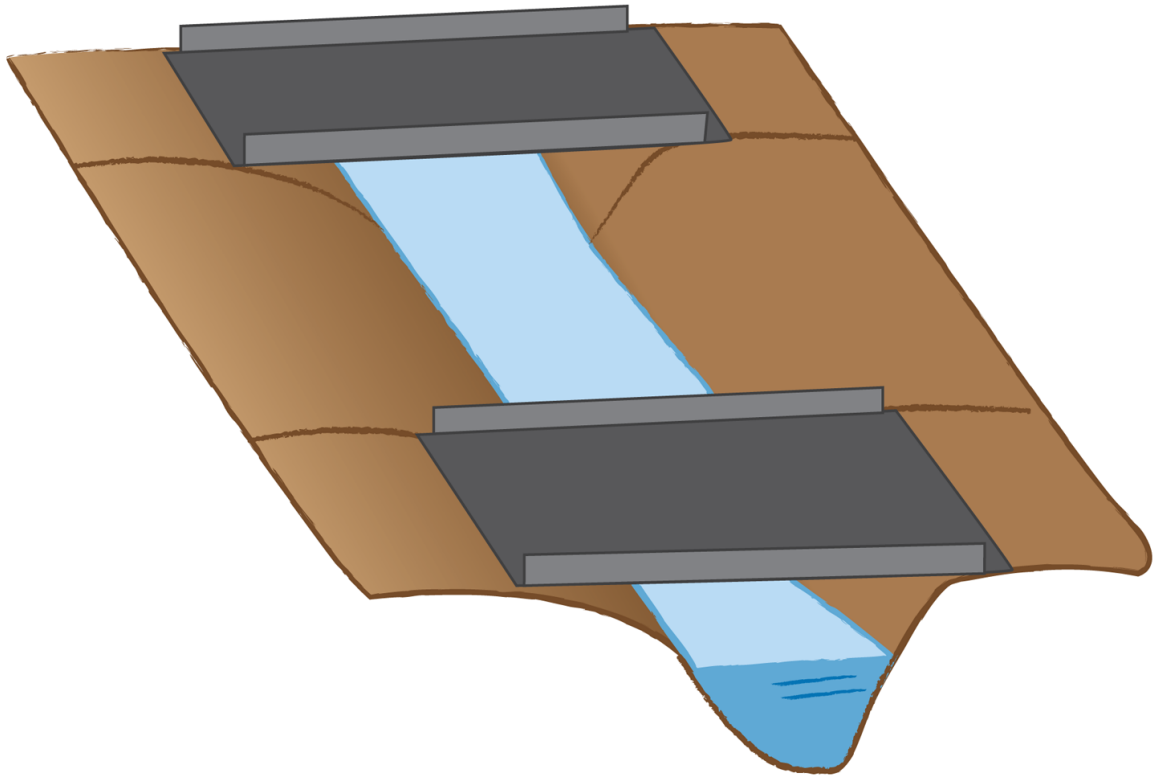

Figure 6.3.16. Schematic of Parallel Bridges

For new highways, these bridges are often identical structures.

Depending on the spacing between the two bridges, the loss may be between 1.3 and 2 times the loss for a single bridge. If the bridges are very close to each other and the flow cannot expand between the bridges, the system can be dealt with as a single structure. If both bridges are modelled, care should be taken in depicting the expansion and contraction of flow between the bridges. Expansion and contraction rates should be based on the same procedures as single bridges.

Some bridges are characterised by more than one opening for flood flow, especially over a very wide flood plain. Figure 6.3.17 shows the situation schematically and illustrates the nomenclature used in the following discussion.

It is necessary to ensure compatibility between the determination of individual flow rates through each opening and the equality of the head loss along each flow path.

With reference to Figure 6.3.17, this requires that:

$$Q_T = \sum Q_i \tag{6.3.7}$$

and

$$H_4 - H_1 = \Delta H_{Q_1} = \Delta H_{Q_2} = \Delta H_{Q_3} \tag{6.3.8}$$

Mutual satisfaction of Equation (6.3.7) and Equation (6.3.8) ensures that the computed energies at the upstream point where flow separates or stagnation point are equal – this is defined by the correct apportioning of flow QI through each opening.

The downstream stagnation point defines where flow merges and the flow path of all the openings are assumed to have equal energy level at this point, ie. downstream boundary.

In HEC-RAS, Up to seven openings (of combinations of open conveyance area, bridges and culverts) can be defined at any one river crossing. The program automatically locates the stagnation points within the range defined by the user unless there are physical stagnation points such as bridge abutments or islands for example.

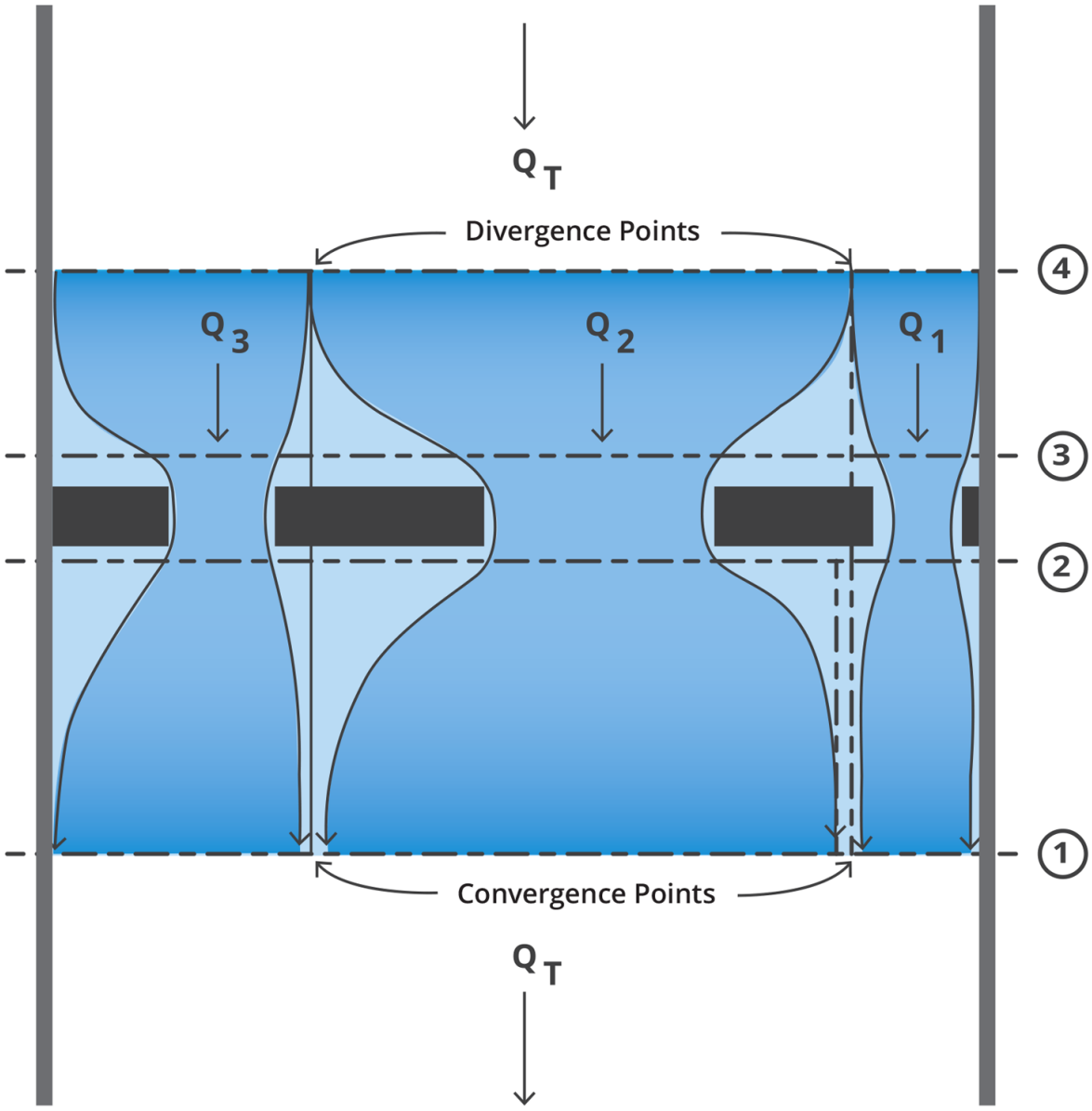


Figure 6.3.17. Schematic of Bridge with Multiple Openings

Alternatively, the divided flow approach can be used whereby the flow paths of each opening are modelled separately with manual adjustment of flow distribution (similar to flow split modelling at upstream of opening and flow combining modelling at downstream of opening).

With this method, the cross section will need to be physically split along assumed stagnation points at each cross sections using the ineffective area option. This method is most suited to anabranches and breakaway flow paths in wide floodplain with multiple road crossings. A typical example is shown in Figure 6.3.18.

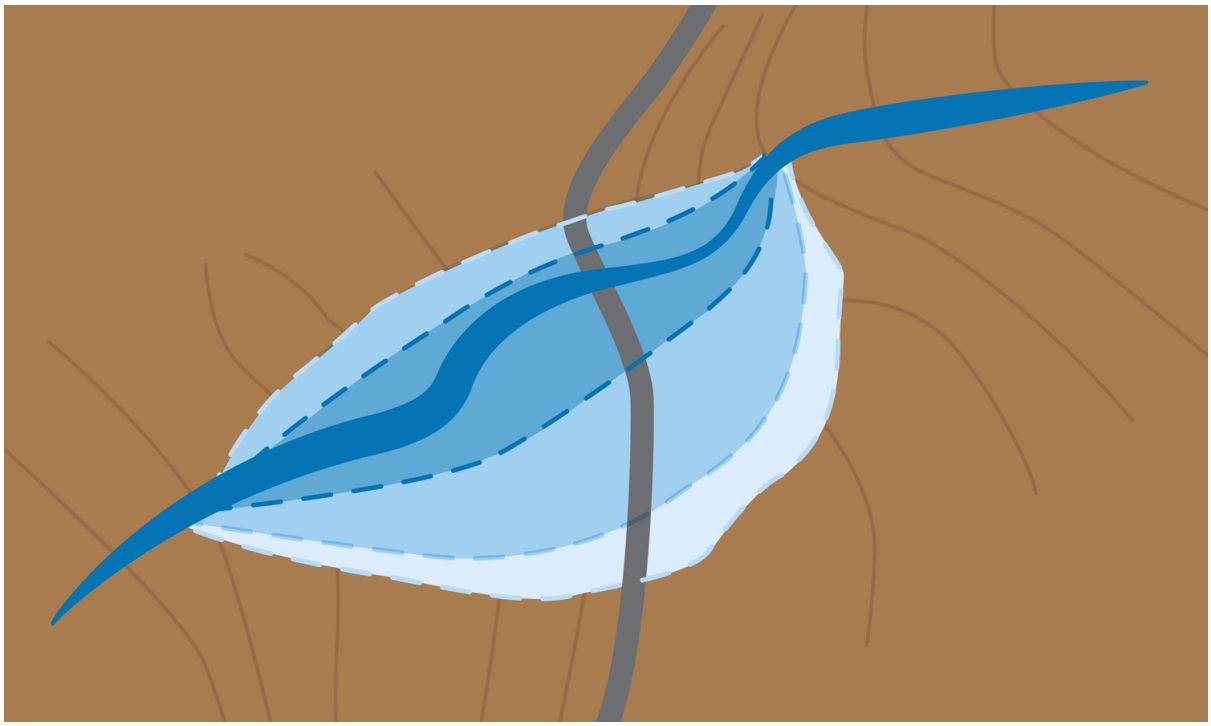

Figure 6.3.18. Illustration of Divided Flow Approach

**Scour at Bridge Sites**

Scour occurs at bridges because of changes to the natural flow conditions and is a serious concern. It can be defined simply as the excavation and removal of material from the bed and banks of streams as a result of the erosive action of flowing water. In the context of this book, it is assumed that this erosive action may potentially expose the foundations of a bridge. Scour is usually considered to be a local phenomenon, but includes degradation that can cause erosion over a considerable length of a river.

Scour at bridges is described in Book 6, Chapter 3, Section 8.

# 3.7. Floodways on Roads

## 3.7.1. Introduction

Floodways are sections of roads that have been designed to be overtopped by floodwater during relatively high annual exceedance probability flood events. These events could be as high as AEP 10% to 5%, but are often designed for overtopping in small floods.

Floodways are therefore planned for locations where flood immunity is not a serious concern or the duration of road closure is low, and are suitable for locations where extensive floodplain width and shallow flows make bridge or culvert construction difficult or expensive. Floodways are often a preferred approach for locations where a relatively cheap floodplain crossing is needed and where flood immunity or flood closures are not a significant concern. They are therefore often preferred for roads with low traffic volumes in arid regions where flood events are infrequent and short duration.

The Queensland Department of Transport and Main Roads Road Drainage Manual (QDTMR, 1986) and the Austroads Guide to Road Design Part 5 (Austroads, 2013) has detailed guidance on floodway design.

Floodways may require costly batter protection and therefore a higher level road together with a larger culvert or bridge option may be more cost effective. Floodways also have smaller waterway (under road) requirements and may be more prone to blockage by debris. These cost related performance factors should be considered as well as trafficability and other requirements in the selection of final road level. Floodways may offer environmental advantages over culverts or bridges, since they will tend to spread flows more widely. This means that the risk of scour to waterway and surrounding land is generally reduced because flow is less concentrated. It is also important that a floodway be designed so that it is not covered by water from ponding or backwater for any significant period of time after a flood event.

The advantages of floodways are as follows:

- Generally, simple to design;
- May offer environmental advantages over culverts and bridges, since they will tend to spread flows more widely, reducing the risk of scour when flow is concentrated in culverts or bridges;
- Typically have low embankments; and
- Risk of scour to waterway and surrounding land is reduced.

There are however some disadvantages, as follows, which mean that design needs careful consideration.

- Allow water flow over road which leads to flood immunity and safety issues;
- Increased disruption to traffic due to overtopping;
- Can have higher construction costs than culverts;
- Batter slopes can be affected by erosion or scour (particularly for higher embankments);
- Generally have costly batter protection requirements;
- Susceptible to stream / channel migration;
- Can have environmental impacts (fauna / fish passage); and
- Potential for failure of embankment (depending on provided protection).

**Geometric and Safety Issues with Floodways**

It is important that adequate approach sight distance be provided to allow drivers time to recognise water over the road and to stop. It is also important that the length of a floodway be limited at about 300 m so that drivers do not become disorientated when confronted with wide open stretches of water. Where a proposed floodway would be longer than 300 m, it is recommended that the proposed floodway be broken into shorter lengths by providing sections of road that are raised above the maximum flood level. As a general principle, floodways should be designed so that the depth of water over the road should be as uniform as possible over the flooded section. Building a floodway on a level grade avoids the possibility of a driver unexpectedly encountering deeper water and possibly stalling or being swept downstream.

Exceptions to the level grading may occur where bridges have been built significantly higher than the flooded approaches on both sides. The bridges have been built on the basis that

the approaches will be raised sometime in the future. Floodways should not be placed on horizontal curves as:

- there are problems in defining the edge of the pavement for motorists;
- any superelevation may change the normal flow distribution ie. push more water to the non-superelevated sections of road; and
- the water depth will be deeper on one side of the road than the other in a superelevated section of road and there is the possibility of the high side being trafficable but not the other, thus creating a safety problem.

Floodways should also not be located on vertical curves to avoid variations in flow depth.

**Hydraulic Design**

A floodway consists not only of the roadway embankment to accommodate flow over the road but also waterway openings to provide for flow under the road. These openings may be required for one or more of the following functions:

- reduce the afflux or rise in water level upstream due to the obstruction (embankment);
- raise the tailwater level so that less batter protection is required on the downstream side e.g. grass instead of concrete; and
- act as anti-ponding structures for low flow stream conditions.

Flow over roadways may be:

- free flow; and
- submerged flow.

In the initial stages of overtopping a low tailwater usually exists and free flow occurs. Under these circumstances flow passes through critical depth over the road and the discharge is determined by flood levels upstream.

Free flowmay be either:

- plunging flow which flows over the shoulder and down the downstream face of the embankment. The flow then penetrates the tailwater surface producing a submerged hydraulic jump on the downstream slope. Velocities are likely to be high and erosive; and
- surface flow which separates from the surface of the road embankment and rides over the surface of the tailwater. This flow will have less erosion potential downstream.

Submerged flowoccurs when the discharge is controlled by the tailwater level as well as the headwater levels. This occurs when the depth of flow over the road is everywhere greater than the critical depth. Typical velocities of flow over a floodway are shown in the Figure 6.3.19 as sourced from *Waterway Design* (Austroads 1994) after *Cameron and McNamara* (1966)Cameron and McNamara (1966).

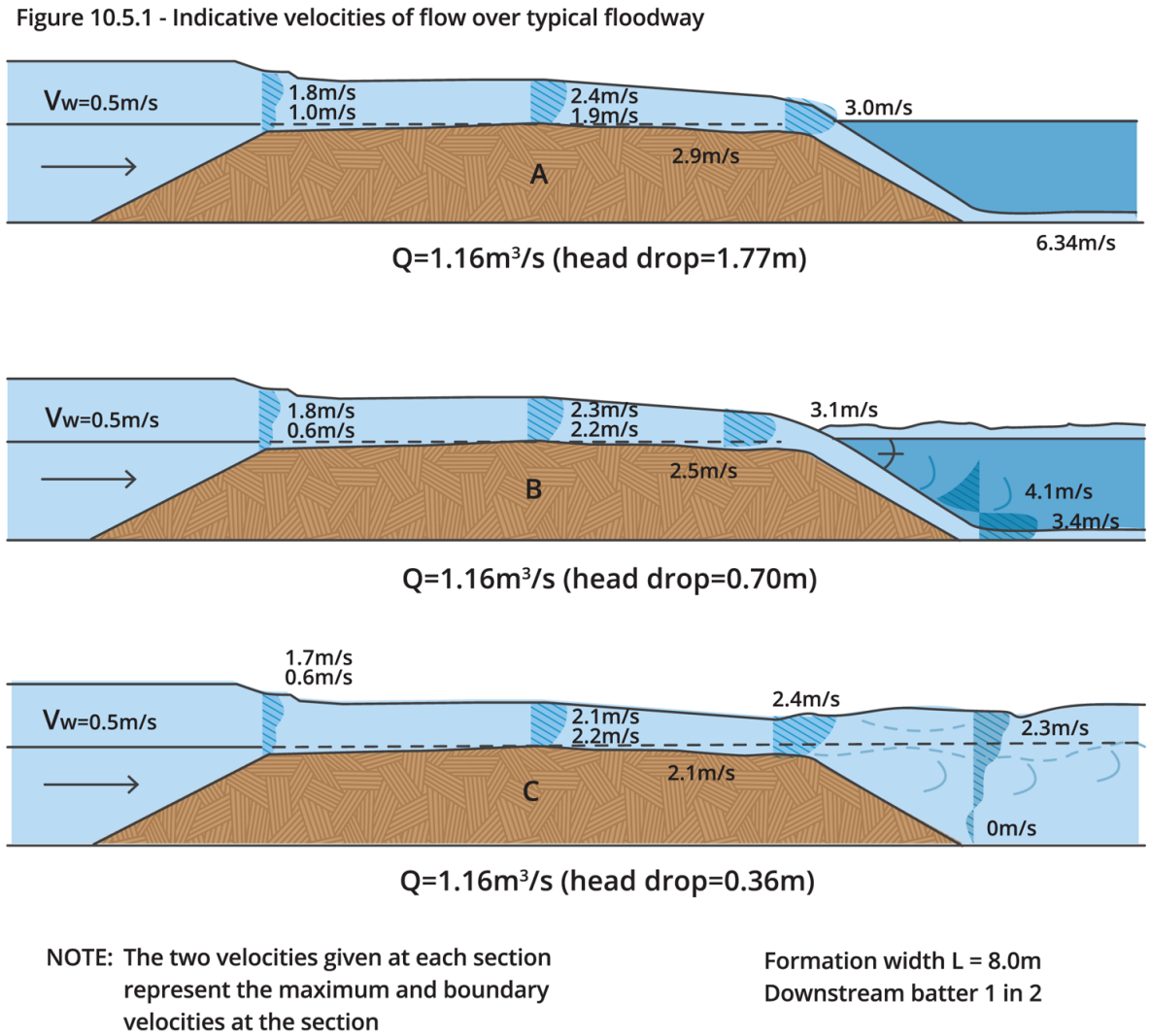


Figure 6.3.19. Floodway flows (DTMR)

**Flow over the road**

Hydraulic calculation for flow over the road embankment is based on the broad crested weir formula as described elsewhere in this Chapter.

With free-flow conditions on the embankment – that is, in the absence of submergence of the control – analysis indicates that the discharge across the embankment may be expressed in terms of the other relevant parameters by an expression of the form:

$$Q = CLH^{\frac{3}{2}} \tag{6.3.9}$$

where Q = the discharge

C = a coefficient

L = the length of the embankment (that is, the width of the flow)

H = the head of the approach flow, determined as shown in Figure 6.3.19 with the elevation of the embankment crown as datum.

The coefficient C embodies numerical coefficients and the gravitational acceleration. For an ideal fluid, the value of C would be 1.70 in SI units. Values of C for real fluids would generally be expected to be somewhat less than this value, incorporating empirically the effects of differences between real and ideal fluid behaviour.

# 3.8. Scour

## 3.8.1. Scour at Bridges

Scour at bridges is an important risk for these structures and design must incorporate mitigation measures. In the case of existing bridges, where scour becomes apparent, measures must be provided to protect the bridge asset and prevent further damage. Scour is a very serious problem. Floods that result in scour are the principal cause of bridge failure.

Some of the observable effects of scour are shown in Figure 6.3.20.

Figure 6.3.20(a) shows the pier caps and pile caps exposed. Figure 6.3.20(b) shows pier and abutment riprap moved downstream. Figure 6.3.20(c) shows a downstream scour hole and bank erosion. Figure 6.3.20(d) shows a downstream scour hole arising from submergence of the opening. Figure 6.3.20(e) shows slumped material at the toe of the bank arising from failure of the riprap or bank. Figure 6.3.20(f) shows erosion and failure of a highway embankment with flow on both sides of the abutment.

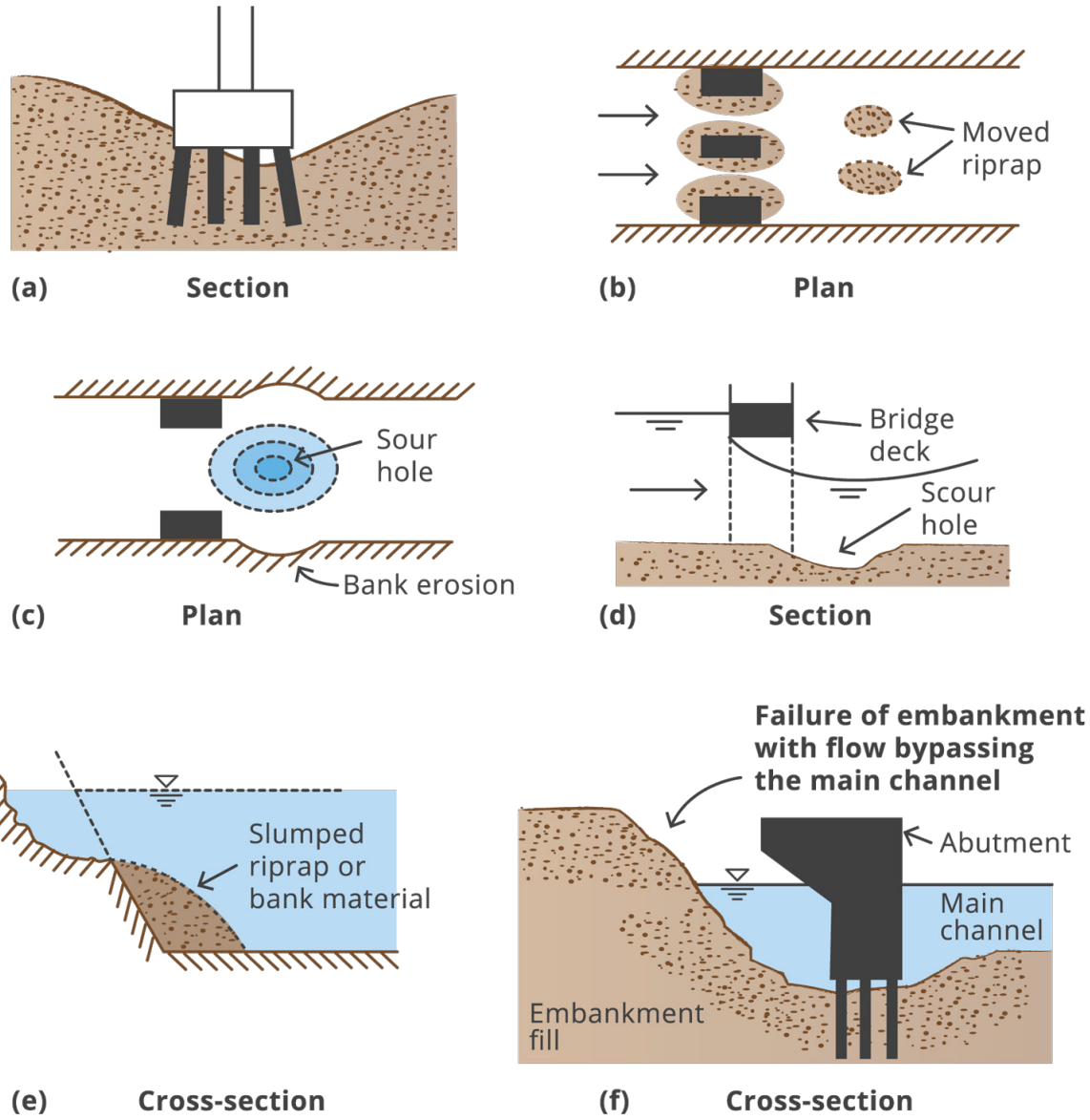


Figure 6.3.20. Some Effects of Scour

The biggest and most frequently encountered scour-related problems usually concern loose sediments that are easily eroded. It is not true, however, to assume that the scour depth in cohesive or cemented soils cannot be as large – it merely takes longer for the scour hole to develop.

Many of the equations for scour were derived from laboratory studies, for which the range of validity is unknown. Some were verified using very limited field data, which itself may be of doubtful accuracy. In the field, the scour hole that develops on the rising stage of a flood, or at the peak, may be filled in again on the falling stage. For this reason, the maximum depth of scour cannot be easily assessed after the event.

Scour can also cause problems with the hydraulic analysis of a bridge. Scour may considerably deepen the channel through a bridge and effectively reduce or even eliminate the backwater. This reduction in backwater should not be relied on, however, because of the unpredictable nature of the processes involved.

When considering scour it is normal to distinguish between non-cohesive or cohesionless (alluvial) sediments and cohesive material. The former are usually of most interest and are considered further in this section. Cohesive materials require special techniques and are outside the scope of this chapter.

The first major issue when considering scour is the distinction between *clear-water* scour and *live-bed* scour. The critical issue here is whether or not the mean bed shear stress of the flow upstream of the bridge is less than or larger than the threshold value needed to move the bed material.

If the upstream shear stress is less than the threshold value, the bed material upstream of the bridge is at rest. This is referred to as the clear-water condition because the approach flow is clear and does not contain sediment. Thus, any bed material that is removed from a local scour hole is not replaced by sediment being transported by the approach flow. The maximum local scour depth is achieved when the size of the scour hole results in a local reduction in shear stress to the critical value such that the flow can no longer remove bed material from the scoured area.

Live-bed scour occurs where the upstream shear stress is greater than the threshold value and the bed material upstream of the crossing is moving. This means that the approach flow continuously transports sediment into a local scour hole. By itself, a live bed in a uniform channel will not cause a scour hole - for this to be created some additional increase in shear stress is needed, such as that caused by a contraction (natural or artificial, such as a bridge) or a local obstruction (e.g. a bridge pier). The equilibrium scour depth is achieved when material is transported into the scour hole at the same rate at which it is transported out.

These concepts are illustrated by Figure 6.3.21.

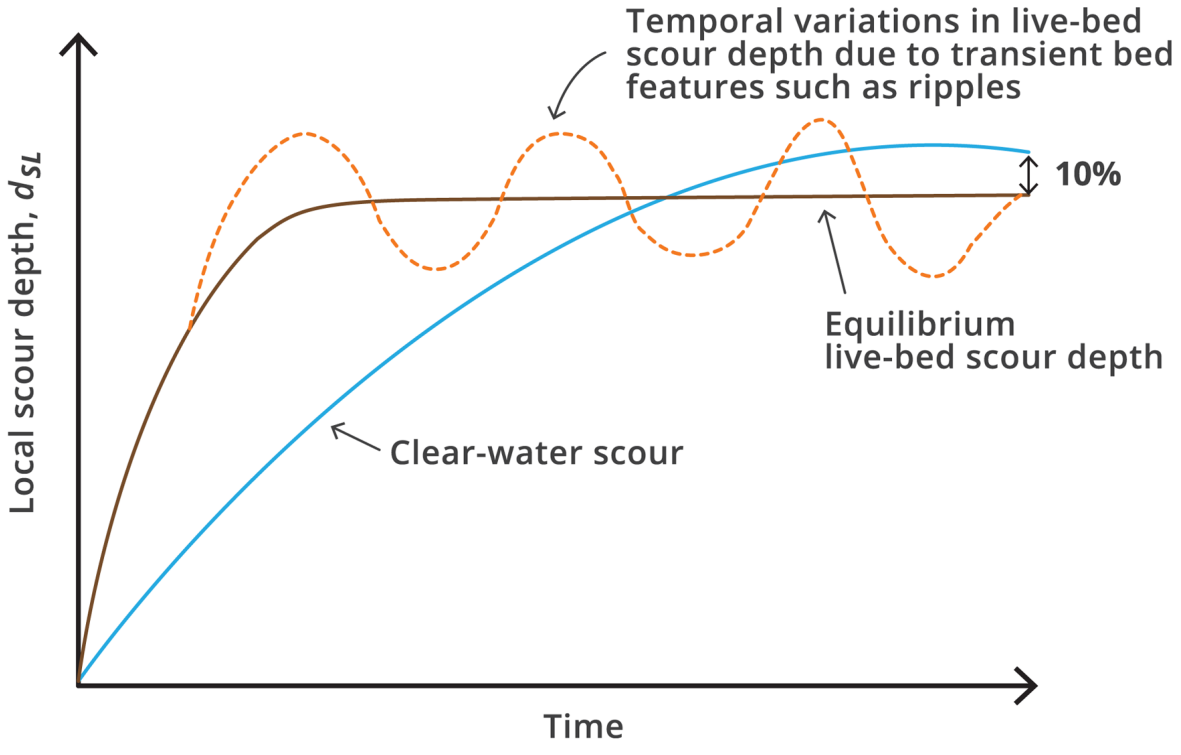


Figure 6.3.21. Development of Clear-water and Live-bed scour with Time

It is noted from Figure 6.3.21 that typically the maximum equilibrium clear-water scour is about 10% larger than the equilibrium live-bed scour. Conditions that favour clear water scour are:

- Channels with flat bed slopes during low flows;
- A coarse bed material that is too large to be transported (e.g. riprap);
- Channels with natural vegetation or artificial reinforcement where velocities are only high enough to cause scour near piers and abutments; and
- Flow over grassed floodplains.

At any particular location both clear-water and live-bed scour may be experienced. During a single flood the bed shear stress will increase and decrease as the discharge rises and falls. Thus, it is possible to have clear-water conditions initially, then a live bed, then finally clear water again. The maximum scour depth may occur under clear-water conditions, not at the flood peak when live-bed scour is experienced. Similarly, relatively high velocities can be experienced when the flow is just contained within the banks, rather than spread over the floodplains at the peak discharge.

It is also possible to have the clear-water and live-bed conditions occurring at the same time. For example, if the floodplains are grassed or composed of material that is larger in diameter than that in the main channel, clear-water conditions may occur on the floodplain with live-bed conditions in the main channel.

It is evident from this discussion that the problem may not always be as simple or as well defined as would be desirable. If there are any uncertainties or if the consequences of failure are large, prompting a conservative approach, it is recommended that clear-water conditions be assumed at the peak flow condition.

Urbanisation has the effect of increasing flood magnitudes and causing hydrographs to peak earlier, resulting in higher stream velocities and degradation. Channel improvements or the extraction of gravel (above or below the site in question) can alter water levels, flow velocities, bed slopes and sediment transport characteristics and consequently affect scour. For instance, if an alluvial channel is straightened, widened or altered in any other way that results in an increased flow-energy condition, the channel will tend back towards a lower energy state by degrading upstream, widening and aggrading downstream.

The significance of degradation scour to bridge design is that the engineer has to decide whether the existing channel elevation is likely to be constant over the 100 year life of the bridge, or whether it will change. If change is probable then it must be allowed for when designing the waterway and foundations.

The lateral stability of a river channel may also affect scour depths, because movement of the channel may result in the bridge being incorrectly positioned or aligned with respect to the approach flow. This problem can be significant under any circumstances but is potentially very serious in arid or semi-arid regions and with ephemeral (intermittent) streams. Lateral migration rates are largely unpredictable. Sometimes a channel that has been stable for many years may suddenly start to move, but significant influences are floods, bank material, vegetation of the banks and floodplains, and land use.

Scour at bridge sites is typically classified as contraction (or constriction) scour and local scour. Contraction scour occurs over a whole cross-section as a result of the increased velocities and bed shear stresses arising from a narrowing of the channel by a constriction

such as a bridge. In general, the smaller the opening ratio ($M = q/Q$ or $b/B$) the larger the waterway velocity and the greater the potential for scour. If the flow contracts from a wide floodplain, considerable scour and bank failure can occur. Relatively severe constrictions may require regular maintenance for decades to combat erosion. It is evident that one way to reduce contraction scour is to make the opening wider.

Contraction scour is caused by a constriction in the floodplain either by a bridge or when overbank flow is confined by road embankments. A decrease in flow area results in an increase in average velocity and bed shear stress. Contraction scour is different from long-term degradation in that contraction scour occurs in the vicinity of the constriction (bridge), it may be intermittent, and/or related to the passing of a particular flood event.

Contraction scour at a bridge is illustrated in Figure 6.3.22.

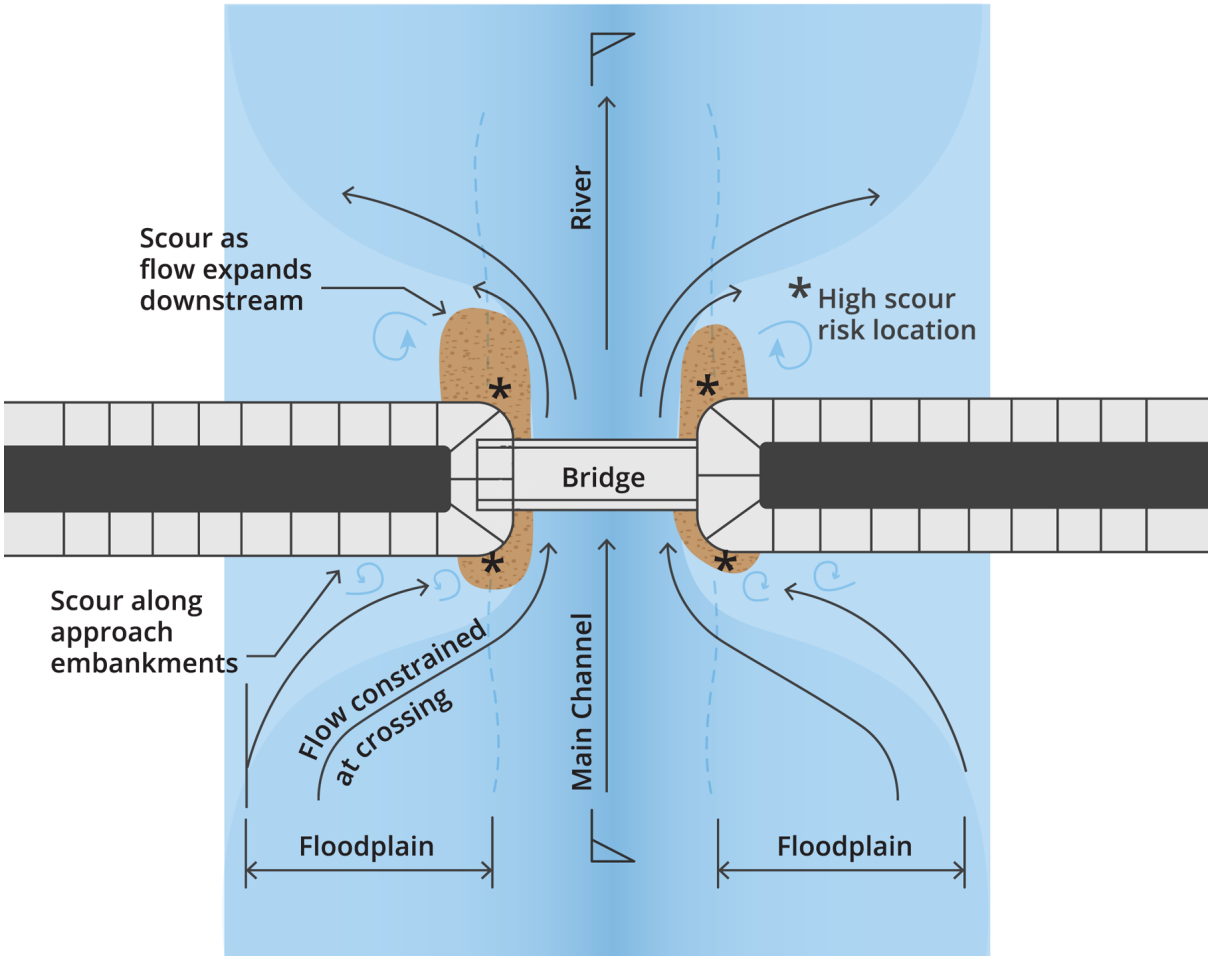


Figure 6.3.22. Contraction scour (QDTMR, 2013)

Contraction scour also occurs in the vertical where flow is contracted vertically as water flows under the bridge and velocity increases, potentially causing a scour hole to develop under the bridge, as shown in Figure 6.3.23.

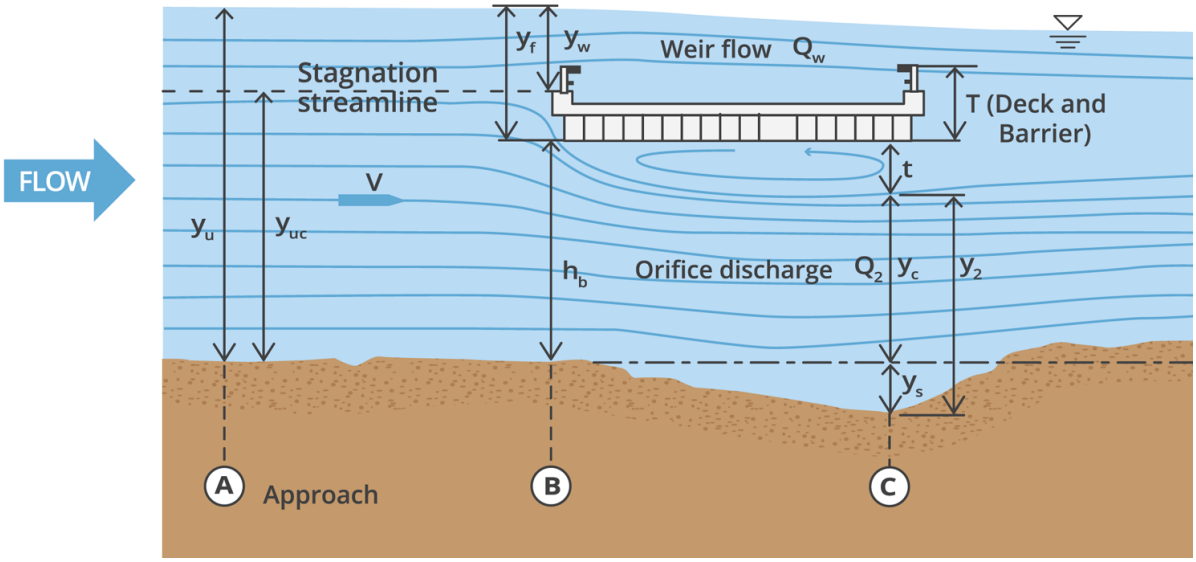


Figure 6.3.23. Vertical contraction scour (QDTMR, 2013)

Local scour arises from the increased velocities and associated vortices as water accelerates around the corners of abutments, piers and spur dykes. The flow pattern around a cylindrical pier is shown in Figure 6.3.24. The approaching flow decelerates as it nears the cylinder, coming to rest at the centre of the pier. The resulting stagnation pressure is highest near the water surface where the approach velocity is greatest, and smaller lower down. The downward pressure gradient at the pier face directs the flow downwards. Local pier scour begins when the downflow velocity near the stagnation point is strong enough to overcome the resistance to motion of the bed particles.

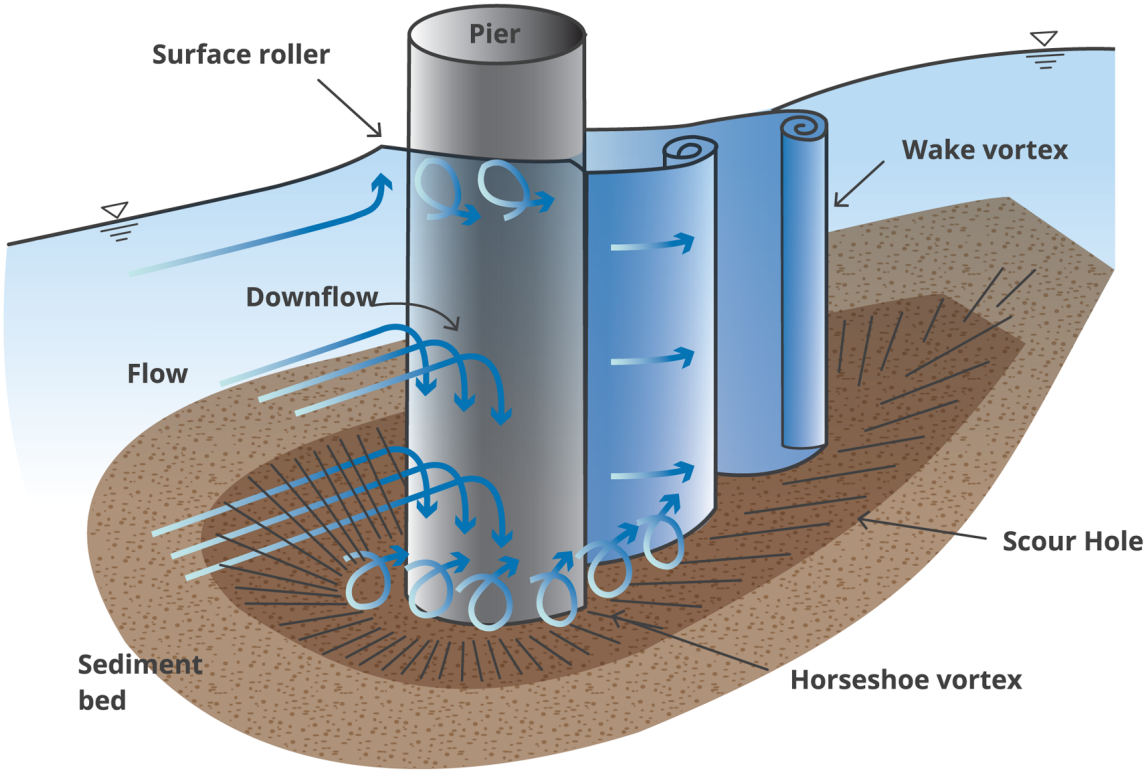


Figure 6.3.24. Schematic of Local Scour at a Bridge Pier

When scour occurs the maximum downflow velocity is about 80% of the mean approach velocity. The impact of the downflow on the bed is the principal factor leading to the creation of a scour hole. As the hole grows the flow dives down and around the pier producing a horseshoe vortex, which carries the scoured bed material downstream.

The combination of the downflow with the horseshoe vortex is the dominant scour mechanism. As the scour hole becomes progressively deeper the downflow near the bottom of the scour hole decreases until at some point in time equilibrium is reached and the depth remains constant.

At the sides of the pier flow separation occurs, resulting in a wake vortex whose whirlpool action sucks up sediment from the bed. As the vortices diminish and velocities reduce, the scoured material is deposited some distance downstream of the pier.

For piers that are essentially rectangular in plan and aligned to the flow the basic scour mechanism is similar to that just described, although rather more severe because of the square corners. However, as the angle of attack to a rectangular pier increases, so does its effective width, so the scour depth increases and the point of maximum scour moves downstream of the nose to a point on the exposed side.

With a large degree of skew the maximum scour may occur at the downstream end of the pier. If the flow direction is likely to change there is merit in using cylindrical piers to avoid these complications.

The scour mechanism at a bridge abutment is similar to that at a pier, although the boundary layer at the abutment or channel wall may result in an additional deceleration of the flow compared with a central pier. The approach flow can be considered as separating into an

upper layer, which forms an upflow surface roller on hitting the abutment, and a lower layer, which becomes the bottom or principal vortex. This is shown schematically in Figure 6.3.25.

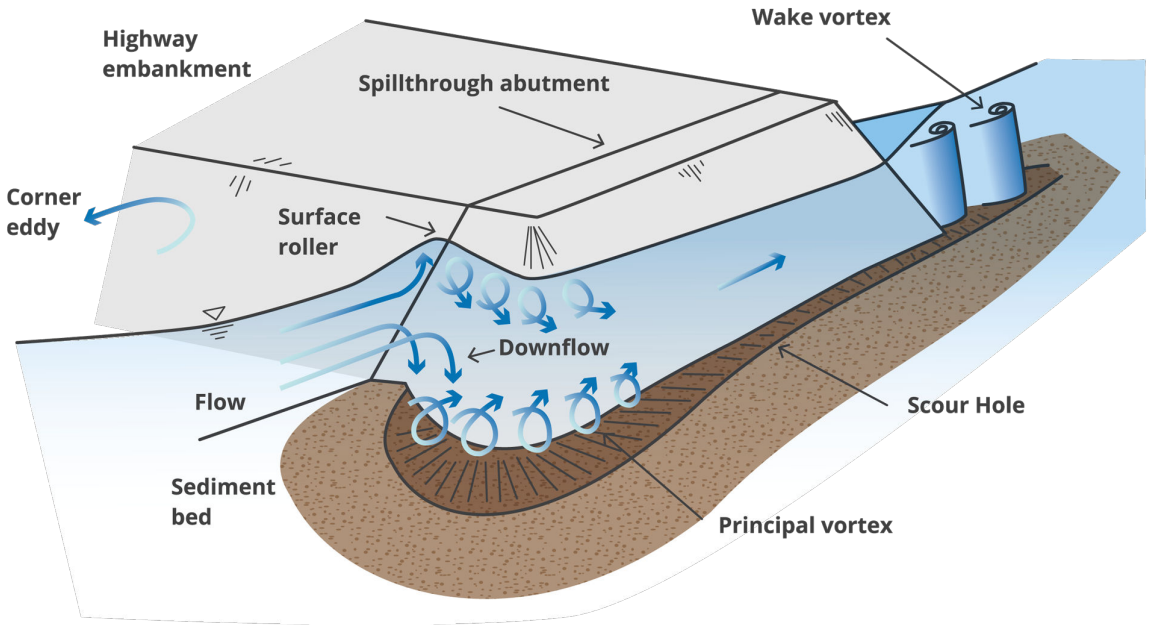


Figure 6.3.25. Schematic of Abutment Scour

Viewed in plan, the upper layer divides or separates, with part of the flow accelerating around the upstream corner of the abutment into the bridge waterway while the remainder slowly rotates in an almost stationary pool trapped against the face of the abutment and the river bank.

In the bottom layer, the flow near the bank forms an almost vertical downflow, while that nearer to the end of the abutment accelerates down and into the waterway, forming the principal vortex. Usually scouring starts in this region of accelerating flow and grows along the faces of the abutment. Wake vortices form downstream of the abutment.

The basic scouring process is the same for most types of abutment, although with wingwall and vertical wall types the stagnation region is larger, and scour is most severe near the end of the abutment where the principal vortex is concentrated.

The total scour depth is obtained by summing degradation, contraction and local scour. This procedure is, strictly, only valid where the scour holes overlap. For instance, contraction scour may have to be added to pier or abutment scour to get the total scour depth. However, pier scour and abutment scour would not be added unless the two scour holes overlap.

This usually has to be determined by drawing a cross-section through the waterway and superimposing the scour depths. If the holes do overlap the resultant scour depth is often larger than the two components, but difficult to predict. Nevertheless, as a general and conservative rule, the total scour depth is the sum of the three components.

The scour computation capability in the HEC-RAS software allows the user to compute contraction scour and local scour at piers and abutments. The details may be found in the HEC-RAS Hydraulic Reference Manual.

## 3.8.2. Design for scour at bridges

The best scour protection measure is to minimise the risk of scour in the bridge design.

Hydraulic modelling of a bridge site is an integral part of any bridge design and these studies should address the sizing of the bridge waterway helping to ensure that the foundations can be designed to minimise scour.

It must be recognised that damage to bridge approaches from rare floods can be repaired relatively quickly to restore traffic service. On the other hand, a bridge which collapses or suffers major structural damage from scour can create safety hazards as well as significant social impacts and economic losses for a prolonged period of time. Therefore, scour resistant bridge foundations should be designed to a higher hydraulic standard. These concepts must be reflected in bridge design procedures.

There are many methods for estimating scour as part of bridge design and these include equations by Holmes, Neill, Faraday and Charlton, Melville and Coleman, the CSU equation, FHWA HEC-18 equation, Froehlich equations and HIRE equations, with details for all provided in QDTMR (2013).

Encroachment in the stream channel by abutments and piers reduces the channel section and may cause significant contraction scour. Severe constriction of floodplain flow may cause approach embankment failures and serious contraction scour in the bridge waterway, where auxiliary (relief) openings can be considered but must be carefully designed. On wide floodplains the design should seek to avoid excessive diversion of floodplain flows towards the main bridge opening and skewed crossings of floodplains should also be minimised as much as possible.

The increase in the velocity through the bridge waterway opening occurs as a result of the increase in the energy head. The restriction in the waterway results in water banking upstream to a level sufficient to develop the additional head to increase the velocity to maintain equilibrium flow.

### 3.8.2.1. Length

In most cases it is not economical to bridge the full width of flood flow and the problem reduces to what is an acceptable length of bridge. As a consequence, the road embankment in the approaches to the bridge causes a restriction on the flow occurring under natural conditions. Consideration of the increase in velocity and hence scour potential and afflux would be the main determining factors for the length of a bridge. Longer bridges increase the cost but reduce the extent of constriction and therefore the risk of scour.

### 3.8.2.2. Height of abutments

The height of abutments should be considered in determining the length of a bridge. High abutments result in large retaining structures and embankments with inherent stability issues both in terms of the surcharge load to underlying material and long term structural issues including rotations and horizontal deflections. Instances have occurred where vertical and horizontal displacements at high abutments in soft soils has resulted in structural distress to the abutment and jamming of expansion joints.

### 3.8.2.3. Bridge height

The bridge height will be influenced by a number of factors being flood height, navigation clearance and span lengths.

### 3.8.2.4. Flood height

For high level bridges the deck level adopted will be above the design flood level. The clearance from the underside of the superstructure to the flood level (including freeboard) should be a minimum of 0.6 – 1.00 m. However the type, amount and size of debris likely may require an increased freeboard depending on local conditions.

### 3.8.2.5. Span lengths

In some cases the minimum span lengths may be determined by the size of the debris carried by the stream. The potential exists for a debris dam to be built up by log lengths greater than the spans.

The total bridge length is an important design feature, but others also need consideration, since this influences the flow velocity through the bridge and therefore the risk of scour. The important design consideration is to minimise the bridge length (and cost of the bridge) while keeping the risk of scour to an acceptable level.

A detailed approach to assessing scour as part of bridge design is given in QDTMR (2013).

## 3.8.3. Countermeasures for existing scour susceptible bridges

The greatest damage to bridges during floods is normally observed between the bridge approach and the abutment. Historically, this is the intersection between the road and bridge designer’s responsibility. Protection of the bridge should consider the impacts of overtopping flows at the roadway.

Scour countermeasures are incorporated at a bridge site to monitor, control, inhibit or minimise stream stability problems and bridge scour. In many cases, the best countermeasure is appropriate design that avoids causing stream instability but scour protection is needed for existing bridges that have experienced scour problems.

Over the last several decades, a wide variety of countermeasure structures, armouring materials and monitoring devices have been used at existing bridges to mitigate scour and stream stability problems.

Since scour susceptible bridges are already in place, options for structural or physical modifications such as replacement or foundation strengthening are limited and expensive. Unless these bridges are programmed for replacement, their continued operation will ultimately require the design and installation of a scour countermeasure.

Riprap is one of the primary scour countermeasures to resist local scour forces at abutments of typical bridges. Riprap is generally abundant, inexpensive and requires no special equipment. However, proper design and placement is essential. Guidelines for proper grading and placement methods are included in QDTMR (2013). When designing riprap countermeasures, maintaining an adequate hydraulic opening through the bridge must be considered. Improperly placed riprap may reduce the hydraulic opening significantly and create contraction scour problems. If placed improperly, riprap can increase local scour

forces. Although riprap is widely used, the following countermeasures can be considered as alternatives to riprap, but are not all covered here:

**Armouring countermeasures:**

- Rock riprap;
- Gabion boxes/ rock mattresses;
- Sack gabions;
- Grouted riprap;
- Grout-filled mats; and
- Articulating concrete blocks.

**River training countermeasures**

River training structures alter stream hydraulics to mitigate undesirable erosional and/or depositional conditions. They are commonly used on unstable stream channels to redirect stream flows to a more desirable location through the bridge, and require specialist design:

- Spurs (both permeable and impermeable);
- Bendway weirs;
- Guide banks; and
- Drop structures and check dams.

**Scour protection design for bridges**

Typical scour repair methods at bridges include:

- Dumped rock over a geofabric layer at piers, abutments and channel banks;
- Gabion mattresses over a geofabric layer at piers, abutments and channel banks; and
- Concrete (shotcrete) at bridge abutments.

Normally the scour protection is used to fill any scour holes that have formed to the original bed levels. Rigid measures such as concrete slabs are not as desirable due to potential for catastrophic failure. Flexible scour protections have an ability to self heal once a failure mode commences.

If shotcrete (concrete) is used at the bridge abutments for scour repair it must be tied into the abutment slope. If it is not properly tied into the slope it can be undermined and result in further damage to the abutment. This method is often not effective, particularly where the scour is being caused by a geotechnical failure of the embankment slopes.

Detailed descriptions of scour repair and protection for existing bridges is included in QDTMR (2013).

## 3.8.4. Scour protection for culverts

Culverts concentrate flow and also allow an increase in flood level upstream of the embankment. These factors increase the flow velocity at the culvert outlet compared to the

natural velocity in the channel. If this increase produces a velocity where scour could be introduced, protection measures are required, though good practice would lead to a design solution where the culvert design maintains a flow velocity at the outlet that is below the rate that causes scour.

Outlet protection is required in situations where:

- outlet velocity exceeds the scour velocity of the bed or bank material;
- an unprotected channel bend exists within a short distance of the culvert outlet;
- the outlet channel and banks are actively eroding; and
- if an erodible channel bank exists less than 10 to 13 times the pipe diameter downstream of the outlet, and this bank is in-line with the outlet jet (ie. likely to be eroded by the outlet jet) the bank should adequately protected to control any undesirable damage as a result of the outlet jetting.

The most appropriate outlet protection is determined by considering the hydraulic performance of the outlet in the prevailing stream environment. At outlet structures, the best hydraulic performance is obtained when the confining sidewalls are parallel and the distribution of flow across the channel is uniform.

Culverts, however, are generally narrower than the natural waterway and a transition section is required to return the flow to the natural channel. When culvert outlet velocities are high, additional measures at the outlet may prove to be necessary for energy dissipation.

To check whether standard inlet and outlet structures with headwalls, wingwalls, aprons and cut-off walls are adequate, the outlet velocity for the culvert requires examination with respect to:

- natural environment (soil and vegetation cover);
- size of peak flow; and
- duration of large flows.

If outlet velocities exceed the acceptable limits, it may be necessary to check for potential bed scour problems. Where the outlet flows have a Froude Number (*Fr*) less or equal to 1.7 and outlet velocities less than 5.0 m/s, an extended concrete apron or rock pad (commonly used) protection is recommended.

Design details are provided by Austroads (2013).

# 3.9. Flow Measurement Structures

## 3.9.1. Introduction

Sharp-crested weirs are often used to measure flow in open channels. Among their advantages, are that they are easy to install, accurate, and relatively inexpensive.

They do, however, have a major disadvantage in flows containing substantial amounts of sediment, in that they trap sediment and other solids behind them, leading to putrescible deposits in sewer applications. For this reason, sharp-crested weirs are most commonly used with relatively clean effluent, or in temporary flow monitoring locations.

The emphasis in this sub-section is on the analytical techniques, weir properties, and choice for particular purposes, and submergence characteristics. In particular, complete details on variations in discharge coefficient are not given, and the reader is referred to specialist texts for such information.

## 3.9.2. Rectangular Sharp-Crested Weir

The analysis of the sharp-crested weir is best illustrated by reference to a weir comprising a vertical plate mounted at right-angles to the flow. This represents the so-called “rectangular sharp-crested weir”.

The flow over such a weir is illustrated schematically in Figure 6.3.26. This figure includes also the necessary nomenclature for the analysis. Before proceeding with the analysis, some comments are provided on the flow situation.

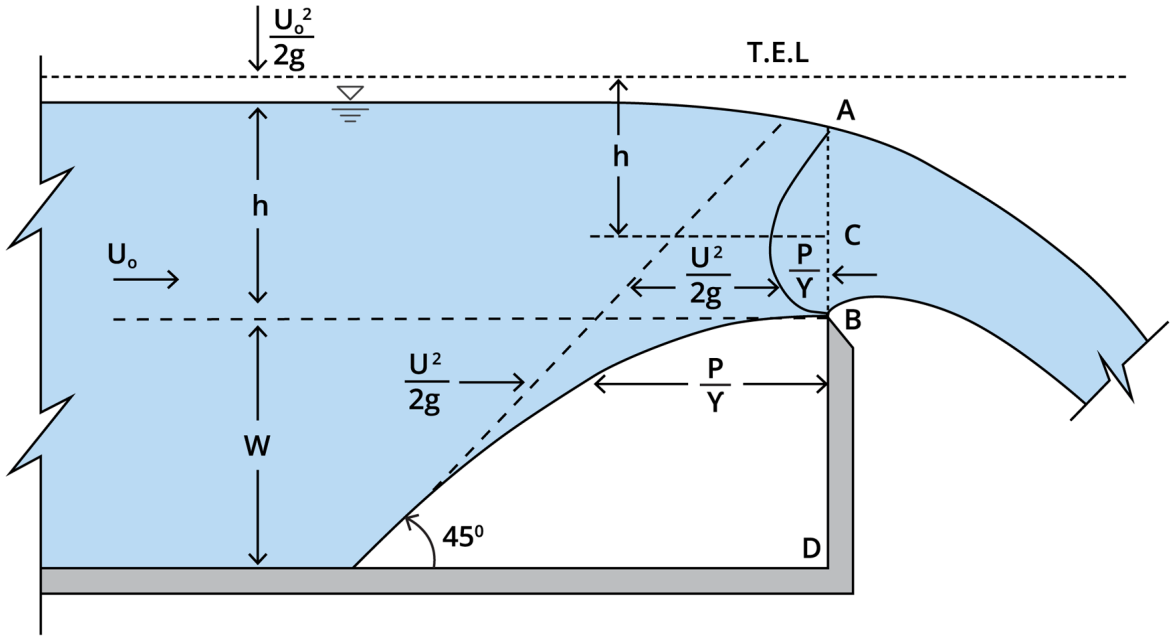


Figure 6.3.26. Schematic of Flow Over Rectangular Sharp-Crested Weir

It is noted first that the pressure distribution at the weir crest is non-hydrostatic. This situation arises because the pressure at both Points A and B is atmospheric by definition, and there are significant vertical components in the velocity as the flow contracts to pass over the weir crest.

Secondly, it is noted that, as expected, the total energy line (TEL) is situated an elevation $\frac{v_0^2}{2g}$ above the free surface, where $v_0$ is the approach velocity. In many cases, the magnitude of the approach velocity head may be considered to be negligible. For simplicity, this is assumed in the following analysis, although the influence of the approach velocity head will be included later.

Two further assumptions are utilised for simplicity:

1. The flow does not contract as it passes over the weir – ie. the elevation of A is the same as that of the upstream water surface; and

2. The pressure is atmospheric across the whole section AB.

With reference toFigure 6.3.26, these assumptions lead to an expression for the velocity at C of:

$$v = \sqrt{2gy} \tag{6.3.10}$$

The flow rate per unit width through an elemental strip of height $dy$ at C, is then given by:

$$d_q = \sqrt{2gy}dy \tag{6.3.11}$$

The integral of Equation (6.3.11) may then be expressed as:

$$q = \int_0^h \sqrt{2gy}dy \tag{6.3.12}$$

where $q$ is the flow rate per unit width.

Equation (6.3.12) is simply integrated and a contraction coefficient, $C_c$, introduced to allow for flow contraction over the crest, to yield:

$$q = \frac{2}{3}C_c\sqrt{2g}h^{\frac{3}{2}} \tag{6.3.13}$$

If the magnitude of the approach velocity head cannot be ignored, the integral form of Equation (6.3.11) is expressed as:

$$q = \int_{\frac{v_0^2}{2g}}^{h+\frac{v_0^2}{2g}} \sqrt{2gy}dy \tag{6.3.14}$$

Evaluation of Equation (6.3.14) yields:

$$q = \frac{2}{3}\sqrt{2g}\left[\left(\frac{v_0^2}{2g} + h\right)^{\frac{3}{2}} - \left(\frac{v_0^2}{2g}\right)^{\frac{3}{2}}\right] \tag{6.3.15}$$

Manipulation and introduction of the contraction coefficient leads finally to the result:

$$q = \frac{2}{3}C_c\sqrt{2g}h^{\frac{3}{2}}\left[\left(1 + \frac{v_0^2}{2gh}\right)^{\frac{3}{2}} - \left(\frac{v_0^2}{2gh}\right)^{\frac{3}{2}}\right] \tag{6.3.16}$$

The equation is made more compact by introducing a discharge coefficient, $C_d$, leading to:

$$q = \frac{2}{3}C_d\sqrt{2g}h^{\frac{3}{2}} \tag{6.3.17}$$

in which:

$$C_d = C_c\left[\left(1+\frac{v_0^2}{2gh}\right)^{\frac{3}{2}} - \left(\frac{v_0^2}{2gh}\right)^{\frac{3}{2}}\right] \tag{6.3.18}$$

It is evident from the form of Equation (6.3.18) that, if the velocity head is negligible compared with $h$, $C_d = C_c$ and Equation (6.3.17) is then identical to Equation (6.3.13).

Early work indicated that the value of $C_d$ is given by:

$$C_d = 0.611 + 0.08\frac{h}{W} \tag{6.3.19}$$

A small value of $h$ relative to $W$ is equivalent to a negligibly small approach velocity head. Under these circumstances, $C_d$ = 0.611 and Equation (6.3.17) becomes:

$$q = 0.407\sqrt{2g}h^{\frac{3}{2}} \tag{6.3.20}$$

The total flow rate over the weir is then given by the product of Equation (6.3.20) and the transverse crest length.

## 3.9.3. V-Notch Sharp-Crested Weir

The triangular sharp-crested weir is analysed under the same assumptions as the rectangular weir. The structure is shown schematically in Figure 6.3.27. The following analysis is again simplified by the assumption that the approach velocity head is negligible.

It needs to be recognised, however, that the concept of “flow rate per unit width” cannot be used because the width varies over the height of the weir. Accordingly, the elemental flow rate through the element of width $b$ is given by:

$$dQ = b\sqrt{2gy}dy \tag{6.3.21}$$

Integration of Equation (6.3.21) requires the expression of $b$ as a function of $y$. From Figure 6.3.27, and using similar triangles:

$$b = 2\tan\frac{\theta}{2}(h-y) \tag{6.3.22}$$

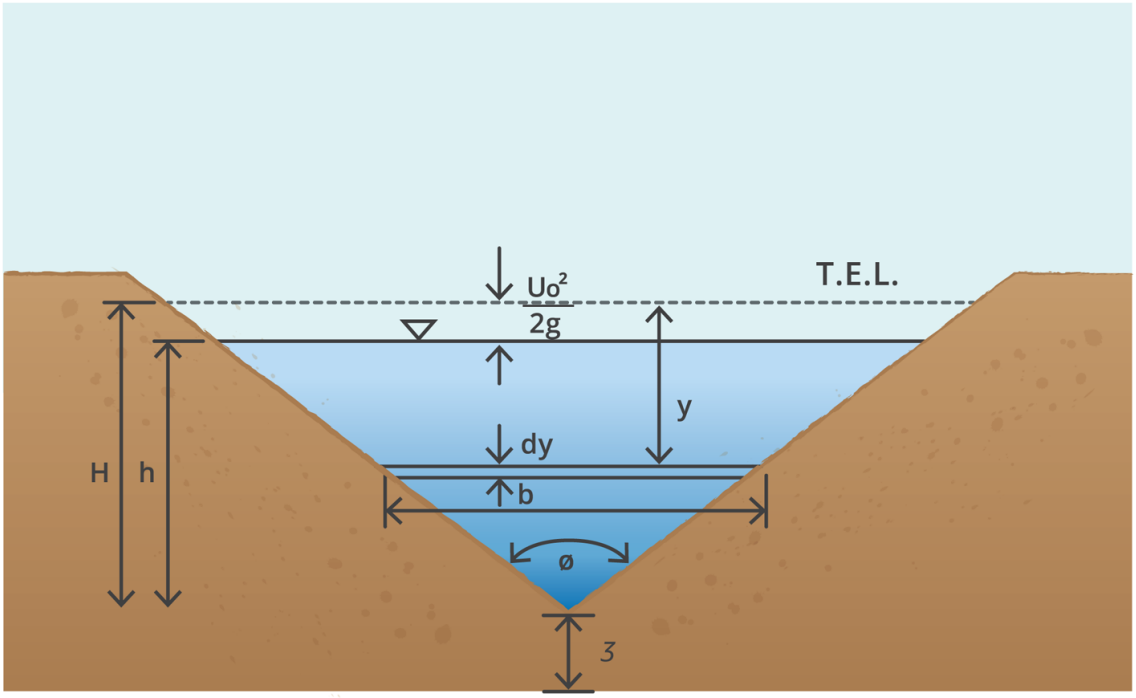


Figure 6.3.27. Schematic of Flow Over V-notch Sharp-Crested Weir

Substitution of Equation (6.3.22) into Equation (6.3.21), integration between the limits of $y = h$ and $y = 0$, and inclusion of the discharge coefficient yields:

$$Q = C_d \frac{8}{15} \sqrt{2g} \tan\frac{\theta}{2} h^{\frac{5}{2}} \tag{6.3.23}$$

The value of $C_d$ is dependent on the ratio of $\frac{h}{w}$ , but more particularly, on the vertex angle, $\theta$. For the commonly used value for θ of $90°$, a value for $C_d$ of 0.58 is commonly assumed. For other situations, values for $C_d$ may be obtained from standard texts on flow measurement.

The analytical techniques discussed above can be applied to any weir crest shape.

## 3.9.4. Submerged Weirs

When the tailwater level is higher than the crest of the weir, the weir is termed *drowned* or *submerged*. This state is not desirable because measurements of flow are more uncertain. Nevertheless, if submerged conditions cannot be avoided, a procedure is required to effect flow measurements.

A submerged weir is shown schematically in Figure 6.3.28.

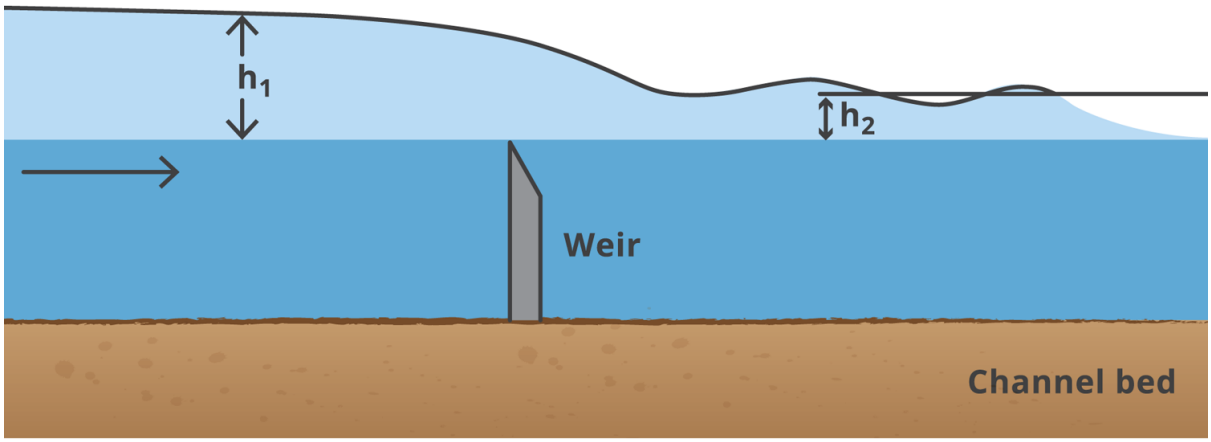


Figure 6.3.28. Schematic of Submerged Weir

A number of experiments were carried out on rectangular, triangular, parabolic, and Sutro submerged weirs and determined that the flow rate could be determined from the following equation:

$$\frac{Q}{Q_1} = \left[1 - \left(\frac{h_2}{h_1}\right)^n\right]^{0.385} \tag{6.3.24}$$

where $Q$ is the flow rate under submerged

conditions $Q_1$ is the flow rate assuming unsubmerged conditions

$h_1$ is the upstream head

$h_2$ is the downstream head

$n$ is the exponent in the unsubmerged flow equation $Q_1 = Ch_1^n$

## 3.9.5. Broad-crested Weirs and Long-Throated Flumes

Because critical flow represents a unique relationship between depth and flow rate, devices which induce critical flow are often used to measure flow in open channels. Most of these devices, however, require calibration in the laboratory because the flow characteristics are not in accordance with the usual theoretical assumptions.

Chief among these is the assumption that the pressure distribution is hydrostatic. In many devices, the strongly curved stream lines negate this assumption, resulting in the necessity for empirical coefficients.

The broad-crested weir and the long-throated flume are devices for which the flow rate can be predicted theoretically without the need for such coefficients. The broadness of the crest and the length of the throat are such that the stream lines are close to horizontal in the region of critical flow, permitting the assumption that the pressure distribution is hydrostatic.

The analysis of both the broad-crested weir and the long-throated flume is identical in that both rely on the determination of the relationship between the upstream water level (which may be measured) and critical depth within the constricted section – which is a known function of the flow rate. Thus, a unique relationship between flow rate and the upstream water surface elevation can be determined.

Broad-crested weirs are more prone to sediment buildup than long-throated flumes and are, consequently, less common in sewerage systems. For this reason, the emphasis in the following is on long-throated flumes, while recognising that broad-crested weirs are analysed in the same manner.

The long-throated flume is widely used in sewerage systems, within the pipe system and to monitor open channel inflows and outflows at sewage treatment plants.

In this section, the advantages of this type of structure are first discussed. The derivation of the theoretical rating curve is then presented for the rectangular flume and it is shown how this can be generalised for arbitrary cross-section shape. Their use in practice is then illustrated.

## 3.9.6. Advantages

The primary advantages of these devices are listed in the following:

- Provided that critical flow occurs in the throat, a rating table can be calculated with an error of less than 2% in the listed discharge. This can be done for any combination of a prismatic throat and an arbitrarily-shaped approach channel.

- The throat, perpendicular to the direction of flow, can be shaped in such a way that the complete range of discharges can be measured accurately, without creating an excessive backwater effect.

- The head loss across the structure required to obtain undrowned flow conditions is minimal, and can be estimated with sufficient accuracy for any of the structures placed in any arbitrary channel.

- Because of their gradually converging transitions, these structures have few problems with floating debris.

- Field and laboratory observations indicate that the structures can be designed to pass sediment transported by channels with subcritical flow. It should be noted, however, that excessively high sediment loads or significant reductions in the velocity of the approach flow may create sedimentation problems.

- Provided that its throat is horizontal in the direction of flow, a rating table based upon post-construction dimensions can be produced, even if errors were made in construction to the designed dimensions.

- Under similar hydraulic and other boundary conditions, these structures are usually found to be the most economical for the accurate measurement of flow.

## 3.9.7. Disadvantages

The major property of a long-throated flume is that it is designed to create a constriction in the flow area sufficient to produce critical flow over the full range of expected flow rates. In

addition, the head loss across the structure should not be excessive and afflux should be kept to a minimum.

A typical long-throated flume is shown schematically in **Figure 6.3.29**. With regard to the hydraulic characteristics of the flume itself, five components may be recognised as follows:

1. The approach channel, where the flow should be stable so that the water level and the energy level can be accurately determined.

2. A converging transition region into the throat, which is designed to provide a smooth acceleration of the flow with no discontinuities or flow separation. The transition may be rounded or consist of plane surfaces.

3. The throat, where the flow is accelerated to the critical condition. The throat must be horizontal in the flow direction, but can, in principle, be of any shape transverse to the flow. The invert of the throat may be higher than the invert of the upstream and downstream channels.

4. A diverging transition to reduce the flow velocity to an acceptable level and to recover head. If there is ample available head, an abrupt transition may be used.

5. The tailwater channel in which a known hydraulic control is exercised by the downstream conditions and the hydraulic properties of the channel.

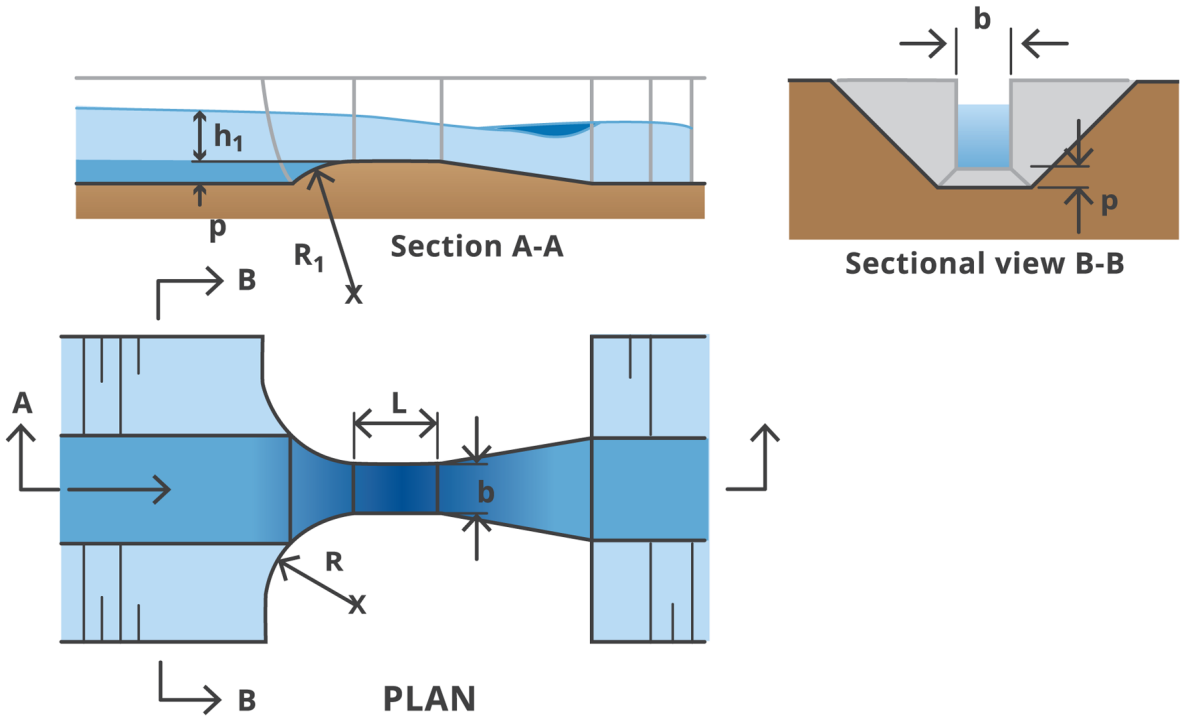


Figure 6.3.29. Schematic of Long-Throated Flume

The general profile of flow through a long-throated flume is shown schematically in Figure 6.3.30. The figure also shows the nomenclature for the theoretical analysis of the flume. In particular, we note that the energy level, $H$, and the stage height, $h$, are referenced to the invert level in the throat. As noted in 3, above, this is not necessarily the same as the channel invert level.

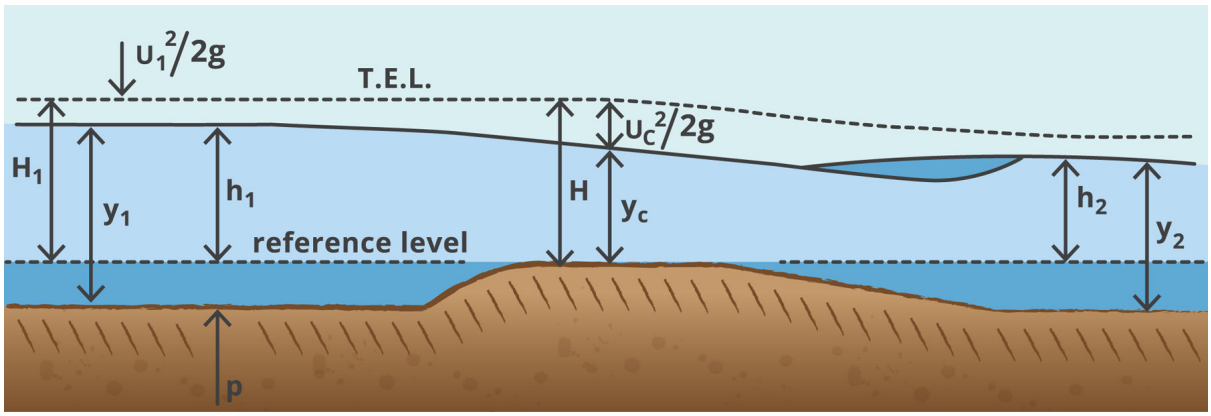


Figure 6.3.30. Flow Profile Through a Long-Throated Flume

The control section is the approximate location of critical flow within the throat of the flume. It is not necessary to know precisely where this occurs because the developed head-flow rate relationship is expressed in terms of the head upstream.

## 3.9.8. Analysis

With reference to Figure 6.3.30, application of the energy equation yields:

$$H_1 = y_c + \frac{v_c^2}{2g} \tag{6.3.25}$$

where subscript $c$ refers to critical conditions.

To proceed further, the shape of the control section must be known. For a rectangular cross-section, the properties of critical flow are such that:

$$y_c + \frac{v_c^2}{2g} = \frac{3}{2}y_c = \frac{3}{2}\sqrt[3]{\frac{q^2}{g}} \tag{6.3.26}$$

where $q$ is the flow rate per unit width within the control section.

Substitution of Equation (6.3.26) into Equation (6.3.25) and expanding yields:

$$H_1^3 = \left(\frac{3}{2}\right)^3 \frac{q^2}{g} \tag{6.3.27}$$

from which:

$$q = \frac{2}{3}\sqrt{\left(\frac{2}{3}g\right)}H_1^{\frac{3}{2}} \tag{6.3.28}$$

In terms of the width of the control section, $b_c$,Equation (6.3.28) is written as:

$$q = \frac{2}{3}\sqrt{\left(\frac{2}{3}g\right)}b_c H_1^{\frac{3}{2}} \tag{6.3.29}$$

where $Q$ is the total flow rate.

The development of Equation (6.3.29) has assumed ideal flow conditions – in particular, that there is no energy loss between the location of the upstream head, $H_1$, and the critical control. This is taken into account by introducing a discharge coefficient, $C_d$, such that:

$$Q = C_d \frac{2}{3}\sqrt{\left(\frac{2}{3}g\right)} b_c H_1^{\frac{3}{2}} \tag{6.3.30}$$

$C_d$ may be determined by an analysis of the boundary layer between the upstream head measurement point and the control section, but the complex procedure is rarely justified. High accuracy can be obtained by using the simpler equation:

$$C_d = \left(1 - \frac{0.006L}{b_c}\right)\left(1 - \frac{0.003L}{h}\right)^{\frac{3}{2}} \tag{6.3.31}$$

However, at the design stage, it is normally sufficient to assume a value for the discharge coefficient of 0.95.

Now,

$$H_1 = h_1 + \frac{v_1^2}{2g} = h_1 + \frac{Q^2}{2gA_1^2} \tag{6.3.32}$$

where $A_1$ is the cross-sectional area at the upstream location.

Equation (6.3.32) demonstrates that Equation (6.3.30) is difficult to use in practice because the head term, $H_1$, contains the unknown flow rate, $Q$, in addition to the measured head, $h_1$. An iteration method can be followed, using the following steps:

1. Assume, as a first approximation, that $h_1 = H_2$ and compute the discharge.

2. Use this approximate discharge to determine the velocity head and then use these data to calculate an improved value of the total head at the gauging section.

3. Compute a more refined discharge value using this total head value.

4. Repeat steps (2) and (3) until the difference between successive discharge values is an order of magnitude less than the required tolerance.

This process, although tedious, will lead to high accuracy.

A much more convenient approach is developed by defining a velocity coefficient, $C_v$, from the equation:

$$Q = C_d C_v \frac{2}{3}\sqrt{\left(\frac{2}{3}g\right)} b_c h_1^{\frac{3}{2}} \tag{6.3.33}$$

Comparison of Equation (6.3.33) and Equation (6.3.32) then shows that:

$$C_v = \left(\frac{H_1}{h_1}\right)^{\frac{3}{2}} = \left(\frac{h_1 + \frac{v_1^2}{2g}}{h_1}\right)^{\frac{3}{2}} = \left(1 + \frac{v_1^2}{2gh_1}\right)^{\frac{3}{2}} \tag{6.3.34}$$

Noting that $v_1 = \frac{Q}{A_1}$, Equation (6.3.34) is expressed as:

$$C_v = \left(1 + \frac{Q^2}{2gh_1A_1^2}\right)^{\frac{3}{2}} \tag{6.3.35}$$

Substitution of Equation (6.3.33) for $Q$ and simplification yields:

$$C_v = \left[1 + \frac{4C_v^2}{27}\frac{C_d^2(b_c h_1)^2}{A_1^2}\right]^{\frac{3}{2}} \tag{6.3.36}$$

We now replace $b_c h_1$ by $A^*$, the imaginary cross-sectional area of the control section if the water depth there was equal to $h_1$, and further simplify to give:

$$C_d\frac{A^*}{A_1} = 2.60\sqrt{\frac{C_v^{\frac{2}{3}} - 1}{C_v^2}} \tag{6.3.37}$$

A plot of $C_v$ against the area ratio, $C_d\frac{A^*}{A_1}$, can then be drawn and is presented in Figure 6.3.31. In this figure, the upper curve is a continuation of the lower curve beyond the right hand limit of the figure.

Because $A^*$ and $A_1$ can be expressed in terms of the measured water surface elevation, $h_1$, the velocity coefficient, $C_v$, can be directly determined.

Corresponding graphs for $C_v$ for non-rectangular cross-sections may be obtained in a similar manner. Such graphs are available in standard texts.

The rating equations for non-rectangular cross-sections are easily determined once the relationship between the critical depth, $y_c$, and the upstream energy level, $H_1$ is known. For example, application of the specific energy principles to the triangular cross-section yields:

$$y_c = \frac{4}{5}H_1 \tag{6.3.38}$$

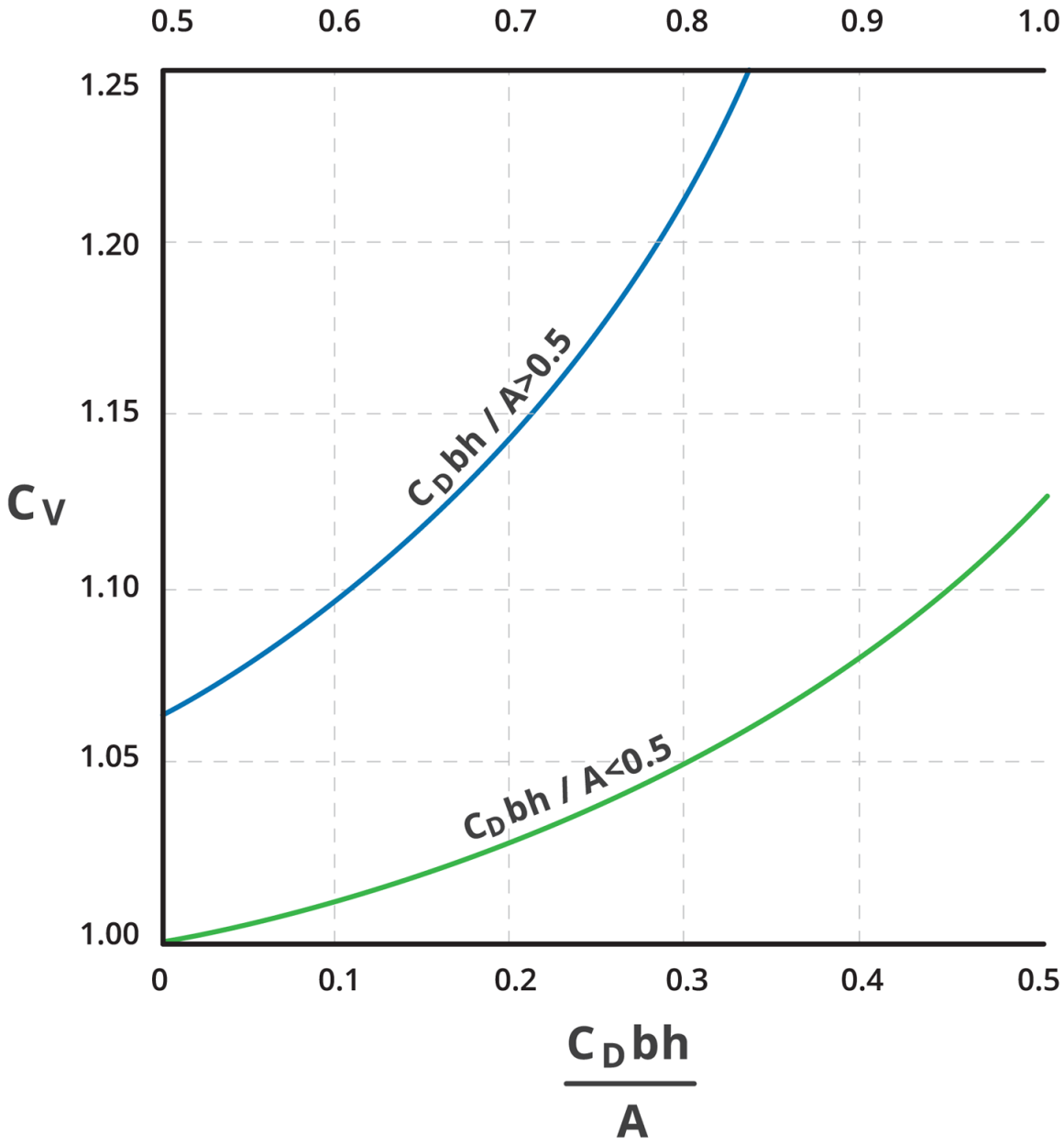


Figure 6.3.31. $C_v$ Relationship for Rectangular Cross-Sections

Substitution of Equation (6.3.38) into Equation (6.3.23) and subsequent manipulation yields:

$$Q = C_d C_v \frac{16}{25}\sqrt{\frac{2}{5}g}\tan\frac{\theta}{2}h_1^{\frac{5}{2}} \tag{6.3.39}$$

where $\theta$ is the vertex angle of the control section.

## 3.9.9. Uncertainty in Flow Measurement Structures

No measurement is perfectly accurate or exact. Many instrumental, physical and human limitations cause measurements to deviate from the true values of the quantities being measured. We refer to these deviations as uncertainties, although, more commonly, the

shorter word error is used. In this review, we will continue to use the word *uncertainty* since it is a more accurate descriptor

## 3.9.9.1. Systematic and Random Uncertainty

Generally, uncertainties can be divided into two broad and rough but useful classes: systematic (or determinate) and random (or indeterminate).

Systematic uncertainties tend to shift all measurements in a systematic way so their mean value is displaced. *Systematic* means that when the measurement of a quantity is repeated several times, the uncertainty has the same size and algebraic sign for every measurement.

Systematic uncertainties may be due to such things as incorrect calibration of an instrument, consistently improper use of equipment or failure to properly account for some effect. A systematic uncertainty is a true error and large systematic errors can and must be eliminated in a good experiment. Every effort should be made to minimise the possibility of these errors, by careful calibration of the apparatus and by use of the best possible measurement techniques. However, small systematic errors will always be present. For instance, no instrument can ever be calibrated perfectly.

Other sources of systematic errors are external effects which can change the results of the experiment, but for which the corrections are not well known.

Systematic errors can be more serious than random uncertainties for three reasons as follows:

1. There is no sure method for discovering and identifying them just by looking at the experimental data;

2. Their effects cannot be reduced by averaging repeated measurements; and

3. A systematic error has the same size and sign for each measurement in a set of repeated measurements, so there is no opportunity for positive and negative errors to offset each other.

Random uncertainties fluctuate from one measurement to the next and are present in all experimental measurements. As such, they cause a measuring process to give different values when a measurement is repeated many times (assuming all other conditions are held constant to the best of the operator’s ability). Random uncertainties can have many causes, including operator errors or biases, fluctuating physical conditions, varying environmental conditions and inherent variability of measuring instruments.

The effect that random uncertainties have on results can be somewhat reduced by taking repeated measurements then calculating their average. The average is generally considered to be a better representation of the true value than any single measurement, because uncertainties of positive and negative sign tend to compensate each other in the averaging process. They yield results distributed about some mean value.

A measurement with relatively small random uncertainty is said to have high precision. A measurement with small random uncertainty and small systematic error is said to have high accuracy. Precision does not necessarily imply accuracy. A precise measurement may be inaccurate if it has a systematic error.

### 3.9.9.2. Determination of Flow Rate Uncertainty from Uncertainty in Measured Head

Frequently, the assessed flow rate will not be measured directly. Rather, it will be determined through a functional relationship from a measurement of head with its own uncertainty. The question is: What is the resulting uncertainty in the assessed flow rate?

The answer depends on the equation linking the flow rate with the directly measured parameters. We first return to the functional relationship derived for the rectangular sharp-crested weir:

$$Q = 0.407B\sqrt{2g}h^{\frac{3}{2}} \tag{6.3.40}$$

Using the rules of differentiation we can determine the derivative of this equation in the form:

$$Q = 0.407B\sqrt{2g}\frac{3}{2}h^{\frac{1}{2}}dh \tag{6.3.41}$$

Now we divide Equation (6.3.41) by Equation (6.3.40). Because of the equality, we can divide the left side of Equation (6.3.41) by the left side of Equation (6.3.40) and the right side of Equation (6.3.41) by the right side of Equation (6.3.40).

Thus:

$$\frac{dQ}{Q} = \frac{3}{2}\frac{dh}{h} \tag{6.3.42}$$

In words, Equation (6.3.42) indicates that the percentage uncertainty in flow rate ($Q$) is equal to (3/2) x the percentage uncertainty in measured head ($h$). We note that the fraction 3/2 is the exponent of the function in Equation (6.3.40).

Indeed, we can now state the completely general equation for uncertainty for a functional relationship of the form $y = Ax^n$ as follows:

If $y = Ax^n$, and there is an uncertainty in the independent variable of $dx$ the consequent uncertainty in the dependent variable is given by:

$$\frac{dy}{y} = n\frac{dx}{x} \tag{6.3.43}$$

Equation (6.3.43) is a very simple equation to apply.

## 3.10. References

Austroads (2013) Guide to Road Design - Part 5: Drainage, Austroads Ltd, Sydney.

Cameron and McNamara, (1966), Model investigations of causeway designs - Report to Commonwealth Department of Works, Cameron and McNamara Consulting Engineers, Brisbane.

Fredrickson, L.H. (1979), Floral and faunal changes in lowland hardwood forests in Missouri resulting from channelization, drainage, and improvement. Report No. FWS/OBS-78/91, Fish and Wildlife Service, U.S. Department of the Interior, Washington, DC.

French, R.H. (1985), Open Channel Hydraulics, McGraw-Hill Book Company, New York.

Henderson, F.M. (1966), Open Channel Flow, Macmillan Publishing Co., New York

Keller, R.J. (1995), Meander re-instatement using submerged weirs. Department of Civil Engineering, Monash University, Final Report, Land and Water Resources Research and Development Corporation Partnership Project P85/05.

Keller, R.J. (1986), Hydraulic Investigation of Proposed Culvert Structures, Report for Road Construction Authority.

Keller, R.J., Peterken, C.J, and Berghuis, A.P. (2012), Design and assessment of weirs for fish passage under drowned conditions, Ecological Engineering, 48: 61-69.

List, E.J and Imberger, J. (1973), Turbulent Entrainment in Buoyant Jets and Plumes, Journal of the Hydraulics Division, ASCE, 99(9), 1461-1474.

Peterka, A.J. (1978), Hydraulic design of stilling basins and energy dissipaters. Engineering Monograph No.25, USER, Denver, Colorado, USA.

Portland Cement Association (1964), Handbook of Concrete Culvert Pipe Hydraulics, Portland Cement Association, Illinois.

QDTMR (Queensland Department of Transport and Main Roads) (2015), 'Road Drainage Manual', Available at http://www.tmr.qld.gov.au/business-industry/Technical-standards-publications/Road-drainage-manual.

QDTMR (Queensland Department of Transport and Main Roads) (2013),'Bridge Scour Manual', available at http://www.tmr.qld.gov.au/business-industry/Technical-standards-publications/Bridge-scour-manual.aspx.

Rouse, J., Bhocta, B.V., Hsu, E.Y (1951), Design of Channel Expansions, Trans. ASCE, 1(116), 347.

U.S. Department of Transportation (1972), Hydraulic Design of Improved Inlets for Culverts, Hydraulic Engineering Circular No.13.

United States Army Corps of Engineers (USACE). (1995), Hydraulic Design of Spillway, Technical Engineering and Design Guides as adapted from the US Army Corps of Engineers, No.12 ASCE.

United States Army Corps of Engineers (USACE) (2000), Design and Construction of Levees, Report #EM 1110-2-1913, April.

US Army Corps of Engineers Waterways Experiment Station (1952), revised in subsequent years. Corps of Engineers Hydraulic Design Criteria.

# Chapter 4. Numerical Models

Andrew McCowan

| Chapter Status | Final |
|---|---|
| Date last updated | 14/5/2019 |

## 4.1. Introduction

Hydrology and hydrologic modelling are generally related to the determination of discharge characteristics of flood flows. By comparison, the main aim of hydraulic modelling is to describe the details of the main water level and velocity characteristics of the hydrologically derived flood flows. An appropriately set-up and calibrated hydraulic model can be used to not only describe the details of flood flows and their distribution throughout a river and floodplain system, but also to predict the likely impacts that any changes to that system may have on these flows. Typical applications for hydraulic models may include:

- Prediction of the behaviour of floods, including extreme flood events;
- Evaluation of the effects of proposed changes that may affect flood flows; and
- Assessment of a range of flood mitigation works

Prior to the advent of computers, hydraulic modelling of river flows could only be carried out in physical models. Although geometrically similar to the physical systems they represent physical models are subject to scaling constraints as described in Book 6, Chapter 2, Section 2. Due to the time and costs involved, physical modelling could only be justified for major projects. Today, the use of physical models is typically limited to modelling complex flows in relatively small reaches of river, and for modelling the behaviour of flows in hydraulic structures.

Although the basic equations governing river flow were derived in the 19th Century, it was not until the development of computers in the 1960s and 1970s that numerical modelling of river flows became practical. With the rapid on-going development of computers and computing power, there has been a continual evolution of numerical modelling and modelling techniques. This has resulted in the availability of a wide range of numerical models with increasing capability, and increased complexity.

The first numerical hydraulic models were little more than computerised backwater calculators for steady flows in one (along stream) dimension. These one-dimensional (1D) models gradually increased in sophistication to include hydraulic structures, unsteady flows, simply connected (dendritic) branched channel networks and, ultimately, multiply connected branched channel networks. With the multiply connected channel models it became possible to separate floodplain flows from main channel flows through the introduction of separate floodplain flow paths or systems of overbank floodplain cells. These models were sometimes called quasi-2D models.

In the early to mid-1990s, numerical modellers began to apply fully two-dimensional (2D) hydraulic models to river and floodplain systems. Many of these models had been originally developed for modelling flows in bays and coastal seas and required modifications to make them more suitable to simulating river and floodplain flows. 2D flood models use square or curvilinear grids, or flexible meshes, to provide much greater resolution of the flows in

floodplains. As a result, 2D modelling was rapidly embraced by the modelling community and, by the early 2000s, had become almost a de facto “standard” for flood modelling in Australia.

Further development saw coupling of 1D channel models with full 2D models to provide a better description of in-bank flows and flows in sub-grid (or mesh) scale channels. These coupled 1D/2D models also allowed the introduction of model structures in localised 1D model branches to provide a better representation of hydraulic structures such as culverts, weirs and bridges. Full 2D models have also been applied extensively to simulating the hydraulics of urban stormwater flows. For these applications 2D models have also been coupled with pipe network models to provide a better description of the flows in underground stormwater drainage systems.

In the early to mid-2000s, the use of full 2D models was extended to also include the effects of rainfall over the model domain. With this “direct rainfall” or “rainfall on grid” approach it is possible to simulate the rainfall/runoff (hydrologic) processes throughout the model area and integrate them with the hydraulic routing of the resulting overland flows. This is particularly useful in urban applications or other situations where the model area includes a significant proportion (or even all) of the catchment contributing to the flow within the model. In these cases, the approach can reduce (and in some cases eliminate) the need for separate hydrologic modelling, but is still the subject of on-going research (Engineers Australia, 2012).

In general, it can be said that the more realistic the modelling approach, the greater the probability of achieving a successful outcome. However, the use of the most sophisticated modelling approach available will not, in itself, guarantee success. This is because the skill of the modeller adapting a generic modelling system to a specific application, and the quality of the data used as model input can be equally (or even more) important in determining the success of a modelling exercise. This can especially true for direct rainfall modelling. Indeed, there will be applications where simplified approaches, suitably applied, may be more appropriate than the use of more sophisticated models.

This chapter introduces the basis of numerical hydraulic models of river and floodplain flows. The differences between steady and unsteady flow models are discussed, and the range of modelling approaches that are currently available are described. More details are then provided on the application of 2D models for describing flood flows.

## 4.2. Development Stages for Numerical Hydraulic Models

The aim of a numerical hydraulic model is to provide a discrete numerical representation of flood flows in what is a physically continuous river and floodplain system. In this respect, the development of a site specific numerical model can be thought of as comprising a sequence of four main steps, as follows:

1. Review and define the physical system (the river and floodplain system to be modelled)

2. Select an appropriate mathematical model (the set of equations or combination of sets of equations to be used to describe the physical system)

3. Select a generic numerical model (the modelling software to be used to solve the equations of the mathematical model)

4. Develop the site-specific numerical model (through the application of site specific inputs to the generic modelling software. These inputs will typically include topographic data, bed-friction coefficients, flow boundary conditions and other parameters such as structure information, as appropriate)

At each step different types of assumptions, approximations and/or simplifications must be made. The steps are discussed briefly below, with further supporting information provided in the following sections. The conceptualisation process is shown schematically in Figure 6.4.1.

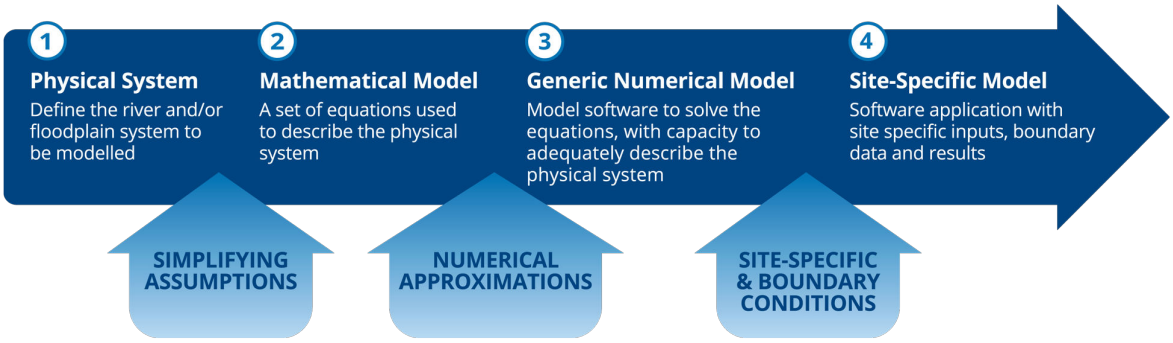


Figure 6.4.1. Stages in Numerical Hydraulic Model Conceptualisation and Development

## 4.2.1. Review of the Physical System

It is essential to have a broad understanding of the hydraulic behaviour of the physical system to be modelled in order to select the most appropriate mathematical model or models to be used. Whilst it is common that detailed hydraulic behaviour of the system is unknown, a good working knowledge of the study area and contributing catchment is required. Aspects such as the study area, shape and slope are important. (Is the subject land low-lying or close to the sea?) The location and dimensions of the main flow paths as well as the effects of any flow controls need to be understood. This can include the effects of flood protection works, such as levees, as well as the effects of formal drainage infrastructure, such channels, hydraulic structures and pipe networks. Land-use is also an important element of the physical system to consider. The distribution of roads, number and type of buildings and the extent and composition of vegetation can all affect the conceptualisation and selections made in following steps.

## 4.2.2. Selection of the Mathematical Model(s)

Selection of the mathematical model (or models) to be used to describe the physical system is the most important decision to be made in this four step process. In this step, the description of the flow in the physical system, which can be complex and highly turbulent, must be reduced to an equation, or set of equations describing the main characteristics of the flow. Here assumptions have to be made as to whether the flow can be considered as being one dimensional (1D), two dimensional (2D), a combination of 1D and 2D, or even three dimensional (3D). Further, a decision must be made as to whether the flow can be described as being steady (i.e., constant with time), or unsteady (time varying).

In 1D models, the flow is described in terms of cross-sectionally averaged discharges and water levels along pre-determined flow paths. In 2D models the flow is described by depth averaged velocity variables in two horizontal directions and water levels across a regular grid or flexible mesh. In all cases (1D, 2D and 3D), the flow equations generally assume there are no vertical accelerations and that the pressure distribution is hydrostatic. As a result, empirical structure equations are frequently used to describe the flow across structures (e.g., weirs, bridges and culverts) and at other locations where vertical accelerations may become important (e.g., across levee banks, or road embankments). It is important that the modeller has an understanding of the limitations of the selected mathematical modelling approach.

### 4.2.3. Selection of the Numerical Model

In going from the mathematical model to the numerical model, continuous mathematical equations have to be approximated by discrete arithmetic equations that can be solved by a computer. This process is generally carried out within a generic numerical model or modelling software package. The errors introduced by the discretization process are called “truncation” errors and reduce with the grid size and/or time step. That is, the smaller the grid size and time step, the smaller the truncation errors. In some models, low-order dissipative numerical truncation errors are deliberately introduced, or can be introduced as an option, to help stabilize the numerical computation.

Numerical solution procedures can involve finite difference, finite element and finite volume techniques. Finite differences are generally used in 1D models, while finite volume techniques are becoming increasingly popular in 2D and 3D applications. The introduction of “parallel processing” through multiple core computers and graphics processing units (GPUs) has dramatically increased the computing power available allowing much larger model domains and/or finer grid/mesh sizes to be used in 2D and 3D modelling applications. Additionally, the various commercially available generic modelling packages can have quite different approaches to modelling different flow characteristics such as flooding and drying, super-critical flows and sub-grid scale processes. It is therefore important that the modeller has an understanding of the capability and any potential limitations that the generic numerical model may have for simulating the flow conditions in any particular application.

### 4.2.4. Development of the Site-Specific Model

The Site-Specific model is developed from the generic Numerical Model (software package) through:

- Selection of a modelling domain,
- Selection of the grid or mesh size and time step,
- The input of site specific data including: topographic data (cross sections and/or topography) and bed-friction data, and
- The application of flow and /or water level boundary conditions.

Once a site-specific model has been developed it must be calibrated and, where possible, validated to ensure that it is capable of providing a reliable description of the flow characteristics within the area of interest. This is described in the following section.

## 4.3. Model Reliability

Assuming that the most appropriate mathematical model has been selected to describe a particular physical system, there are two main steps for determining the accuracy and reliability of the model results. These are model verification and model calibration and validation. These are described briefly below.

### 4.3.1. Model Verification

Model verification is the process whereby checks are made to ensure that the generic numerical model (i.e., the modelling software package) is actually solving the equations of the mathematical model. Most hydraulic modelling work will generally involve the use of well-

tried and proven software packages. In these cases, it can be assumed that the modelling software has been validated and that it is capable of solving the equations of motion correctly. Nevertheless, it can be useful for inexperienced modellers to carry out their own verification runs using standard test cases to provide confidence that they are operating the model correctly. These verification runs could include reproduction of uniform channel flow and/or reproduction of standard backwater or drawdown cases.

Modellers should be aware that all software packages have “bugs”, which can lead to spurious results and/or instability, particularly when used in modelling high velocity flows and in “non-standard” applications. Modellers should also be aware that different modelling packages can use different forms of the under-lying equations, different numerical solution procedure, and different approaches and assumptions to modelling special flow cases such as super-critical and flows at structures. Here it is important for a modeller to be aware of the assumptions that are used in the selected modelling package, and to be confident that they are appropriate for the physical system to be modelled.

Finally, there is a tendency for modellers to be innovative and to use models in situations well beyond the range of conditions for which they were originally developed. Typical examples might include the use of a 2D model to simulate flows where there may be significant vertical accelerations, or where there may be a significant three-dimensional component to the flow. Caution should always be used when using a package in these types of applications. Wherever possible, model results should be compared with analytical results, physical model results, or more appropriate (e.g., 3D or CFD) model results to obtain an estimate of the likely magnitude of the errors involved.

## 4.3.2. Model Calibration and Validation

Model calibration and validation provides an overall check of the reliability of a model. That is, how well the final site-specific model is representing the flow conditions in the physical system to be modelled. Ideally, calibration and validation is a two stage process, as follows.

Model calibration is the process of comparing model results against measured flood levels and extents and adjusting model parameters to obtain a “best-fit”. For flood studies, model calibration is typically carried out on the largest flood for which reliable water level data is available. In studies where more frequent flooding may be important, the model should also be calibrated against measurements taken from a more frequent flood event. During the calibration process, model parameters (typically bed-friction coefficients) are adjusted and the model re-run until the results give the best reproduction of the measured data.

In the first instance, the calibration process is also used to identify any inconsistencies in the model terrain data and boundary conditions. If after repeated efforts, it is not possible to obtain a reasonable representation of the measured data or, if this can only be achieved by the use of physically unrealistic input parameters, then it will be necessary to look more closely at: the assumptions made in the selection of the generic mathematical model, the appropriateness of the selected modelling package for reproducing the flow conditions under consideration, and the reliability of the boundary conditions that have been applied to the model.

Model Validation is the process whereby the calibrated model is used to simulate an independent flood event to provide a check on the reliability of the calibration process. The flood event will typically be somewhat lower than the calibration case and, in some cases, the results may be used to further refine the calibration process.

## 4.4. Steady vs Unsteady Hydraulic Models

Numerical hydraulic models can be described as being either steady flow models, where the depth of flow remains constant with time, or unsteady flow models, where the depth of flow can vary with time. These models typically assume the flow to be gradually varying in space. That is, variations in flow depth are small in relation to the distance over which they occur. Under these conditions the pressure distribution can be assumed to be hydrostatic.

In the early days of numerical hydraulic modelling, the models were limited to 1D and the distinction between steady flow and unsteady flow models was quite marked. This was because Hydrolic Engineering Center of the US Army Corps of Engineers made their River System, HEC-RAS, a relatively sophisticated 1D steady flow model, freely available to anyone who wanted to use it. By comparison, unsteady flow modelling required modellers to either have specialist modelling skills to develop or adapt research-based models, or to purchase what was then quite expensive specialised modelling software packages. As a result there was a tendency for modellers to “push” the use of HEC-RAS well beyond the range of application for which it was originally designed.

With the advent of more readily available and relatively sophisticated 1D and 2D unsteady flow models, the distinction between steady and unsteady flow models has become less marked. This is because there is less reliance on specialised steady flow models and, where required, much of the steady flow modelling is carried out by unsteady flow models using steady flow boundary conditions.

### 4.4.1. Steady Flow Models

In steady flow modelling, the flow velocity $u$ and discharge $Q$ can be assumed to be locally constant and do not vary in time. Under these conditions, the acceleration terms in the equations of motion, described in Book 6, Chapter 4, Section 6, can be assumed to be negligible. This means that the flow is assumed to be in equilibrium with any potential increase in momentum or energy as water flows downstream being balanced by bed-friction and other friction losses such as may occur at structures.

1D steady flow models such as 1D steady flow version of HEC-RAS (USACE, 2010) can be used to compute flood profiles in a wide range of situations. This version of HEC-RAS is based on the numerical solution of the profile equation presented in Book 6, Chapter 2, Section 8. This in turn is based on the 1D energy equation. Manning’s equation is used to compute energy losses due to bed-friction, and other contraction and expansion losses are calculated using a coefficient times the change in velocity head. The momentum equation is used in situations where there are rapid variations in the water surface profile, such as at hydraulic jumps. The computations can also include empirical structure equations to describe rapidly varying flows at a range of structures including bridges, culverts, weirs and spillways.

When using steady flow models, such as HEC-RAS, or using unsteady flow models with steady flow boundary conditions, it is noted that the main underlying assumptions of steady flow are effectively that:

- The discharge is constant (usually calculated by a hydrologic model);
- The peak flood levels coincide with the peak discharge; and
- The peak discharge and corresponding flood levels occur simultaneously over the full length of the reach of channel under consideration.

For these reasons, and for the reasons described in the following section, steady flow models are best suited to modelling flows along relatively short reaches of river with well-defined flow paths, and/or for modelling flows at structures. Steady flow models should not be used to describe flows where there are:

- Rapidly changing hydrographs;
- Flat channel slopes where wave propagation effects can become important;
- Wide floodplains and/or other features where storage effects may affect the flow; and
- Channel networks where the flow splits are not well defined.

**The Manning Equation**

The Manning equation for uniform flow can be considered as the simplest form of steady flow model. Here the average velocity *u* across a cross-section can be related to a Manning roughness coefficient *n*, the hydraulic radius *Rh*, and the bed slope *S*:

$$u = \frac{1}{n} R_h^{\frac{2}{3}} S^{\frac{1}{2}} \tag{6.4.1}$$

For a wide open floodplain, the hydraulic radius can, to a first approximation, be replaced by the flow depth y:

$$u = \frac{1}{n} y^{\frac{2}{3}} S^{\frac{1}{2}} \tag{6.4.2}$$

These equations can be used by modellers as a sanity check to ensure that their models are providing results with flow velocities of the correct order of magnitude. For example, a relatively smooth floodplain with $n = 0.04$, a moderate slope of $S = 0.001$, and a depth of $y = 1.0$m would be expected to have a flow velocity of approximately $u = 0.8$ m/s.

## 4.4.2. Unsteady Flow Models

Unsteady flow models are not restricted by the steady flow assumption, and can be applied to a much wider range of flow conditions. Referring to the limitations of steady flow models, described above, situations in which an unsteady flow modelling should be used are discussed below.

**Rapidly Changing Hydrographs**

With rapid changes in flow, the inertial (acceleration) terms in the equations of motion become important. (These terms are not included in steady flow models). Examples include modelling of dam-breaks and structure operations, as well as modelling of reaches where the time of propagation of a flood wave through the reach cannot be considered insignificant relative to the duration of the flood hydrograph.

**Flat Channel Slopes**

For flat channel slopes, flow velocities and, correspondingly, the effects of bed friction can become small relative to the main time-varying acceleration terms in the equations of motion. This is particularly true in lakes and estuaries. For this reason, the American Society of Engineers (1996) recommends that unsteady flow modelling should be carried out for

channel slopes less than about $4x10^{-3}$ and, depending on the study objectives, for slopes up to about $1x10^{-3}$.

**Storage Effects**

In reaches where there are significant storage effects, the rating curve on the rising limb of a flood hydrograph will be different to the rating curve on the falling limb. This results in a "looped" rating curve, as shown in Figure 6.4.2. Under these conditions the peak water level will not correspond to the peak discharge. As a result, unsteady models should be used to simulate these effects.

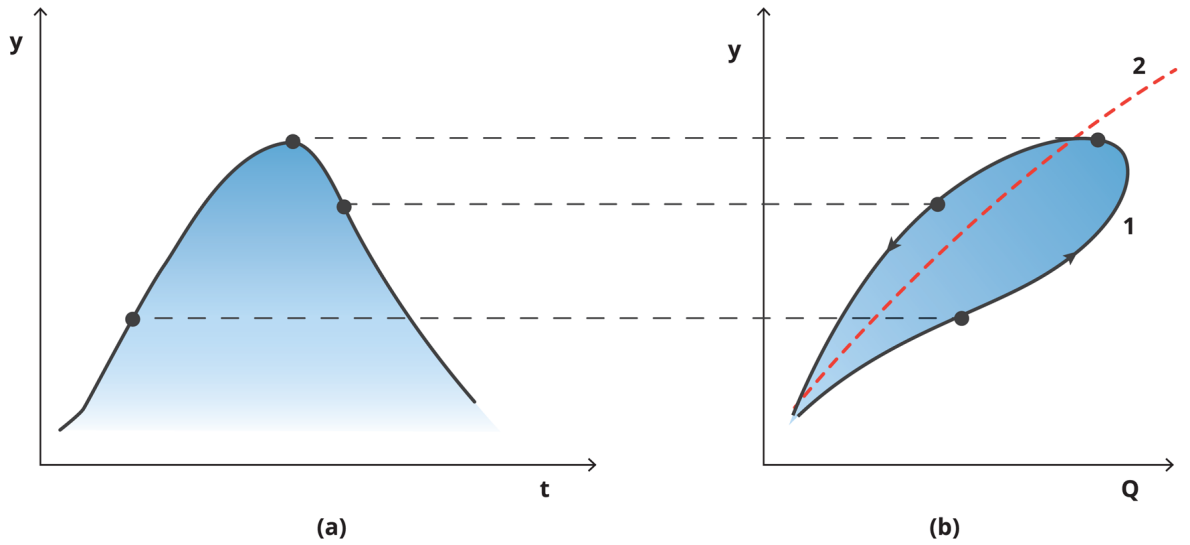


Figure 6.4.2. Storage Effects on the Rating Curve; (a) Flood Hydrograph, (b) Corresponding Rating Curve (Cunge et al., 1980)

**Channel Networks**

Unsteady flow models have the ability to compute the distribution of flows throughout a channel network or across a model domain, whereas steady flow models can only modelled on the basis of pre-determined flow splits. In real-life situations peak flows in tributaries rarely correspond with the peak flow in the main channel and, in some cases, backwater effects from one part of a network (e.g., a main channel) can cause time-varying flow reversals in another part (e.g., a tributary). Unsteady flow models are required to simulate these effects.

## 4.5. Types of Unsteady Flow Models

With the exception of the steady 1D form of HEC-RAS most models currently in use have unsteady modelling capability. In order of increasing level of sophistication, the main types of unsteady flow model that can be applied to flood investigations, include:

- 1D models
- 2D models
- Coupled 1D/2D models
- 3D models

- CFD, physical and other non-hydrostatic models

These are described briefly below. More details on the use of 1D, 2D and coupled 1D/2D models in flood modelling applications are then provided in the following sections.

### 4.5.1. 1D Models

1D flow models are based on the numerical solution of the Saint Venant equations for describing gradually varying unsteady flow in one horizontal dimension. Early 1D models required the main channel and flood plain of a river to be schematised as a single one-dimensional channel. The use of these early 1D models was generally restricted to modelling single river branches, or simply connected (dendritic) branched river systems. As part of the evolutionary process of model development these relatively simple models have been replaced by more sophisticated models that allow arbitrary connections of multiple channel systems. In these models, floodplains can be represented as separate flow paths and there can be multiple flow paths within a single floodplain. This makes it possible to provide a somewhat more realistic description of the flows in real river and floodplain systems.

1D models are computationally quick to run and are well suited to modelling flows along well-defined channel and floodplain flow paths. Their more general use in flood studies has been largely superseded by 2D models which can provide a much more detailed description of flood flows in overbank areas. 1D models are still used in applications where large numbers of multiple model runs are required and computational time requirements make 2D modelling impractical. 1D models have also been integrated with 2D models in order to make the most of the relative advantages of both types of model.

### 4.5.2. 2D Models

2D flow models are based on the numerical solution of the depth-averaged equations describing the conservation of mass and momentum in two horizontal dimensions. These equations assume that the flow velocity is uniform over the depth, both in magnitude and direction. This assumption is reasonable in most floodplain applications where the flow depth is relatively shallow with respect to the horizontal dimensions of the main physical features to be resolved in the model.

The 2D model equations are solved at each active water grid point or mesh element over a two-dimensional model grid or mesh. The computational domain may be a square, rectangular or curvilinear grid, or may be a flexible mesh comprising triangular and/or quadrilateral mesh elements. With these models survey information for the area of interest is digitised onto the two-dimensional model grid or mesh. This capable of providing a detailed description of the flow in floodplains and overbank areas.

2D models can have problems in providing adequate resolution of in-bank flows and, compared with 1D models, are heavy computationally. With respect to the latter, it is noted that the use of parallel processing coupled with multi-core computers and/or graphics processing units (GPUs) has significantly enhanced the computational capability of 2D models.

### 4.5.3. Coupled 1D/2D Models

Coupled 1D/2D models are aimed at making the most of the best features of both 1D and 2D models. Depending upon the particular software package being used the coupling can occur

in two ways. In the first, an overall 1D model of an extended reach of river may be coupled dynamically to one or more detailed 2D model domains to provide a more detailed description of the flows in local areas of interest. In the second, one or more 1D model branches may be dynamically coupled within a 2D model domain to provide a better description of in-bank channel flows, and flows through hydraulic structures such as culverts, weirs and bridges. In some software packages, the 1D/2D coupling has also been extended to include 1D pipe network models. This has extended the range of application of coupled 1D/2D models to providing a more detailed description of the flooding associated with urban stormwater flows.

## 4.5.4. 3D Models

3D flow models are based on the numerical solution of the Reynolds-averaged Navier-Stokes equations describing the conservation of mass and momentum in three-dimensions. For most 3D river and estuarine modelling applications, these equations are simplified by assuming that the pressure distribution is hydrostatic. This assumption is consistent with the equations used in 1D and 2D modelling, described above. As for 2D models, the computational domain of a 3D model may be formed using a square, rectangular or curvilinear grid, or using a flexible mesh comprising triangular and/or quadrilateral mesh elements. With 3D models there are additional grid cells or mesh elements in the vertical dimensional for describing the variations in flow with depth.

The use of a full 3D model should be considered in cases where it is important to simulate three-dimensional flow effects. These can include: stratified flows and wind-driven over-turning circulations in lakes and estuaries, “helicoidal” flows around river bends, flows associated with hydraulic structures, and flows where the water depth is of the same order of magnitude as, or greater than, the horizontal dimensions of the main physical features to be resolved.

3D models require significantly more computing time (typically an order of magnitude or more) than equivalent 2D models, even with the use of parallel processing. Further, in most floodplain applications, many of the three-dimensional flow effects noted above are of secondary importance, relative to the main flood flows, or can be accounted for through relatively well defined additional loss parameters. In these cases, the additional complexity and computing time associated with using a 3D model is considered to be unnecessary and unwarranted. As such, 3D models are best suited to modelling the details of complex flows in relatively short reaches of rivers, around structures and in other flows cases where three-dimensional effects become important in determining localized flood effects.

## 4.5.5. 1D, 2D and 3D Model Limitations

The 1D, 2D and 3D models that have been discussed so far generally assume that the pressure distribution in the flow to be modelled is hydrostatic. This assumption is applicable for most flood flows but becomes invalid in flow situations where vertical accelerations become significant. The most common cases where this might occur include flows over weirs and levee banks, and flows through hydraulic structures. This is one of the reasons why most 1D, 2D and even 3D models incorporate structure equations for describing flows at structures such as weirs, levee banks and culverts.

Additionally, the numerical methods used to solve the equations of motion are generally based on the assumption that the flow is sub-critical. As such, super-critical flows can usually only be modelled through locally simplifying the momentum equation(s) and/or through the addition of significant amounts of numerical dissipation. These approaches

make it possible to maintain the numerical computation through regions of super-critical flow. Modellers should, however, be aware that these approaches only provide approximate solutions to super-critical flow. Care should be taken when interpreting the results in these regions, and in the transition zones between super-critical and sub-critical flow (and, in particular, in the location and size of any resulting hydraulic jumps).

### 4.5.6. CFD and other Non-Hydrostatic Models

In cases where it becomes important to describe the details of non-hydrostatic flow and/or of super-critical flow, it will become necessary to use more sophisticated numerical modelling approaches such as Computational Fluid Dynamics (CFD) or Smoothed Particle Hydrodynamics (SPM), or to use a physical model.

Computational Fluid Dynamics (CFD) refers to a class of models that are based on the numerical simulation of the more generalised form of the Navier-Stokes equations. (See for example, Roache (1998)). CFD can be used to model the details of non-hydrostatic flows, including flows where there is no free-surface (e.g., internal flows within a structure). CFD can also be used to model supercritical flows, as well as the transitions between super-critical and sub-critical flows. CFD models require significantly more computing time than the 3D models discussed above and are more demanding with respect to model set-up and boundary condition requirements. As such, the use of CFD in flood modelling is generally limited to simulating the details of complex flows at or within hydraulic structures (e.g., flow over a dam spillway or flow through a complex system of culverts).

CFD and the other types of model considered above typically operate in what is known as an “Eulerian” reference frame. This involves the computation of the fluid flow relative to a fixed model grid or mesh. By comparison, Smoothed Particle Hydrodynamics (SPM) uses a “Lagrangian” reference frame (See for example, Violeau (2012)). Here the fluid itself is broken down into small individual “particles” and, rather than using a fixed grid or mesh, the computation follows the movements of these particles. This makes SPM particularly well suited to modelling the dynamics of interactions at the water-air interface. For reliable results SPM requires the use of very large numbers of particles. SPM has similar disadvantages to CFD in relation to computational time and the demands associated with model set-up and the application of appropriate boundary conditions. As for CFD, the use of SPM in flood modelling is generally limited to simulating the details of complex flows at or within hydraulic structures.

Physical models are geometrically scaled reproductions of the physical system to be modelled and are disscussed in more detail in Book 6, Chapter 2, Section 12. They typically use the same fluid (i.e., water) and operate under the normal laws of gravity. This makes physical models suitable for modelling non-hydrostatic flows and super-critical flows, including the transitions between super-critical and sub-critical flows. As a result, physical models can be used to model flow cases similar to those for 3D, CFD and SPM models discussed above. The main limitation on the more general use of the physical models is the restriction on the scales that can be used in order to avoid “scale effects”. This generally restricts the use of physical models to modelling the details of flows in relatively short reaches of rivers. Although “distorted scale” models can be used to reduce scale effects when modelling larger areas, distorted models should not be used when accurate reproduction of three-dimensional flow effects is required.

## 4.6. 1D Unsteady Hydraulic Models

Commercially available 1D unsteady hydraulic models typically solve the full one-dimensional unsteady Saint Venant equations. They can be applied to branched and looped

channel and river and floodplain systems, and can be used to simulate flows in a wide range of physical systems from steep river reaches to tidal estuaries. The capabilities of these models typically include most, if not all of the following features:

- Hydraulic structures such as bridges, culverts, weirs, levees, etc., through the use of in-built structure routines.
- Options for including user-defined structures for describing structures such as flow regulation gates and pumps.
- The capability to approximate super-critical flows, including super-critical to sub-critical flow transitions.
- Options for specifying simplified diffusive wave or kinematic wave approximations to the equations of motion to improve computational speed, where appropriate

## 4.6.1. 1D Equations of Motion

The main properties of one-dimensional flow along a channel can be uniquely defined by two dependent variables, the water level or stage *h,* and the averaged discharge *Q*, as shown in Figure 6.4.3. These can be described as a function of the two main independent variables: the chainage or distance along centreline of the channel *x*, and the time *t*

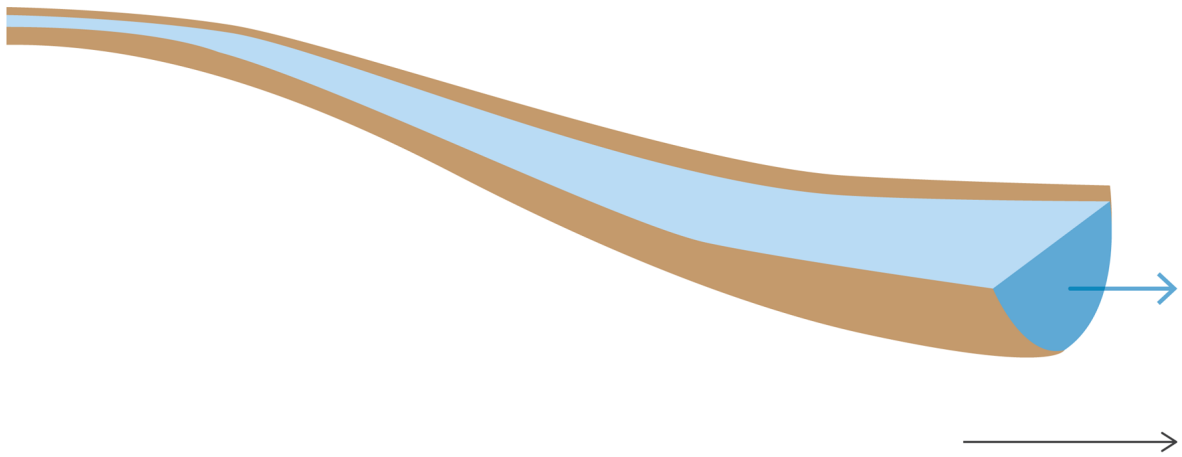

Figure 6.4.3. The main dependent variables for the 1D model equations

With two dependent variables it is necessary to have two equations to describe the flow in terms of the stage height *h* and discharge *Q* at any given point in *x* and *t*. The equations used are the Saint Venant equations. These equations describe the cross-sectionally averaged conservation of mass and conservation of momentum. The momentum equation is used in unsteady flow models in preference to the energy equation that is used in steady flow models. This is because momentum is a vector and introduces directionality into the computation. By comparison, energy is a scalar and cannot. Additionally, the momentum equation can be used to maintain the computation through discontinuities such as hydraulic jumps.

**The Mass Equation:**

The one-dimensional unsteady continuity equation as derived in Book 6, Chapter 2, Section 8 can be given as:

$$\frac{\partial A}{\partial t} + V\frac{\partial A}{\partial x} + A\frac{\partial V}{\partial x} = 0 \tag{6.4.3}$$

By combining the two spatial derivatives, the conservation law form of the cross-sectionally averaged mass equation can be given as:

$$\frac{\partial A}{\partial t} + \frac{\partial Q}{\partial x} = 0 \tag{6.4.4}$$

For modelling applications, this equation is transformed into terms of the required water level *h* through the introduction of a storage width $b_{st}$ and, when a lateral inflow of $q_l$ per unit length of channel is included, the mass equation becomes:

$$b_{st}\frac{\partial h}{\partial t} + \frac{\partial Q}{\partial x} = q_1 \tag{6.4.5}$$

**The Momentum Equation:**

In a similar form, the equation describing the one-dimensional cross-sectionally averaged conservation of momentum can be given as:

$$\frac{\partial Q}{\partial t} + \beta\frac{\partial}{\partial x}\left(\frac{Q^2}{A}\right) + gA\left(\frac{\partial h}{\partial x} + S_f\right) = q_1 u_l \tag{6.4.6}$$

Where: *A* is the cross-sectional area, *g* is the gravitational constant, $S_f$ is the friction slope, $\beta$ is the momentum correction factor, and $q_l$ is a lateral discharge with a downstream velocity component $u_l$ relative to the velocity of the main stream.

With the introduction of a bed friction term based on Manning's equation, the momentum equation can be expressed as:

$$\frac{\partial Q}{\partial t} + \beta\frac{\partial}{\partial x}\left(\frac{Q^2}{A}\right) + gA\left(\frac{\partial h}{\partial x} + \frac{n^2Q^2}{A^2R^{4/3}}\right) = q_1 u_l \tag{6.4.7}$$

Where: *n* is Manning's roughness coefficient and *R* is the hydraulic radius (defined as the cross-sectional area divided by the wetted perimeter)

**Equation Assumptions:**

The Saint Venant equations for unsteady flow, as described above, are based on the following assumptions:

- The flow is one-dimensional (i.e., the flow velocity is uniform and the water surface is horizontal across each cross-section).
- The pressure is hydrostatic (i.e., streamline curvature is small and vertical accelerations can be neglected).
- The effects of bed friction and turbulence can be included through resistance laws (e.g., Manning's equation) that have been derived for steady flow conditions.
- The flow is nearly horizontal (i.e., the average channel bed slope is small)

Unsteady flow models based on the numerical solution of the full de Saint Venant equations are sometimes called "dynamic wave" models.

## 4.6.2. Simplified Forms of the 1D Momentum Equation

The water surface slope in the hydrostatic pressure term of the momentum equation can be expressed as:

$$\frac{\partial h}{\partial x} = \frac{\partial y}{\partial x} - S_b \tag{6.4.8}$$

Where *y* is the water depth and $S_b$ is the bed slope.

Ignoring the effects of lateral inflows for the purpose of this exercise, the momentum equation can then be rewritten as:

$$\frac{\partial Q}{\partial t} + \beta \frac{\partial}{\partial x}\left(\frac{Q^2}{A}\right) + gA\left(\frac{\partial y}{\partial x} - S_b + S_f\right) = 0 \tag{6.4.9}$$

**Diffusive Wave Approximation**

In the diffusive wave approximation, the local acceleration term $\delta Q/\delta t$ and the convective acceleration term $\delta(Q^2/A)/\delta x$ are neglected, and the momentum equation reduces to:

$$\frac{\partial h}{\partial x} = \frac{\partial y}{\partial x} - S_b = -S_f \tag{6.4.10}$$

That is, the water surface slope is balanced by the friction slope.

This approximation includes backwater effects, but the “dynamic” or wave propagation effects associated with the “inertial” acceleration terms have been excluded. As a result, a model based on the diffusive wave equation does not have the same stability constraints as an equivalent full dynamic wave model, and can use much larger time steps.

The diffusive wave approximation is valid for describing gradually varying flows in reaches with moderate to steep slopes. It should not be used for rapidly varying flows such as in dam-breaks, or in reaches with flat-bed slopes, including lakes and estuaries, where the acceleration terms become important. Diffusive wave models are sometimes used to describe regional scale flows where the use of larger time steps can provide significant reductions in the amount of computation required.

**Kinematic Wave Approximation**

In the kinematic wave approximation, it is assumed that the momentum equation can be further reduced to:

$$S_b = S_f \tag{6.4.11}$$

That is, the friction slope is equal to the bed slope. Backwater effects are excluded from this approximation and water can only flow downstream.

The kinematic wave approximation is only valid for describing gradually varying flows in reaches with moderate to steep slopes where bed-friction dominates and backwater effects can be neglected. As such it is not well suited to general modelling applications. The kinematic wave approximation is very stable and is sometimes used to describe super-critical flows in localized regions of an otherwise dynamic wave model.

## 4.6.3. Model Set-up

Topographic input to 1D models is generally specified in terms of survey cross-sections of the channel and floodplain system to be modelled. These cross-sections are given as a series of x–z co-ordinates specified perpendicular to the direction of flow. At each cross-section key computational parameters may be pre-computed as a function of water level. These parameters include cross-sectional area, storage width and conveyance. The effects of varying roughness across a cross-section (e.g., between in-bank and over-bank areas) may also be included in the conveyance calculations.

The computation can be carried out on a “staggered” grid where water level *h* and discharge *Q* grid points are specified alternately along each model branch, or on a “non-staggered” grid where the water level *h* and the discharge *Q* are specified at each grid point, as shown in Figure 6.4.4. Grid points are typically allocated to each surveyed cross-section; water level *h* points for staggered grids, and combined water level *h* and discharge *Q* grid points for non-staggered grids. If necessary, additional intermediate grid points may be allocated between cross-sections. For the staggered approach, discharge *Q* grid points are located midway between adjacent water points.

Implicit finite difference procedures are typically used to solve the equations of motion along each model reach. The scheme first attributed to Abbot and Lonescu (1967) is commonly used with staggered grid models. With this scheme, numerical approximations to the mass equation are centred on each water level *h* grid point, while numerical approximations to the momentum equation are centred on each discharge *Q* grid point. The Preissmann (1961)Preissmann (1961) scheme is generally used in non-staggered grid models. With this scheme, the numerical approximations to both the mass and momentum equations are centred on the mid-point between each combined water level *h* and discharge *Q* grid point.

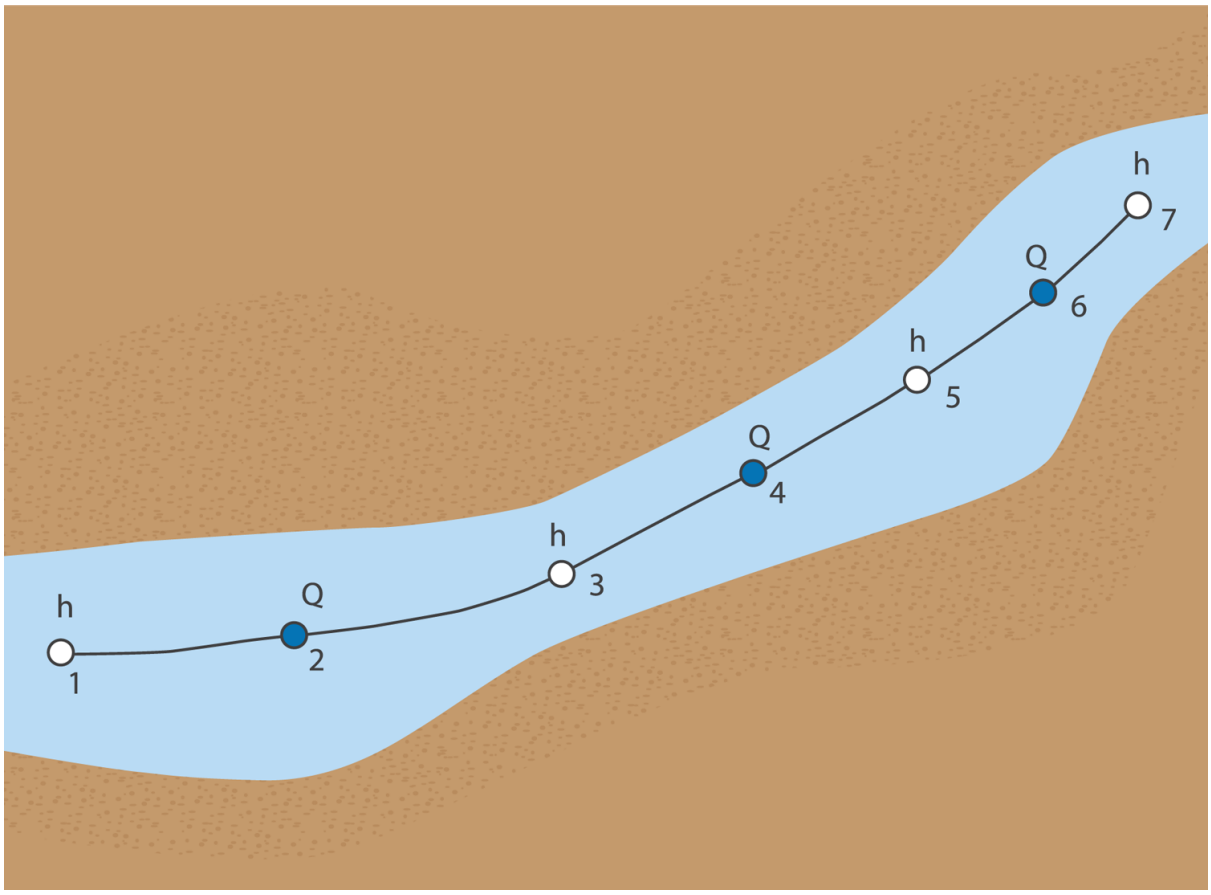


Figure 6.4.4. The Computational Grid

The staggered Abbot and Lonescu (1967) scheme has some advantages with the way in which structures can be incorporated. This is discussed briefly below. By comparison, the non-staggered Preissmann (1961) scheme has the advantage that the model grid size can be varied from one grid point to another with no loss of numerical accuracy.

**Initial Conditions**

Before starting a model simulation, initial water level *h* and discharge *Q* values must be specified at each water level and discharge point, irrespective of whether a staggered or non-staggered grid is being used. Depending upon the particular modelling package being used, these initial values can be obtained from:

- User specified values;
- Hot start conditions obtained from the results of an earlier model run;
- Internally generated “auto-start” conditions computed using an assumed initial steady state flow solution; and
- A combination of user defined and auto-start conditions (e.g., using user defined conditions in initially dry flood plains).

**Boundary Conditions**

The main input to the model is generally provided by the boundary conditions. These must be specified at each upstream or downstream open boundary. In most flood studies the

upstream boundary conditions are generally specified as discharge hydrographs (typically computed by a hydrologic model). Corresponding downstream boundary conditions are generally specified as tail water levels (either constant or time varying), or through some means of relating the model discharge to a corresponding water level. This can be done by specifying a rating curve, where the discharge is explicitly linked to the water surface elevation, or through the use of the kinematic wave approximation at the boundary. The latter effectively links the discharge to the water surface elevation through the Manning equation. In tidal estuaries the downstream boundary will generally be specified in terms of a fixed or time-varying tidal elevation.

**Model Structures**

1D hydraulic models typically incorporate a range of structure formulations for including flow control structures within a model. These may include:

- Weirs: for describing flows over weirs, levees, road and rail embankments and overtopping of bridges, etc. A range of weir formulations may typically be available for describing different weir characteristics (e.g., broad-crested or sharp-crested) and different flow combinations (e.g., free overflow or drowned flow). Special weir formulations may also be included through which user-defined flow relationships can be specified.

- Culverts: for describing flows through culverts, bridges and pipes. Different formulations are used for a range of different upstream and downstream controlled flow conditions. User-defined culvert relationships can also be used.

- Regulating structures: where flows at structures such as gates or pumps can be specified as a level or discharge at another point in the model.

For simplicity, the remianing discussion has been limited to the use of staggered grid models. In these models, structures are located at discharge grid points, and water level grid points (and therefore cross-sections) must be specified immediately upstream and downstream of the structure, as shown in Figure 6.4.5. For these cases, the momentum equation at the discharge grid point is replaced by a structure equation. Flow through the structure then becomes a function of the upstream and/or downstream water levels, depending on the flow conditions (e.g., free overflow or drowned flow for weirs, or inlet or outlet control for culverts).

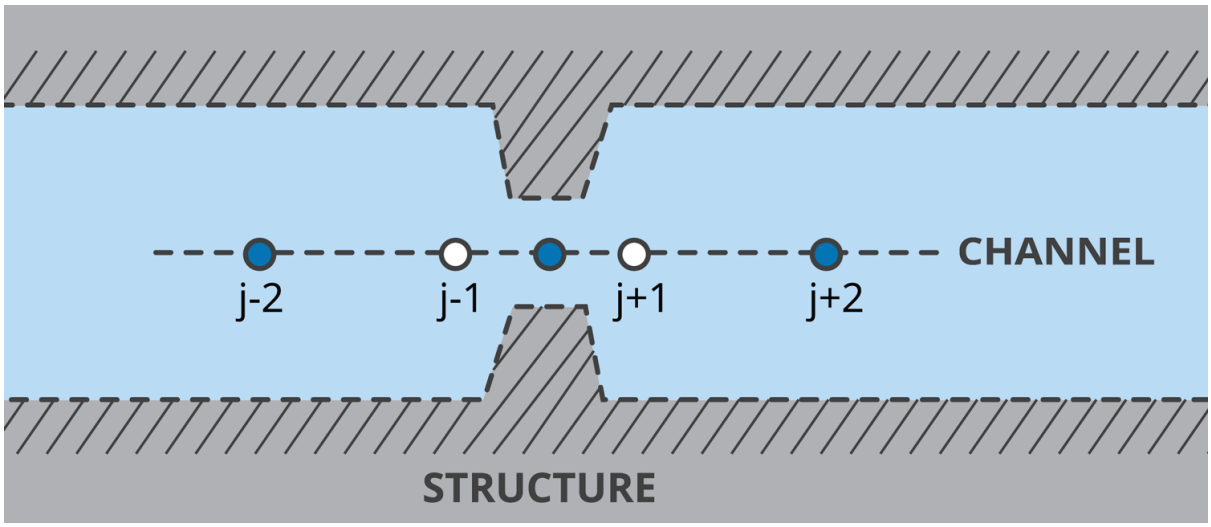


Figure 6.4.5. Schematisation of a Channel and Structure Grid

Multiple structures can be defined at a single discharge point. For example, a bridge which can be overtopped can be described by the combination of a culvert, for normal flow conditions, and a weir, for overtopping flows.

**Floodplain Flows**

The treatment of floodplain flows can be very different depending on the main characteristics of the river channel and floodplain system. For floodplains that drain naturally to the river channel, as shown in Figure 6.4.6(a), the water level can be the same in both the river and the floodplain. Under these conditions the effects of storage and flow along the floodplain can be included directly in a single combined river channel and floodplain branch.

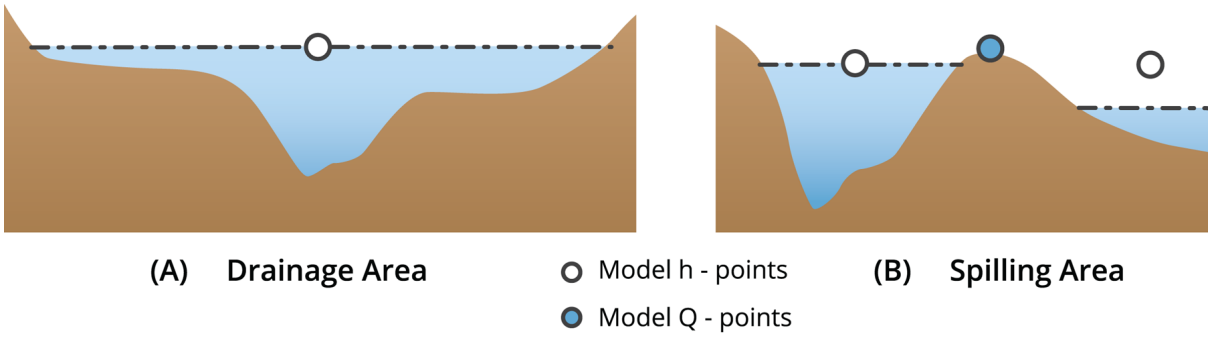


Figure 6.4.6. Different Types of Flood Plain Flow

For floodplains where the river flows spill out over a natural or man-made levees, as shown in Figure 6.4.6(b), the water level in the floodplain can be very different to the water level in the main channel. Under these conditions, the effects of storage and flow along the floodplain should be incorporated in a separate model branch. Flow exchange between the river channel and floodplain branches can then be controlled by a link branch with a broad-crested weir representing the levee bank.

A simple river channel/floodplain branch system is schematised in Figure 6.4.7. Combinations of multiple river channel and floodplain branches can be used to describe the flows in quite complex river and floodplain systems.

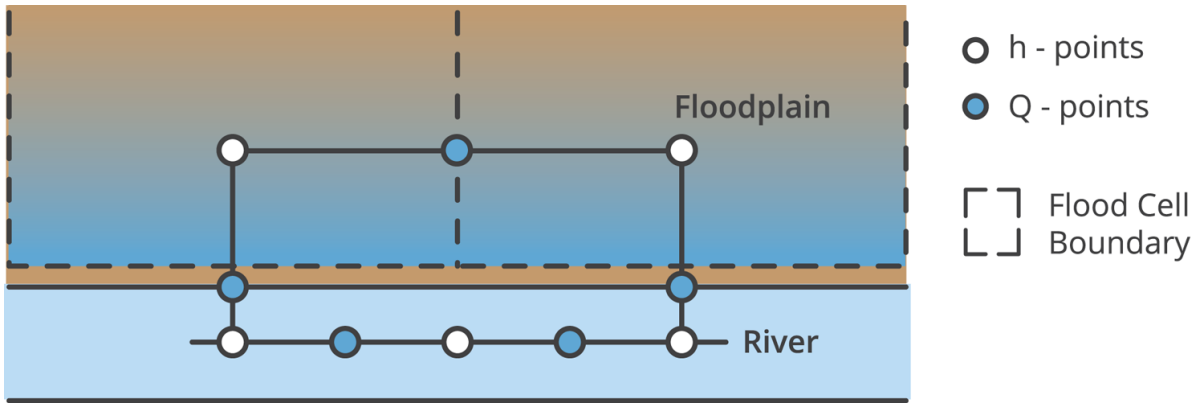


Figure 6.4.7. Schematisation of a Simple River Channel/Floodplain Branch System

## 4.6.4. Data Requirements

To construct a 1D model of a river and floodplain system, it is necessary to have the following data:

- A knowledge of the main flow paths throughout the system.
- Survey cross-sections at representative locations across the river channel and floodplain.
- Survey levels along flow controls such as levees, weirs and road embankments.
- Survey of control structures such as bridges and culverts.
- Survey cross-sections immediately upstream and downstream of branch junctions, and flow control structures.

Additionally, data on historic flood levels is required for model calibration. Ideally, a 1D model should be calibrated against water level hydrographs at various locations throughout the model area. This will provide a measure of how well the model can reproduce the timing of a flood and the shape of the hydrograph. In many cases, however, water level hydrographs of historic flood events do not exist. Consequently, most models are calibrated against peak water levels surveyed after a flood.

Figure 6.4.8 shows a plan view of a branched 1D model of the Lindsay and Murray River system in northwest Victoria and southwest New South Wales. The 1D model is able to provide a good description of the flows along the main channels of the Lindsay River in the south, the Murray River to the north, and a range of older flow paths across the flood plain, including Mullaroo Creek. Figure 6.4.9 shows a water surface profile along one particular branch of the model.

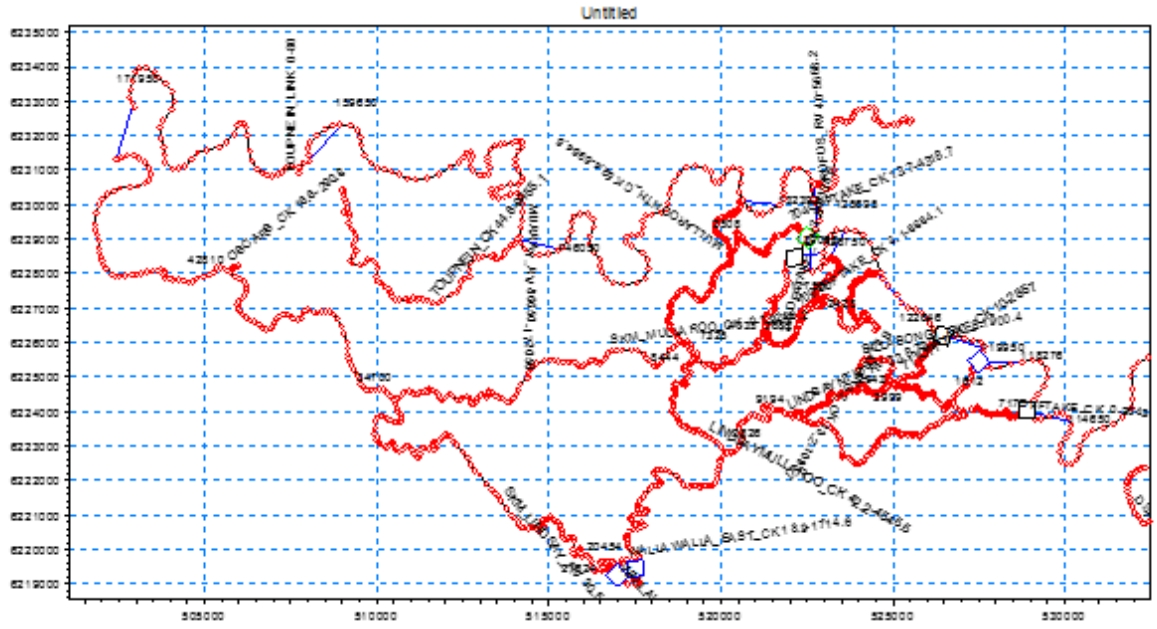


Figure 6.4.8. A Branched 1D Model Network of the Lindsay and Murray River Systems

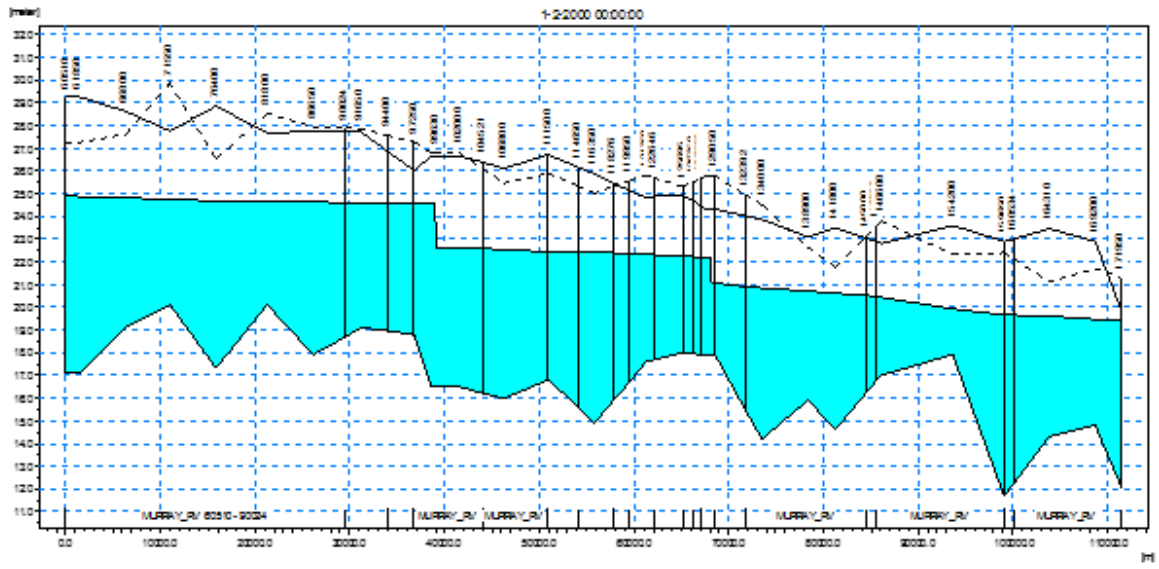

Figure 6.4.9. Lindsay River

## 4.6.5. Advantages and Limitations

The main advantages of a 1D model are that the model simulations are relatively quick to run computationally (i.e., relative to full 2D models), and that the main river channels can be well defined by survey cross-sections. As such, 1D models are well suited to modelling long reaches of river systems, and to modelling of river and floodplain systems where the flow paths are reasonably well defined.

The main disadvantages of 1D models are that they are based on cross-sectionally averaged one-dimensional equations of motion. As such:

- The floodplain flow paths must be pre-determined by the user.
- The flow paths are by definition 1D and no information is available on the distribution of flows within individual flow paths.
- Losses due to two-dimensional effects such as bends, flow separations, etc., must all be lumped into the bed-friction parameter (making detailed calibration essential).
- There can be problems in interpreting model results for mapping flood extents and depths of inundation.

As such, 1D models are not well suited to modelling the details of flood flows within the floodplain.

# 4.7. 2D Unsteady Hydraulic Models

Due to the limitations 1D models, there was a trend in the early 1990s towards the use of full 2D models in urban flood studies and other flood studies where the details of the flow distribution across the floodplain became important. (See for example Bishop et al. (1995)). This trend continued through to the early 2000s. By this time 2D modelling had become a virtually a standard for most rural and urban flood modelling studies.

## 4.7.1. Model Equations

2D unsteady hydrodynamic models are based on the numerical solution of the depth-averaged shallow water wave or long wave equations. These equations describe the conservation of mass and momentum in two horizontal dimensions *x* and *y*. In a form used in many 2D flood models, these equations can be expressed as:

**Mass**

$$\frac{\partial \varsigma}{\partial t} + \frac{\partial (d.u)}{\partial x} + \frac{\partial (d.v)}{\partial y} = \text{Sources} - \text{Sinks} \tag{6.4.12}$$

**x-Momentum**

$$\frac{\partial u}{\partial t} + u\frac{\partial u}{\partial x} + v\frac{\partial u}{\partial y} + g\frac{\partial \varsigma}{\partial x} = -\frac{gu\sqrt{u^2+v^2}}{C^2 d} + E\left(\frac{\partial^2 u}{\partial x^2} + \frac{\partial^2 u}{\partial y^2}\right) + \text{Source/Sink} \tag{6.4.13}$$

**y-Momentum**

$$\frac{\partial v}{\partial t} + v\frac{\partial v}{\partial y} + u\frac{\partial v}{\partial x} + g\frac{\partial \varsigma}{\partial y} = -\frac{gv\sqrt{u^2+v^2}}{C^2 d} + E\left(\frac{\partial^2 v}{\partial x^2} + \frac{\partial^2 v}{\partial y^2}\right) + \text{Source/Sink} \tag{6.4.14}$$

This coupled system of equations provides the three equations necessary to solve for the three dependent variables; ς the free surface elevation, *u* the velocity in the *x* direction and *v* the velocity in the *y* direction. It is noted that in this secton and the following sections, *d.u* and *d.v* refer to the depth *d* multiplied by the *x*-velocity component *u* and the *y*-velocity component *v*, respectively.

The mass and momentum equations include sources and sinks for describing the effects of localised inflows and outflows. The *x* and *y* momentum equations also include a quadratic Chezy-type friction formulation and a simple eddy viscosity formulation (with eddy viscosity coefficient *E*). For practical modelling applications, the Chezy coefficient *C* can be related to the more usual (for Australian applications) Manning's *"n"* by the Strickler relation:

$$n = d^{1/6} C^{-1} \tag{6.4.15}$$

In some European models, the friction coefficient is sometimes specified in terms of Manning's *"M"*, where:

$$n = M^{-1} \tag{6.4.16}$$

For modelling large expanses of open water, such as in lakes and estuaries, these 2D model equations can be extended to include the effects of wind shear and/or Coriolis forces.

## 4.7.2. Assumptions

In the derivation of the 2D model equations, it has been assumed that:

- The flow is incompressible
- The pressure is hydrostatic (that is, vertical accelerations can be neglected and the local pressure is dependent only on the local depth).

- The flow can be described by continuous (differentiable) functions of ς, *u* and*v* (that is, the flow does not include step changes in ς, *u* and *v).*
- The flow is two-dimensional (that is, the effects of vertical variations in the flow velocity can be neglected).
- The flow is nearly horizontal (that is, the average channel bed slope is small).
- The effects of bed friction can be included through resistance laws (e.g., Manning's equation) that have been derived for steady flow conditions.

## 4.7.3. Other Forms of the Equations

The equations presented in Book 6, Chapter 4, Section 7 form the basis of many of the 2D numerical models currently in use. Another form of the equations that is finding increasing popularity is the so-called "conservation law" form described for example by Abbott (1979). In this form of the equations, the depth average momentum "fluxes" (*d.u* and *d.v* in the *x* and *y* directions, respectively) are used as the time dependent velocity variables in the momentum equations. In a form similar to that considered above, , the resulting conservation law form of the shallow water equations can be expressed as:

**Mass**

$$\frac{\partial \varsigma}{\partial t} + \frac{\partial (d.u)}{\partial x} + \frac{\partial (d.v)}{\partial y} = \text{Sources} - \text{Sinks} \tag{6.4.17}$$

**x-Momentum**

$$\frac{\partial (d.u)}{\partial t} + \frac{\partial}{\partial x}\left(d.u^2 + \frac{1}{2}g.d^2\right) + \frac{\partial (d.u.v)}{\partial y} = -\frac{gu\sqrt{u^2+v^2}}{C^2 d} + E.d\left(\frac{\partial^2 u}{\partial x^2} + \frac{\partial^2 u}{\partial y^2}\right) + \text{Source/Sink} \tag{6.4.18}$$

**y-Momentum**

$$\frac{\partial (d.v)}{\partial t} + \frac{\partial (d.u.v)}{\partial x} + \frac{\partial}{\partial y}\left(d.v^2 + \frac{1}{2}g.d^2\right) = -\frac{gv\sqrt{u^2+v^2}}{C^2 d} + E.d\left(\frac{\partial^2 v}{\partial x^2} + \frac{\partial^2 v}{\partial y^2}\right) + \text{Source/Sink} \tag{6.4.19}$$

This is effectively the form of the equations that provides the basis of the finite difference solution procedure used by DHI (2005). A distinct advantage of the conservation law formulation of the equations is that, when the depth average momentum fluxes *d.u* and *d.v* are used as the dependent velocity variables, the mass equation becomes linear and, barring coding errors, the numerical solutions should remain mass conservative.

## 4.7.4. Numerical Solution Procedures

Development of numerical solution procedures for the shallow water wave equations is an active area of on-going research. There are three main approaches that have used; finite difference, finite element and finite volume techniques. The main characteristics of, and the differences between, these methods are discussed in detail by, for example, Sherwin and Peiro (2005). The main features of each of these approaches are outlined below.

**Finite Difference Methods:** With finite differences, the differential forms of the equations of motion described above are used directly. The dependent water level and velocity variables are defined at individual grid points on a structured rectilinear or curvilinear grid. Spatial derivatives are approximated by taking arithmetic differences between the dependent variables in adjacent grid points, while time derivatives are approximated by taking arithmetic differences between the variables at different time levels. The main advantages of finite difference methods are that they are relatively simple to implement and are easy to use. The main disadvantage is that complex geometries cannot be readily resolved without the use of fine scale grid resolution. Finite difference techniques for providing solutions to the shallow water wave equations have been described by, for example, Abbott (1979); Stelling (1984); and Abbott and Basco (1989).

**Finite Element Methods:** With finite elements, the equations of motion are transformed into integral formulations. Weighting or trial functions are introduced and the resulting equations are then solved numerically over an mesh of regular or irregularly shaped elements. The shapes of these elements are typically triangles and/or quadrilaterals, but can take other forms. Finite element methods provide solutions that are smooth and continuous over each element and which have matching values at the interfaces between elements. One of the main advantages of finite elements is that the integral formulation of the equations does not require a structured mesh. This makes it possible to use an unstructured flexible mesh which can be aligned with the local flow direction, or which can provide greater resolution in particular areas of interest. The main disadvantage with flood modelling with standard finite element techniques is that mass is not necessarily conserved. Finite element techniques for providing solutions to the shallow water wave equations have been described by, for example, Connor and Brebbia (1976); and Zienkiewicz et al. (2014).

**Finite Volume Methods:** Finite volume methods are similar to finite elements in that they use integral formulations of the equations of motion and can be solved over an unstructured flexible mesh of irregularly shaped (typically triangular and/or quadrilateral) mesh cells. The main differences are that finite volume methods use integral forms of the conservation law form of the equations of motion and each mesh cell is treated as a control volume represented by volume-averaged values of the conserved variables (mass and momentum). The rates of change of these conserved variables are derived by integrating the cell-interface fluxes. A key step in these methods involves calculating the numerical fluxes at the cell interfaces. As for finite elements, the integral formulation of the equations used in finite volumes makes it possible to use unstructured flexible meshes that can be aligned with the local flow directions and which can provide greater resolution in particular areas of interest. The main advantage of finite volumes over finite elements is that mass is conserved. Finite volume techniques for providing solutions to the shallow water wave equations have been described by, for example, LeVeque and Bale (2012).

Finite difference methods have been used extensively in the historical development of numerical 2D flood modelling practice (e.g., Bishop et al. (1995); Stelling et al. (1998); McCowan et al. (2001) and Syme (2001)) and are still used widely today. Early flexible mesh flood model development was mostly carried out using finite element techniques (e.g., King and Roig (1988)). However, due to potential mass conservation issues, more recent flexible mesh model development has focussed more on finite volume techniques. In this respect, it is noted there are also hybrid approaches that combine the finite element and finite volume schemes. Further, the conservation law formulation of the shallow water wave equations can be used to develop finite difference solution procedures that apply the finite volume approach to a structured rectilinear or curvilinear grid.

**Explicit vs Implicit Solution Procedures**

The way in which these different solution procedures move forward in time can be described as being either “explicit” or “implicit”. In this respect it is noted that the “Courant” number *Cr* is a key parameter for defining the differences between explicit and implicit solution procedures. The Courant number expresses the number of grid or flexible mesh cells that flow information can travel in one timestep. The Courant number *Cr* can be defined as:

$$C_r = \left[\frac{(u + \sqrt{gd}) \,.\, \Delta t}{\Delta x}\right] \tag{6.4.20}$$

With an explicit solution procedure, the solutions to the water surface elevations and flow velocities at the new timestep are computed directly (explicitly) as a function of the known values at the old timestep. Explicit schemes tend to be computationally efficient, but have a stability constraint that information can only travel a maximum of one grid/mesh element in a single timestep. That is, that the Courant number must always be less than or equal to one (i.e., $Cr \leq 1$). This provides a stability constraint on the timestep $\Delta t$, that is commonly called the “Courant” stability criterion, where:

$$\Delta t_{\max} \leq \left[\frac{\Delta x}{(u + \sqrt{gd})}\right]_{\min} \tag{6.4.21}$$

By comparison, in an implicit solution procedure, the water surface elevations and flow velocities at the new timestep are expressed as a combination of both the known values at the old timestep and adjacent unknown values at the new timestep. As a result, the solutions at one grid/mesh element are linked to those in the neighbouring cells. These solutions are, in turn, linked to those in their neighbouring cells, and so on. In this way, the solutions to the discrete numerical approximations to the mass and *x* and *y* momentum equations for each grid/mesh cell are linked “implicitly” to those in every other cell over the entire model domain. This approach allows flow information to travel much further than one grid point per timestep. As a result, the Courant stability criterion does not apply to implicit solution procedures and model time steps can be determined more by accuracy requirements rather than by stability constraints.

**ADI Solution Procedures**

Most of the early 2D model developments were for coastal and marine applications where the use of high Courant numbers was found to provide significant computational advantages. Following Leendertse (1967) many of these models used finite difference schemes which used what is known as an “alternating direction implicit” or ADI algorithm. This approach involves the use of a series of implicit 1D sweeps alternating along x-grid lines and y-grid lines which is much simpler to implement than a fully two-dimensional implicit solution procedure.

The ADI approach can be shown to be independent of the Courant stability criterion and has been used extensively in two-dimensional flood modelling (e.g., Stelling et al. (1998); McCowan et al. (2001) and Syme (2001)). It should be noted, however, that the ADI approach is not directly equivalent to a fully two-dimensional implicit scheme. Although the timestep is not subject to the Courant stability criterion, it is subject to accuracy constraints, particularly when the solution involves flow in relatively narrow channels at an angle to the grid (Benque et al., 1982). In practice, the timestep should be selected such that the Courant number is less than the minimum number of grid cells used to describe the width of a channel. In many cases this tends to restrict the timestep such that the Courant number is of order Cr ≈ 1 in narrow channels, although higher Courant numbers can occur in other parts of the model.

**Parallel Processing and GPUs**

With the advent of multiple-core processors and graphics processing units (GPUs) it became possible to carry out multiple computations in parallel. This has provided significant increases in computational speed for models with code that could be readily “parallelised”. The direct explicit relationships between water surface elevations and flow velocities at the new timestep and the corresponding values at the old time step make explicit solution procedures particularly well suited to parallel processing. As a result, much of the recent development in 2D flood modelling has focussed on explicit finite volume numerical solution procedures (need references here). These models have the capability to increase the effective computational speed by one to two orders of magnitude, depending upon what features are, or are not, included in the model.

## 4.7.5. Discretisation Errors

Irrespective of the numerical method being used, the modeller should be aware that the resulting Numerical Model is only a numerical approximation to the Equations of Motion (the Mathematical Model). Discretisation errors are introduced when the continuous mathematical equations have to be approximated by discrete (discontinuous) arithmetic expressions that can then be solved by the computer. These errors are called “truncation” errors. They are different to computer “round-off” errors, and can have significant implications on the accuracy of a model’s results.

To illustrate this effect, a simple first-order finite difference approximation to the $u\delta u/\delta x$ “convective momentum” term in the x momentum equation has been examined more closely. This term is to be discretised on a square “staggered” grid similar to that shown in Figure 6.4.10.

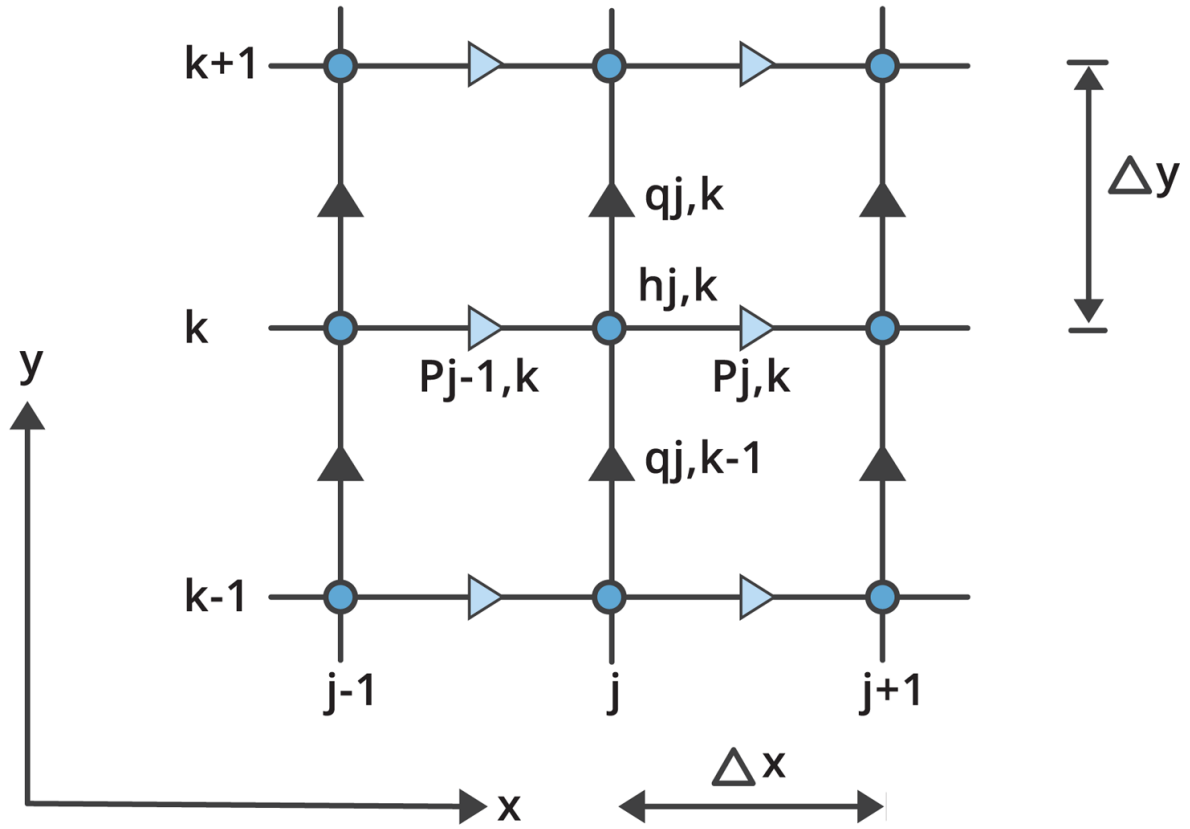


Figure 6.4.10. Example of a Computational Grid

For a given timestep $n\Delta t$ and $x$ grid line at $k\Delta y$, the term $u\delta u/\delta x$ can be approximated by:

$$u\frac{\partial u}{\partial x} \approx u\frac{\Delta u}{\Delta x} = u_j\frac{(u_{j\Delta x} - u_{(j-1)\Delta x})}{\Delta x} \tag{6.4.22}$$

With this approximation, the continuous derivative of the velocity $u$ with respect to $x$ is approximated by the linear gradient of the velocity between the grid point at which the derivative is to be taken, and the grid point immediately upstream. As a result, this approach is often termed “upwind” differencing. The errors associated with this approximation can be determined by using Taylor’s Series to expand the terms in the right hand side of this equation in terms of the velocity $u$ velocity at the centre-point, $j\Delta x$. This results in the following expression:

$$u\frac{(u_{j\Delta x} - u_{(j-1)\Delta x})}{\Delta x} = u\frac{\partial u}{\partial x} - u\frac{\Delta x}{2}\frac{\partial^2 u}{\partial x^2} + u\frac{\Delta x^2}{6}\frac{\partial^3 u}{\partial x^3} - u\frac{\Delta x^3}{2}\frac{\partial^4 u}{\partial x^4} + \text{.....} \tag{6.4.23}$$

This shows that, the discrete finite difference approximation is equal to the original continuous partial differential term $u.\delta u/\delta x$, but with additional second, third, fourth and higher order truncation error terms. Further, it can be seen that the truncation error includes a second order term which is of the same form as one of the eddy viscosity terms in the $x$-momentum equation. That is, upwinding of the convective momentum term $u.\delta u/\delta x$ can be seen to be equivalent to introducing a numerical eddy viscosity term with, in this case, an eddy viscosity coefficient of:

$$E_N = u\frac{\Delta x}{2} \tag{6.4.24}$$

This numerical eddy viscosity coefficient is grid size and flow velocity dependent. For typical floodplain flow conditions and model dimensions, the numerical eddy viscosity introduced by first-order upwind differencing can be an order of magnitude or more greater than the corresponding physically realistic values. Issues associated with first-order upwind differencing of the convective momentum terms are discussed in detail by Leonard (1979).

Similar truncation error terms can be developed for numerical approximations to the other terms in the mass and momentum equations. The properties of these truncation errors can have a significant effect on the accuracy and stability of the numerical procedures being used.

**Accuracy and Stability**

From the above, it can be seen that first-order schemes have second-order truncation errors that are proportional to the grid or mesh size *Δx* (or timestep *Δt* for time derivatives). In a similar manner, it can be shown that second-order schemes have third-order errors that are proportional to the square of the grid or mesh size *Δx2* (or of timestep *Δt2*). If the grid or mesh size *Δx* and timestep *Δt* are treated as fractions of representative length and time scales of the flood under consideration, the truncation errors of a second-order scheme can be shown to reduce quadratically with decreasing grid size and timestep. That is, the finer the grid or mesh size or shorter the timestep, the smaller the numerical truncation errors.

In general, it can be said that first-order schemes are “diffusive”. That is, they tend to damp out sharp gradients in water levels and flow velocities. The artificially high levels of numerical eddy viscosity, discussed above, help to smooth out flow irregularities and make the model calculations very stable. However, the unrealistically high levels of smoothing results in the suppression of flow separations and eddy formation and makes it impractical to compute channel/overbank interactions, where the specification of appropriate eddy viscosity coefficients becomes important.

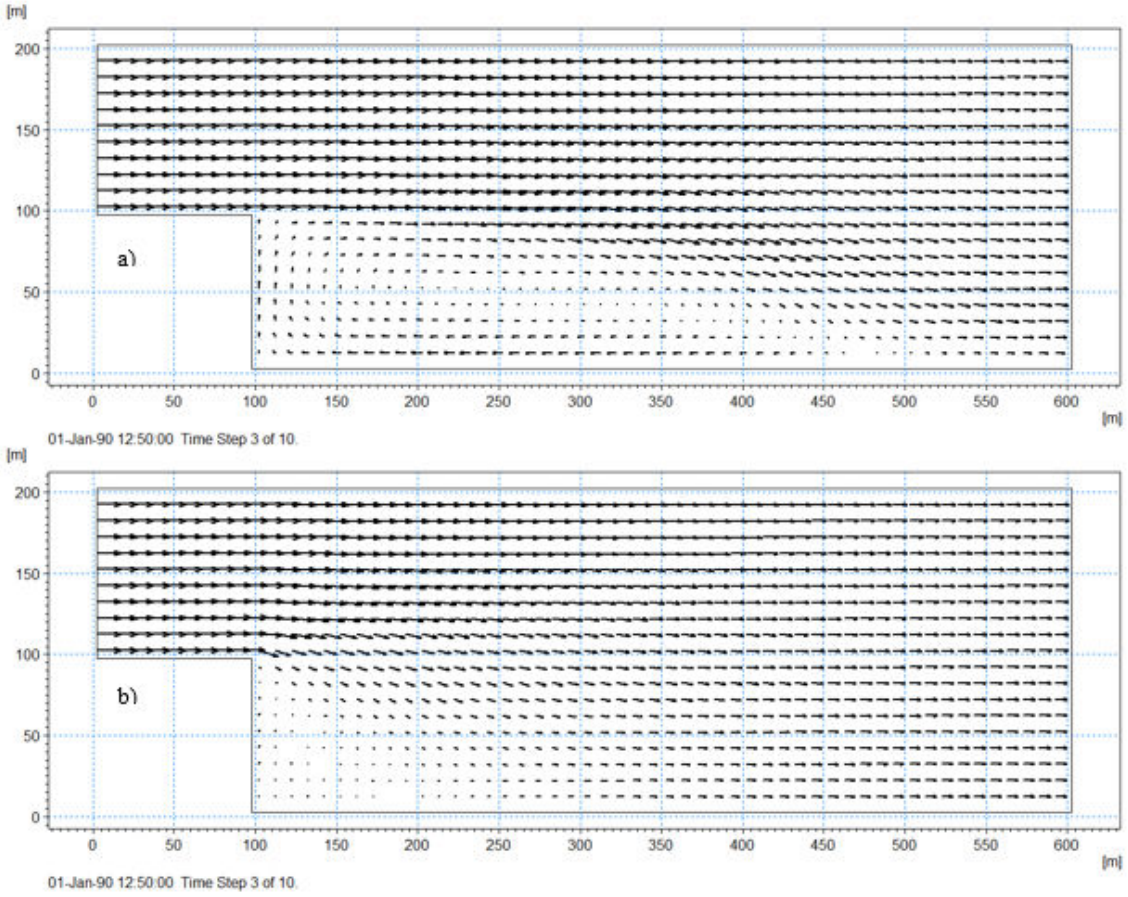


Figure 6.4.11. Figures showing (a) flow separation and eddy formation, and (b) suppression of flow separation with numerical eddy viscosity form a first order upwind scheme

By comparison, second-order schemes are “dispersive”. That is, high frequency components of flood flow can travel at different speeds. This is not normally a problem with the propagation of flood waves which tend to be very long (low frequency) with respect to the model grid or mesh size and timestep. As a result, second-order schemes are generally well suited to modelling the wave propagation properties of flood flow. They are, however, not as well suited to modelling high velocity flows and flows where there are strong velocity gradients. Under these conditions, the convective momentum terms in the momentum equations become more important and the use of second-order schemes can result in artificial “zig-zagging” of the flow and non-linear instabilities (Abbott and Rasmussen, 1977). As a result, Leonard (1979) advocates the use of higher third-order schemes for modelling transport dominated flows.

## 4.7.6. Model Applications

Most of the 2D flood models in common use are based on the numerical solution of the full mass and momentum equations, described above. This generally works well in straight-forward flow situations. However, many of the commonly used solution procedures can have stability issues when modelling high velocity flows, and most, if not all, become ill-conditioned when modelling super-critical flows. This is generally approached by either deliberately introducing numerical stabilising terms, or by using simplified forms of the momentum equation to describe the flow.

Stelling et al. (1998) describe a finite difference model based on first-order upwind differences. The model provides smooth stable solutions for high velocity flows. However, as discussed above, the high levels of numerical diffusion (numerical eddy viscosity) may result in reduced accuracy under flow conditions where the use of more physically realistic values of eddy viscosity may be required. To avoid this problem, McCowan et al. (2001) use a second order scheme for the main part of the computation, but gradually introduce first-order upwinding in localised areas where the Froude number exceeds Fr = 0.25. In both cases, the numerical diffusion introduced in this way is sufficient to maintain the numerical computation through regions of super-critical flows.

As an alternative, BMT WBM (2008) uses the kinematic wave approximation to describe flow conditions in regions with super-critical flow. This approach is reasonable for most flooding applications as super-critical flows are upstream controlled and are normally friction dominated. However, whenever simplified forms of the equations are used, it is important for the modeller to understand their limitations, and care may be required in interpreting the results, particularly in transition areas.

It is noted that the full set of the equations should always be used for describing flows in relatively flat river reaches, and in regions of relatively flat, deep water such as in estuaries and lakes

Clearly, there is a wide range of models with quite different solution procedures with varying orders of accuracy available to the numerical flood modeller. It is important for the modeller to be aware of the type of solution procedure being used, and of any constraints that that this may impose on the timestep, model accuracy, and on the way in which the computation is carried out.

## 4.7.7. Site Specific Model Development

To this point the discussion has focussed on the different types and properties of 2D Generic Numerical Models. The process of developing a Site Specific 2D Model is discussed at length by Engineers Australia (2012) and only an overview of the key stages of model development have been summarised here. They include:

- Selection of the Generic 2D Numerical Model to be used
- Model schematisation (model domain, cell size, time step)
- Key model inputs (topography, bed resistance, eddy viscosity)
- Inclusion of flow controls and hydraulic structures
- Initial Conditions
- Boundary Conditions
- Hydraulic Structures

**Generic Numerical Model Selection**

In practice, the selection of the Generic Numerical Model or modelling software package to be used can be limited to the software available within the modeller's organisation or, in the case of a consulting project, may even be specified externally by the client. Where a choice is available some of the key factors to be considered in selecting the particular software to be used include:

- The skill, experience and personal preferences of the modeller;
- The choice of finite difference or finite volume solution procedures;
- The choice of the use of a structured grid or an unstructured flexible mesh: and
- The availability of any particular features required in the modelling.

**Modeller Experience:** The skill level and experience of the modeller is an important factor in determining the success of any modelling exercise and should be taken into account when selecting the software package to be used.

**Finite Difference vs Finite Volume:** A big advantage with finite volume models and finite difference models based on finite volume techniques is that, barring coding errors, they conserve mass. This is a very important property in a flood model, as any loss or gain of mass caused by the approximations made in the numerical solution procedure can invalidate the model results. It should be noted that this does not preclude the use of finite difference models. It only means that care should be taken when using finite difference models to ensure that there is no significant loss or gain of mass during the model simulations.

**Structured Grid vs Unstructured Flexible Mesh:** Until relatively recently, most of the commercially available flood models operated with a structured rectilinear (square or rectangular) grid. The advantages of these structured grid models are that they are easy to set-up and can be very computationally efficient. A disadvantage is that they do not provide a good description of flows along relatively narrow channels aligned at an angle to the grid, as shown in Figure 6.4.12(a). To get adequate resolution of these flow paths may require reduction in the model grid size, as shown in Figure 6.4.12(b), with a corresponding significant increase in computational requirements.

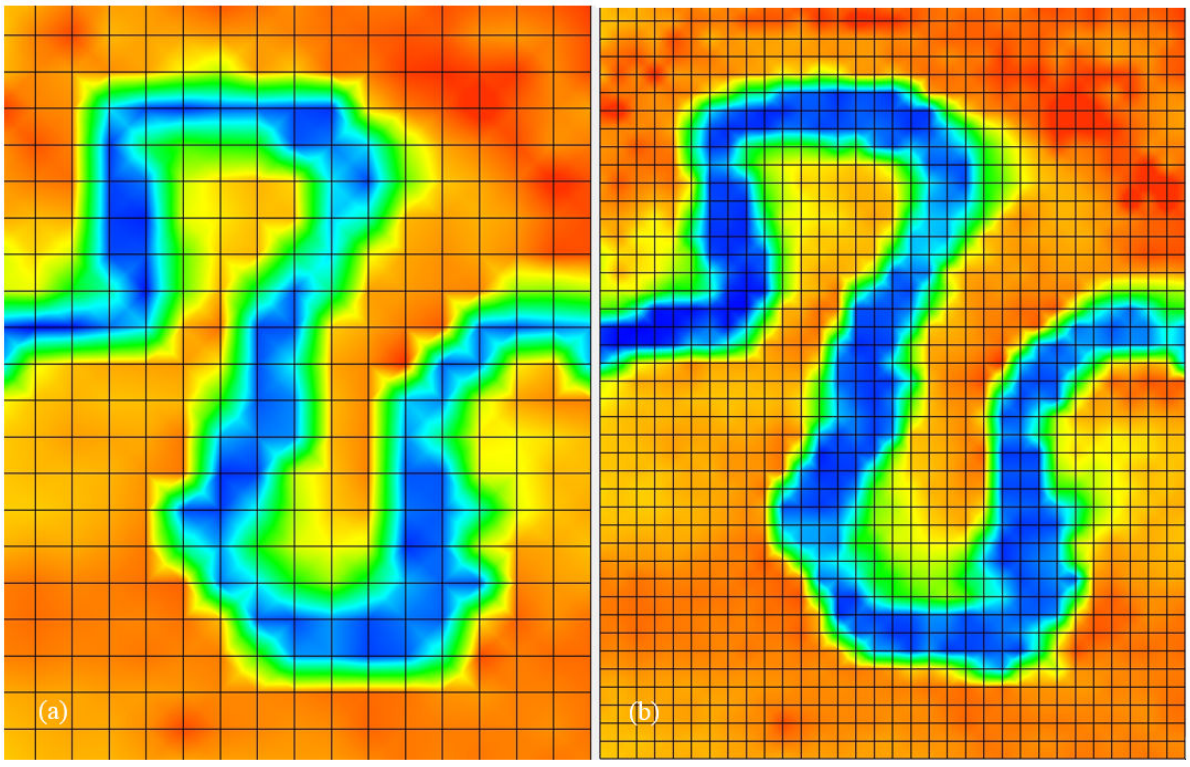


Figure 6.4.12. Showing (a) poor resolution of a sinuous flow path on a coarse square grid, and (b) improved, but still relatively poor resolution at a finer grid scale.

By comparison, flexible mesh models typically use a combination of unstructured triangular and quadrilateral mesh cells as shown in Figure 6.4.13(a). These can be aligned more closely with the main flow paths allowing good resolution with larger mesh cells than with a corresponding structured grid model, as shown in Figure 6.4.13(b). Larger mesh sizes can sometimes also be used in regions with relatively uniform flow and away from particular areas of interest. The main disadvantages of the flexible mesh models are that they take more time and skill to set up the initial model mesh and, due to their increased complexity, they generally take more computer time to run, even with the use of larger mesh sizes.

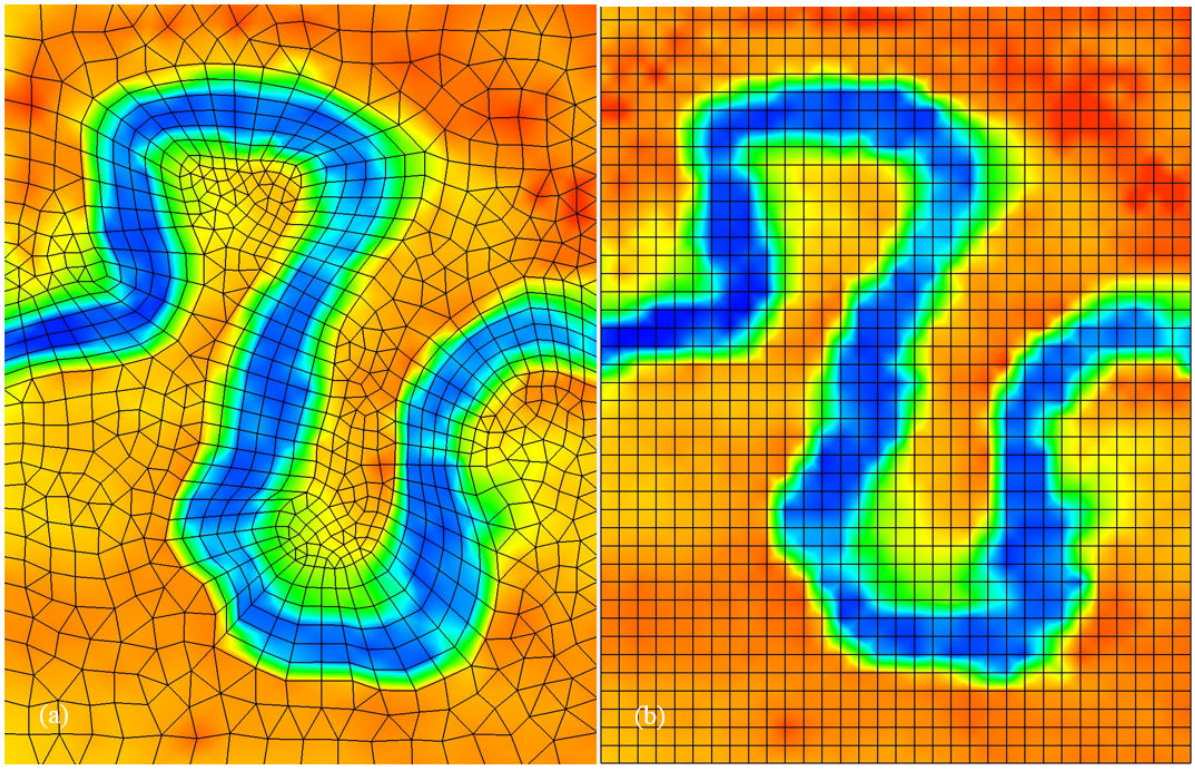


Figure 6.4.13. Showing (a) improved resolution of a sinuous flow path using a flexible mesh, relative to (b) a fine square grid.

**Model Schematization**

The first task in schematizing a model is to decide on the model domain. This is the area to be included within the model. It should include the main area of interest and should extend out far enough to include all the areas that are likely to be inundated in the most extreme flood to be considered. It should also extend sufficiently upstream and downstream such that any irregularities in the flow at the model boundaries will not affect the model results in the main area of interest. Wherever possible, the model boundaries should be located in areas of relatively uniform flow.

For structured grid models, a square or rectangular is overlaid on the model domain. This grid should, where possible, be aligned with the main flow direction. The grid size should be selected to provide adequate resolution of the main features to be modelled (e.g., channels, levees, bridges, etc). Care should be taken to ensure that the main flow paths to be considered can be adequately described, particularly when they are aligned at an angle to the grid.

For unstructured flexible mesh models, a model mesh covering the model domain must be developed. This mesh may typically be formed using triangular mesh cells, or a combination

of triangular and quadrilateral mesh cells, although some software allows the use of other shapes as well. As seen in Book 6, Chapter 4, Section 7, one advantage of the flexible mesh approach is that the mesh cells can be aligned to the main flow paths irrespective of their orientation. Another is that finer cell sizes can be used to provide greater resolution in particular areas of interest. Conversely, larger cell sizes can be used to reduce computational requirements in less important areas.

Clearly, the smallest feature that can be resolved will be one grid or mesh cell wide. However, if realistic simulation of flow separation and eddy formation behind structures such as bridge abutments is required, then these structures will need to be resolved by a minimum of 6 to 8 grid or mesh cells.

The selection of the appropriate cell size is generally a trade-off between model resolution and computational requirements. In this respect it is noted that the computational time required by a model is roughly proportional to the cube of the cell size. That is, halving the cell size could be expected to increase the computational time by a factor of 8.

The time step is generally set to the largest value that can be used without affecting the accuracy of the model results. For explicit models, the time step is set close to the maximum allowable under the Courant stability criterion, discussed in Book 6, Chapter 4, Section 7. Although implicit models are not affected by this constraint, their timestep is usually limited by accuracy requirements, and the optimum timestep is typically determined by sensitivity testing during model calibration.

**Key Model Inputs**

Some of the key inputs to a 2D model include: the model topography, bed resistance values and, where appropriate, the eddy viscosity formulation. These are discussed briefly below.

**Topography:** The model topography forms the basis of any 2D hydraulic model. It is the numerical analogue of the actual terrain over which the water flows. It comprises survey data (e.g., from a digital terrain model) that has been interpolated onto the model grid or mesh. Following the initial interpolation process, some degree of manipulation may be required to ensure that the main flow paths and flow controls, such as road embankments or levee banks, have been adequately resolved. For flow paths that are less than a few cell widths wide, some degree of schematization may be required to ensure that the model flow path provides a realistic description of the flow path conveyance. This is particularly true for structured grid models. Care taken in setting up the model topography can significantly reduce the amount of time required to calibrate a 2D model.

**Bed Resistance:** 2D models also require bed-friction coefficients to be specified for application to each computational cell. These are generally specified in terms of different Mannings “n” coefficients that are assigned to a range of different land-use categories. These can be determined on the basis of a combination of information gained through site inspections, from aerial imagery and from cadastral data.

**Eddy Viscosity:** Eddy viscosity is used in 2D models to represent the effects of turbulence and sub-grid scale processes. The use of appropriate eddy viscosity values is necessary in simulations where the realistic representation of flow separations and eddy formation, or of momentum transfers between the main channel and overbank areas are important. Depending on the software being used eddy viscosity coefficients can be described as constant values, spatially varying values, or values computed internally by a turbulence closure model. In this respect, it is noted that a “Smagorinsky-type” eddy viscosity formulation has been found to be suitable for describing the effects of sub-grid scale processes in many applications.

**Initial Conditions**

For any model computation to move forward in time there must be a known starting point. For numerical hydrodynamic models this starting point is known as the model "initial conditions". The initial conditions necessary for two-dimensional hydrodynamic models consist of water surface elevation $\zeta$ and $u$ and $v$ velocity values at every grid/mesh element that is "active" at the start of the computation.

These values can be specified by:

- A "cold start", where initial estimates of the water surface elevation $\zeta$ values are made, and the $u$ and $v$ velocity values are set to zero (i.e., no flow).
- A "hot start", where the initial water surface elevation $\zeta$, and $u$ and $v$ velocity values are specified from the results of a previous model simulation.

***Cold Starts:*** In many flood modelling applications, the precise values of the initial conditions are not that critical, provided the model computation starts in a reasonably realistic manner; that is, relatively smoothly and with no initial instabilities. However, in applications where there are lakes, wetlands, retarding basins, or other depressions that may provide initial flood storage, it is important that the initial water surface elevations provide the correct amount of initial storage in these areas. If the initial amount of water in these storage areas is underestimated, this may cause the model to artificially attenuate the flood peak. Conversely, if it is overestimated, the flood peak may be artificially enhanced.

***Hot Starts:*** Hot starts are not used extensively in practice. Their main uses tend to be limited to:

- Providing initial conditions for model simulations where significant computing time may be required for the model "warm-up" period required. In these cases, the results of a single prolonged "warm-up" simulation can be used to provide initial conditions for a subsequent series of model simulations.
- Breaking-up very long model simulations into more manageable sub-sections.

***Urban Applications:*** In many urban applications, the area to be modelled may be initially dry. In these cases, the initial water surface elevation $\zeta$ values will typically be set to the corresponding ground surface elevation $z$ values, and the initial $u$ and $v$ velocity values set to zero. This approach could be considered as a special case of the cold start. It is applicable in model simulations where there is no initial overland flow, including direct rainfall on grid applications.

**Boundary Conditions**

With the initial conditions specified, the model boundary conditions are the remaining pieces of necessary information required for the model computation to proceed. In this respect it is noted that boundary conditions are required at every grid/mesh element along the model boundaries. These boundaries include both external boundaries and internal boundaries, where:

- External boundaries are located along the external edges or boundaries of the model, where water can flow into or out of the model domain.
- Internal boundaries are located within the model domain, and include the interface between wet (water) cells, where the computation is to be carried out, and dry (land) cells where there is no computation.

The subject of boundary conditions for two-dimensional flow models is quite complex and the following discussion is, of necessity, relatively superficial.

***External Boundaries:*** The model requires boundary conditions in terms of either water levels or discharges along both the upstream and downstream boundaries.

The upstream boundary conditions for a 2D flood model are generally provided by a discharge hydrograph. This has to be converted to discharges or flow velocities and water depths at each boundary cell. For this to be done, some assumptions need to be made with respect to the distribution of the flows along the boundary, and to the direction of the flow. Depending on the modelling package being used, the flow distribution along the boundary may be computed internally using a range of possible assumptions (e.g., uniform flow or the use of Manning's equation). There may also be options for providing user specified flow distributions and directions.

The downstream boundary conditions are generally specified in terms of water surface elevations. These may be specified as a constant, a times series, or computed internally using a rating curve. As a first approximation, it can be assumed that the water surface elevations along the boundary are horizontal. As such, the water surface elevation specified at each individual boundary cell will be the same. Depending on the modelling package being used, the flow directions may be specified as being normal to the boundary, or there may be options for them to be computed as a function of the upstream flow conditions, or specified externally by the user.

Whatever forms of boundary conditions that are being used, it is important to recognise that the model has no information regarding the flow conditions upstream or downstream of the model boundaries. As such, it is important that, wherever possible, the model boundaries should be located in areas where the flow is expected to be relatively uniform. The model boundaries should also be placed far enough upstream and downstream of the area of interest to ensure that any errors in flow distribution and/or direction do not have a significant effect on the model results.

***Internal Boundaries:*** There are two types of internal boundaries used in 2D models:

- The first occurs at the land/water interfaces within the interior of the model domain. These internal boundaries can be considered as a special case of a velocity boundary where the flow velocity between adjacent pairs of wet and dry cells is set to zero. The locations of these internal boundaries are dynamic as different cells are brought into the computation as the flood rises, and taken out again as the flood recedes.

- The second type of internal boundary occurs where there are source or sink terms (related to local inflows and outflows), hydraulic structures, or where there are links to embedded 1D model branches.

**Hydraulic Structures**

Depending upon the particular software being used, hydraulic structures such as weirs, culverts, bridges and regulating structures can be introduced into the model. This may be done either by introducing a structure equation to replace the momentum equation between two adjacent computational cells (similar to the 1D model approach), or by introducing a 1D model branch containing the required structures (see Book 6, Chapter 4, Section 5) and coupled to the 2D model domain via internal boundaries.

## 4.7.8. Advantages and Disadvantages

The main advantage of a full 2D model is that it can provide a more realistic description of the flows and flow distributions throughout a river and flood plain system. When compared with the disadvantages of 1D models discussed above, it can be said that:

- The floodplain flow paths do not need to be pre-determined by the user, as they are computed directly as a function of the model terrain and the applied flows.
- The flow paths can change with increases in water level in much the same way as they do in real life.
- Losses due to two-dimensional effects such as bends, flow separations, etc, are automatically included within the computation, and do not need to be lumped into the bed-friction parameter (as such, the bed-friction coefficients can be specified directly as a function of bed-roughness only).
- Model results can provide details of the flow distribution within individual flow paths.
- Model results can be used directly for mapping flood extents and depths of inundation.

In the early days of full 2D modelling, the main disadvantages of the 2D models were that they required significantly more survey data than 1D models, and that they were very heavy computationally. The advent of LiDAR has, to some extent, overcome some of the survey requirements. There have also been significant increases in computing power, which combined with the introduction of parallel processors and GPUs has greatly increased the computational capacity of modern computers. However, along with the increase in computing capacity, there has been a tendency for modellers to use smaller cell sizes, to get better resolution, and also to use much larger model domains. As a result, long simulation times can still be an issue with 2D models. Further, the result files of these model runs can become very large, and can make significant demands on data storage and processing capability.

Another disadvantage of 2D models is that flow paths and channels can only be resolved at the same scale as the model grid or mesh. Even when a channel may be several computational cells wide, the in-bank flows may not be described as well as in a 1D model with detailed cross-sections.

Figure 6.4.14 shows the topography of the floodplain region of the Lindsay and Murray River system considered in Book 6, Chapter 4, Section 6, where the channel of the Murray River is shown in white. To provide adequate resolution of the complex channel system throughout the floodplain in a 2D model would require a relatively fine grid or mesh size resulting in very large computational arrays and correspondingly long run times.

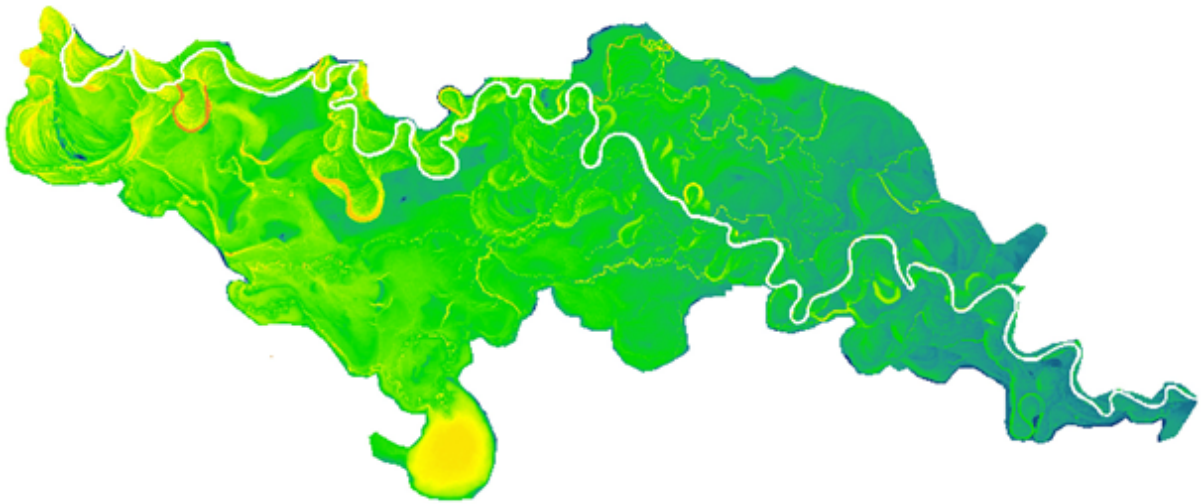

Figure 6.4.14. Topography of The Lindsay and Murray River System

## 4.7.9. Coupled 1D/2D Hydraulic Models

From the discussions above, it can be seen that 1D models are well suited to modelling in-bank flows and flows along long river and floodplain reaches (of the order of 10s to 100s or even 1,000s of kilometres) while full 2D models are well suited to modelling the details of the flow in smaller areas (of order 100s of metres to 10s of kilometres). This led to the proposal for integrated modelling (Carr and McCowan, 1988) whereby overall 1D models are used to provide water level and discharge boundary conditions for use in a detailed 2D model of a particular area of interest. This concept of model integration has been taken further (references needed) with 1D models being dynamically coupled with 2D models.

The coupling can work in different ways depending upon the particular software package being used. These can include:

- The use of a 1D model to simulate an overall river and floodplain system dynamically coupled to a 2D model providing detailed flow computations in particular areas of interest.
- The use of dynamically coupled 1D model branches to provide a better description of in-bank channel flows within a 2D model domain. The coupling of these branches can provide for the exchange of water between the 1D in-bank flows and the 2D model flood plain flows.
- The use of dynamically coupled 1D model branch to introduce hydraulic structures (such as weirs, culverts, bridges, etc.) into the 2D model domain.

A further extension of the integrated 1D/2D modelling concept has been the dynamic coupling of 2D models with 1D pipe network models. This has significantly enhanced the capabilities of 2D models for urban flood modelling applications.

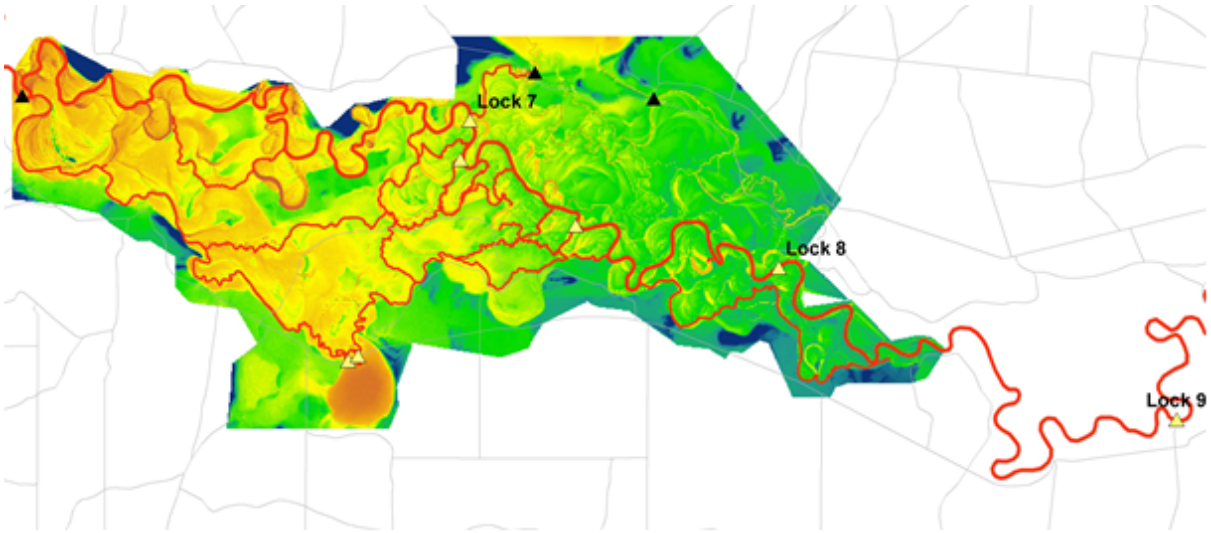


Figure 6.4.15. Example of a Coupled 1D/2D Model of the Lindsay River System

## 4.7.10. Direct Rainfall Models

A relatively recent development in 2D hydraulic modelling models has been the use of direct rainfall to estimate flows in catchments or sub-catchments where the local rainfall within the 2D model domain is contributing to the flow that we are interested in. Under these circumstances it is difficult to use traditional approaches such as the use a hydrologic model to provide flows at the model boundaries.

With the direct rainfall approach, the rainfall-runoff process is simulated by applying rainfall directly to each cell within the model domain. Losses are accounted for using different approaches depending upon the software package being used. With the simplest approach, the losses are applied directly to the rainfall with only a resulting rainfall “excess” being applied to the model cells. More sophisticated approaches may use infiltration models incorporated within the 2D modelling software and, ultimately, may involve coupling with a groundwater model.

The use of direct rainfall on a 2D model makes it possible to simulate the rainfall-runoff process, as well as the hydraulic routing of the resulting overland flows throughout model domain. This provides a more realistic representation of catchment storage and runoff effects. It is, however, essential to have good topographic data. The selection of appropriate roughness coefficients is critical to the success of this approach (Muncaster et al., 2006). Further, roughness values may need to be increased for describing shallow flows in rural areas, or decreased to allow for more rapid runoff from rooves and some paved areas in urban applications (Caddis et al., 2008).

The use of a 2D hydraulic model in this way integrates both the hydrologic and hydraulic aspects of the rainfall-runoff process into a single model. The use of direct rainfall is, however, an area of on-going research and care should be used when interpreting the model results. Wherever possible models should be calibrated to measurements. Where calibration is not possible (as in many cases), sensitivity testing should be carried out to assess the sensitivity of the model to variations in the main model parameters.

## 4.7.11. Limitations of 2D Hydraulic Models

One of the main limitations associated with 2D hydraulic models is that they can provide plausible results in situations where the underlying data may be inadequate, the model schematization does not adequately describe all the physical system being represented, or in flow cases where the assumptions of two-dimensional flow or of hydrostatic pressure becomes invalid.

Examples of situations where the two-dimensional assumption becomes invalid include:

- Modelling the details of “helicoidal” flows around river bends
- Modelling the details of flows at bridges, culverts and intake and outlet structures
- Modelling separation zones and wakes behind structures where the horizontal dimensions of the structure, and of the cell size, are much smaller than the water depth

In these situations care needs to be taken in interpreting the model results. In some models the effects of three-dimensional flows can be included through additional loss terms, or the inclusion of sub cell-scale pier loss formulae. If, however, it is necessary to model the details of these types of flow, then a full three-dimensional model should be used.

Situations where the hydrostatic pressure assumption becomes invalid include free overflows of water over levees and embankments. In these cases the hydrostatic pressure assumption can lead to a significant over-estimation of the overflows. Depending upon the software being used, these effects can be overcome by incorporating weir equations into the computation, or by widening the model description of the levee or embankment to include two cell widths.

# 4.8. Summary and Conclusions

The aim of a hydraulic flood model is to provide a realistic representation of flood flows in river and floodplain systems. In general, it can be said that the more realistic the modelling approach, the greater the probability of achieving a successful outcome. However, the use of the most sophisticated modelling approach available will not, in itself, guarantee success. This is because the skill of the modeller adapting a generic modelling system to a specific application, and the quality of the data used as model input can be equally (or even more) important in determining the success of a modelling exercise.

The reliability of a hydraulic model is determined by a three stage process:

- Validation: to confirm that the modelling software is doing what it is supposed to do.
- Calibration: the process of adjusting model parameters to obtain a best fit with measured flood data.
- Verification: ideally, a check of the model calibration against an independent set of flood data.

In cases where there is insufficient or no calibration data, sensitivity tests should be carried out to assess the sensitivity of the model to variations in the main model parameters

Steady flow hydraulic models are best suited to modelling flows along relatively short reaches of river with well-defined flow paths, and/or for modelling flows at structures. However, unsteady hydraulic models should be used to describe flows where there are:

- Rapidly changing hydrographs;
- Flat channel slopes where wave propagation effects can become important;
- Wide floodplains and/or other features where storage effects may affect the flow; and
- Channel networks where the flow splits are not well defined.

With respect to the different types of unsteady hydraulic models that are available, it can be said that:

- The use of CFD and other non-hydrostatic models, including physical models, is generally limited to simulating the details of complex flows in relatively short reaches of a river, or at or within hydraulic structures.
- 3D models are very heavy computationally, and are best suited to modelling the details of complex flows in relatively short reaches of rivers, around structures and in other flows cases where three-dimensional effects become important in determining localized flood effects.
- 1D models are computationally quick to run and are well suited to modelling flows along well-defined channel and floodplain systems. However, the more general use of 1D models in flood studies has been largely superseded by 2D models.
- 2D models can provide a much more detailed description of flood flows and flow distributions within individual flow paths and have become virtually the standard for rural and urban flood studies. 2D models are, however, more demanding on input data and on computing resources.
- The integration of 1D models with 2D models has made it possible to include 1D model branches within a 2D model domain to provide a better description of in-bank flows and/or to introduce hydraulic structures (such as weirs, culverts, bridges, etc.) into the 2D model domain.
- The integration of 1D pipe network models with 2D models has significantly enhanced the capabilities of 2D models for urban flood modelling applications.
- The use of rainfall on grid has made it possible to integrate both the hydrologic and hydraulic aspects of the rainfall-runoff process into a single model. The use of direct rainfall is, however, an area of on-going research and care should be used when interpreting the model results.

## 4.9. References

Abbott, M.B. and Ionescu, F. (1967), On the Numerical Computation of Nearly Horizontal Flows, Journal of Hydraulic Research.

Abbott, M.B. (1979), Computational Hydraulics - Elements of the Theory of Free Surface Flows, Pitman, London.

Abbott, M.B. and Basco, D.R. (1989), Computational Fluid Dynamics: an Introduction for Engineers, Longman.

Abbott, M.B. and Rasmussen, C.H. (1977), On the Numerical Modelling of Rapid Contractions and Expansions in Models that are Two-Dimensional in Plan, Proc. 17th Congress IAHR, Baden-Baden.

American Society of Engineers (1996), River Hydraulics - Technical Engineering and Design Guides as Adapted From the US Army Corps of Engineers, No. 18, ASCE Press, New York.

BMT WBM (2008), TUFLOW User Manual. GIS Based 2D/1D Hydrodynamic Modelling.

Benque, J.P., Hauguel, A. and Viollet, P.L. (1982), Numerical Models in Environmental Fluid Mechanics, Pitman.

Bishop, W.A., McCowan, A.D., Sutherland, R.J. and Watkinson, R.J. (1995), Application of Two-Dimensional Numerical Models to Urban Flood Studies, 2nd International Symposium on Stormwater Management, Melbourne.

Caddis, B.M., Jempson, M.A., Ball, J.E. and Syme, W.J. (2008), Incorporating Hydrology into 2D Hydraulic Models - the Direct Rainfall Approach, (9th Aust. Conf. on Hydraulics in Water Engineering, Darwin.

Carr, R.S. and McCowan A.D. (1988), An Integrated Approach to Two?Dimensional Flood Plain Modelling, ACADS Workshop on 2D Flood Plain Modelling, Monash University.

Connor, J.J. and Brebbia, C.A. (1976), Finite Element Techniques for Fluid Flow, Newnes-Butterworths

Cunge, J.A., Holly, F.M. and Verwey, A. (1980), Practical Aspects of Computational River Hydraulics, Pitman, London (Reprinted by University of Iowa).

DHI Water and Environment (2005), MIKE 21 - Coastal Hydraulics and Oceanography - Hydrodynamic Module, Scientific Documentation, DHI Software, Hørsholm.

Engineers Australia (2012), Australian Rainfall and Runoff Revision Project 15: Two-Dimensional Modelling in Urban and Rural Floodplains.

King, I.P. and Roig, L.C. (1988), Recent Applications of RMA's Finite Element Models for Two-Dimensional Hydrodynamics and Water Quality, Proc 2nd Int. Conf. on Finite Elements in Water Resources, Pentech Press.

LeVeque, R.J and Bale D.S. (2012), Wave Propagation Methods Conservation, Journal of Hyperbolic Problems, Zurich.

Leendertse, J. (1967), Aspects of a Computational Model for Long-Period Water Wave Propagation, Rand Memorandum RM-5294-PR, Santa Monica.

Leonard, B.P. (1979), A Stable and Accurate Convective Modelling Procedure Based on Quadratic Upstream Interpolation. Computer Methods in Applied Mechanics and Engineering, 19(1), 59-98.

McCowan, A.D., Rasmussen, E.B. and Berg, P. (2001), Improving the Performance of a Two-dimensional Hydraulic Model for Floodplain Applications, Proceedings of the 6th Conference on Hydraulics in Civil Engineering, Hobart.

Muncaster, S.H., Bishop, W.A. and McCowan, A.D. (2006), Design Flood Estimation in Small Catchments Using Two-Dimensional Hydraulic Modelling - A Case Study, 30th Hydrology and Water Resources Symposium, Launceston.

Preissmann, A. (1961), Propagation des Intumescences dans les Canaux et Rivieres, First Congress of the French Association for Computation, Grenoble.

Roache, P.J. (1998), Fundamentals of Computational Fluid Dynamics, Hermosa.

Sherwin S.J., Peiro J., (2005), Finite difference, finite element and finite volume methods for partial differential equations, Handbook of materials modeling, Editors: Yip, Berlin, Publisher: Springer, pp: 1-30, ISBN: 9781402032875

Stelling, G.S. (1984), On the Construction of Computational Methods for Shallow Water Flow Problems, Delft University of Technology.

Stelling, G.S., Kernkamp, H.W.J and Laguzzi, M.M. (1998), Delft Flooding System: A Powerful Tool for Inundation Assessment based upon a Positive Flow Simulation, in Hydroinformatics '98, V. Babovic and L.C. Larsen (ed's), Balkema.

Syme, W.J. (2001), TUFLOW - Two and One-Dimensional Unsteady Flow Software for Rivers, Estuaries and Coastal Waters, I.E.Aust Workshop on 2D Flood Modelling, Sydney.

United States Army Corps of Engineers (USACE) (2010), HEC-RAS River Analysis System, Hydraulic Reference Manual, Version 4.1, Hydrologic Engineering Center.

Violeau, D. (2012), Fluid Mechanics and the SPH Method, Theory and Applications, Oxford University Press.

Zienkiewicz, O.C., Taylor, R.L. and Nithiarasu, P. (2014), The Finite Element Method for Fluid Dynamics, 7th Edition, Butterworth-Heinemann.

# Chapter 5. Interaction of Coastal and Catchment Flooding

Seth Westra, Michael Leonard, Feifei Zheng

| Chapter Status | Final |
|---|---|
| Date last updated | 14/5/2019 |
| Minor edits | 27/08/2024 |

## 5.1. Introduction

Floods in estuarine areas can be caused by runoff generated by an extreme rainfall event, an elevated ocean level generated by a storm surge and/or a high astronomical tide, or a combination of both processes occurring simultaneously or in close succession. Research in Australia (Zheng et al., 2013) and internationally (Svensson and Jones, 2002; Svensson and Jones, 2004; Hawkes and Svensson, 2006) has shown that extreme rainfall and storm surge processes are statistically dependent, and therefore their interaction needs to be taken into account for areas affected by both processes.

This chapter describes procedures that can be used to estimate design flood levels in the 'joint probability zone', defined as the region in which the dependence between riverine and ocean processes has the potential to influence the design flood level. This region is illustrated in Figure 6.5.1, and shows that the range of possible flood levels corresponding to a given Annual Exceedance Probability are enclosed in an envelope bounded by cases where flood events and ocean levels are perfectly dependent (upper curve) and independent (lower curve).

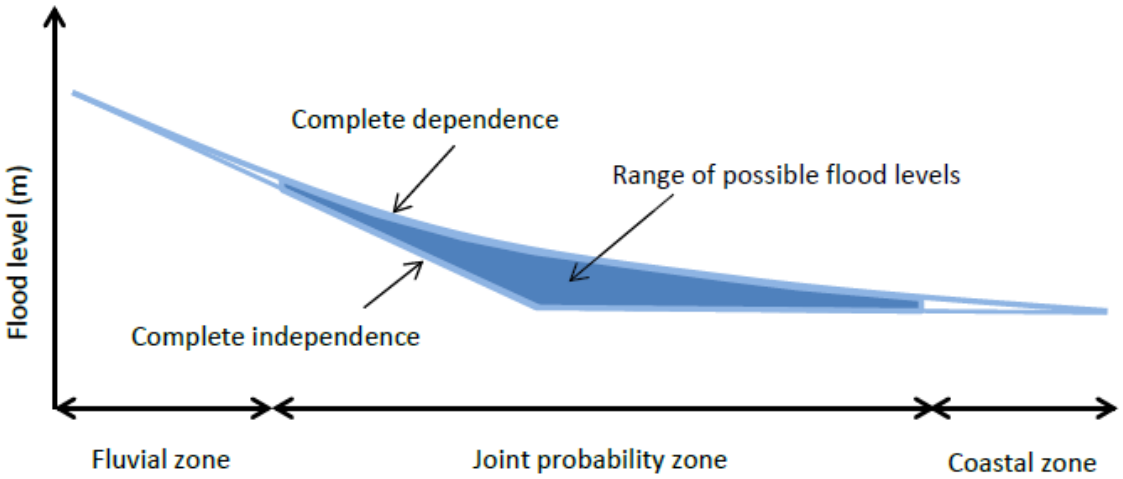


Figure 6.5.1. Schematic of a longitudinal section of an estuary, which shows two hypothetical water levels: the level obtained by assuming that fluvial floods will always coincide with storm tides of the same exceedance probability (upper curve); and the level assuming fluvial processes and ocean processes are completely independent and thus will almost never coincide (lower curve).

This chapter provides practical guidance on estimating the exceedance probability of floods in the joint probability zone. The focus of this chapter is on the 'design variable method', which has been developed as a flood estimation approach that can be applied across Australia's diverse climates. The method has been tested for design floods from 50% to 1% Annual Exceedance Probabilities , and can account for the influence of climate change by adjusting both the design rainfall and design ocean levels that are required as inputs.

The theory and practice of flood estimation in the joint probability zone is considerably more complex than many traditional flood estimation problems, and engineering judgement is required on whether the design variable method described in this chapter is suitable for a given situation. This judgement should be based on a sound knowledge of joint probability theory, combined with an understanding of riverine and oceanic flood processes. Alternative methods that may be appropriate under certain conditions are discussed briefly in Book 6, Chapter 5, Section 3. The approach presented in this chapter is also valid for overland flooding problems.

## 5.2. Background to Flood Processes in Estuarine Areas

The combination of processes that can cause flooding in the joint probability zone is illustrated using a hypothetical flood occurring in an estuarine region bounded above by flow from an upstream catchment and below by ocean water levels at the estuary mouth (Figure 6.5.2)**.** Factors that can influence the magnitude of a flood in this region have been numbered in Figure 6.5.2, and each factor is described is more detail below.

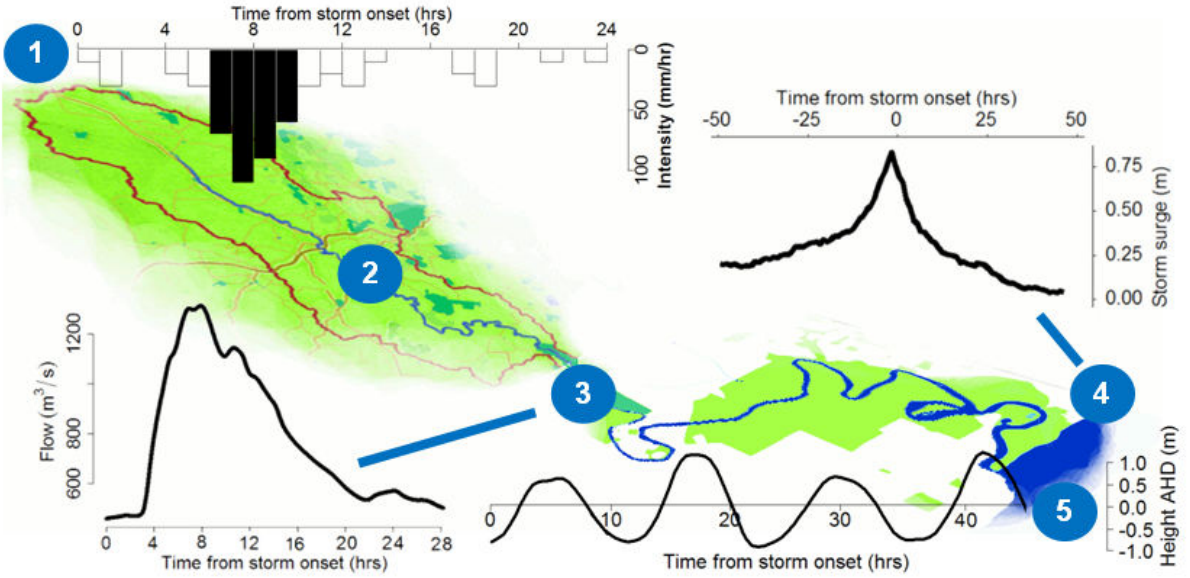


Figure 6.5.2. Timing factors affecting the magnitude of a flood in the joint probability zone

1. *Rainfall* - A flood can be initiated by a sustained burst of intense rainfall (often referred to as a storm burst, shown in Figure 6.5.2 as the shaded four hour period) over an estuarine catchment. This storm burst can be characterised by its duration, spatial extent, temporal pattern and rainfall intensity. The storm burst is often embedded in a longer period of rainfall, which can be caused by large-scale meteorological features such as a frontal rainfall system or a tropical cyclone.

2. *Runoff Generation*- The shape, size, slope, soil type, vegetation and level of urbanisation all contribute to the way a catchment translates rainfall into runoff. The time of concentration refers to the time it takes all of the catchment to contribute runoff at the

catchment outlet, and is often assumed to be equivalent to the time taken for water to travel from the most distant point in the catchment to the catchment outlet. The time of concentration of the hypothetical catchment in Figure 6.5.2 is four hours, which is equivalent to the duration of the storm burst.

3. *Hydrograph at Catchment Outlet:* - The time it takes for the hydrograph to enter the joint probability zone causes a lag between the flood producing rainfall event and the hydrograph peak. The hydrograph represents the fresh water contribution to floods in the joint probability zone, and may form the upstream boundary condition for hydrodynamic models of this region.

4. *Storm surge* - The ocean level forms the downstream boundary to the system, and typically comprises a deterministic component (the astronomical tide) and a random component (usually dominated by the storm surge). The storm surge is caused by anomalous wind and atmospheric pressure that are linked to large-scale weather patterns, and the magnitude of the surge at a particular location will be influenced by the coastal geography and bathymetry. Figure 6.5.2 shows a composite of ten storm surge events near Perth, with the composite exhibiting a sharp peak lasting several hours, yet with some effects still apparent for a day or longer both before and after the peak.

5. *Astronomica*l tide- Tidal patterns, whether diurnal (24 hour), semi-diurnal (12 hour) or mixed, can vary substantially with location. The astronomic tide level is usually assumed to be independent of the rainfall intensity.

As illustrated in Figure 6.5.2, the question of whether or not a large fluvial flood will coincide with an elevated ocean level will depend on several timing issues, which are influenced by a combination of meteorological, catchment scale and oceanographic processes. In particular, the timescale of both rainfall and storm surge events are determined by meteorological influences, whereas the timescale of the runoff depends on specific catchment features that are related to the catchment's time of concentration.

A further complicating factor is that the same meteorological events can drive both rainfall and storm surge events, and this has led to the finding in Australia (Zheng et al., 2013) and internationally (Svensson and Jones, 2002; Svensson and Jones, 2004; Hawkes and Svensson, 2006) that extreme rainfall and storm surge is statistically dependent. The dependence strength between extreme rainfall and storm surge in Australia was found to vary as a function of geographic location and the duration of the rainfall burst (Zheng et al., 2013; Zheng et al., 2014a). Each of these factors will need to be taken into account when selecting a method for estimating flood exceedance probabilities in Australia's estuarine catchments.

## 5.3. Flood Estimation Approaches for the Joint Probability Zone

Several approaches have been developed to estimate the exceedance probability of floods in the joint probability zone, each with different assumptions, data and modelling requirements. The three most commonly used approaches are described here, with key features summarised in Table 6.5.1:

*Flood Frequency Analysis (FFA)* - This approach involves fitting a probability distribution to a time series of historical streamflow. The approach is relatively easy to implement, but requires long, high-quality historical flood records at the location of interest. The advantage of this approach is that, by directly focusing on the statistical characteristics of historical

floods, it may be possible to avoid modelling the complex processes that lead to estuarine floods as depicted in Figure 6.5.2**.**

However, the approach assumes that the upstream catchment conditions and the bathymetry of the estuary are unchanged over the historical record and are reflective of future conditions, and that the statistical characteristics of the upper and lower boundary conditions (e.g. extreme rainfall, sea level, storm surge) will remain constant into the future. For most of Australia's estuarine catchments, one or more of the assumptions underpinning FFA will be violated; therefore this approach is unlikely to be practically applicable in most situations.

Further information on implementation of flood frequency approaches is provided in Book 3, Chapter 2.

*Continuous simulation* - As discussed in Book 6, Chapter 5, Section 2, floods in the joint probability zone can be influenced by a large number of processes operating at a range of timescales, including sub-daily variability in tides, storm surges and the flood hydrograph from the upstream catchment, superimposed on lower-frequency variability at daily, seasonal, annual and inter-annual timescales. In many cases, dynamical features, such as the progression and attenuation of tides up the estuary, can significantly influence flood behaviour.

Continuous simulation approaches aim to simulate these complex dynamics, by running continuous hydrological and hydraulic models to generate a long time series of a response variable (e.g. flood level) that can then serve as the basis for Flood Frequency Analysis. To capture these dynamics, the models will usually need to be run at fine sub-daily timescales. Furthermore, the hydrological and hydraulic model will require long continuous observational time series of rainfall (representing the upstream boundary condition) and storm tides (representing the downstream boundary condition). To estimate flood characteristics such as level at specified exceedance probabilities, it is possible to apply a univariate Generalised Extreme Value analysis to extreme simulated flood values. Alternatively, it is possible to stochastically generate long continuous time series of the forcing variables and then use the empirical probabilities.

The computational load of continuously running hydrological and hydraulic models at the short time steps required for capturing tidal dynamics—while producing long runs required for estimating floods with low exceedance probabilities—is often extremely high. Furthermore, in many cases, long historical time series of both extreme rainfall and storm tides are unlikely to be available at the location of interest. If implemented correctly, continuous simulation is likely to be a technically rigorous approach for flood estimation in the joint probability zone, but given its numerous practical challenges, the design variable method has been developed as an alternative approach for flood estimation problems along the Australian coastline.

Further information on implementation of continuous simulation approaches is provided in Book 2, Chapter 7.

*The design variable method* -This approach has been developed as a simpler alternative to continuous simulation, without the limiting assumptions of Flood Frequency Analysis. For further information on the theory and practical limitation of the method, refer to Book 6, Chapter 5, Section 4 and Book 6, Chapter 5, Section 5, respectively. The primary assumptions of the approach are:

- The statistical dependence between extreme rainfall and storm surge can be represented through a bivariate logistic extreme value dependence model, discussed in further detail in (Zheng et al., 2014a);
- The dependence strength can be interpolated between gauged locations along the Australian coastline, and therefore can be represented by a map of dependence strength (given in Figure 6.5.13 and discussed further in Book 6, Chapter 5, Section 5); and
- The Annual Exceedance Probability of the rainfall event is equivalent to the Annual Exceedance Probability of the flood event (probability neutral);
- Ocean water levels are assumed to be 'static', as tidal dynamics are not considered explicitly in the method; and
- Anthropogenic climate change will have negligible effect on the strength of dependence between extreme rainfall and storm surge, although the effects of climate change can be accounted for by changing the marginal distributions (ie. the extreme rainfall intensity and the ocean level).

The validity of the assumptions of the design variable method need to be considered when applying the method to a specific flood estimation problem, and weighed against assumptions associated with alternative approaches. For many situations, the design variable method is a pragmatic approach that can be applied across a range of estuarine flood estimation approaches.

A comparison between each of the methods is provided in Table 6.5.1.

Table 6.5.1. Comparison design flood estimation methods in the joint probability zone

| Aspect \ Model | Flood Frequency Analysis | Design Variable Method | Continuous Simulation |
|---|---|---|---|
| Domain of Applicability | Analysis restricted to locations with gauged data. | Can be applied throughout the joint probability zone. | Can be applied throughout the joint probability zone. |
| Models Required | Univariate extreme value model or other statistical model of extremes (see Book 6, Chapter 4). | Event-based hydrological and hydraulic models, and a bivariate extreme value model. | Continuous hydrological and hydraulic models, and a univariate extreme value model. |
| Technical Complexity | Low | Intermediate | Advanced |
| Computational Demand | Low | Medium | High |
| Capacity to Account for Dynamic Tidal Effects | N/A | Static ocean levels only | Dynamic Tides. |
| Parametric Uncertainty | Well understood likelihoods and methods for parameter uncertainty (refer to Book 3, Chapter 2 on FLIKE). | It is feasible to estimate the uncertainty of each parameter in a bivariate extreme value model, but this | Model-dependent. |

| Aspect \ Model | Flood Frequency Analysis | Design Variable Method | Continuous Simulation |
|---|---|---|---|
| | | is beyond the scope of this Chapter. | |
| Capacity to Account for Climate Change | Cannot account for climate change. | The method enables the distribution of both the extreme rainfall and ocean level to be modified by adjusting AEPs. The dependence between extreme rainfall and storm surge is assumed to remain constant in a future climate. | Requires the full distribution of future changes to rainfall and ocean levels to be modified, rather than just the extremes. This is likely to require some form of dynamical and/or statistical downscaling. |

## 5.4. Theory of Joint Probability

This section describes the theory of joint probability concepts in general, and also provides a more detailed overview of the design variable method. A practical description of the implementation of the design variable method is provided in Book 6, Chapter 5, Section 5, and worked examples in Book 6, Chapter 5, Section 6 are provided in.

### 5.4.1. Joint, Marginal and Conditional Distributions

Consider two random variables, $X$ and $Y$[1]. The joint probability distribution (or, equivalently, the bivariate probability distribution) of these variables describes the probability that ($X$, $Y$) equals a particular set of values ($x$, $y$) or falls in any particular range of values for that variable. This enables the relationship between two variables to be considered. The joint probability distribution can be generalised to any number of random variables, in which case it is referred to as a multivariate probability distribution. The following text presents basic statistical properties of the joint, marginal and conditional distributions, using bivariate distributions by way of illustration. For more information on the theory of joint, marginal and conditional distributions, the reader is referred to statistics references such as Ang and Tang (2006).

The joint probability density function is written as $f_{x,y}(x,y)$, and has the property:

$$\int_x \int_y f_{X,Y}(x,y)dydx = 1 \tag{6.5.1}$$

For independent variables, the joint probability distribution can be expressed as:

$$f_{X,Y}(x,y) = f_X(x)f_Y(y) \tag{6.5.2}$$

The conditional probability density function given the occurrence $X = x$ is given as:

[1]In this chapter, the variable X can be thought of as denoting daily or sub-daily rainfall, and Y denotes either storm surge or storm tide. However, the theory can be applied more generally to any pair of variables.

$$f_{Y|X}(y|X=x) = \frac{f_{X|Y}(x,y)}{f_X(x)} \tag{6.5.3}$$

A corollary of the definition of independence in Equation (6.5.2) is that substitution into Equation (6.5.3) leads to:

$$f_Y(y|X=x) = \frac{f_X(x)f_Y(y)}{f_X(x)} = f_Y(y) \tag{6.5.4}$$

In other words, the conditional distribution becomes equivalent to the marginal distribution of $Y$ when the two variables are independent.

Finally, a marginal distribution can be written as:

$$f_X(x) = \int_y f_{X,Y}(x,y)dy = \int_y f_{X|Y}(x|y)f_Y(y)dy \tag{6.5.5}$$

These concepts are illustrated in Figure 6.5.3. The main panel shows a joint Gaussian probability density function $f_{x,y}(x,y)$with simulated data that has been drawn from this distribution function given as light blue dots. The marginal distributions $f_y(y)$ and $f_x(x)$ are shown as solid lines in the left and bottom panels, respectively. A conditional distribution $f_y(y|X)=x)$ is represented as a slice through the joint density at X=2, and the conditional probability density function is shown as the dashed line in the left panel.

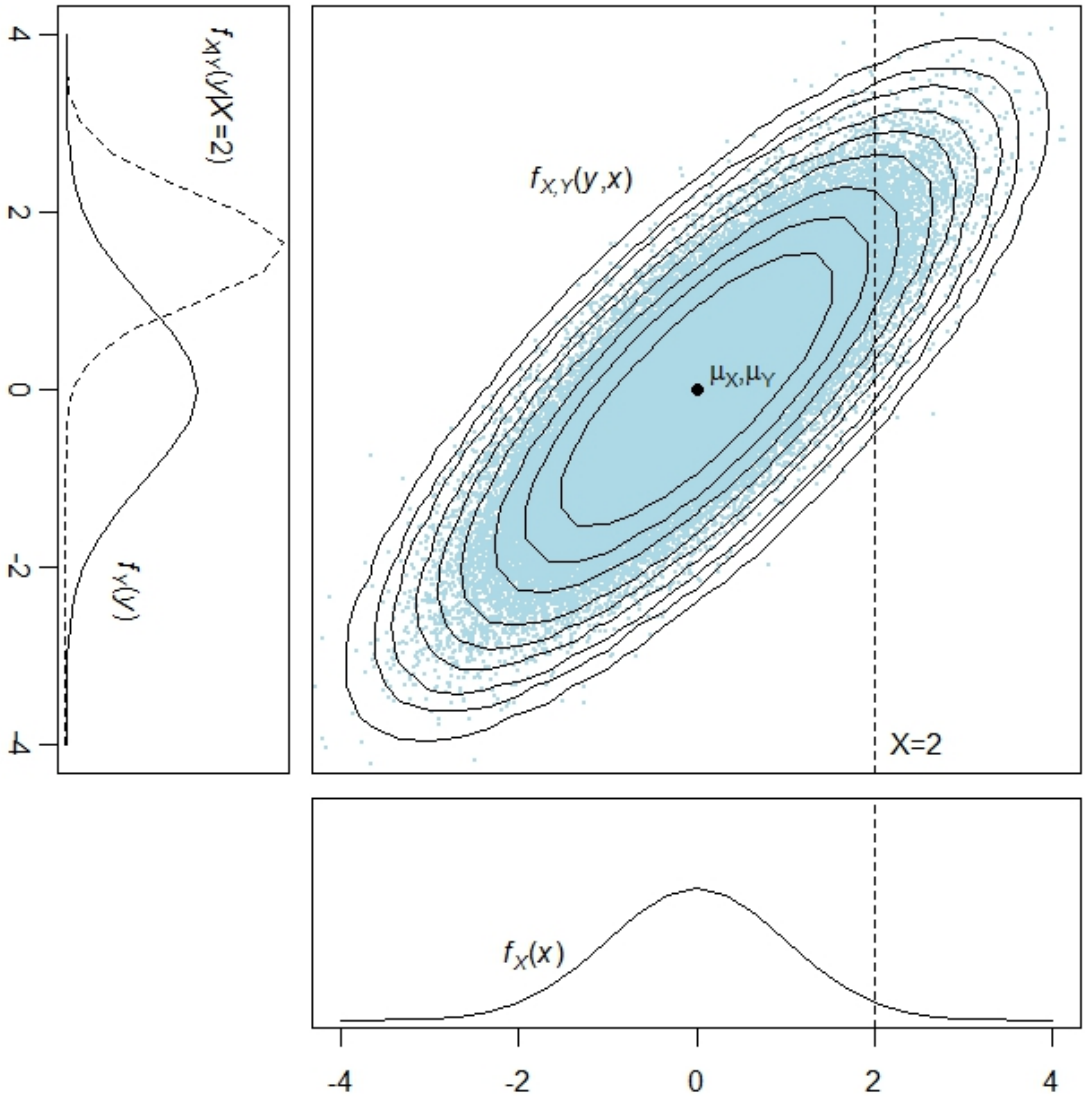


Figure 6.5.3. Joint, Marginal and Conditional Probability Density Functions

## 5.4.2. Representations of Univariate and Multivariate Extremes

Extreme value theory focuses on the statistical behaviour of the extremes of a random variable. Most of the theory is derived asymptotically as one or multiple variables become increasingly extreme, however a large body of literature now shows that the theory performs well in modelling finite extremes commonly encountered in hydrological applications (e.g. Refer to discussion in Coles (2001)).

Univariate extreme value theory is now a mature field, and the reader is referred to the text by Coles (2001) for a detailed overview of the theory and practical applications of extreme value models. Probably the most well-known representation of univariate extremes are 'block maxima', which are the maximum values of a process of independent and identically distributed random variables over a period of time such as a year. These maxima are commonly modelled using a Generalised Extreme Value (GEV) distribution, with the cumulative GEV distribution function given as:

$$F(x;\mu,\sigma,\xi) = \exp\left\{-\left[1+\xi\frac{x-\mu}{\sigma}\right]^{-1/\xi}\right\} \quad (6.5.6)$$

for $1+\xi(x-\mu)/\sigma > 0$, where $\mu \in \mathbb{R}$ is the location parameter, $\sigma > 0$ is the scale parameter, $\xi \in \mathbb{R}$ is the shape parameter, and $F_{(x)}$ is the cumulative distribution function.

An alternative representation that is widely used is the 'threshold-excess' representation, which is defined as exceedances $(x-u)$ over some suitably high threshold $u$. These maxima are commonly modelled using the Generalised Pareto distribution, with the cumulative distribution function given as:

$$F(y) = 1-\left(1+\frac{\xi y}{\sigma}\right)^{-1/\xi},\ y = x-\mu \quad (6.5.7)$$

For both univariate representations, the definition of an ‘extreme’ event is clear. In contrast, the definition of an ‘extreme’ event becomes more ambiguous in the multivariate context. Four characterisations were identified in Zheng et al. (2014b), and are summarised briefly herein (refer also to the illustration in Figure 6.5.4). For more theoretical treatment of multivariate extremes, the reader is referred to Kotz and Nadarajah (2000) and Beirlant et al. (2004).

*Component-wise block maxima* -This is a direct analogue of univariate block maxima, but has the limitation that the component-wise maxima may occur at different times in the block. As such, the joint maxima will not necessarily correspond to 'real' (ie. simultaneously occurring) events. This representation is also very wasteful of data, as only the maximum values in each block contribute to the analysis. In practice these are severe limitations, and therefore component-wise are rarely used in multivariate extreme value analyses.

*Threshold-excess extremes* - (Figure 6.5.4, left panel): A high threshold $(u_x \, and \, u_y)$ is set for both variables X and Y, and the multivariate threshold-excess model simulates the dependence between extremes that exceed both thresholds (illustrated by blue 'plus' symbols in Figure 6.5.4). Identifying appropriate thresholds $(u_x \, and \, u_y)$ represent a compromise between maximising the amount of data exceeding both thresholds, and ensuring that the asymptotic assumptions that support the Generalised Pareto distribution are approximately valid; diagnostics for threshold identification are discussed in more detail in Coles (2001). A disadvantage to this characterisation is that, by only focusing on cases where both thresholds are exceeded, situations where only one variable is extreme are not modelled.

*Point process representation* - (Figure 6.5.4, middle panel): In this representation, the data are first transformed to radial $(r = x+y)$ and angular $(w = x/(x+y))$ components, which is a transformation from Cartesian to pseudo-polar coordinates. Here, $r$ represents the distance of each data point from the origin (and therefore describes the ‘extremeness’ of the observation), and $w$ measures the angle on a [0,1] scale (and thus describes whether the variable is mostly influenced by $x, y$, or a combination of both variables) (Coles, 2001). Extreme events are those above the radial threshold $r_0$ (red 'plus' symbols in Figure 6.5.4), and the identification of an appropriately high threshold $r_0$ is based on asymptotic arguments, with diagnostic measures given in Coles (2001). As can be seen from the figure, this representation characterises the situation where both margins are extreme as well as the situation where only a single margin is extreme.

*Conditional extremes distribution* - (Figure 6.5.4, right panel): This representation is based on conditional distributions in both the X and Y dimensions, with the distribution of Y

conditioned on the threshold exceedances in X (ie. $Y|X > u_{Y|X}$) and vice versa. The threshold $u_{Y|X}$ (vertical green line in Figure 6.5.4) needs to be specified, and then all points with $X > u_{Y|X}$ (green open circles) are defined as extremes when modelling the distribution of $Y|X$. The extremes when modelling the distribution of $X|Y$ are defined analogously, with the horizontal green line representing $u_{X|Y}$ and the green 'plus' symbols representing extremes above this threshold. The extreme events in the upper right quadrants (the combination of green circles and plus symbols) are based on combining $Y|X$ and $X|Y$, with further details in Heffernan and Tawn (2004). Similar to the point process representation, this characterisation models the situation where both margins are extreme as well as the situation where only a single margin is extreme.

The decision of how to represent multivariate extremes can have important implications in the context of estimating flood exceedance probabilities in the joint probability zone, with different models potentially leading to different probability estimates. In particular, given that the dependence between extreme rainfall and storm surge is generally statistically significant but not very strong (refer to Book 6, Chapter 5, Section 5 ), it is necessary to assess the probability of floods for situations when only a single variable is extreme, as well as when both variables are extreme, suggesting that the point process and conditional representations may be most suitable for coastal flood problems.

A detailed study in Zheng et al. (2014b) compared the three methods illustrated in Figure 6.5.4, with results summarised in Table 6.5.2. Zheng et al. (2014b) generated synthetic data from a bivariate logistic model with dependence α = 0.9 and Gumbel margins, and the threshold-excess, point process, and conditional methods were used to fit an extreme value model to this simulated data. Zheng et al. (2014b) concluded that the point process representation was most suitable for estimating the exceedance probability of floods in Australia's estuarine regions, as the conditional model tended to underestimate the dependence strength, and the parameter estimates are also highly variable. It was noted, however, that the dependence parameter estimates can be biased when simulating extremes using the point process representation, and that to overcome this issue it may be appropriate to estimate the dependence parameter the threshold-excess model. This was the approach taken to develop Figure 6.5.13, and is discussed in more detail in Zheng et al. (2014a).

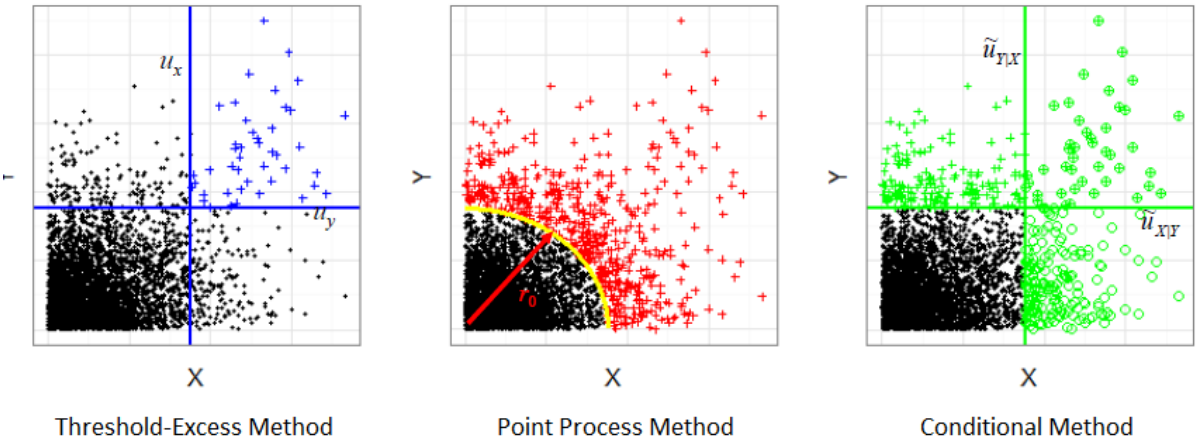


Figure 6.5.4. Three Representations of 'Extreme Values' Following Different Extreme Value Methods ( After (Zheng et al., 2014b))

Table 6.5.2. Advantages and Disadvantages of Alternative Representations of Joint Extremes(based on Zheng et al (Zheng et al., 2014b))

| Method | Advantages | Disadvantages |
|---|---|---|
| Component-wise Block Maxima | Some of the original theory on multivariate extremes has been developed using component-wise maxima, but there are few benefits of using this approach to estimate the exceedance probability of floods in estuarine regions. | Does not necessarily correspond to 'real' events, since the maxima of each variable can occur at different times of the year. |
| Threshold-excess Extremes | Corresponds to 'real' meteorological events, and enables unbiased estimates of the dependence parameter. | Does not represent the situation where only a single variable is extreme. |
| Point process | Corresponds to 'real' meteorological events, including the situation when only one variable is extreme. The models are typically parsimonious, and the variance is often low. | The dependence parameter is typically biased for weak dependence parameter values (α>0.8), and will lead to an overestimate of the dependence strength. |
| Conditional Extremes | Corresponds to 'real' meteorological events, including the situation when only one variable is extreme. | The dependence parameter is typically biased for weak dependence parameter values (α>0.8), and will lead to an underestimate of the dependence strength. The variance of the estimator is also high, and the model can be difficult to implement in practice. |

## 5.4.3. External Dependence

In addition to the large number of alternative definitions of a ‘multivariate extreme’ discussed in Book 6, Chapter 5, Section 4, there are also a range of statistical models available for simulating extremal behaviour of multivariate processes. Five alternative models were compared in Zheng et al (Zheng et al., 2014b): the logistic, negative logistic, bilogistic, negative bilogistic and dirichlet models (refer also to Kotz and Nadarajah (2000)). The conclusion was that the differences in the performance of each model were minor. The bivariate logistic model was the simplest and most widely used model, and has therefore been recommended for use in implementing the design variable method ( Book 6, Chapter 5, Section 5).

The cumulative distribution function of the bivariate logistic model is given as (Tawn, 1988):

$$F(x,y) = \exp\left\{-\left(\tilde{x}^{-1/a} + \tilde{y}^{-1/a}\right)^{a}\right\},\ \tilde{x} > 0, \tilde{y} > 0, 0 < a \leq 1 \qquad (6.5.8)$$

where $\tilde{x}$ and $\tilde{y}$ are standard Fréchet-transformed values of original observations x and y, and α represents the dependence strength with α→0 and α=1 representing complete dependence and independence, respectively.

The Fréchet transformation is given as:

$$\tilde{z} = \begin{cases} -\left(\log\left\{1-\hat{\varsigma}_{u_z}[1+\frac{\hat{\xi}(z-u_z)}{\hat{\sigma}_z}]^{-1/\hat{\xi}_z}\right\}\right)^{-1}, & z>u_z, \xi_z \neq 0 \\ -\left(\log\left\{1-\hat{\varsigma}_{u_z}\exp(-\frac{z-u_z}{\hat{\sigma}_z})\right\}^{-1/\hat{\xi}_z}\right)^{-1}, & z>u_z, \xi_z = 0 \\ -\left\{\log\hat{F}(z_i)\right\}^{-1}, & z \leq u_z \end{cases} \quad (6.5.9)$$

where z represents one of the original margins (either x or y), $\tilde{z}$ is the standard Fréchet value corresponding to the z in the original scale. $\hat{\varsigma}_{u_z} = \Pr\{Z > u_z\}$, and $u_z$ is an appropriately high threshold for the margin z, and $\hat{\sigma}_z$ and $\hat{\xi}_z$ are the maximum-likelihood estimated parameters of the Generalised Pareto distribution. Finally, $\hat{F}$ is the empirical distribution function of z, estimated by $\hat{F}(z_i) = i/(n+1)$, where i is the rank of $z_i$ and n is the total number of data points.

The application of the bivariate logistic model (Equation (6.5.8)) and the Fréchet transformation (Equation (6.5.9)) are illustrated in Figure 6.5.5 for an example dataset near Perth, Western Australia. First, a pairwise scatterplot of daily rainfall and daily maximum storm tide is presented (Figure 6.5.5a). Prior to applying the Fréchet transformation, it is necessary to identify marginal thresholds $u_x$ and $u_y$. The choice of threshold values represents a trade-off between bias and variance: if the threshold is too low, then the parameters will likely be biased as the asymptotic justification of the extreme value model may not be valid; conversely if the threshold is too high then the limited sample size will result in parameter estimates with high variance. Based on visual inspection of two diagnostic plots—the mean residual life plot and the plot of parameter estimates against threshold - at multiple rainfall-storm surge pairs across Australia, it was found that the 1% daily exceedance probability (ie. the top 1% of rainfall and storm tide days) led to reasonable model performance for most locations along the Australian coastline (Zheng et al., 2013). These thresholds are shown as grey lines in Figure 6.5.5b.

The Frechet transformation in Equation (6.5.9) is applied to each margin, and the transformed data are shown on a logarithmic scale in Figure 6.5.5c. As discussed in Book 6, Chapter 5, Section 4, the point process representation focuses only on data above a radial threshold $r_0$; values below this threshold are represented in the figure as solid blue shading. The bivariate logistic model can then be fitted to this transformed data, with dependence represented using a single dependence parameter, $\alpha$. For this case, a weak dependence parameter ($\alpha$=0.95) was used. The bivariate probability density function, $f(x,y)$, and the bivariate cumulative distribution function, $F(x,y)$, are presented as dashed blue contours and solid black contours, respectively, in Figure 6.5.5d.

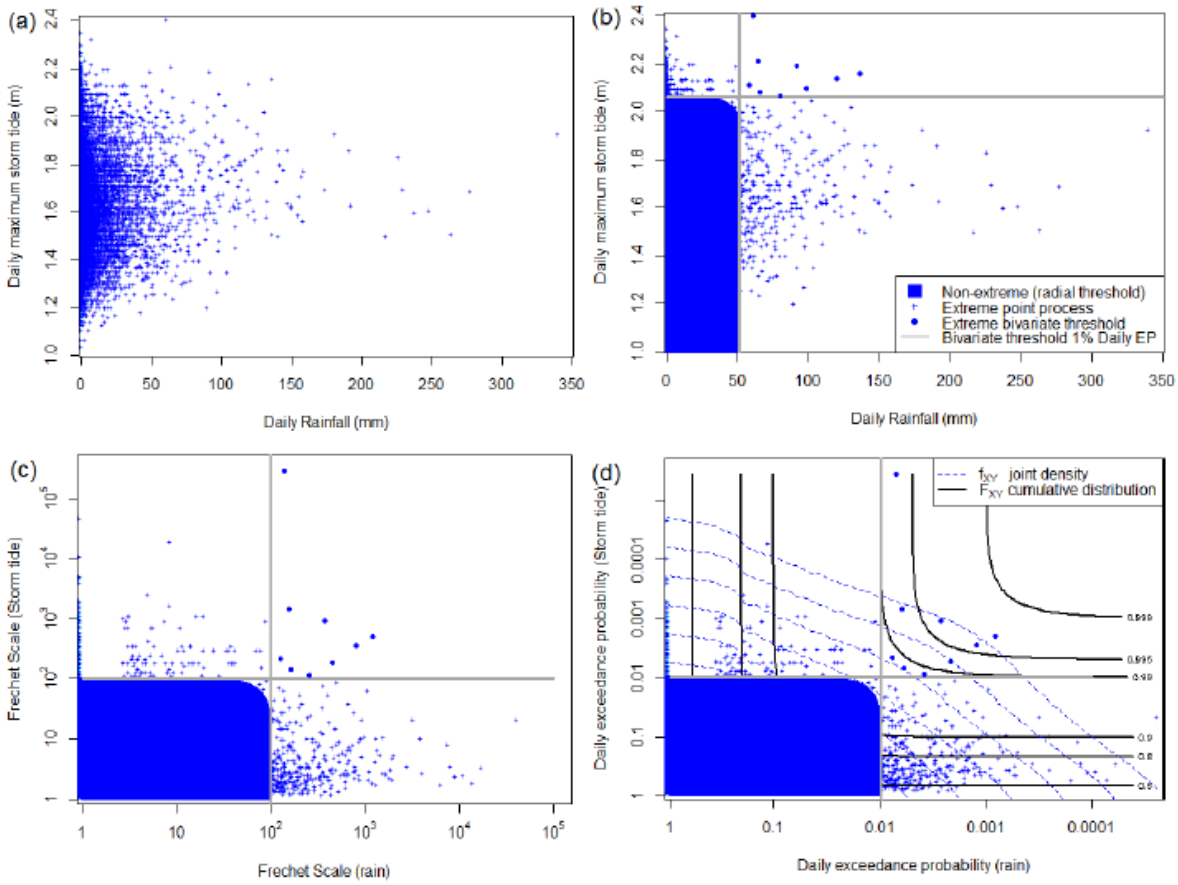


Figure 6.5.5. (a) Pairwise Plot of Daily Maximum Storm Tide and Daily Rainfall; (b) Application of Marginal Thresholds (Based on the 1% Daily Exceedance Probability for Each Margin), with Events Below the Radial Threshold $r_0$ Shaded in Blue; (c) Transformation of Events to Unit Fréchet Scale; and (d) Fitting the Joint Probability Distribution

To assist in the interpretation of the dependence parameter ($\alpha$), the relationship between $\alpha$ and the number of events that exceed a bivariate threshold are shown in Figure 6.5.6 (refer also to Zheng et al. (2013)). The analysis was based on a study of 13 414 pairs of daily rainfall and daily maximum storm surge data located throughout the Australian coastline, and a marginal threshold of the 99$^{th}$ percentile of observed rainfall or storm surge data was used, which corresponds to an average of 3.65 exceedances per year. Assuming statistical dependence, it would be expected on average that one event every 100 x 100 = 10 000 days exceeds the joint threshold by random chance. The actual number of exceedances was then plotted against the fitted dependence parameter $\hat{\alpha}$, to see the relationship between this parameter and the number of events exceeding the joint threshold.

There is a close relationship between $\hat{\alpha}$ and the number of joint exceedances of both thresholds. As will be discussed in Book 6, Chapter 5, Section 5, the value of $\hat{\alpha}$ typically varies from about 0.8 to 0.95 throughout most of the Australian coastline, therefore it is expected between eight and 27 more exceedances above the joint 99% threshold compared to what might be expected had the processes been independent. This is an order of magnitude increase in the probability of a 'joint' flood event (ie. a flood event caused by the combination of extreme rainfall and storm surge), and highlights the importance of accounting for joint probability issues in the Australian estuarine zone.

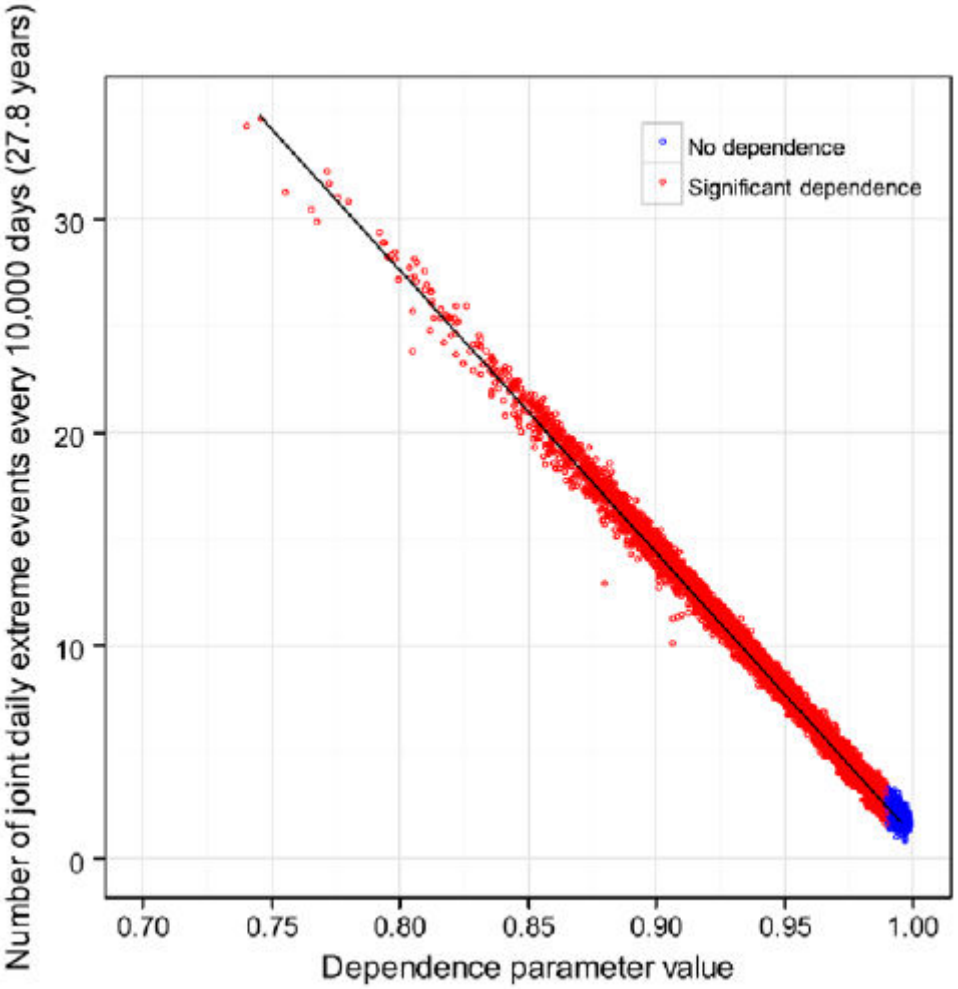


Figure 6.5.6. The Relationship Between the Dependence Parameter and the Number of Joint Extreme Events per 10 000 days

## 5.4.4. Design Variable Method

In this section, the theory is presented for translating information on extremal dependence into estimates of flood exceedance probability, commencing with a brief review of univariate flood estimation concepts. Further details on the design variable method can be found in Coles and Tawn (1994), with a more recent review by Zheng et al. (2015).

Univariate estimation methods are used for many flood estimation problems, whereby the frequency of a single forcing variable (e.g. extreme rainfall or storm tide) is assumed to be equivalent to the frequency of the corresponding flood level. The exceedance probability $\Pr(H \geq h)$ for a given flood level, *h* can be defined as:

$$\Pr(H \geq h) = \int_{x=x_0}^{\infty} f(x)dx, \quad h = B(x_0) \tag{6.5.10}$$

where $B(x)$ is a function relating the flood level to a single forcing variable $X$ (e.g. rainfall or storm tide); $x_0$ is the value of the forcing variable that causes the flood level $h$, and $f(x)$ is a density function of X at extreme levels. To obtain $\Pr(H \geq h)$, one needs to first estimate the corresponding $x_0$ that causes the flood level $h$, then estimate the exceedance probability that

a value of the forcing variable will be greater than $x_0$, and assign this to $\Pr(H \geq h)$, ie. $\Pr(H \geq h) = \Pr(X \geq x_0)$. Typically, an annual maximum, $r$-largest or a peak-over-threshold method is used to obtain the tail distribution of X (Coles, 2001).

The estimation procedure becomes complicated in a multivariate setting since the exceedance probability of any given forcing process is no longer equivalent to the exceedance probability of the flood level, ie. $\Pr(X \geq x_0) \neq \Pr(H \geq h)$. Considering the design variable $H$ forced by two variables $X$ and $Y$, Coles and Tawn (1994) defined a 'failure region' $A_h$ as:

$$A_h = \left\{(x, y) \in \mathbb{R}^2 : B(x, y) > h\right\} \tag{6.5.11}$$

where $B(\mathrm{x,y})$ is a 'boundary function' that maps the two dimensional space of the forcing variables to the one dimensional response variable. In flood estimation, a combination of hydrologic and hydraulic models are typically used to obtain a flood level $h = B(x, y)$ as a function of boundary conditions such as rainfall and storm tide (x, y). The failure region $A_h$ can be interpreted as the set of values of the constituent processes (x, y) that cause flood levels greater than a specified design flood level $h$. The corresponding exceedance probability $\Pr(H \geq h)$ is given as:

$$\Pr(H \geq h) = \int\int_{A_h} f(x, y) \tag{6.5.12}$$

where $f(x, y) = \partial F(x, y) / \partial x \partial y$ is the joint density function of the two variables X and Y at extreme levels, and $F(x, y)$ is their corresponding joint cumulative distribution function.

Figure 6.5.7 illustrates the difference between the univariate method (top panel) and the design variable method as an example of a joint probability method (bottom panel) for a hypothetical scenario in which floods are caused by two forcing variables $X$ and $Y$. In the top panel, the grey shaded region represents the exceedance probability $\Pr(H \geq h)$, where $h$ (the red dashed line) is determined by a single forcing variable (e.g. rainfall or storm tides). The grey shaded region in the bottom panel illustrates the exceedance probability for the region $A_h$ where $h$ (the solid red line) depends on both forcing variables. In the bivariate case, the probability $\Pr(H \geq h)$ can then be evaluated as the integral of the joint density $f(x, y)$ (thin blue contours) across the whole failure region $A_h$ (Equation (6.5.12)).

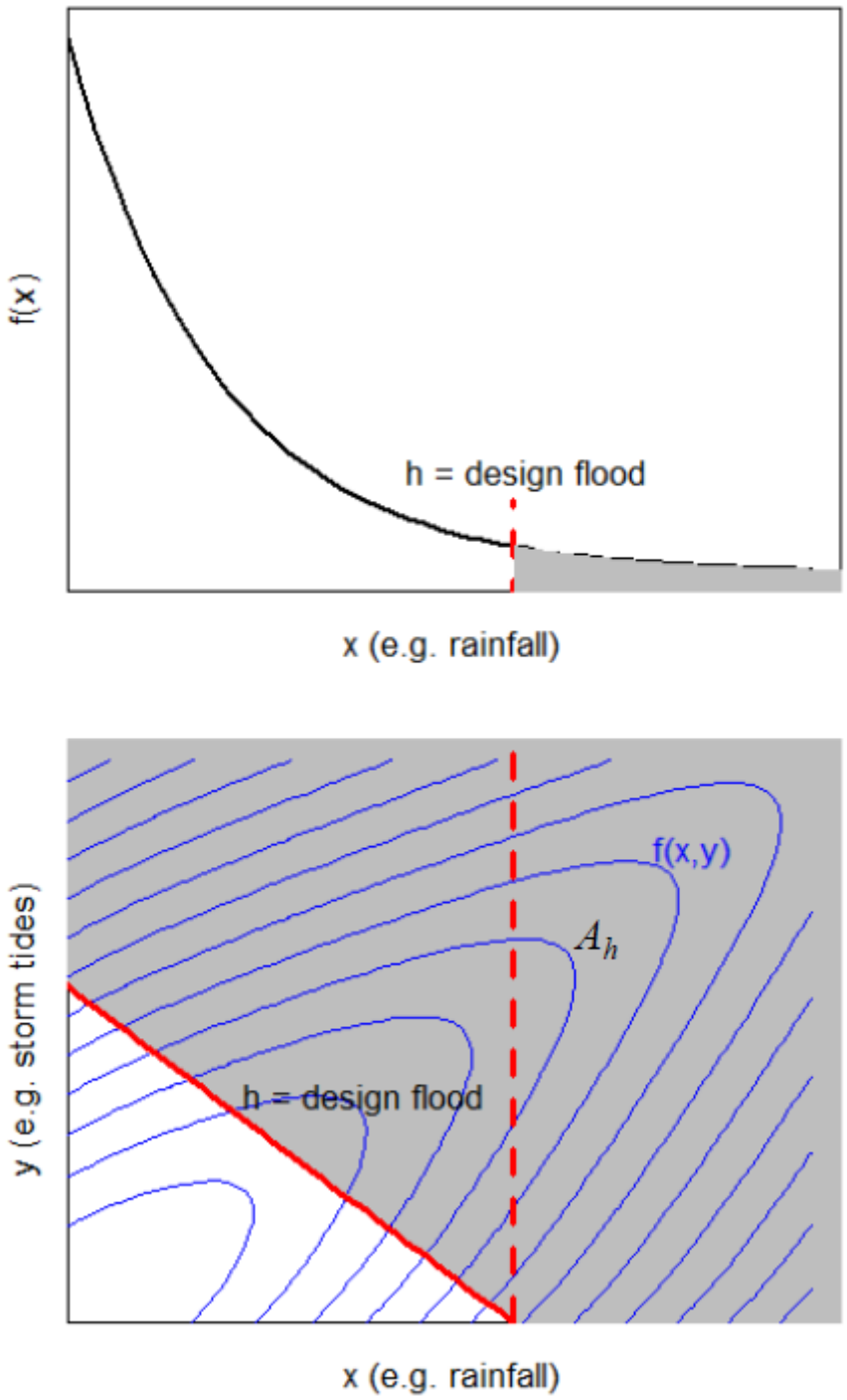


Figure 6.5.7. Exceedance Probabilities Obtained from a Univariate Analysis (top panel) and a Bivariate Analysis (bottom panel)

It is possible to compute the integral in Equation (6.5.12) using two dimensional numerical integration or Monte Carlo techniques, but these approaches can be slow for the required levels of precision. It is more computationally efficient to exploit the properties of the joint cumulative distribution function $F(\mathrm{x},\mathrm{y})$ to reduce the bivariate integral to a univariate line-integral along the boundary function $B(\mathrm{x},\mathrm{y}) = h$. This is implemented numerically as:

$$\Pr(H \geq h) = 1 - \Pr(H < h) = 1 - \sum_{j=1}^{m-1} \left[ F\left(x_j, y_j\right) - F\left(x_j, y_{j+1}\right) \right] \quad (6.5.13)$$

defined as $(x_j, y_j) : B(x_j, y_j) = h, y_{j+1} - \Delta y$ , where $m$ is the number of points $(x_j, y_j)$ that are used to discretise the boundary line $h$ (the red solid line in Figure 6.5.7) and $\Delta y \geq 0$. By taking the finite difference of $F(\mathrm{x,y})$ in only one dimension, the probability of being less than $x_j$ is obtained for an increment of width $\Delta y$. Moving along the boundary function line, the probability increments are obtained for all corresponding pairs $(x_j, y_j)$, and the non-exceedance probability $\Pr(H \geq h)$ is the sum over all increments.

Finally, the exceedance probability of flood event from the univariate method (the grey shaded region in the top panel) is also illustrated on the bivariate plot (the grey shaded region to the right of the red dashed line in the bottom panel). The univariate failure region is smaller than the $A_h$ that would be obtained by the joint probability method, demonstrating that the univariate method will underestimate the exceedance probability of the flood in this case.

**Asymptotic Dependence or Independence?**

Flood estimation is often concerned with understanding the behaviour of the upper tail of a probability distribution. In the context of multivariate extremes, this requires assumptions about how the dependence between variables changes as the variables become increasingly extreme.

Multivariate probability distributions can be classified based on how they behave in the limit as each variable becomes increasingly extreme (refer to Coles (2001) for additional coverage of the theory of asymptotic dependence). Examples of an asymptotically independent and an asymptotically dependent distribution are given the Figure 6.5.8: the dependence between variables for the Gaussian distribution decreases with extremity of $X$ or $Y$ (evidenced by the increased scatter of points away from the leading diagonal), where dependence remains high for the asymptotically dependent bivariate logistic distribution.

A detailed study along the Australian coastline ((Zheng et al., 2013)) found that at most locations, the bivariate distribution between extreme rainfall and storm surge was asymptotically dependent, meaning that rarer events are more likely to occur jointly compared to more frequent events. This is the basis for the recommendation to use a bivariate logistic distribution for dependence analysis, and provides a cautionary note for using correlation-based measures (which assume Gaussianity) for representing joint dependence.

## 5.4.5. Illustration of Joint Probability Concepts

Several of the theoretical concepts of joint probability described above are now illustrated through a set of joint probability problems. The solution to each problem has been derived based on the simplifying assumptions of statistical independence or complete dependence, which means that the solutions in the tables below can be easily verified using hand calculations. For situations with intermediate levels of dependence, it is necessary to apply the full design variable method to calculate flood exceedance probabilities.

Results are presented both in terms of Annual Exceedance Probabilities (AEPs) and Average Recurrence Intervals (ARIs), using the conversion $AEP = 1 - e^{\frac{-1}{ARI}}$

The probability of two independent events Z = X>x or Y>y: Consider two independent random variables, X and Y. What is the probability of a 'failure event' Z = X > x or Y > y? This type of question might arise when (i) a system is considered to 'fail' when any component of the system fails, and (ii) the failure of any component of the system is independent of the failure of any other component. For example, a road might 'fail' when either of two bridges are overtopped, and the bridges are sufficiently far from each other so that it is possible to assume the flood producing mechanisms are approximately independent[2].

The set of events X>x is shown by the vertical blue lines in Figure 6.5.8, and the set of events Y>y is shown by the horizontal blue lines in Figure 6.5.8. Start by considering only the probability of two variables exceeding their respective thresholds in a given year (but potentially on different days). The question of calculating the probability of the two events coinciding (ie. occurring at the same time) is considered in a later example.

The exceedance probabilities corresponding to those thresholds is $AEP_x$ = Pr{X>x} and $AEP_y$ = Pr{Y>y}. The Annual Exceedance Probability of the failure event, Z, is then given as $AEP_z$ = Pr{X>x or Y>y}. With reference to the illustration in Figure 6.5.8, it is straightforward to see that $AEP_z = AEP_x + AEP_y - (AEP_x * AEP_y)$; the reason for the subtraction term is because the cross-hatched region in Figure 6.5.8 would otherwise have been counted twice. Example calculations of $AEP_z$ assuming a number of different combinations of $X$ and $Y$ are presented in Table 6.5.3.

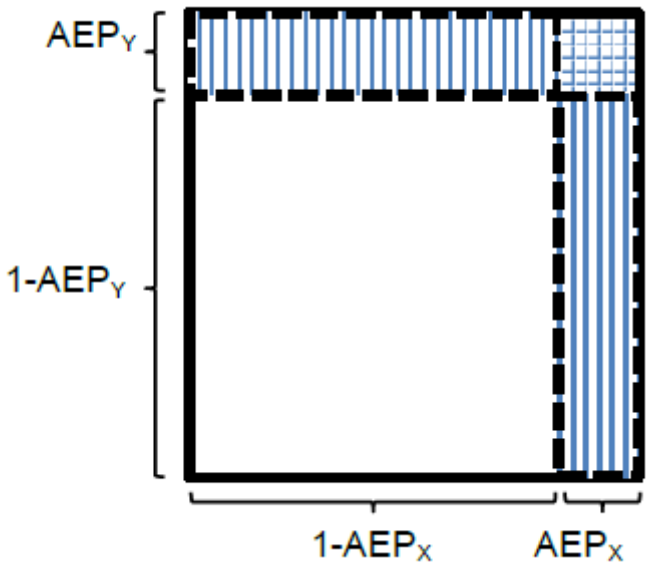


Figure 6.5.8. Illustrating the Probability of Two Independent Events Z = X>x or Y>y

Table 6.5.3. Worked Examples of the Probability of Two Independent Events Z = X>x or Y>y

| $AEP_X$ | $AEP_Y$ | $AEP_X$(years) | $AEP_Y$(years) | $AEP_Z$ | $ARI_Z$ (years) |
|---|---|---|---|---|---|
| 1.00% | 65.0% | 99.5 | 1.0 | 65.4% | 0.94 |
| 2.00% | 40.0% | 49.5 | 2.0 | 41.2% | 1.88 |
| 5.00% | 20.0% | 19.5 | 4.5 | 24.0% | 3.64 |

[2]Given that rainfall is a spatial process, the assumption that extreme rainfall at two nearby locations is statistically independent is unlikely to be valid; it is made here for illustration purposes only.

| | | | | | |
|---|---|---|---|---|---|
| 10.00% | 10.0% | 9.5 | 9.5 | 19.0% | 5.75 |

**The probability of Two Independent Events Z = X>x and Y>y:** An alternative question concerns the probability of *both* X and Y exceeding their specified thresholds.

This situation is illustrated as the hatched region in Figure 6.5.9. Defining $AEP_z$ as Pr{X>x and Y>y}, $AEP_z$ = $AEP_x$ * $AEP_x$ can be estimated, with a number of specific examples shown in Table 6.5.4.

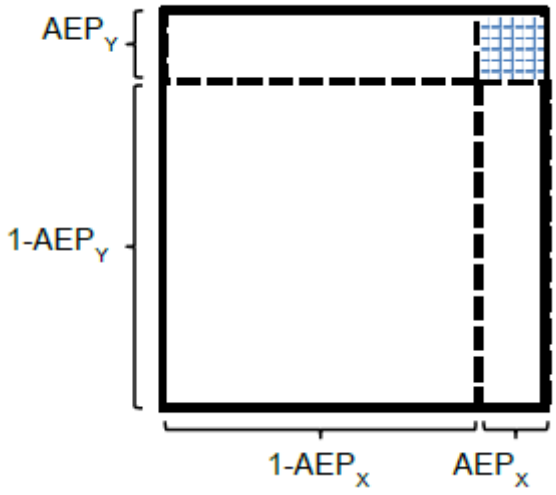


Figure 6.5.9. Illustrating the Probability of Two Independent Events Z = X>x and Y>y

Table 6.5.4. Worked Examples of the Probability of Two Independent Events Z = X>x and Y>y

| **$AEP_X$** | **$AEP_Y$** | **$AEP_X$(years)** | **$AEP_Y$(years)** | **$AEP_Z$** | **ARI $_Z$(years)** |
|---|---|---|---|---|---|
| 1.00% | 65.0% | 99.5 | 1.0 | 0.65% | 153.3 |
| 2.00% | 40.0% | 49.5 | 2.0 | 0.80% | 124.5 |
| 5.00% | 20.0% | 19.5 | 4.5 | 1.00% | 99.5 |
| 10.00% | 10.0% | 9.5 | 9.5 | 1.00% | 99.5 |

**The Probability of Two Completely Dependent Events Z = $X$>$x$ and $Y$>$y$:** In situations of perfect dependence between $X$ and $Y$, the probability of $X$>$x$ would be equal to the probability of Y>y for all x and y. Because of this, Pr{$X$>$x$} = Pr{$Y$>$y$} = Pr{$X$>$x$ and $Y$>$y$}. For example, if $AEP_x$ and $AEP_y$ are both 10%, then $AEP_z$ = 10%.

**The probability that Two Events X>x and X>y with Specified Annual Exceedance Probabilities Pr{$X$>$x$} and Pr{$Y$>$y$} Occur on the Same Day:** In the previous examples, the interest was in the probabilities that two random variables $X$ and $Y$ exceeded thresholds $x$ and $y$ in a given year. However, when estimating the exceedance probability of floods, our interest is in the probability of these two variables coinciding. Therefore, one must consider the probability that both variables reach their maxima at the same time within a given year.

This issue can be illustrated by considering the case where the daily maximum storm tide is assumed to coincide with the daily maximum rainfall. This is still a conservative assumption (since the peak of the hydrograph will not always occur at exactly the same time as the peak

of the storm surge within a given day), but less conservative than the assumption that the annual maximum of variable $X$ will always occur at the same time as the annual maximum of variable $Y$.

The conversion between an AEP and a Daily Exceedance Probability (DEP) is DEP=AEP/365. For the example of 1 year ARI event, there is a 63% chance that any given year will exceed that level (AEP), and a corresponding 0.17% chance that any given day will exceed that same level (DEP).

The earlier example is now revisited (the probability of two independent events Z = $X>x$ and $X>y$), but now first converting to daily values. Table 6.5.5 shows the results using the example of two coinciding 10% AEP events. It is clear from this example that the joint exceedance probability is much lower than the results presented in Table 6.5.4 (since, in the absence of dependence, the most likely case is that the two extreme events would occur on different days). In contrast, had complete dependence been assumed, then $AEP_z$ would remain at 10%, as by the definition of complete dependence, high values of $X$ and $Y$ will always occur at the same time.

Table 6.5.5. Calculating the Probability of Two Independent Events Z = X>x and Y>y, When Adding the Constraint that Both Events Must Occur on the Same Day

| $AEP_X$ | $AEP_Y$ | $DEP_X$ | $DEP_Y$ | $ARI_X$(years) | $ARI_Y$(years) | $DEP_Z$ | $AEP_Z$ | $ARI_Z$ (years) |
|---|---|---|---|---|---|---|---|---|
| 10.0% | 10.0% | 0.027% | 0.027% | 9.5 | 9.5 | (7.51E-06)% | 0.00274 % | 36500 |

**Why the Probability That $X>x$ or $Y>y$ is Non-commensurate with the Probability that $H>h$ Where $h = B(x,y)$, Even When Random Variables $X$ and $Y$ are Independent:** This illustrates a basic problem in joint probability analysis of floods in the coastal zone, where interest is in a quantity such as a flood level (*h*) that is some complex function of forcing variables such as rainfall ($X$) and storm tide ($Y$). A 'boundary function' $B()$ is used to represent the complex mapping from rainfall/storm tide to the flood level. In most practical applications this mapping would be achieved using hydrologic and hydraulic models that take rainfall and storm tide as their boundary conditions, and produce flood level as their output.

Consider the situation concerning the exceedance probability of a flood of height $H>h$, and after a hydrological/hydraulic analysis concluded that this height can be caused by a rainfall event with $AEP_x$= 5% but with no significant storm tide, or a storm tide event with $AEP_y$= 20% but with no significant rainfall. Furthermore, assume that the processes *X* and *Y* are independent. In this case, it is tempting to refer to Table 6.5.3 and suggest that the AEP of the flood becomes 24.0%.

A problem with this calculation is that it neglects floods that can occur through a combination of smaller values of rainfall and storm tide. This is illustrated by the red hatched region in Figure 6.5.10. Therefore, even if it is assumed that extreme rainfall and storm tide are statistically independent, it will still be necessary to apply the design variable method to compute flood exceedance probabilities.

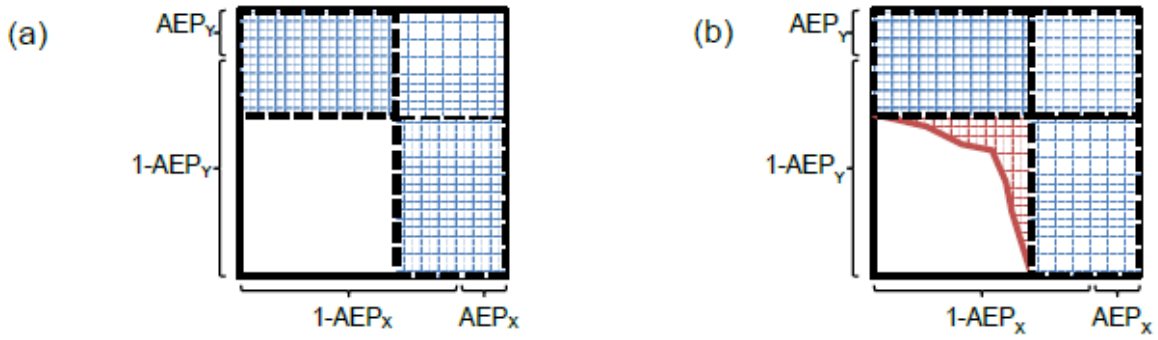


Figure 6.5.10. Conceptual Diagram (a) Probability of Floods Caused by Either a Significant Rainfall Event or a Significant Storm Tide Event, and (b) Additional Probability of Floods Produced by Combinations of Smaller Rainfall and Storm Tide Events

**Accounting for Intermediate Levels of Dependence Between $X$ and $Y$:** The previous examples illustrated the extreme situations whereby the processes $X$ and $Y$ were either completely independent, or perfectly dependent. The design variable method has been designed to cater for cases with intermediate levels of dependence. The method superimposes the joint probability distribution of the forcing variables $X$ and $Y$ onto the boundary function $B()$ describing the relationship between forcing variables and flood level. The practical implementation of this method is discussed in Book 6, Chapter 5, Section 5.

## 5.5. The Design Variable Method

This section describes a practical approach to implement the design variable method, which comprises four distinct steps (Book 6, Chapter 5, Section 5). Further detail on each step is given below.

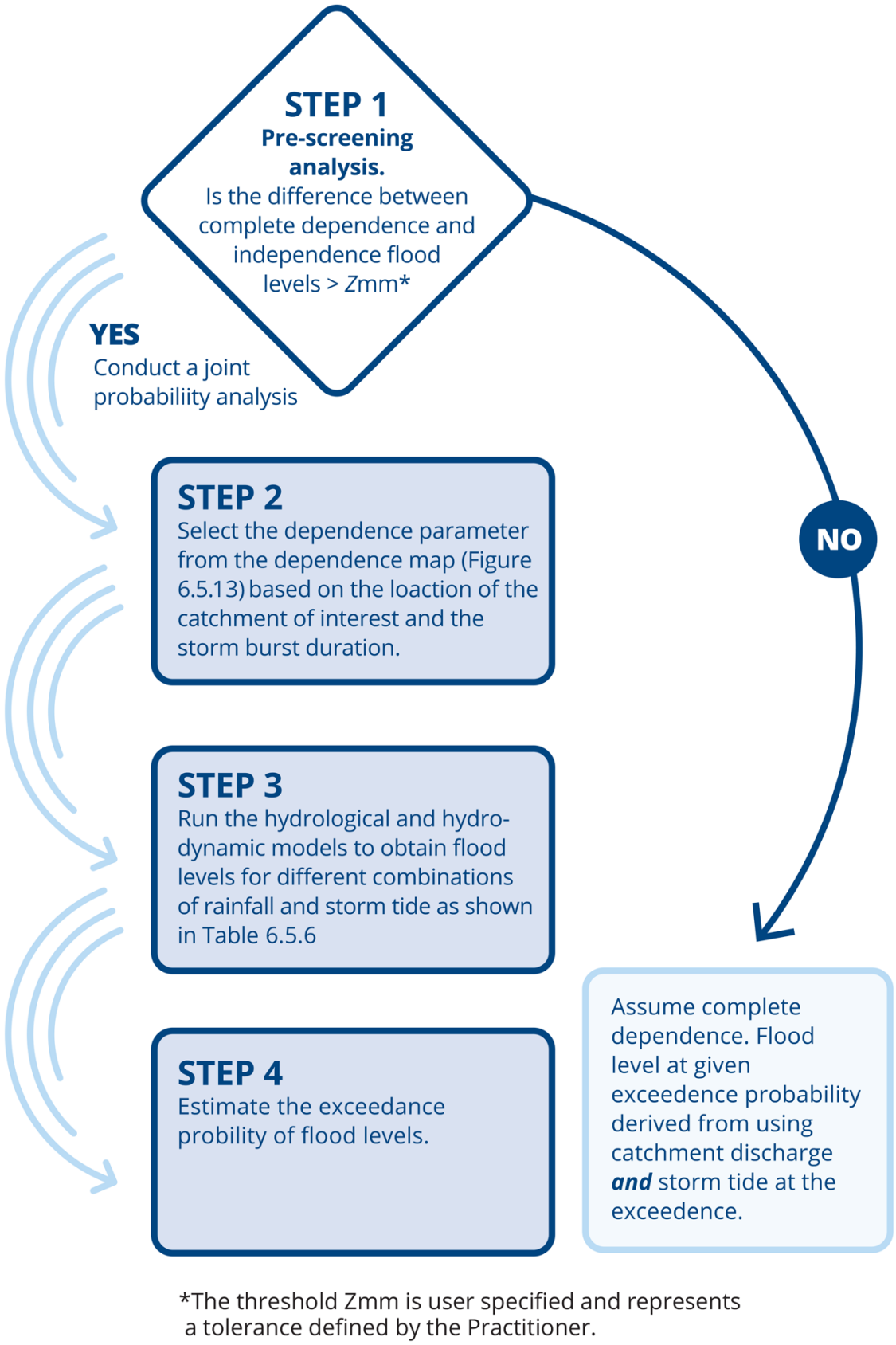


Figure 6.5.11. The Design Variable Method

**Step 1: Pre-Screening Analysis**

Accounting for dependence between extreme rainfall and storm surge as part of estuarine flood assessments represents significant additional computational effort when compared to traditional univariate methods. Therefore, a pre-screening analysis is recommended to determine whether the additional complexity of a joint probability analysis is warranted.

The aim of this step is to calculate the outer envelope of flood estimates obtained from the joint probability method. This involves calculating a minimum number of cases to determine the magnitude of flood differences between independence and full dependence:

1. the independence case where a fluvial flood occurs in the absence of an ocean event; (2) the independence case where a coastal flood occurs in the absence of a rainfall event; and

2. the full dependence case where both a fluvial flood and a coastal flood occur simultaneously.

The specific number of runs required in the pre-screening analysis will depend on the number of AEPs that need to be evaluated. Table 6.5.6 presents the pre-screening analysis for three AEPs, which requires nine instances ('runs') of a hydrological and hydrodynamic model. The boundary conditions are specified in terms of their AEP rather than in their corresponding dimensional value (e.g. $m^3/s$, m, etc), so that it will be necessary to consider the probability distribution of the extremes of each boundary to enable translation between an AEP and the dimensional value.

Table 6.5.6. Flood Levels of Different Combinations of Rainfall and Storm Tide in Terms of Annual Exceedance Probability, for a Particular Storm Burst Duration. Only the highlighted cells need to be evaluated.

| **Rainfall Events in AEPs** | **Storm Tide Events in AEPs** | | | |
|---|---|---|---|---|
| | Lower Bound | 20% | 2% | 1% |
| No Rainfall | | blue | blue | blue |
| 20% | green | red | | |
| 2% | green | | red | |
| 1% | green | | | red |

The pre-screening analysis should be undertaken at each cross-section or grid cell in the floodplain where information is required, with a longitudinal profile of the independence and complete dependence cases illustrated for a single exceedance probability in Figure 6.5.12. The pre-screening analysis involves classifying each cross-section and AEP into one of the following cases.

*Case 1* - If the flood levels in the green cells are similar to those in the red cells for each rainfall AEP (ie. the difference is less than some tolerance threshold value of $Z$ mm), the flood levels for the catchment of interest are completely dominated by the rainfall (the 'fluvial zone' in Figure 6.5.12). Normally such catchments are in upstream reaches of the river. For this case, complete dependence should be assumed; the AEP of a flood level is obtained when the same AEP of the rain and storm surge are assumed to coincide (red cells). While this is a conservative assumption, it eliminates the need for modelling a much larger number of combinations.

*Case 2* - If the flood levels in the blue cells are very close to those in the red cells for each storm tide AEP (ie. the difference is less than the tolerance threshold of $Z$ mm), the flood levels are completely dominated by the storm tide (the 'coastal zone' in Figure 6.5.12). Normally this location is in lower reaches of the river. As with Case 1, complete dependence should be assumed, and the flood level should be obtained based on the combinations in the red cells.

*Case 3* - If the flood levels in the red cells are significantly higher than those in the green and blue cells (ie. the difference is greater than the tolerance threshold of $Z$ mm) with the same rainfall and storm tide AEPs, this indicates that the joint dependence has a significant influence on the flood level (the 'joint probability zone' in Figure 6.5.12). It will be necessary to continue to Step 2 and conduct a full joint probability analysis.

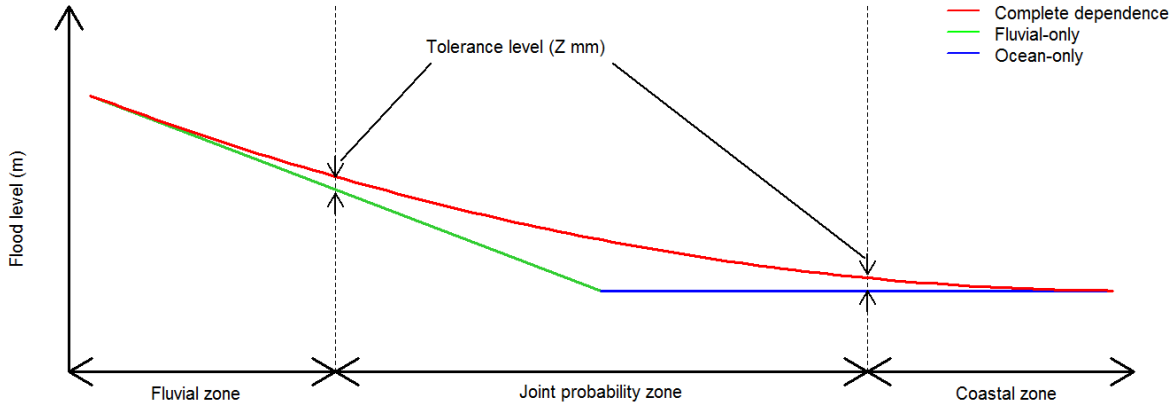


Figure 6.5.12. Pre-Screening Step, which Involves Calculating the Outer Envelope of the Possible Flood Levels.

The threshold value of $Z$ represents a tolerance defined by the practitioner. This tolerance is a trade-off between the benefit of a more accurate assessment of flood exceedance probabilities (obtained through the joint probability calculation) and the additional effort required to implement a joint probability analysis. A joint probability analysis has additional computational cost and this cost should be proportional to the benefit of the additional precision. This trade-off will vary according to different locations and design problems. As illustrated in Figure 6.5.12, the tolerance is also used to formally define the 'joint probability zone' that was first introduced in Figure 6.5.1.

It should be noted that if one is only interested in a single AEP (rather than a range of AEPs) then only three runs are required instead of the nine runs in Table 6.5.11. For example, if only the 1% AEP is of interest, then the three model runs are: (i) an event with 1% AEP rainfall combined with the lower bound of the storm tide; (ii) an event with 1% AEP storm tide combined with no rainfall; and (iii) an event with the 1% AEP rainfall combined with the 1% AEP storm tide.

If a joint probability analysis is required then proceed to Step 2.

**Step 2: Dependence Parameter Selection**

A map of dependence parameters from the bivariate logistic extreme value model has been created for the Australian coastline (Figure 6.5.13). The map was derived based on an analysis of the joint dependence using data from 64 tide gauges, 7684 daily rainfall gauges and 70 sub-daily rainfall gauges, and is described in more detail in Zheng et al (Zheng et al.,

2014a). The dependence parameters are available for storm burst durations shorter than 12 hours, between 12 and 48 hours, and between 48 and 168 hours. Note that values closer to one represent weaker dependence, and values closer to zero represent stronger dependence.

This step involves selecting the dependence parameter from the map (Figure 6.5.13). The duration should be estimated with reference to the catchment time of concentration. Values closer to 1 represent weaker dependence, and values closer to 0 represent stronger dependence.

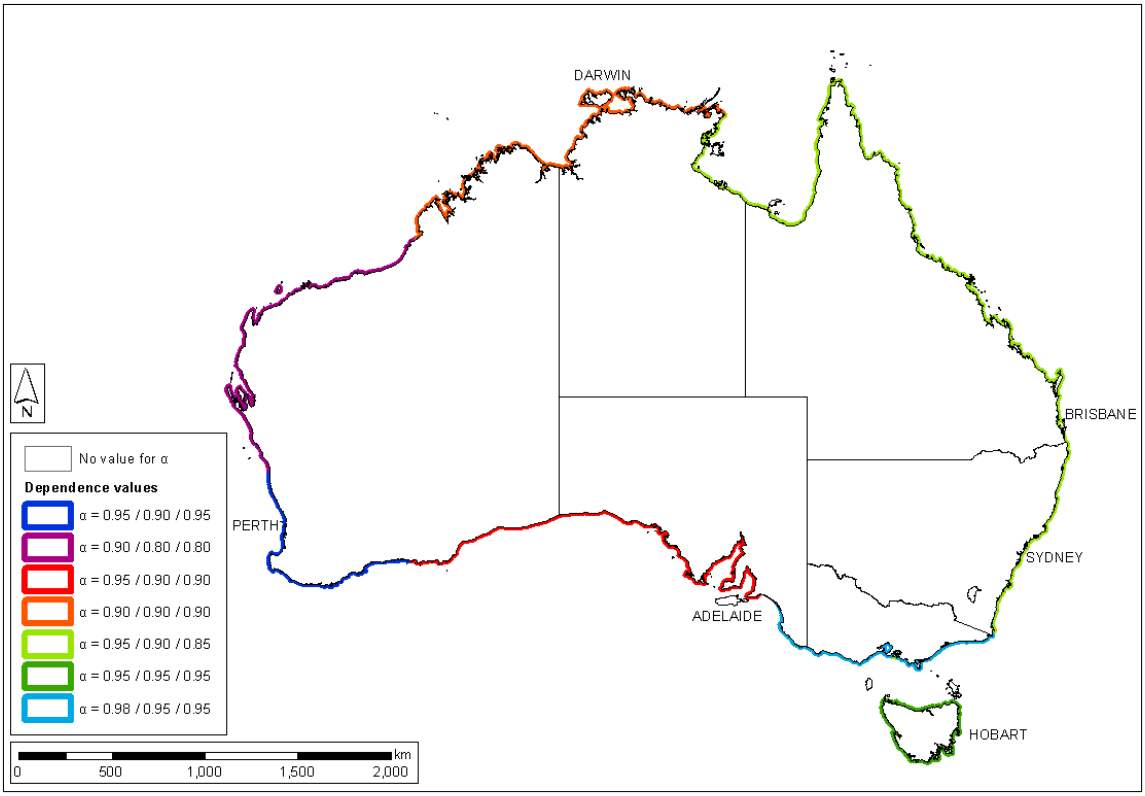


Figure 6.5.13. Dependence Parameter (α) Map for the Basins of the Australian Coastline - shorter than 12 hours, 12 to 48 hours, and 48 to 168 hours

**Step 3: Flood Level Modelling**

In this step, the flood level corresponding to a number of scenarios of rainfall and storm tide needs to be evaluated to accurately estimate flood levels incorporating dependence. The scenarios should include no rainfall and the lower bound of the storm tide cases to represent the lowest possible value of each variable. The scenarios should also consider cases with exceedance probabilities lower than the smallest AEP (ie. largest flood level) of interest. Up to the 1% AEP, a typical example is given in Table 6.5.7 which has seven cases for each variable leading to 49 runs of a hydrologic and hydrodynamic models.

Table 6.5.7. Flood Levels of Different Combinations of Rainfall and Storm Tide in Terms of Annual Exceedance Probability with a Particular Storm Burst Duration

| | **Storm Tide Events (AEP)** |
|---|---|

| | | Lower Bound | 50% | 20% | 10% | 2% | 1% | 0.2% | 0.05% |
|---|---|---|---|---|---|---|---|---|---|
| **Rainfall Events (AEP)** | **No Rain** | | | | | | | | |
| | **50%** | | | | | | | | |
| | **20%** | | | | | | | | |
| | **10%** | | | | | | | | |
| | **2%** | | | | | | | | |
| | **1%** | | | | | | | | |
| | **0.2%** | | | | | | | | |
| | **0.05%** | | | | | | | | |

**Step 4: Estimate the Exceedance Probability of Flood Levels**

The final step of the analysis involves superimposing the flood level table (Table 6.5.7) onto the joint probability density function of the bivariate logistic extreme value distribution, and in the context of estimating the probability of a specific design flood level, *h* will involve the following steps:

1. Using the bivariate logistic extreme value model of Equation (6.5.8) with the dependence parameter estimated in Step 2, estimate the bivariate probability distribution function corresponding to the extreme rainfall and storm tide. This is represented as the blue contours the hypothetical example that was presented in Figure 6.5.7.

2. Using the data obtained in Step 3 (Table 6.5.7), estimate the set of all possible combinations of extreme rainfall and storm tide that would produce flood level h. This involves interpolating over the values in Table 6.5.7. The contour of fixed, *h*, was illustrated as a solid red line in the hypothetical example presented in Figure 6.5.7.

3. Integrate the bivariate probability distribution function to the right of (ie. above) the design flood level to obtain the exceedance probability of that flood event. This is represented in Figure 6.5.7 as the integration of the blue contours over the grey shaded region.

If the objective of the analysis is to find the design flood level corresponding to a specific AEP, then the above steps need to be repeated for a number of flood levels until the flood level corresponding to the desired AEP is identified.

A software tool[3] has been developed to perform these calculations. This tool requires as inputs the dependence parameter and the flood level table, and will produce a plot of water levels against AEPs. Implementation of the software is illustrated using worked examples in Book 6, Chapter 5, Section 7. At present the software implementation of the method has been tested for flood levels for the 50% to 1% AEP. The software tool is needed primarily for Step 4.2 and 4.3. To determine contour lines in Step 4.2 there are a number of standard libraries, but to determine the integral in Step 4.3 a customised routine is required for implementing Equation (6.5.13).

Finally, a note of caution is required regarding the identification of the storm burst duration in Step 2. In that step, it was recommended that the storm burst duration was selected based on the time of concentration of the catchment, with the reasoning that this would lead to the

[3] http://p18.arr-software.org/

maximum flow rate. Assuming static tailwater levels (which is a fundamental assumption of the design variable method; see Book 6, Chapter 5, Section 3) and a constant dependence parameter, this would be equivalent to the duration that would lead to the largest flood event. However, because the dependence parameter depends on duration, it is possible that some storm burst duration could result in a lower peak flow rate but nonetheless lead to a higher flood level because the peak flow is more likely to coincide with the peak ocean level. Therefore, if the identified storm burst duration identified in Step 2 is close to a threshold between dependence parameters, it may be necessary to test the implications of an adjacent duration with a lower dependence parameter (ie. stronger dependence).

**Accounting for Climate Change**

Anthropogenic climate change is likely to increase the exceedance probabilities of flooding in estuarine regions, owing to a combination of elevated ocean levels arising from increases in both mean sea level and possible changes in storm surges, as well as increases in extreme rainfall. Furthermore, climate change may result in changes to the frequency and magnitude of different types of extreme weather events, which may affect the magnitude of dependence between extreme rainfall and storm surge/tide.

Information on how the dependence between extreme rainfall and storm surge/tide may change in a future climate is currently unavailable, and therefore guidance on possible changes to the dependence parameters in Figure 6.5.13 cannot be provided at this stage. Guidance is available, however, on possible changes to both extreme rainfall and mean sea level (Book 1, Chapter 6). As an interim measure, it is recommended that estimates of the impact of climate change on flooding in the joint probability zone be accounted for as follows[4]:

- Changes to extreme rainfall and ocean level should be estimated using the approach described in Book 1, Chapter 6); and
- The dependence parameters described in Figure 6.5.13 that correspond to the historical climate situation should be used unless more precise estimates of future dependence parameters are available.

The implication of changing both the extreme rainfall intensity and the ocean levels is illustrated in Figure 6.5.14. Using the adjusted rainfall and ocean levels, the four step methodology described earlier in this section then can be applied. It is noted that a possible effect of climate change is that the tidally affected part of a river is likely to change (for example, it may reach further upstream due to the effects of sea level rise), and this will influence the area classified requiring a full joint probability analysis. Therefore the pre-screening analysis in Step 1 will also need to be repeated when considering climate change.

[4] This section was written before the latest climate change guidance in Book 1, Chapter 6 (2024). A minor change to the text has been made to reflect the change in guidance.

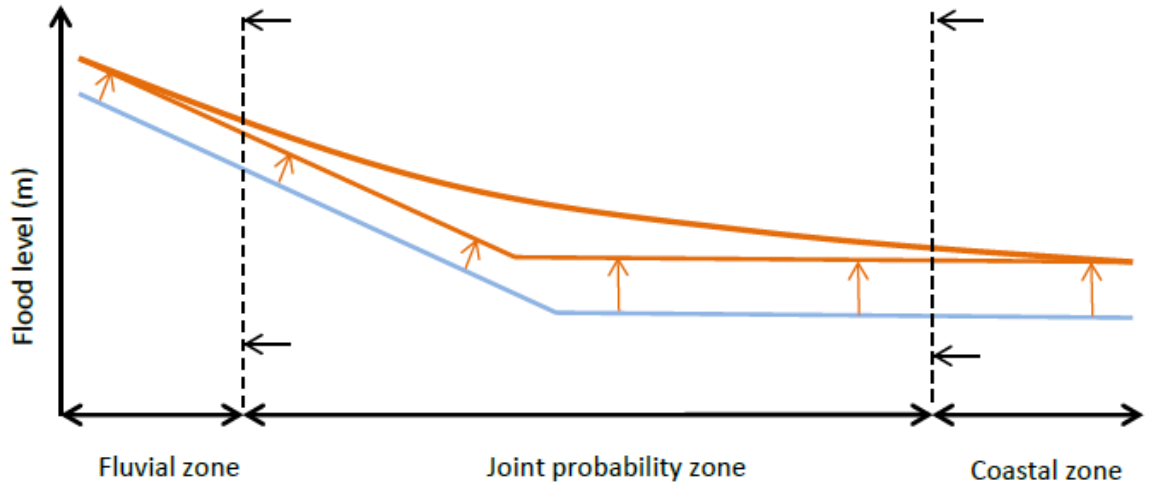


Figure 6.5.14. Interim Approach to Account for the Effects of Climate Change

To account for climate change, two alternative methods for adjusting the flood level table (Table 6.5.7) are proposed:

- The table can be populated using the climate change-affected rainfall and ocean levels as upper and lower boundary conditions to the hydrologic/hydraulic models, which would require repeating all the simulations to account for the changes in the rainfall and ocean level values; or
- The historical flood level table can be used but the exceedance probabilities of the extreme rainfall and storm tide can be modified to reflect future exceedance probabilities. This can eliminate the need for additional hydrologic and hydraulic runs, although it is possible that additional simulations may still be required for low exceedance probability events.

## 5.6. Worked Example 1 — Hawkesbury/Nepean River

This worked example illustrates the basic implementation of the design variable method and should be read in conjunction with Book 6, Chapter 5, Section 5. The example demonstrates each of the four steps of the method applied to multiple sections of a river reach, and provides flood level estimates with respect to location, dependence level and AEP.

The hydraulic and hydrologic models for the Hawkesbury-Nepean River system were originally developed as part of an Environmental Impact Statement in the 1990s for works to upgrade the spillway capacity of Warragamba Dam. The study included a detailed analysis of the existing flooding behaviour and was carried out by Webb McKeown and Associates (1996). The outcomes were subject to rigorous technical reviews by a range of parties including Sydney Water, the then Department of Land and Water Conservation, the Bureau of Meteorology and other experts.

The hydrologic model used was RORB, and the hydraulic model was RUBICON. The RORB model was calibrated and then evaluated using historical records available for five of the events between June 1964 and April 1988. The RUBICON hydrodynamic model software was used to quantify the hydraulic aspects of the flood behaviour (e.g. flood levels and velocities). RUBICON is a fully dynamic one dimensional (1D) model and uses different elements to simulate complex flow over floodplains and through channel systems. The

hydraulic model covers the entire area from Lake Burragorang to the ocean at Broken Bay. The process of calibrating and evaluating the RUBICON model was undertaken using recorded information for 11 individual historical events. The models were then used to determine design flood behaviour of the system. The calibrated RUBICON model of the Hawkesbury-Nepean has been maintained by WMAwater (previously Webb McKeown and Associates) since this original study and was selected for this project as there is a very high flood gradient along the river even though the river is tidal for 140 km upstream of the estuary inlet under non-flood conditions.

**Step 1: Pre-Screening Analysis**

As described in Book 6, Chapter 5, Section 5, a pre-screening analysis is recommended as a first step to identify whether a full joint probability analysis is warranted for the problem being considered. The basis of the pre-screening analysis is to assess whether flood levels corresponding to the extreme cases of complete dependence and complete independence are sufficiently different from each other, which is determined with reference to a tolerance threshold.

Consider the location of Liverpool which is 80 km upstream from the ocean boundary. Assume that the practitioner specifies a tolerance of 0.1 m for the design in question. Assume also that the user is interested in a design at the 2% AEP level. Three model runs are required:

1. *Completely dependent* — flow boundary at 2% AEP and ocean boundary at 2% AEP.

2. *Flow boundary only* — flow boundary at 2% AEP and ocean boundary at 100% AEP.

3. *Ocean boundary only* — flow boundary at 100% AEP and ocean boundary at 2% AEP.

The water levels resulting from these three runs are summarised in Table 6.5.8. For the dependent case, the water level is 9.590 m. For the independent case, the water level is obtained by taking the highest water level from either the flow boundary only case or the ocean boundary only case. For this location, the flow boundary only case dominates, and leads to a flood level of 9.537 m. The difference between the dependence and independence cases is 0.053 m, which is within the specified tolerance. This implies that this cross-section is not highly sensitive to the ocean level, and is thus in the 'fluvial zone'. The fully dependent value of 9.590 m is therefore used as the best approximation to the 2% AEP event, without having to implement the design variable method. This analysis is only valid for the 2% AEP level, and should be repeated for other AEPs if there is interest in analysing other exceedance probabilities.

Table 6.5.8. Model-Derived Water Levels (mAHD) for Given Pairs of Tide and Rainfall Boundary Input Conditions for a Cross-section Located at Liverpool (Chainage–80 300)

| | | **Storm Tide (% AEP)** | |
|---|---|---|---|
| | | **Lower Bound** | **2** |
| **Flow (% AEP)** | **No Rain** | | *1.381* |
| | **2** | *9.537* | *9.590* |

By repeating the pre-screening analysis at multiple locations along a river, the extent of the joint probability zone can be defined. Two examples of dependent locations for this case study are Olga Bay and Spencer, with 2% AEP model runs shown in Table 6.5.9 and Table 6.5.10 respectively. The difference between the dependent and independent cases at

both these locations is greater than the tolerance of 0.1 m, indicating the influence of both boundary conditions. At these locations, it is therefore necessary to implement the design variable method to determine the 2% AEP water level. AtSpencer, in particular, the difference in flood level based on the dependent and independent cases is 0.614 m, suggesting potentially significant discrepancies depending on the joint probability assumption at this location.

Table 6.5.9. Pre-Screen Analysis Pairs at Olga Bay (Chainage–20 400)

| | | **Storm Tide (% AEP)** | |
|---|---|---|---|
| | | **Lower Bound** | **2** |
| **Flow (% AEP)** | **No Rain** | | *1.258* |
| | **2** | *0.286* | *1.397* |

Table 6.5.10. Pre-Screen Analysis Pairs at Spencer (Chainage–34 700)

| | | **Storm Tide (% AEP)** | |
|---|---|---|---|
| | | **Lower Bound** | **2** |
| **Flow (% AEP)** | **No Rain** | | *1.306* |
| | **2** | *1.876* | *2.490* |

**Step 2: Dependence Parameter Selection**

For the location of this case study, assume that the dependence parameter is 0.9 (refer Figure 6.5.9).

**Step 3: Flood Level Modelling**

The design variable method requires many combinations of boundary conditions. Table 6.5.11 and Table 6.5.12 are examples of the hydraulic response at Olga Bay and Spencer, respectively. The design variable method does not require the same number of runs for each boundary condition (here there are five storm tide cases and 10 flow cases), nor do the marginal probabilities have to be identical. Where there is sufficient prior opportunity, the marginal probabilities could be selected to be standard values (e.g. 1, 2, 5, 10, …) but in many instances (as in Table 6.5.11 and Table 6.5.12), they will be back-calculated from existing model runs.

The hydraulic response table should include runs where the 100% exceedance probability of each margin is considered, and there should be a wide range of AEPs. The range of AEPs for the margins should include events that are rarer than the AEPs being calculated for the water level (since, for example, a 1% AEP water level could hypothetically arise from the combination of a 10% AEP flow and a 0.1% AEP storm tide). The total number of model runs (here 5 x 10 = 50 runs) is likely to be the limiting factor for the feasibility of the method (especially where two dimensional (2D) hydrodynamic models are used) and this will govern the resolution at which the table is evaluated (Zheng et al., 2015).

Table 6.5.11. Model-Derived Water Levels (mAHD) for Given Pairs of Storm Tide and Rainfall Boundary Input Conditions for a Cross-section Located at Olga Bay (Chainage–20 400).

| | **Storm Tide (% AEP)** |
|---|---|

| | | Lower Bound | 30 | 2 | 0.25 | 0.0025 |
|---|---|---|---|---|---|---|
| **Flow (% AEP)** | **No Rain** | 0.001 | 1.048 | 1.258 | 1.466 | 1.678 |
| | **18.1** | 0.114 | 1.084 | 1.279 | 1.482 | 1.687 |
| | **9.5** | 0.129 | 1.094 | 1.292 | 1.494 | 1.696 |
| | **4.9** | 0.175 | 1.129 | 1.321 | 1.515 | 1.708 |
| | **2** | 0.286 | 1.209 | 1.397 | 1.586 | 1.776 |
| | **1** | 0.429 | 1.316 | 1.498 | 1.682 | 1.866 |
| | **0.5** | 0.686 | 1.509 | 1.681 | 1.854 | 2.03 |
| | **0.2** | 0.982 | 1.735 | 1.895 | 2.057 | 2.222 |
| | **0.1** | 1.364 | 2.033 | 2.177 | 2.325 | 2.476 |
| | **0.01** | 1.449 | 2.101 | 2.241 | 2.387 | 2.534 |

Table 6.5.12. Model-Derived Water Levels (mAHD) for Given Pairs of Storm Tide and Rainfall Boundary Input Conditions for a Cross-section Located at Spencer (Chainage–34 700)

| | | Storm Tide (% AEP) | | | | |
|---|---|---|---|---|---|---|
| | | Lower Bound | 30 | 2 | 0.25 | 0.0025 |
| **Flow (% AEP)** | **No Rain** | 0.002 | 1.09 | 1.306 | 1.519 | 1.737 |
| | **18.1** | 0.913 | 1.626 | 1.782 | 1.941 | 2.104 |
| | **9.5** | 1.007 | 1.694 | 1.845 | 2.000 | 2.159 |
| | **4.9** | 1.29 | 1.909 | 2.049 | 2.193 | 2.341 |
| | **2** | 1.876 | 2.374 | 2.49 | 2.612 | 2.737 |
| | **1** | 2.497 | 2.895 | 2.99 | 3.089 | 3.194 |
| | **0.5** | 3.343 | 3.643 | 3.714 | 3.791 | 3.873 |
| | **0.2** | 4.122 | 4.345 | 4.402 | 4.462 | 4.526 |
| | **0.1** | 4.919 | 5.091 | 5.134 | 5.181 | 5.231 |
| | **0.01** | 5.083 | 5.247 | 5.286 | 5.334 | 5.378 |

Figure 6.5.15 is a plot of the water level contours that have been interpolated from the hydraulic response tables for Olga Bay and Spencer. These plots provide a consistency check of the water levels in the tables. Vertical lines imply that the storm tide (in this case the $X$ variable) is the dominant process affecting the water level, whereas horizontal lines imply that the flow (the $Y$ variable) dominates the water level. Any other slope between these two indicates variation with respect to both inputs.

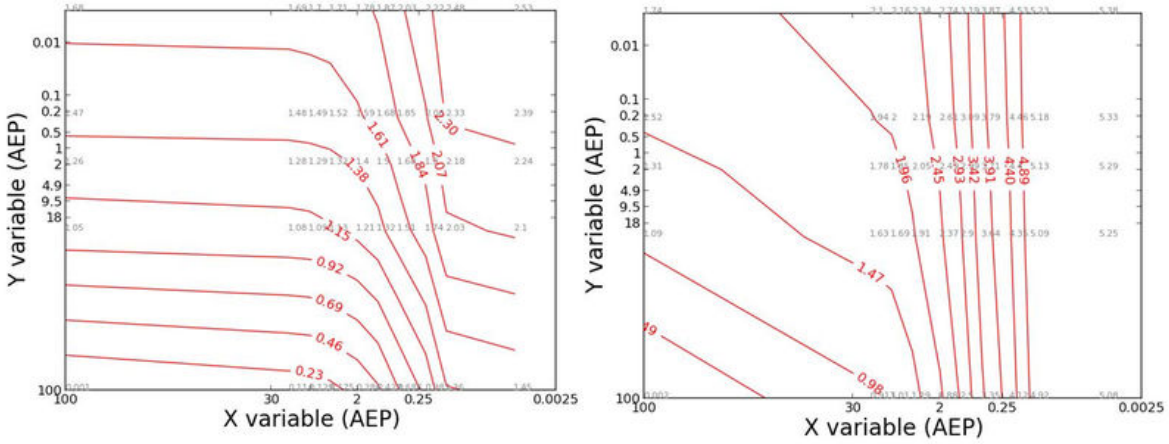


Figure 6.5.15. Interpolated Contours for Olga Bay (left) and Spencer (right) Corresponding to the Water Levels in Table 6.5.11 and Table 6.5.12.

**Step 4: Estimate the Exceedance Probability of Flood Levels**

Figure 6.5.16 shows the output water levels at the two locations. For Olga Bay the best estimate (solid black line) is very similar to the independence case. Figure 6.5.16 also shows that the difference between complete dependence and independence is a function of the AEP (AEPs >10% are very similar, but AEPs <10% diverge between these two cases). For Spencer, the best estimate lies approximately midway between the complete dependence and independence cases. This demonstrates that the relationship of $\alpha$ is non-linear with respect to the resulting water levels and that it varies with location. Specifically, although $\alpha$ varies from zero (complete dependence) to one (independence), $\alpha$=0.90 does not necessarily mean the water level is 'near independence'.

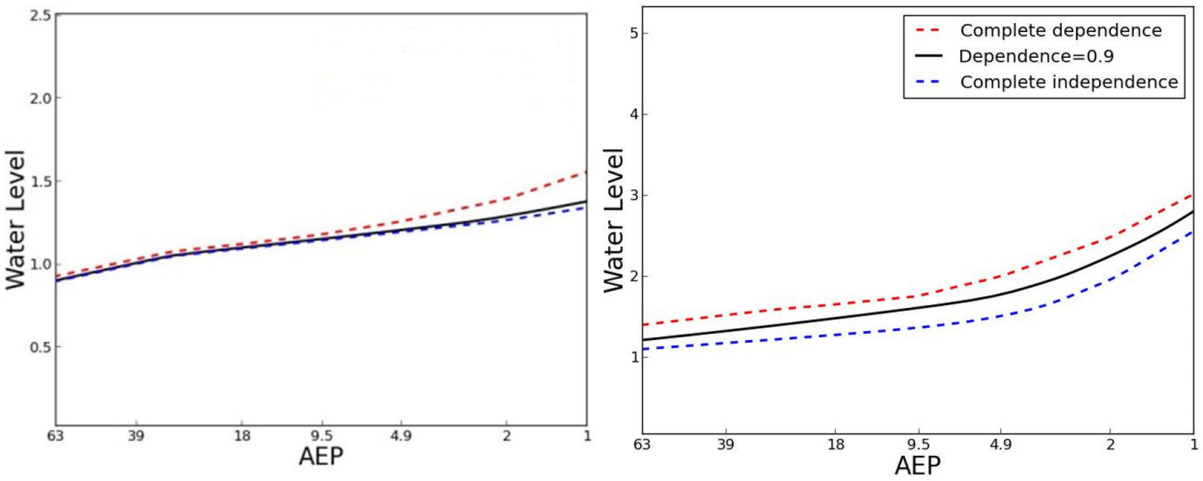


Figure 6.5.16. Water Levels at Olga Bay (left) and Spencer (right) Corresponding to Cases of Complete Dependence, Complete Independence and the Best Estimate when α=0.9

A longitudinal plot can be generated by repeating the analysis for multiple cross sections (Figure 6.5.17). The joint probability zone is indicated as the region where the difference between the complete dependence and independence cases is greater than the defined tolerance. From Figure 6.5.17 it is clear that Spencer is situated in the middle of this zone, and that Olga Bay – being closer to the ocean boundary – is less affected by the joint dependence. The extent of the zone also depends on AEP, as the joint dependence is more

important for more frequent events, and this leads to a longer extent of the zone (e.g. compare the range of distance over which there is a noticeable difference between dependence and independence cases, for the 10% and 1% AEP respectively).

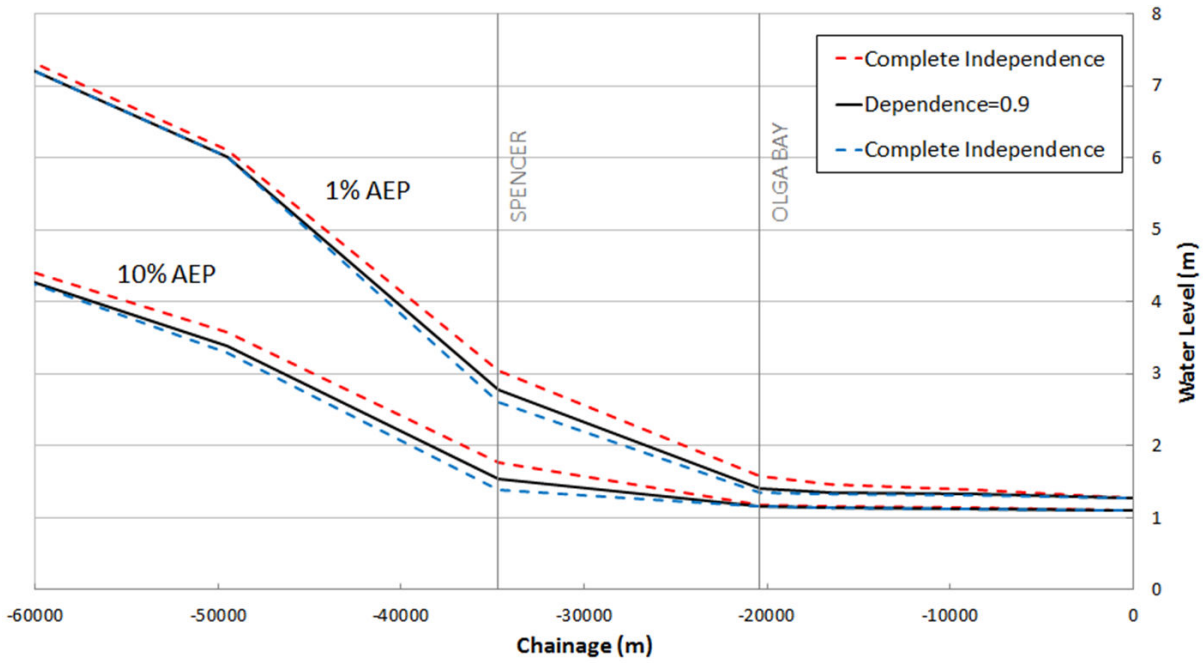


Figure 6.5.17. Longitudinal Comparison of 1% AEP and 10% AEP Water Levels

# 5.7. Worked Example 2 — Nambucca River

The Nambucca River catchment is located in northern New South Wales. Based on work prepared for the Nambucca Shire Council, modelled flood levels for combinations of boundary conditions were provided from a Tuflow 1D-2D hydrodynamic model ((WMAwater, 2013)). The model is of the Nambucca River, Warrell Creek and tributaries, and covers a catchment area of 1315 km$^2$. The model was calibrated to peak flood survey levels (1890-2011) and large historical events (1972, 1977, 2009) recorded at gauges located at Bowraville, Macksville, Stuarts Island and Utungun.

**Step 1 Pre-Screening Analysis**

Model runs for a pre-screening analysis at three different AEPs (9.5%, 2% and 1%) are shown in Table 6.5.13. For the 9.5% AEP the difference between independence and complete dependence is 0.21 m, for the 2% AEP it is 0.12 m and for the 1% AEP it is 0.12 m. The importance of accounting for joint probability effects therefore appears to be greater for more frequent events. If a tolerance of $Z$=0.1 m was specified for the design, a joint probability analysis would be required for each AEP to obtain more accurate estimates of the water level corresponding to a specified exceedance probability.

Table 6.5.13. Pre-Screening Analysis Pairs for Macksville

| | **Storm Tide (% AEP)** | | | |
|---|---|---|---|---|
| | **Lower Bound** | **9.5%** | **2%** | **1%** |

| | | | | | |
|---|---|---|---|---|---|
| **Flow (% AEP)** | **No Rain** | | 1.45 | 1.52 | 1.55 |
| | **9.5%** | 2.26 | 2.47 | | |
| | **2%** | 3.32 | | 3.46 | |
| | **1%** | 3.68 | | | 3.80 |

**Step 2 Dependence Parameter Selection**

The critical duration of the Nambucca River catchment is between 36 and 48 hours. Given this storm burst duration and the location of the Nambucca River catchment, $\alpha$ =0.90, taken from Figure 6.5.13, was used to represent the dependence between extreme rainfall and storm tide.

**Step 3 Flood Level Modelling**

Table 6.5.14 shows flood levels at Macksville for various combinations of critical-duration rainfall and storm tides in terms of AEP.

Table 6.5.14. Flood Levels for Various Combinations of Rainfall and Tide Levels at Macksville (Pacific Highway Bridge) Nambucca River

| | | **Storm Tide (% AEP)** | | | | | | | | | | | |
|---|---|---|---|---|---|---|---|---|---|---|---|---|---|
| | | **Lower Bound** | **63.1 %** | **39.3 %** | **18.1 %** | **9.5%** | **4.9%** | **2%** | **1%** | **0.5%** | **0.2%** | **0.1%** | **0.05 %** |
| **Rainfall levels (AEPs)** | **No Rain** | 0.60 | 1.35 | 1.38 | 1.42 | 1.45 | 1.48 | 1.52 | 1.55 | 1.58 | 1.62 | 1.65 | 1.68 |
| | **63.1 %** | 1.29 | 1.70 | 1.73 | 1.75 | 1.77 | 1.80 | 1.82 | 1.84 | 1.87 | 1.90 | 1.92 | 1.94 |
| | **39.3 %** | 1.61 | 1.92 | 1.94 | 1.96 | 1.98 | 2.00 | 2.02 | 2.04 | 2.06 | 2.08 | 2.10 | 2.12 |
| | **18.1 %** | 1.83 | 2.08 | 2.09 | 2.11 | 2.12 | 2.14 | 2.16 | 2.18 | 2.19 | 2.21 | 2.23 | 2.25 |
| | **9.5%** | 2.26 | 2.43 | 2.44 | 2.46 | 2.47 | 2.49 | 2.21 | 2.52 | 2.54 | 2.56 | 2.58 | 2.59 |
| | **4.9%** | 2.82 | 2.96 | 2.96 | 2.98 | 2.98 | 2.99 | 3.00 | 3.01 | 3.02 | 3.04 | 3.05 | 3.06 |
| | **2%** | 3.32 | 3.42 | 3.42 | 3.43 | 3.44 | 3.45 | 3.46 | 3.46 | 3.47 | 3.48 | 3.49 | 3.50 |
| | **1%** | 3.68 | 3.76 | 3.76 | 3.77 | 3.78 | 3.78 | 3.79 | 3.80 | 3.81 | 3.82 | 3.82 | 3.83 |
| | **0.5%** | 4.20 | 4.27 | 4.27 | 4.28 | 4.28 | 4.29 | 4.29 | 4.30 | 4.30 | 4.31 | 4.32 | 4.32 |
| | **0.2%** | 4.95 | 4.99 | 4.99 | 4.99 | 5.00 | 5.00 | 5.00 | 5.01 | 5.01 | 5.02 | 5.02 | 5.03 |
| | **0.1%** | 5.48 | 5.51 | 5.51 | 5.51 | 5.52 | 5.52 | 5.52 | 5.52 | 5.53 | 5.53 | 5.53 | 5.53 |
| | **0.05 %** | 5.91 | 5.93 | 5.93 | 5.93 | 5.93 | 5.94 | 5.94 | 5.94 | 5.94 | .595 | 5.95 | 5.95 |

**Step 4 Estimate the Exceedance Probability of Flood Levels**

Figure 6.5.18 shows the flood levels at the Macksville cross-section (Pacific Highway Bridge) for various AEPs. As with the pre-screening analysis, the difference between the flood levels

is larger for more frequent AEPs. For rarer AEPs, the small difference between the independence and complete dependence-based estimates indicates that one flood-producing mechanism has negligible effect and that the other dominates. Based on the results in Table 6.5.14 rainfall is the dominant mechanism (there is a larger variation with changes in rainfall than with changes in tide).

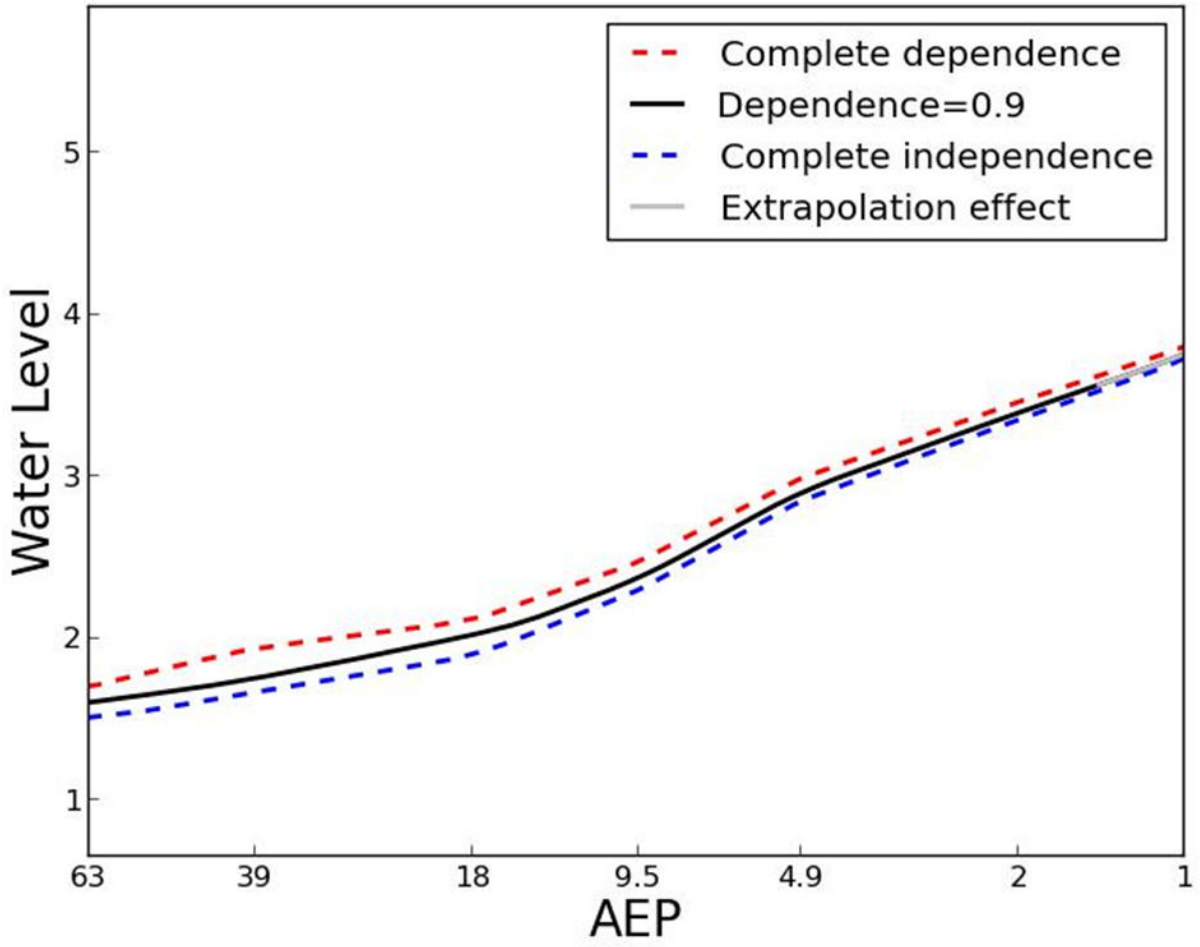


Figure 6.5.18. Water Levels at Macksville Corresponding to Cases of Complete Dependence, Complete Independence and the Best Estimate when α=0.95

**Evalaution Against Observed Water Levels**

Given that the location is jointly affected by storm tides and streamflow, it is preferable to compare the modelled water levels to observed levels (rather than flows). The observation gauge at Macksville has records from 1890 to 2011, giving 121 annual maximum events. Of these, 93 were censored below the 2 m threshold due to the tidally influenced nature of the location, leaving 28 uncensored gauged values. Of the 28 values, one value – the largest on record – could not be specified precisely but instead was suggested to have a range between 3.5 m-4 m ((WMAwater, 2013)).

Figure 6.5.19compares the observed water levels at Macksville (blue points) to the range of estimates from the design variable method, from complete dependence to independence, with the range depicted in the figure as grey shading. The fitted model gives reasonable agreement for less frequent events (AEP < 5%) that were the focus of hydraulic model calibration, but there is noticeable discrepancy for more frequent events (AEP > 5%). These

observations lie outside the bounds produced by the dependence parameter, suggesting that variability in the dependence between extreme rainfall and storm tide is insufficient to explain this discrepancy.

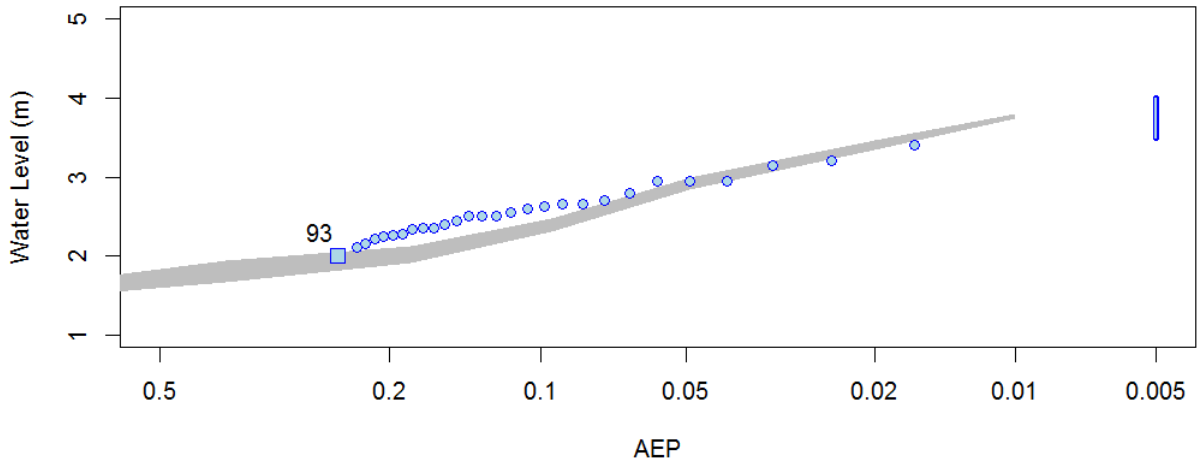


Figure 6.5.19. Comparison of Observed Water Levels at Macksville with Range of Estimates from Design Variable Method from Complete Dependence to Complete Independence

In addition to uncertainty in the representation of dependence (grey shading in Figure 6.5.19), alternative explanations for the discrepancy between simulated and observed water levels could include:

1. Parametric uncertainty in the rainfall, storm tide and observed water levels;

2. The hydraulic model and how it is represented via the hydraulic response table;

3. The assumed entrance conditions being too efficient for these more frequent events; and

4. The upper and lower boundary models (ie. the hydrological and storm tide models).

**Uncertainty Assessment**

When comparing models to observations, uncertainty assessment provides a useful mechanism for assessing the relative magnitude of a discrepancy. Uncertainty intervals were estimated for the frequency analysis of both the observed water levels and the rainfall/storm tide data, to enable an assessment of the magnitude of the discrepancy between observed and modelled water levels relative to their uncertainty intervals.

To estimate the 90% confidence intervals for the water levels, the procedures outlined in Book 3, Chapter 2 were used to implement a Flood Frequency Analysis. The 90% confidence limits from a fitted Generalised Extreme Value distribution are represented as grey dashed lines in Figure 6.5.20, and appear to encompass the simulated flows for most AEPs.

There is also uncertainty in the distributions used to model the design variable method, such that the rainfall AEPs and storm tide AEPs may differ from those in Table 6.5.14. To estimate the 90% confidence intervals to account for the effects of rainfall and storm tide, the censored threshold likelihood of (Zheng et al., 2015) was used. In the analysis, the joint distribution of storm tides at Stuart Island and rainfall from the Utungun gauge were extracted, jointly dependent Generalised Pareto distributions were fitted and the corresponding parameters were sampled using a Markov Chain Monte Carlo method to

adjust the AEPs in Table 6.5.14. This method is beyond the scope of this chapter, but it is nonetheless useful for diagnosing the discrepancy with observations. Figure 6.5.20 shows the 90% confidence limits of the uncertainty analysis of the design variable method.

Comparing the observations to the confidence limits in Figure 6.5.20, the design variable method has considerable uncertainty in the upper tail, but less uncertainty in the lower tail. The observed water levels in the lower tail lie outside the confidence limits, which suggests that this discrepancy is not accounted for by considering parametric uncertainty. Nonetheless, the confidence intervals between the two methods overlap for the majority of AEP estimates suggesting general agreement.

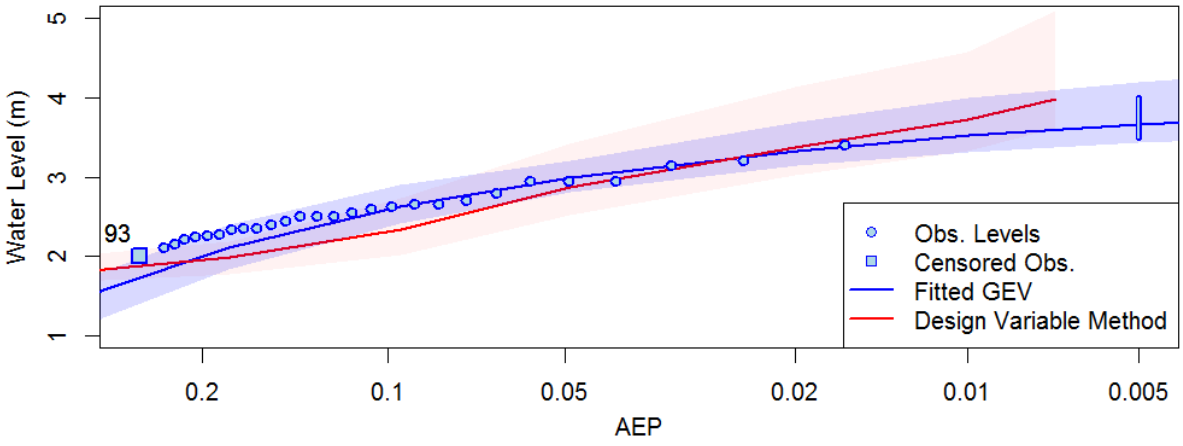


Figure 6.5.20. Comparison of Observed Water Levels to 90% Confidence Limits from Generalised Extreme Value Distribution and Design Variable Method

**Hydraulic Model**

The hydraulic model entails a number of assumptions that could lead to misspecification of water levels for a given set of boundary conditions. For example, typical issues such as simplified model representations and coarse grids could affect the flood level estimates. If the water levels specified for Table 6.5.14 are different, this leads to different water level contours and exceedance probabilities. For this study a two dimensional model was used with a rigorous calibration ((WMAwater, 2013)). The focus of the calibration was to less frequent events, whereas the discrepancy in Figure 6.5.19 is with respect to the more frequent events. One potential issue with respect to more frequent events is an assumption about the river entrance. The model assumed that events generated sufficient flow to blow-out the river entrance, but for more frequent events this may not hold, leading to higher observed water levels than those modelled. This issue will be further considered in the following section by adjusting AEPs corresponding to the water levels (since it is computationally expensive to rerun the hydraulic model).

A related issue may be due to the coarseness and range of the hydraulic response table (Zheng et al., 2015), but Table 6.5.14 extends to a 0.05% AEP event and has a relatively large number (twelve) increments for each dimension. Based on these considerations, the discrepancy does not seem to be due to the coarseness or extent of AEPs in Table 6.5.14.

**Boundary Model**

The boundary model refers to the methods by which the boundary conditions of the hydraulic model were derived and linked with exceedance probabilities (e.g. the AEPs in Table 6.5.14). For example, the probability distribution for the ocean boundary may have been specified

using a surrogate location or may itself be derived from a coastal model. The probability distribution for the streamflow boundary may have assumptions in how the streamflow was derived from rainfall, for example, loss parameter values, temporal patterns, representativeness of the rainfall gauge, and the coincidence of rainfall across multiple tributaries. In short the probabilities associated with water levels in Table 6.5.14 may not be correct.

Visual inspection of Table 6.5.14 shows that the water level at Macksville is more responsive to the rainfall distribution rather than storm tide. This suggests that the design variable method at this location will be more sensitive to the assumptions made when associating the rainfall AEPs to water levels. Rather than reassess the hydrological model, a heuristic method is to manually adjust the AEPs and determine whether an improved fit to water levels is plausible. Taking this approach, the frequent rainfall AEPs in Table 6.5.14 were modified from {63.1%, 39.3%, 18.1%} to {63.1%, 50%, 39.1%} with all other AEPs remaining the same. The result of this approach is shown in Figure 6.5.21 giving the strongest indication that the discrepancy is due to the association of water levels to the frequent rainfall AEPs. As noted previously, the hydraulic model assumption that the river entrance is blown-out for frequent events is the most likely plausible explanation for this observation. However, it cannot be ruled out that the issue may instead be with the hydrological model and further inspection would be required to isolate the specific issue (beyond the scope of this chapter).

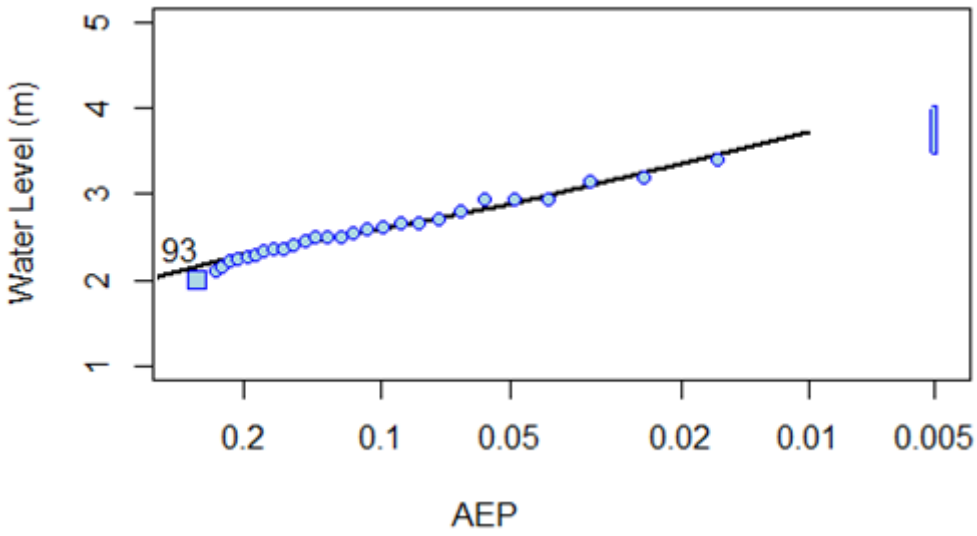


Figure 6.5.21. Comparison of Observed Water Levels at Macksville to Best Fit Estimates from Design Variable Method Assuming Correction to Frequent Rainfall AEPs

From this example, it is clear that care is required when interpreting the results from the design variable method. This example has illustrated the type of issues that should be taken into account, including the uncertainty of data sources, hydraulic model assumptions and boundary model assumptions.

**Consistency of Flood Level Table**

The flood level table for Macksville was constructed from output from a 2D hydraulic model. At other locations the flood level table may be only partially complete because some flow/ tide combinations do not cause the water level to exceed the base elevation of that grid cell. As an example, Table 6.5.15 presents a water level table from a different location, and has a

number of NA (not available) values indicating that for these combinations the free water surface was not high enough to wet the grid cell. Provided that there are not too many NAs and they are in a consistent block, the design variable method can handle partially wetted flood level tables by ignoring the region of missing values.

Another issue is that the hydraulic model output should be 'well behaved' for all combinations of boundary conditions. This issue can be seen in Table 6.5.15 for the column of 0.05 % AEP storm tide, which shows two instances where a larger rainfall value results in a lower water level. When a rarer rainfall (or, equivalently, storm tide) event yields a lower water level this is referred to as being non-monotonic increasing. Strictly, this is not physically possible, but could be produced by a model for various reasons. One explanation is that the hydraulic model itself has spurious numerical artifacts.

Another explanation is cases where the boundary conditions have been derived inconsistently. For example, the practitioner may have switched between critical durations, used different temporal patterns or changed the way hydrographs are derived from tributary catchments. A practical workaround is to enforce monotonicity by artificially raising the water levels to be at least as high as water levels from more frequent events (in Table 6.5.15, the two events would be set to be 10.44 m). See the underlined cases of tide= 0.05% with rain = (5% or 0.05%) that are not monotonic increasing when compared to the values at lower AEPs.

Table 6.5.15. Hydraulic Response Table for cell (294, 200)

| | | **Storm Tide (% AEP)** | | | | | | | | | | | |
|---|---|---|---|---|---|---|---|---|---|---|---|---|---|
| | | **Lower Bound** | **63%** | **39%** | **18%** | **10%** | **5%** | **2%** | **1%** | **0.5%** | **0.2%** | **0.1%** | **0.05 %** |
| **Rainfall levels (AEPs)** | **No Rain** | NA | NA | NA | NA | 5.68 | 7.04 | 7.63 | 8.31 | 8.79 | 9.43 | 9.98 | 10.44 |
| | **63%** | NA | NA | NA | NA | 5.73 | 7.04 | 7.63 | 8.31 | 8.79 | 9.44 | 9.99 | 10.44 |
| | **39%** | NA | NA | NA | NA | 5.73 | 7.04 | 7.63 | 8.31 | 8.79 | 9.44 | 9.99 | 10.44 |
| | **18%** | NA | NA | NA | NA | 5.73 | 7.04 | 7.63 | 8.31 | 8.79 | 9.44 | 9.99 | 10.44 |
| | **10%** | NA | NA | NA | NA | 5.73 | 7.04 | 7.63 | 8.31 | 8.79 | 9.44 | 9.99 | 10.44 |
| | **5%** | NA | NA | NA | NA | 5.74 | 7.04 | 7.63 | 8.31 | 8.79 | 9.44 | 9.99 | 10.43 |
| | **2%** | NA | NA | NA | NA | 5.74 | 7.04 | 7.63 | 8.31 | 8.79 | 9.44 | 9.99 | 10.44 |
| | **1%** | NA | NA | NA | NA | 5.74 | 7.04 | 7.63 | 8.31 | 8.79 | 9.44 | 9.99 | 10.44 |
| | **0.5%** | NA | NA | NA | NA | 5.75 | 7.05 | 7.63 | 8.31 | 8.79 | 9.44 | 9.99 | 10.44 |

| | | | | | | | | | | | | |
|---|---|---|---|---|---|---|---|---|---|---|---|---|
| | **0.2%** | NA | NA | NA | NA | 5.75 | 7.05 | 7.63 | 8.31 | 8.79 | 9.44 | 9.99 | 10.44 |
| | **0.1%** | NA | NA | NA | NA | 5.75 | 7.05 | 7.64 | 8.31 | 8.79 | 9.44 | 9.99 | 10.44 |
| | **0.05%** | NA | NA | NA | NA | 5.76 | 7.05 | 7.64 | 8.31 | 8.79 | 9.44 | 9.99 | 10.43 |

## 5.8. Summary

Flood estimation in estuarine regions is generally more complicated than for other locations due to the range of processes and timescales that can lead to flood events. As described in Book 6, Chapter 5, Section 2, these processes can include extreme rainfall events on the upstream catchment, combined with storm surges and high astronomical tides in the lower reaches of the estuary. The strengths and limitations of three alternative methods - Flood Frequency Analysis, continuous simulation and the design variable method—were reviewed in Book 6, Chapter 5, Section 3, with the design variable method identified as the most appropriate method for general application in Australia.

A detailed overview of the theory joint probability modelling was presented in Section Book 6, Chapter 5, Section 4, and a practical approach to implementing the design variable method was provided in Book 6, Chapter 5, Section 5. The recommended approach includes a pre-screening analysis that can be used to ensure that a detailed joint probability analysis is only conducted for cases where the additional complexity is warranted. The implementation of the method has been designed to be generally applicable to a range of situations across the Australian coastline, and the method is able to accommodate changes to extreme rainfall and ocean levels as a result of anthropogenic climate change. Worked examples describing the implementation of the method were provided in Book 6, Chapter 5, Section 6 and Book 6, Chapter 5, Section 7.

The additional complexity of joint probability modelling means that the methods described here should only be implemented by users with sufficient understanding of the theoretical basis of each method. In all cases, the assumptions and limitations of each method (summarised in Book 6, Chapter 5, Section 3) should be taken into account to ensure that the selected method is appropriate for the problem. The theory, computational methods and supporting datasets required to implement joint probability approaches will continue to advance, and users should maintain familiarity with on-going developments in this field.

## 5.9. References

Ang, A.H.S. and Tang, W.H. (2006), Probability Concepts In Engineering Planning and Design. Emphasis on applications in Civil and Environmental Engineering, John Wiley and Sons.

Beirlant, J., Goegebeur, Y., Segers, J. and Teugels, j. (2004), Statistics of Extremes - Theory and Applications, 490 pp., John Wiley and Sons, West Sussex, England.

Coles, S.G. (2001), An Introduction to Statistical Modelling of Extreme Values, pp.208, Springer, London.

Coles, S. G. and Tawn, J.A. (1994), Statistical Methods for Multivariate Extremes: An Application to Structural Design, Journal of the Royal Society. Series C (Applied Statistics), 43(1), 1-48.

Hawkes, P.J. and Svensson, C. (2006), Joint Probability: Dependence Mapping and Best Practice. R&D Technical Report FD2308/TR1Rep., DEFRA.

Heffernan, J. and Tawn, J.A. (2004), A conditional approach for multivariate extreme values (with discussion), Journal of the Royal Society. Series B (Methodological), 66(3), 497-546.

Kotz, S. and Nadarajah, S. (2000), Extreme Value Distributions: Theory and Applications, Imperial College Press.

Svensson, C. and Jones, D.A. (2002), Dependence between extreme sea surge, river flow and precipitation in east Britain, International Journal of Climatology, 22: 1149-1168.

Svensson, C. and Jones, D.A. (2004), Dependence between sea surge, river flow and precipitation in south and west Britain, Hydrological Earth Systems Science, 8(5), 973-992.

Tawn, J. (1988), Bivariate extreme value theory: Models and Estimation, Biometrika, 75(3), 397-415.

WMAwater (2013), Hydraulic modelling report - Nambucca River and Warrell CreekRep.

Webb McKeown and Associates (1996), Warragamba Dam Auxiliary Spillway EIS flood study parts A-ERep.

Zheng, F., Westra, S. and Sisson, S.A. (2013), The dependence between extreme rainfall and storm surge in the coastal zone, Journal of Hydrology, 505: 172-187.

Zheng, F., Leonard, M. and Westra, S. (2015), Efficient joint probability analysis of flood risk, Journal of Hydroinformatics, in press (accepted 14/1/2015).

Zheng, F., Westra, S. and Leonard, M. (2014a), Australian Rainfall and Runoff Revision Project 18, Stage 3: Coincidence of fluvial flooding and coastal water levels in estuarine areasRep., pp: 145.

Zheng, F., Westra, S., Leonard, M. and Sisson, S.A. (2014b), Modelling dependence between extreme rainfall and storm surge to estimate coastal flood risk, Water Resources Research, 50(3), 2050-2071.

# Chapter 6. Blockage of Hydraulic Structures

William Weeks, Ted Rigby

| Chapter Status | Final |
|---|---|
| Date last updated | 14/5/2019 |

## 6.1. Introduction

### 6.1.1. Background and Scope

The capacity of drainage systems can be severely impacted by blockage. However, there are situations where significant blockage may not impact flood behaviour to any great extent. Determination of likely blockage levels and mechanisms, when estimating design flows, is therefore an important consideration in quantifying the potential impact of blockage of a particular structure on design flood behaviour.

This chapter provides guidance on the assessment of blockage in drainage systems to assist in drainage analysis and design for both urban and rural catchments. While there are a range of locations and conditions where blockage of a drainage network may be a concern in hydraulic design, this chapter concentrates specifically on blockage of cross drainage structures, in particular culverts and small bridges.

Blockage of drainage structures is a subject where a range of advice has been provided in different guidelines. Many drainage guidelines do not mention blockage at all (Pilgrim, 1987), therefore blockage is ignored in many cases. In other situations, especially where there has been an observed blockage problem in historical flood events, blockage may be specified for extreme conditions. Other guidelines provide inconclusive advice.

In fact, the actual evidence for the impact of blockage on design flood events is very limited and the evidence for any clear quantitative design advice is lacking. This is the case internationally as well as in Australia.

This chapter is not a definitive approach, but is an attempt to provide an approach that allows a consistent analysis methodology, while not becoming too extreme in either direction since there are risks in either under- or over-estimating the influence of blockage on design flood levels. It draws heavily on the findings of an earlier report prepared by the ARR Revision Project 11 team (Weeks et al., 2009). Materials upon which this guideline has been based are referenced in the Bibliography of this chapter and in the earlier project reports and papers released on the ARR website (http://arr.ga.gov.au/).

It is expected that this chapter will be updated and revised as more information becomes available and designers gain experience in the assessment of blockage and how it affects the drainage system and calculated design flood behaviour.

### 6.1.2. Limitations of the Procedure

This procedure has been developed to quantify the most likely blockage level and mechanism for a small bridge or culvert when impacted by sediment or debris laden

floodwater. It has not been developed for and is not appropriate when considering the impact of what are known as hyperconcentrated flows, mudflows or debris flows, on blockage of a structure. Hyperconcentrated flows are typically defined by a solids content of 20% or more by volume (or about 40% by weight) of the water column. Mud and debris flows include even higher levels of solids. At these much higher levels of suspended or fully integrated solids, blockage levels are likely to be much higher than those assessed in accordance with this chapter. Care should be taken in the review of catchment conditions where bed grades are relatively steep (say > 3%), to confirm bed and banks would remain relatively stable, such that flows would remain in the sediment or debris laden category and not become hyperconcentrated during the event under consideration.

While this procedure includes consideration of the impact of non-floating (sediment) on blockage of a structure, it is restricted to the likely impact of such material arriving at the structure during a design event. It cannot reflect the impact of any pre-existing build-up of sediment on the subsequent blockage of a structure.

## 6.2. Types of Structures and Drainage Systems

The types of structures or drainage elements affected by blockages can generally be grouped as follows:

***Bridges and Culverts***

These cross drainage structures carry roads, railways, pipelines or other infrastructure across watercourses. These structures can be affected by a number of different types of blockage mechanisms, resulting in consequences including increased flood levels, changes to stream flow patterns, changes to erosion and deposition patterns in channels, and physical damage to the structure. Blockage of these structures is the subject of this chapter.

***Drainage system inlets and pipes***

This includes components of urban drainage systems located within road reserves and urban overland flow paths. Frequently blockage of this type of system is generally less likely to cause the same extent of damage associated with blockage of bridges and culverts, but the consequences can still be serious from a traffic and safety perspective, and can cause serious inconvenience and nuisance. However in certain circumstances, in densely developed urban areas, pit blockage can cause significant monetary damage due to flooding of buildings upstream. While this type of blockage can be a significant nuisance, it is not covered in this chapter.

***Open channels and waterways***

Blockage of natural and constructed waterways can occur at any location, typically as a result of large debris snagged against bank vegetation, or debris passing slowly down the channel. The consequences of such blockage are increased flood levels, diversion of surface flows and the possible relocation of the waterway channel as a result of severe bank erosion. Blockage of these structures is not covered in this chapter.

***Overland flow paths***

This category covers various surface flow paths that are not normally recognised as drainage channels but do act to convey surface flows in larger events. Blockage of these flow paths can result from the deposition of sediment or the material blockage of structures built across the flow, such as property fences blocked by litter and grass clippings. Blockage of these structures is not covered in this chapter.

***Weirs and dams***
Debris can cause blockage within the spillways of weirs and dams, especially where there is a significant constriction to the flow area. This could increase the water level in the storage, possibly threatening the security of the structure. The sudden release of large debris rafts from dam spillways can cause significant damage to downstream road crossings. Blockage of these structures is not covered in this chapter.

# 6.3. Factors Influencing Blockage

## 6.3.1. Overview

The factors that most influence the likely blockage of a bridge or culvert structure are:

***Debris Type and Dimensions***
Whether floating, non-floating or urban debris present in the source area and its size;

***Debris Availability***
The volume of debris available in the source area;

***Debris Mobility***
The ease with which available debris can be moved into the stream;

***Debris Transportability***
The ease with which the mobilised debris is transported once it enters the stream;

***Structure Interaction***
The resulting interaction between the transported debris and the bridge or culvert structure; and

***Random Chance***
An unquantifiable but significant factor.

These various factors which impact debris movement and interaction with the structure are discussed further in the following sections.

## 6.3.2. Debris Type and Dimensions

### 6.3.2.1. Overview

All blockages that do occur arise from the arrival and build-up of debris at a structure. There are three different types of debris typically present in debris accumulated upstream of or within a blocked structure. This debris may be classified as

- Floating (e.g. trees);
- Non-floating or depositional (e.g. sediment); and
- Urban (e.g. cars and other urban debris).

Debris comprising natural materials is discussed in Book 6, Chapter 6, Section 3 and Book 6, Chapter 6, Section 3 and urban debris in Book 6, Chapter 6, Section 3. A means of determining the relevant dimensions of the debris is discussed in Book 6, Chapter 6, Section 4.

## 6.3.2.2. Floating Debris

Floating debris in rural or forested streams is generally vegetation of various types:

***Small floating debris***
: less than 150 mm long, can include small tree branches, sticks, leaves and refuse from yards such as litter and lawn clippings and all types of rural vegetation. This type of debris can also be introduced into a stream by earlier windstorms, bank erosion and land mass failures or from seasonal leaf falls. It is important to note that this material is available in both urban and rural catchments, and is usually available for transportation at any time.

***Medium floating debris***
: typically between 150 mm and 3 m long, mainly consists of tree branches of various sizes. This material is usually introduced into the flow path by channel erosion undermining riparian vegetation or through wind gusts during storms. It can also be present as a result of the breakdown of larger floating debris.

***Large floating debris***
: more than 3 m long, consists of logs or trees, typically from the same sources as for medium floating debris. Transport and storage of this material depends on discharge, channel characteristics, the size of the drift pieces relative to the channel dimensions, and the hydraulic characteristics (depth and slope) of the system. In small and intermediate size channels, this material is not easily transported and can easily become snagged mid-stream acting as a collection point for smaller material (i.e. a debris raft or log-jam). Whole trees can be retained within streams by being temporarily anchored either to the bed or banks of the stream. Large floating debris is usually transported during larger floods or prolonged periods of high river-stage where the floodplain is engaged and the ability of the debris to become snagged is reduced. This type of debris can cause significant problems for both culverts and bridge structures.

Small items of vegetation will usually pass through drainage structures during floods, while larger items may be caught in the structure. Once larger items are caught, this then allows smaller debris to collect on the structure.

## 6.3.2.3. Non-Floating Debris

Non-floating debris in rural or forested streams is usually sediment of all types. These can be classified as:

***Fine sediments (silt and sand)***
: typically consist of particles ranging from 0.004 to 2 mm. The deposition of finer clay-sized particles is normally a concern in tidal areas, with lower flood surface gradients and velocities. This type of debris is either transported along the streambed as bed load or within the water column as suspended load. Such material is normally sourced from sheet and rill erosion, landslip and landmass failures and channel erosion. Yield rates for this material can be significantly influenced by the conditions of, and changes to, a catchment due to urbanisation and/or rural land use practices.

***Gravels and cobbles***
: consist of rock typically ranging in size from 2 to 63 mm and 63 to 200 mm respectively. The source of this material may be from gully formation, channel erosion, landslips or land mass failure although landslips and/or land mass failures of any size will likely create hyperconcentrated or even debris flows which are not covered by this guideline.

Once mobilised, gravels and cobbles are primarily transported as bed load within high gradient streams. The deposition of cobbles can readily block the entrance of culverts or reduce the flow area under bridges.

***Boulders***

comprise rocks greater than 200 mm. The source of boulders is mostly from gully and channel erosion, landslips and the displacement of rocks from channel stabilisation works. Like gravel and cobbles, this material is typically transported as bed load in high gradient streams. This material can readily block the entrance to a structure and/or cause damage to the structure from the force of impact/collision.

### 6.3.2.4. Urban Debris

Urbanisation of catchments introduces many different man-made materials that are less common in rural or forested catchments and which can cause structure blockage. These include fence palings, building materials, mattresses, garbage bins, shopping trolleys, fridges, large industrial containers and vehicles. Garbage bins can for example be easily washed down a street and into a stream or drainage structure, a situation made worse if a large rainfall event occurs on the same day as rubbish collection within the catchment, when bins are placed in streets for collection. Urban Debris can be floating or non-floating.

## 6.3.3. Debris Availability

Defining the source area is an important consideration, when discussing debris availability and mobility. The source area is that area from which debris could be sourced during an event. In a small event it may be restricted to the immediate confines of the creek and its banks but in larger events will likely extend to the full extent of the floodplain and possibly the full extent of the upstream catchment area. As this procedure is used to initially establish debris potential in a 1% Annual Exceedence Probability (AEP) event , the relevant source area will typically be limited to the 1% AEP flood extents. Steep sided tributaries and larger rills may however extend the source area beyond the limits of the 1% AEP flood.

The following factors affect the availability of debris material within a source area:

***Potential for soil erosion***

Soil erosion exposes soil and rock particles, thus increasing their availability. The potential for soil erosion is dependent on a number of factors including soil erodibility, rainfall erosivity, surface slope length and gradient, vegetation cover and changes in catchment hydrology, this latter factor being often closely linked to the effects of urbanisation.

***Local geology***

The geology of the debris source area, particularly the exposed geology of the watercourse, influences the availability of materials such as clay, silt, sand, gravel, rocks and boulders.

***Source area***

Increasing the area supplying debris typically increases the quantity of available blockage material. It is noted however, that once blockage occurs at a given structure, the debris source area for the next downstream structure may be much less than that of the upstream structures source area.

***Amount and type of vegetative cover***

Cover can vary from grasses and shrubs to thick forests and plantations as well as a variety of crops and agricultural uses. Increasing the cover density in the source area will

typically increase the availability of debris. Some types of cover are also more prone to produce debris than others (eg Cora trees). The type of cover in the source area can also impact availability

***Land clearing***

This is associated with both rural and urban land use practices. Deforestation and urbanisation can alter the long-term flow regime of streams and may lead to gully erosion and channel expansion.

***Preceding wind and rainfall***

The occurrence of frequent flood events typically reduces the availability of debris in the source area, however, the occurrence of frequent windstorms will typically increase the quantity of debris available in the source area.

***Urbanisation***

Such areas make available a wide range of debris typically influenced by the extent of flood inundation and proximity of such debris to the stream. In most circumstances this a manageable factor linked to town planning and drainage design.

## 6.3.4. Debris Mobility

The following factors affect the mobilisation of debris material within the catchment:

***Rainfall erosivity***

Different regions experience a range of frequencies of rainfall intensity, and in general, those areas that experience more intense rainfall have a greater potential to mobilise debris than areas of lower rainfall intensity.

***Soil erodibility***

This can vary from weathered rocks to cohesive clays, all soils have different abilities to become eroded, entrained and available for mobilisation.

***Slope***

For sediment and boulder movement, there is a relationship between the mobilisation of such debris and the slope of the catchment, with respect to overbank areas where debris may be sourced and the stream channel which conveys the debris.

***Storm duration***

The mobilisation of materials generally increases with increasing storm duration.

***Vegetation cover***

Sparse vegetation cover can increase sediment mobility.

## 6.3.5. Debris Transportability

Once debris has been mobilised, it then needs to be transported down the stream if it is to present a hazard to downstream structures. Stream power, velocity, depth, presence of snags and bends and the overall dimensions of the water course play a large part in determining whether the mobilised debris lodges where it first enters the stream or is transported downstream to a receiving structure. There is a reasonably strong correlation between the waterway width and the maximum size of floating debris that a stream can transport. The event magnitude is also a major factor in controlling the quantity of debris transported. Rarer events produce deeper and faster flowing floodwaters which are able to transport large quantities and larger sizes of debris, smaller events may not be able to transport larger bridging material at all.

## 6.3.6. Structure Interaction

The likelihood of blockage at a particular structure depends on whether or not debris is able to bridge across the structure's inlet or become trapped within the structure. As bridging occurs, the clear expanse of each opening reduces, thus increasing the likelihood of further bridging and further blockage by smaller or similar material. Smaller blockage matter is unlikely to cause full blockage of a structure without the presence of suitable larger bridging matter, the material that initially bridges across the opening or inlet of a structure. Bridging matter can be as small as leaves caught on a kerb inlet grate, or as large as logs, cars and shipping containers caught at a culvert inlet or on bridge piers.

Exposed services attached to the face of culverts or bridges or obstructing the culvert waterway opening can significantly increase the risk of blockage. Similarly, some through-culvert features introduced to improve fish passage can also collect and hold debris increasing the risk of internal blockage problems. Many other factors such as skew alignments, opening aspect ratios, opening height to overtopping height ratios, culvert hoods, sloping inlet walls and the smoothness of transitions can also modify the likely interaction between the arriving debris and the bridge or culvert structure.

In urban drainage systems, any individual culvert in the system is not an individual structure, it is part of a system, generally with culverts and other structures in a series down the water course. As a consequence, upstream culverts are likely to collect a portion of the transported debris in the stream, reducing the quantity of debris that would otherwise reach the downstream culverts so the risk of blockage in these downstream structures is reduced.

Consideration of multiple structures is discussed further in Book 6, Chapter 6, Section 4.

## 6.3.7. Random Chance

While an unquantifiable factor, random chance plays a significant role in the blockage of structures. Antecedent conditions can in particular substantially alter the likely level of blockage at a structure. Recent floods can for example reduce the availability of debris but increase the transportability of debris of a particular size by cleaning out the waterway. Even the alignment of a limb approaching a structure can substantially alter its likelihood of being caught on the inlet and triggering a more substantial blockage. Blockage of a structure in any event of a particular magnitude will therefore vary in response to these random changes in behaviour, creating a distribution of blockage levels associated with such an event. This chapter attempts to quantify the average or most likely blockage level associated with a design event of a particular magnitude, as this presents an probability neutral approach to simulation of the resulting flood surface.

# 6.4. Assessment of Design Blockage Levels

## 6.4.1. Overview

Blockage of cross drainage structures such as culverts and bridges could have an impact on the capacity of these structures and also on flood levels. Hydraulic analysis of these structures should include some consideration of these impacts. This section describes a procedure for the inclusion of the impacts of blockage in analysis.

The design blockage is the blockage condition that is most likely to occur during a given design storm and needs to be an “average” of all potential blockage conditions to ensure that the calculated design flood levels reflect the defined probability. For example, an

assumption of a higher than average level of blockage would lead to the calculated design flood level upstream of the structure being higher than would be appropriate for the defined probability. Downstream flood levels would be lower because of the additional flood storage created upstream of the structure. On the other hand, an assumed lower than average level of blockage would result in lower flood levels upstream and higher flood levels downstream. This is a similar concept to that of probability neutrality used in various aspects of design flood event analysis. It is also noted that actual blockage levels vary greatly from event to event with a potential spread from “all clear” to “fully blocked” even in floods of comparable magnitude. Antecedent catchment conditions and random chance are major factors in determining blockage levels in an actual event. The selected design blockage must aim for probability neutrality (the concept of ensuring that the AEP of the design flood discharge is the same as the AEP of the design rainfall input) so design floods are appropriate for the particular circumstances. As with other similar aspects of design flood estimation, such as losses, each individual historical flood may have quite different amounts of blockage compared to the design event.

Flood mapping is an exercise in probabilities that involves the estimation of ‘average’ catchment conditions for various storm and flood frequencies to ensure that the rainfall of the defined probability produces a flood event of the same probability. In such work, design blockage conditions must be considered when predicting flood levels of a given frequency. In situations where the consequences of flooding (including the impact of blockage) are high, planning rules typically require design for a lower probability (rarer) event. An increase in the design event probability is typically adopted for planning purposes, when the consequences of flooding are low.

This chapter is based on a design event type analysis, where a flood of a defined flood probability is required. For Monte Carlo analysis of flood risk, a probability distribution of blockage is required, as an input. Considering the uncertainty in the assessment of blockage, analysis of probability distributions is even more difficult. This topic is discussed more detail in Book 6, Chapter 6, Section 5. The procedure presented in this chapter is based on a qualitative assessment of debris likely to reach a structure, and the likely interaction between that debris and the structure regarding its potential for blockage. It is based on the various papers prepared by Barthelmess, Rigby, Silveri and others.

The procedure initially involves a series of decisions leading to estimation of the likely magnitude of debris reaching a structure in a 1% AEP event and the most likely blockage level that would develop at the structure under consideration. Subsequent adjustments are then made to reflect the most likely design blockage levels in lesser or greater AEP events and to establish the associated most likely blockage mechanism. This procedure provides an probability neutral approach to the assessment of an appropriate level of blockage for the simulation of design flood behaviour , but may not reflect specific conditions in an equivalent historical event. Such is the random nature of the many variables controlling blockage behaviour.

## 6.4.2. Appropriate Investigation

It is important to recognise the impact that different levels of investigation can have on the confidence associated with any blockage estimate. Estimates based on aerial imagery alone cannot for example provide the level of confidence that would be obtained from a field visit to the site, specifically aimed at assessing the various factors influencing blockage levels at the site or likely blockage mechanisms.

Where the structure/site under consideration is located in a particularly flood sensitive area and blockage of the structure could significantly impact flood behaviour in that area, then a

high level of investigation is warranted. This should include a field inspection of the upstream catchment/source area to confirm the types of debris likely to reach the site, their availability, mobility and transportability together with the average size of the largest 10% of each debris type likely to reach the site. Any structures upstream of the target structure/site should be inspected and consideration given to their ability to trap debris reaching the target structure/site. Any photographs/records of past blockage material and extents should be used to validate the choice of $L_{10}$ and debris type. Although seldom available, any photos/records of the blockage mechanism (Location – Type – Timing) that have been observed in past events will help to validate the chosen blockage mechanism to be used in the hydraulic model. However it must be stressed that it is the most likely (probability neutral) blockage mechanism that is required, not the worst case scenario. Flood mapping, aerial photography, annual rainfall and rainfall IFD data, rainfall and soil erosivity maps, topographic maps, vegetation and soil maps should be consulted when available to further consolidate conclusions as to the types of debris likely to reach the site and the quantum of such debris.

Conversely, when the structure under consideration is in an area where changes in flood behaviour would have no significant consequences on safety, property damage or amenity, then an extensive investigation to support the blockage assessment process, as outlined above, may not be warranted. This decision should be documented.

The final decision as to what is an appropriate level of investigation must ultimately be the responsibility of the person making the assessment. It will vary greatly between sites and will to some extent be constrained by what information is available. Whatever the approach adopted, it is important that the level of investigation undertaken should be relevant to the importance of the assessment of blockage at the site and is documented, so that others relying on the assessment can be aware of the confidence limits attaching to that particular assessment.

## 6.4.3. History of Blockage

The history of blockage in the drainage system is an important input to any risk based approach to blockage, and should always be explored in so far as available data permits. While the procedure outlined in this chapter provides a generic assessment of likely design blockage levels and mechanisms, local observations and history can be important in ensuring that this procedure results in reasonable answers. All available history should be sought from relevant local stakeholders, including residents, in assessing the reasonableness of blockage levels and mechanisms produced by this chapter.

In particular, if there has been no long term history of blockage at a particular structure and similar drainage structures in the catchment have not demonstrated blockage problems, blockage may not need to be considered, or a nominal allowance only may be appropriate in design.

## 6.4.4. Assessment Procedure

### 6.4.4.1. Debris Types and Dimensions

In using this procedure it is necessary to first assess the type of debris likely to arrive at the structure under consideration and the likely dimensions of that debris. Where more than one type of debris is present in quantity in the source area, the procedure will need to be repeated for each debris type to establish the debris type with the most impact on the performance of the blocked structure.

The types of debris available in their respective source areas will normally be readily apparent during a field visit or from aerial photographs, but relevant dimensions may be more difficult to assess.

The ratio of the opening width of the structure (e.g. diameter or width of the culvert or bridge pier spacing) to the average length of the longest 10% of the debris that could arrive at the site (termed here as $L_{10}$) is a well correlated guide to the likelihood that this material could bridge the openings of the structure and cause blockage. This $L_{10}$ value is defined as the average length of the longest 10% of the debris reaching the site and should preferably be estimated from sampling of typical debris loads. However, if such data is not available, it should be determined from an inspection of debris on the floor of the source area, with due allowance for snagging and reduction in size during transportation to the structure.

For debris of any particular type and size to reach the structure, the debris must:

- be available in the source area;
- be able to be mobilised into the stream and not snagged by bank vegetation as it enters the stream; and
- be delivered into a stream able to transport the debris from the source area down to the structure, without floating debris being snagged by bank vegetation or stream bends or constrictions, or without non-floating debris being deposited prior to reaching the structure as the stream grade and velocities reduce. For smaller more turbulent streams (less than say 6 m bank to bank) the width between banks of the stream through the source area will normally limit the size/length of larger floating debris to less than the stream width. The bed grade immediately upstream of the structure will normally limit the size of the larger non-floating debris reaching the structure to that capable of being moved by the flow.

Any loose material and pockets of debris lying within or in close proximity to the channel are likely to be representative of the debris that could cause downstream blockage. A detailed inspection of the waterway upstream of the target structure, particularly after a flood, will assist with assessing the above factors and deriving a realistic value for $L_{10}$.

In an urban area the variety of available debris can be considerable with an equal variability in $L_{10}$. In the absence of a record of past debris accumulated at the structure, an $L_{10}$ of at least 1.5 m should be considered as many urban debris sources produce material of at least this length such as palings, stored timber, sulo bins and shopping trolleys.

## 6.4.4.2. Debris Availability

The availability of a particular type of debris (floating, non-floating or urban) in a source area limits the level of that particular debris that can be ultimately mobilised and transported to a structure. As noted in Book 6, Chapter 6, Section 4, there may be significant quantities of more than one type of debris present in the source area, requiring more than one type of debris to be assessed. The characteristics of high, medium and low availability are hard to quantify, so there is some judgment required in their evaluation. Table 6.6.1 describes typical source area characteristics and a corresponding ranking for the likely availability of a particular type of debris in that source area. It should be noted that the characteristics included are not exhaustive or presented in any particular order. Some will only be applicable in respect to certain debris types. They are provided to provoke thought about the factors that could be relevant to the level of availability. As this procedure is based on a 1% AEP flood (with later adjustment for other AEPs) the effective source area is that associated with a 1% AEP event.

Table 6.6.1. Debris Availability - in Source Area of a Particular Type/Size of Debris

| Classification | Typical Source Area Characteristics (1% AEP Event) |
|---|---|
| High | • Natural forested areas with thick vegetation and extensive canopy cover, difficult to walk through with considerable fallen limbs, leaves and high levels of floor litter.<br>• Streams with boulder/cobble beds and steep bed slopes and steep banks showing signs of substantial past bed/bank movements.<br>• Arid areas, where loose vegetation and exposed loose soils occur and vegetation is sparse.<br>• Urban areas that are not well maintained and/or where old paling fences, sheds, cars and/or stored loose material etc., are present on the floodplain close to the water course. |
| Medium | • State forest areas with clear understory, grazing land with stands of trees.<br>• Source areas generally falling between the High and Low categories. |
| Low | • Well maintained rural lands and paddocks with minimal outbuildings or stored materials in the source area.<br>• Streams with moderate to flat slopes and stable bed and banks.<br>• Arid areas where vegetation is deep rooted and soils are resistant to scour.<br>• Urban areas that are well maintained with limited debris present in the source area. |

### 6.4.4.3. Debris Mobility

The ability for debris to become mobilised from the source area into a stream has an effect on the amount of debris that can then be ultimately transported to a structure. Table 6.6.2 describes typical source area characteristics and a corresponding rank for the likely mobility of debris from the sorce area into receiving streams.

Table 6.6.2. Debris Mobility - Ability of a Particular Type/Size of Debris to be Moved into Streams

| Classification | Typical Source Area Characteristics (1% AEP Event) |
|---|---|
| High | • Steep source areas with fast response times and high annual rainfall and/or storm intensities and/or source areas subject to high rainfall intensities with sparse vegetation cover.<br>• Receiving streams that frequently overtop their banks.<br>• Main debris source areas close to streams. |
| Medium | • Source areas generally falling between the High and Low mobility categories. |
| Low | • Low rainfall intensities and large, flat source areas.<br>• Receiving streams infrequently overtops their banks. |

| Classification | Typical Source Area Characteristics (1% AEP Event) |
|---|---|
| | • Main debris source areas well away from streams. |

## 6.4.4.4. Debris Transportability

The ability for debris to be transported by a stream down to a structure has an effect on the amount of debris arriving at the structure. Table 6.6.3 describes typical stream characteristics and a corresponding rank for the likely transportability of debris.

Table 6.6.3. Debris Transportability - Ability of a Stream to Transport Debris Down to the Structure[a]

| Transportability | Typical Transporting Stream Characteristics (1% AEP Event) |
|---|---|
| High | • Steep bed slopes (> 3%) and/or high stream velocity (V > 2.5 m/s)<br>• Deep stream relative to vertical debris dimension (D > $0.5L_{10}$)<br>• Wide stream relative to horizontal debris dimension.(W > $L_{10}$)<br>• Stream relatively straight and free of major constrictions or snag points.<br>• High temporal variability in maximum stream flows. |
| Medium | • Stream generally falling between High and Low categories. |
| Low | • Flat bed slopes (< 1%) and/or low stream velocity (V < 1m/s).<br>• Shallow depth relative to vertical debris dimension (D < $0.5L_{10}$).<br>• Narrow stream relative to horizontal debris dimension (W < $L_{10}$).<br>• Stream meanders with frequent constrictions/snag points.<br>• Low temporal variability in maximum stream flows. |

[a]Where V = velocity, D is depth, W is width and $L_{10}$ is average length of the longest 10% of the debris that could arrive at the site

## 6.4.4.5. Debris Potential

Where reliable long term data is available on the quantity and type of debris typically present at a structure, this should be used to directly quantify the debris potential at the structure. Where such data is not available, the potential quantity of debris reaching a structure at a site from a contributing source area in a 1% AEP event can be estimated from Table 6.6.4. If there is a significant quantity of more than one type of debris in the source area that could induce blockage, this will require more than one type of debris to be assessed.

Table 6.6.4. 1% AEP Debris Potential

| Classification | Combinations of the Above (any order) |
|---|---|
| High | HHH or HHM |
| Medium | MMM or HML or HMM or HLL |
| Low | LLL or MML or MLL |

## 6.4.4.6. Adjustment for Annual Exceedence Probability

Observation of debris conveyed in streams strongly suggests a correlation between an event's magnitude and debris potential at a site. This is accommodated in Table 6.6.5 as follows.

Table 6.6.5. AEP Adjusted Debris Potential

| Event AEP | (1% AEP) Debris Potential at Structure | | |
|---|---|---|---|
| | High | Medium | Low |
| AEP > 5% | Medium | Low | Low |
| AEP 5% - AEP 0.5% | High | Medium | Low |
| AEP < 0.5% | High | High | Medium |

## 6.4.4.7. Design Blockage Level

### Inlet Blockage (Floating or Non-Floating)

In conjunction with the quantity of debris likely to arrive at the site, Table 6.6.6 provides an estimate of the 'most likely' inlet blockage level should a blockage form from floating or non-floating debris bridging the inlet.

Table 6.6.6. Most Likely Inlet Blockage Levels - $B_{DES}$%

| Control Dimension Inlet Clear Width (W) (m) | AEP Adjusted Debris Potential At Structure | | |
|---|---|---|---|
| | High | Medium | Low |
| $W < L_{10}$ | 100% | 50% | 25% |
| $L_{10} \leq W \leq 3*L_{10}$ | 20% | 10% | 0% |
| $W > 3*L_{10}$ | 10% | 0% | 0% |

### Barrel Blockage (Non Floating)

An alternative blockage mechanism is however possible for non-floating material (typically sediment) when this material progressively arrives and is deposited at the inlet and in the barrel or waterway of the structure. This typically leads to a bottom up blockage of both the barrel and inlet to the structure. Blockage in this form can arise because velocities through the structure fall below the level required to maintain the material in motion or, in extreme cases, because the depth of sediment in the bed load is sufficient to overwhelm the inlet, leading to sediment with little water completely blocking the inlet and filling a substantial proportion of the barrel of the structure.

Table 6.6.7 classifies the likelihood of deposition in the barrel or waterway based on sediment size and velocity through the structure. Using this likelihood of deposition Table 6.6.8 then combines the likelihood of deposition with the debris potential to provide a most likely depositional barrel or waterway blockage level for the structure.

Table 6.6.7. Likelihood of Sediment Being Deposited in Barrel/Waterway (HML)

| Peak Velocity Through Structure (m/s) | Mean Sediment Size Present | | | | |
|---|---|---|---|---|---|
| | Clay/Silt 0.001 to 0.04 mm | Sand 0.04 to 2 mm | Gravel 2 to 63 mm | Cobbles 63 to 200 mm | Boulders >200 mm |
| >= 3 | L | L | L | L | M |
| 1.0 to < 3.0 | L | L | L | M | M |
| 0.5 to < 1.0 | L | L | L | M | H |
| 0.1 to < 0.5 | L | L | M | H | H |
| < 0.1 | L | M | H | H | H |

*Based on Hjulstrom's diagram as modified by Sundborg (Sundborg, 1956)*

Table 6.6.8. Most Likely Depositional Blockage Levels – $B_{DES}$%

| Likelihood that Deposition will Occur (Table 6.6.7) | AEP Adjusted Non Floating Debris Potential (Sediment) at Structure | | |
|---|---|---|---|
| | High | Medium | Low |
| High | 100% | 60% | 25% |
| Medium | 60% | 40% | 15% |
| Low | 25% | 15% | 0% |

It is noted that Table 6.6.8 (blockage caused by non-floating debris) is to be read in conjunction with Table 6.6.6 (blockage caused by floating debris) and the blockage mechanism creating the worst impact on flood behaviour should be used in design.

While the above tables provide a means of estimating a realistic value for the magnitude of a likely (probability neutral) blockage, they do not address the other characteristics required to properly describe the blockage mechanism (viz the blockage type, location and timing) and its impact on the hydraulics of flow through the structure. These issues are discussed further in Book 6, Chapter 6, Section 4.

## 6.4.4.8. Minimum Opening Height Considerations

Consideration of likely inlet blockage levels as presented in Table 6.6.6 assumes that the greatest dimension (length) of debris relative to the structures opening width is the dominant factor influencing inlet blockages. All debris however has three dimensions and a lesser dimension, such as the debris height, could also trigger vertical bridging across the opening height if the structure's opening height was substantially less than the structures opening width. In the absence of detailed data on likely debris geometry, it is recommended that structures be designed with a clear opening height of at least one third their width to reflect the assumptions inherent in this procedure. In an existing structure where the opening height is less than one third of the opening width, it is recommended that analysis be based on the likely vertical dimension of the debris and the vertical opening height of the structure in lieu of the likely debris length and horizontal opening width. Unless data is available to support the choice of $L_{10}$ (vertically), it should be taken as not less than one half of the assessed debris $L_{10}$ (length).

## 6.4.4.9. Blockage of Multi Cell/Span Structures

Limited observation of blockages at multi cell culverts or multi span bridges suggests that all cells/spans often do not block to the same extent. The main factors influencing this variability appear to be the main stream approach alignment and location relative to the multiple culverts or spans and the relative width of flow carrying debris to the total opening width. These two factors are somewhat related as they both influence the uniformity of presentation of debris, carried by the flow, to the individual cells or spans.

Where the main stream width is considerably less than the total structure width, it is likely that more debris will be delivered to and accumulate at or in the cells/spans falling within the main stream width, than at the cells/spans located on the adjacent floodplains. This may not be the case when the mainstream flow is only a small proportion of the total flow reaching the structure. In such cases the presentation of debris to the multiple cells/spans may become more uniform resulting in more consistent levels of blockage.

As an initial guide it is suggested that, where the width of that part of the approach flow that is capable of transporting the debris under consideration, is comparable with or greater than the total width of the structure, then the assessed $B_{DES}$ be applied uniformly to all cells/ spans.

Where the width of that part of the approach flow that is capable of transporting the debris under consideration is significantly less than the total width of the structure, then the culverts/spans within the effective transport width be assessed as blocked to $B_{DES}$ and those outside of that zone be reduced to half $B_{DES}$. Measurements of observed distributions are however essentially non-existent at this time. More information, to permit refinement of guidelines for blockage of multiple spans/cells, is needed.

## 6.4.4.10. Assessment of Multiple Structures

It is fundamental to the consideration of the interaction between multiple culverts that any individual culvert/bridge could be ‘all clear’ or ‘guideline blocked’ in a design event.

The question then arises as to what are the ‘likely’ probability neutral combinations of blockage that could occur across a catchment. Clearly an ‘all clear’ ($B_{DES}$=0) global solution is possible in any event and even probable in lesser events. In these lower probability events the single site $B_{DES}$ is probably also low so the change in catchment floods behaviour between different mixes of sites with $B_{DES}$>0 and $B_{DES}$=0 may not be great. In larger events however substantial differences in flood behaviour can be created from different mixes of ‘all clear’ and $B_{DES}$ structures across the catchment. Simple math shows that n independent sites with two choices for blockage presents 2n combinations. A catchment with 6 interacting culverts therefore could involve 64 possible blockage scenarios. In analysing these combinations it is therefore critical both with respect to probability neutrality and computation time that only likely combinations are considered. Seldom will all structures be responding in a truly independent manner. There is unfortunately no pre-prepared solution for this problem – all catchments will be different. While not a truly probability neutral approach, modelling all structures 'all clear' and 'guideline blocked' ensures individual structure impacts are properly simulated in the envelope solution together with the 'all clear' impacts. If these scenarios are then augmented with 'likely' mixtures of clear and 'guideline blocked' structures, the resulting flood surface envelope should reasonably represent the likely envelope flood surface levels that could be reached at any site in the catchment. It should be noted however that in any single historic event of a given AEP, the recorded flood surface will likely only reach the envelope levels at some locations (due to the variability in actual historic blockages).

As previously noted, where there are multiple structures on a contiguous water course, the debris availability will normally reduce downstream since debris will be captured by the upstream structures. Therefore for downstream structures, the debris availability, as defined in Table 6.6.1 will normally be reduced.

### 6.4.4.11. Risk Based Assessment of Blockages

In general, the consequences of a flood event of given probability will be used to establish risk in an area or at a site and this level of risk will in turn be used to establish the appropriate event AEP to be used as the planning event for that particular area or site. What this approach does not reflect is the relative uncertainty in all of the various parameters influencing design flood estimation. With even the most careful approach to the selection of parameters like design rainfall intensity, rainfall temporal patterns, stream roughness or most likely blockage levels, there is a significant likelihood that error in the assessment of these parameters may in turn lead to errors in the predicted design flood behaviour.

In an event based approach to modelling it is therefore prudent to undertake various sensitivity runs to quantify how reasonable variation in the chosen parameters could affect the model's results. Where such an analysis generates significant changes in the flood surface, it indicates that the parameter creating that change needs very careful review to confirm that the value selected was as appropriate as available data permits. A sensitivity analysis of alternate reasonable blockage levels and mechanisms is therefore strongly recommended for design or analysis involving blockages. It is recommended that the sensitivity to such a variation in design blockage levels be incorporated into analysis by considering both an 'all clear' and blocked at twice the calculated 'guideline blocked' level (max 100%) scenarios, to identify sites where flood behaviour upstream or downstream of the structure is particularly sensitive to the adopted design blockage level. Where such a site is identified, all inputs into the assessment process should be carefully reviewed to confirm the adopted design blockage level before proceeding with design or analysis based on that level.

As blockage of a structure with significant upstream available flood storage can lead to a reduction in flood flow and levels downstream of the structure, effectively protecting downstream properties, it is important to review the all clear analysis to see if the all clear scenario results in significantly increased flows downstream of the structure. If this is found to be the case then the all clear and 'guideline blocked' results should be enveloped for design flood estimation purposes.

In reviewing risk, inclusion of blockage in a Monte Carlo analysis is a valuable means of quantifying the impact of blockage on uncertainly in the flood assessment process. A distribution of blockage values is however needed for Monte Carlo analysis. Considering the uncertainty inherent in the factors influencing blockage levels and the lack of data in respect to the variation of blockage levels over time, it is however difficult to determine a suitable distribution. What little research has been done on this distribution suggests that the probability distribution is likely to be dual peaked with the 'all clear' and 'most likely' values ranking higher than adjacent values. Much more data is however needed before these characteristics can be confirmed.

## 6.4.5. All Clear

This is the condition where there is no allowance for blockage, and the hydraulic analysis assumes that the structure flows freely.

This condition should be considered as referenced above as an important sensitivity case, since the 'all clear' condition will reduce the upstream flood level and may increase flood levels downstream depending on the storage and flood immunity of the structure being considered.

Secondly, and perhaps more importantly, as referenced in Book 6, Chapter 6, Section 4, blockage may not need to be considered at all or may need consideration as a nominal allowance, if there is no history of blockage at this site or at similar neighbouring sites, especially if there is low risk of damage or disruption caused when blockage is neglected.

### 6.4.6. Implementation

A form has been prepared to assist in implementing this procedure and is available on the ARR website[1].

## 6.5. Hydraulic Analysis of Blocked Structures

### 6.5.1. Overview

Where blockage has historically been included in analysis or design, it has often been applied as a reduction factor to the 'all clear' flow through the structure. This is a simple and rapid means of making some allowance for blockage and in the absence of information on likely blockage mechanisms and extents can provide an answer commensurate with the associated uncertainty in such an approach.

This chapter enhances our understanding of likely design blockage mechanisms at a structure by quantifying likely blockage levels at a structure based on assessable catchment and structure parameters and understanding the blockage mechanism that will likely develop at the structure. Given this information, a more deliberate approach to hydraulic analysis of design blockages is now available, although most current hydraulic modelling software currently lacks the functionality to simulate the blockage mechanisms described in this chapter. It is hoped that this functionality will however be made available in the more capable software packages, in use in Australia, in the not too distant future.

### 6.5.2. Blockage Types

As previously noted, a blockage mechanism can be described by its type, its location and its timing and extents. With respect to type, there are three types of blockages that could occur:

***A top down blockage***
: occurs, when a floating debris raft builds up at the entrance to a structure, obstructing the inlet. This is a very dynamic type of blockage with the raft volume and elevation varying over time. These changes occur in response to both the flow rate and the difference between debris being added and lost from the raft as the blockage develops. On the flood recession this material may settle to fully block the inlet even though the inlet may have been only partly blocked by the raft at the flow peak. While rarely available, the temporal history of such a blockage, in an historic event, can be an important factor in realistically reproducing the actual flood behaviour at the blocked structure. While top down blockages are common in heavily vegetated areas, realistic simulation of this form of blockage is very complex.

[1]BLOCKAGE ASSESSMENT FORM via http://arr.ga.gov.au/downloads-and-software/revision-project-reports

***A bottom up blockage***

occurs, when non-floating material is deposited at the inlet and/or in the barrel or waterway of the structure. This also is a dynamic type of blockage with sediment being both added and removed from the blockage as time passes. Because of the dynamic nature of this process, the debris apparent at the conclusion of the event may have little relationship to the debris level at any point in time during the event. As with the top down blockage, the temporal history of blockage in an historic event can be important in realistically reproducing actual flood behaviour during the event. Bottom up blockages are relatively common in steep lightly vegetated catchments with unstable stream banks or easily eroded stream beds. As the geometry of a bottom up blockage does not directly vary with flood stage (as in a top down blockage), hydraulic analysis of a bottom up blockage is more straightforward.

***A porous plug blockage***

typically occurs when larger vegetative debris (often rapidly) bridges across the inlet of the structure covering the entire inlet but with sufficient porosity to allow some flow through the plug. It typically arises from a rapid bank or slope collapse, releasing a substantial pulse of vegetation and sediment into the stream. Unlike a top down or bottom up blockage, the porosity of this plug will likely only diminish as the event continues, with ever finer material being trapped on the bridging material that triggered the initial blockage. As blockage geometry does not vary with flood stage (as in a top down blockage), hydraulic analysis of a porous plug blockage is also more straightforward.

## 6.5.3. Blockage Mechanisms

While the number of possible blockage mechanisms is considerable, there appears to be a strong correlation between the dominant debris type arriving at a structure and the blockage mechanism it triggers. This correlation forms the basis of Table 6.6.9 where the blockages ‘most likely’ location, timing and extents are described. It should be noted that this table is based heavily on limited observations and should be updated as further data becomes available.

Progressive floating raft inlet blockages are assumed in this chapter to significantly impact flow through the structure only after the flow peaks (being mostly clear at higher flows as the raft lifts clear of the inlet and possibly overtops the structure. Pulse like blockages of floating material at an inlet mostly arise from vegetation injected into the stream from collapsing banks, as floodwater rise or from litter swept off the floodplain as streams overtop their banks. Neither of the above blockage types is likely to create a significant barrel/waterway or outlet blockage although non-floating debris, if present in any quantity can build up under the raft at the inlet and in the barrel, particularly as the flood recedes. It should be noted that factoring of 'all clear' flow will not necessarily provide a good estimate of the impact of either of these mechanism as both are inlet control mechanisms and the 'all clear' structure could be operating under strong outlet control.

Non-floating material reaching a culvert or bridge will mostly build up progressively but can occur as a pulse of debris in streams with unstable banks. Typically, non-floating material (sediment) will build up throughout the structure (inlet, barrel and outlet) as increasing flows mobilise ever increasing amounts of bed and bank material. Material will be continuously lost from the accumulated debris mass, but the rate of supply is likely to exceed the rate at which material passes on downstream, at least while flows are increasing and new material is being mobilised.

These observations and assumptions on the likely type, location and timing of a blockage are summarised in Table 6.6.9 In this table, the following designations are used to describe the timing of key trigger points in the blockage process.

$T_{TOTB/SA}$
Is the time when flow that first overtops the stream's banks in the source area reaches the structure.

$T_{OT/F\ \&\ OT/L}$
Are the times when flow first and last overtops the structure.

$T_P$
Is the time at which the upstream water level peaks at the structure.

$T_{OBV/FL}$
Is the time on the falling limb when the upstream water level drops back to the obvert level of the structure.

Table 6.6.9. Likely Blockage Timing and Extents

| Dominant source material | Delivery and Type | Likely Blockage Locations and Timings | | | |
|---|---|---|---|---|---|
| | | Inlet | Barrel | Outlet[a] | Handrails[b] |
| FLOATING | Progressive Top Down | 0 @ $T_P$ to $B_{DES}$ @ $T_{OBV/FL}$ | Unlikely | Unlikely | $B_{DES}$ @ $T_{OT/F}$ to $B_{DES}$ @ & $_{TOT/L}$ |
| | Pulse Porous Plug | $B_{DES}$ @ $T_{OTB/SA}$ | N.A | N.A | $B_{DES}$ @ $T_{OT/F}$ to $B_{DES}$ @ & $T_{OT/L}$ |
| NON FLOATING | Progressive Bottom Up | 0 @ $T_{OTB/SA}$ to $B_{DES}$ at $T_P$ | $T_{OTB/SA}$ to $B_{DES}$ at $T_P$ | $T_{OTB/SA}$ to $B_{DES}$ at $T_P$ | Unlikely |
| | Pulse[c] Porous Plug | Unlikely[d] | N.A | N.A | Unlikely |

[a]Unlikely - but could become likely if inlet is open and outlet grated.

[b]$B_{DES}$ is for the handrail geometry and will normally be much higher than for the culvert/bridge waterway as $L_{10}$ is likely to be much greater than the horizontal opening width/spacing of the balusters. In modelling $B_{DES}$ can be assumed at t=0 as the model will not apply handrail blockages until flow reaches the level of the handrails.

[c]Pulse blockage is more likely in systems subject to irregular flooding and/or streams with unstable banks.

[d]Unlikely – but could become likely if upstream bed/banks unstable and/or prone to scour.

As previously noted in Book 6, Chapter 6, Section 5, modelling the hydraulics of a progressively accumulating floating raft is quite complex as the blockage is not fixed in regard to its own geometry or in relation to the structure's opening geometry. While applying a blockage progressively from $T_P$ to $T_{OBV/FL}$ provides a reasonable approximation of when a floating blockage most impacts flow through a culvert or bridge that overtops, it does not sensibly reflect behaviour when floodwater carrying floating debris does not reach the obvert of the structure. In the absence of any better information it is recommended that a progressive top down blockage by floating debris that does not reach the structures obvert be initiated at $T_{OTB/SA}$ and ramped up to $B_{DES}$ at $T_P$. It should also be noted that a floating raft creates a top down blockage only as a consequence of the projection of floating debris below its water surface. Relative to the structures opening height this projection will lift on the rising limb and fall on the falling limb creating a quite variable level of blockage of the structure itself during the event. Under such circumstances, blockage levels of the structure will be controlled by both the water depth and projection of the raft below the water level. Detailed simulation of such a process is however considered beyond the scope of this

chapter. This chapter assumes that a top down blockage will be simplistically modelled by lowering the obvert of the structure over the tabulated time to then reflect the tabulated blockage level. Where the consequences of this form of blockage are high, and more realistic simulation is deemed necessary, it may be necessary to develop a site specific procedure. More information on this process can be found in Parola (2000), US DOTFHA (2005) and USGS (2013).

While the temporal pattern of a structure's blockage when it blocks prior to the flood peak in a system with little flood storage will have minimal impact on downstream peak flows or upstream peak flood levels, it can substantially alter the duration that upstream flood levels are above a certain level (floor or structure overtopping) level. In a system with significant flood storage, the timing of a structure's blockage can significantly alter upstream peak flood level, downstream peak discharge and overtopping duration. Consideration of the temporal pattern of a blockage can therefore be extremely important in realistically simulating the hydraulic impact of a blockage.

In establishing the key timings referred to in Table 6.6.9, it will normally be necessary to first run a simulation with estimated blockage levels and timings in place.

When modelling a historic event, hydraulic analysis will need to reflect (as far as available data permits) the actual blockage mechanism that developed at the structure during the event. It should be noted that this may vary significantly from what this chapter provides as the ‘most likely’ blockage scenario for the structure, such is the impact of near random chance on the many parameters influencing actual blockage. However, where data for multiple historic events is available and blockage appear to consistently differ from these chapter recommendations, further investigation is warranted, with historic data, if of reasonable quality, being given precedence.

# 6.6. Management of Blockage

## 6.6.1. Design Considerations

Even though floodway crossings can be subject to blockage issues, by far the greatest attention is given to the management of blockage at culvert and bridge crossings.

To minimise the adverse impacts of debris blockage on bridges the following design considerations should be given appropriate consideration:

- Minimise the number of in-stream piers.
- Minimise the exposure of services (i.e. water supply pipelines) on the upstream side of the bridge, and/or minimise the likelihood of debris being captured on exposed services.

To minimise the effects of debris blockage on culverts the following design consideration should be noted:

- Take all reasonable and practicable measures to maximise the clear height of the culvert, even if this results in the culvert hydraulic capacity exceeding the design standard. This minimises the likelihood of debris being caught between the water surface and obvert, and also minimises the risk of a person drowning if swept through the culvert (i.e. the culvert is more likely to be operating in a partially full condition).
- The risk of debris blockage can also be reduced by using single-cell culverts, or in the case of floodplain culverts, spacing individual culvert cells such that they effectively operate as single-cell culverts without a common wall/leg (Figure 6.6.1 and Figure 6.6.2).


Figure 6.6.1. Series of Floodplain Culverts


Figure 6.6.2. Floodplain Culvert

- One means of maintaining the hydraulic capacity of culverts in high debris streams is to construct debris deflector walls (1V:2H) as shown in Figure 6.6.3 and Figure 6.6.5. The purpose of these walls is to allow the debris that normally collects around the central leg to rise with the flood, thus maintaining a relatively clear flow path under the debris. Following the flood peak, the bulk of the debris rests at the top of the deflector wall allowing easier removal (Figure 6.6.4).


Figure 6.6.3. Debris Deflector Walls


Figure 6.6.4. Post Flood Collection of Debris on Top of Deflector Walls

- Sedimentation problems within culverts may be managed using one or more of the following activities:
  - Formation of an in-stream sedimentation pond or trap upstream of the culvert.
  - Formation of a multi-cell culvert with variable invert levels such that the profile of the base slab simulates the natural cross section of the channel (Figure 6.6.6).
  - Installation of sediment training walls on the culvert inlet (Figure 6.6.3 and Figure 6.6.5). Sediment training walls reduce the risk of sedimentation of the outer cells by restricting minor flows to just one or two cells.

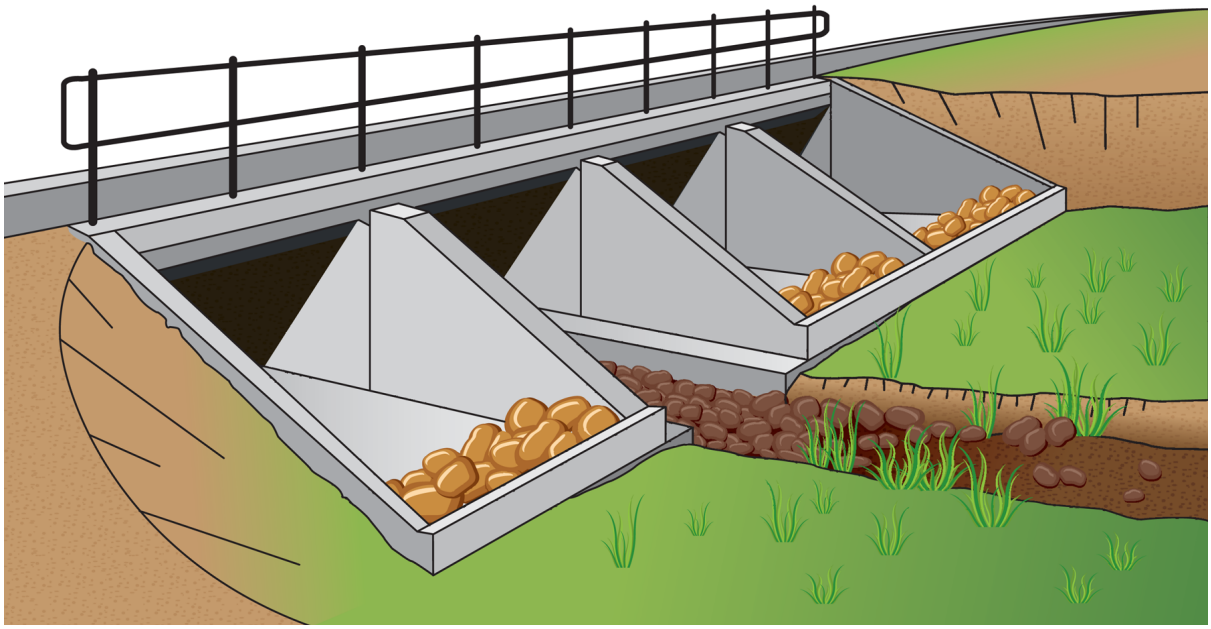

Figure 6.6.5. Sediment Training Walls Incorporated with Debris Deflector Walls (Catchments & Creeks Pty Ltd)


Figure 6.6.6. Multi-Cell Culvert with Different Invert Levels


Figure 6.6.7. Debris Deflector Walls and Sediment Training Wall Added to Existing Culvert

- Where space allows, a viable alternative to increased culvert capacity (in response to the effects of debris blockage) may be to lengthen the roadway subject to overflow (i.e. the effective causeway weir length).

- Where high levels of floating debris are present and frequently become trapped on hand rails, collapsible hand rails may be considered. Such systems typically include pins or bolts designed to fail when water becomes backed up by the handrails and therefore require ongoing maintenance. If used as traffic barriers the downstream rail fixing can be problematic. They can however limit rises in floodwater levels upstream of the structure.

## 6.6.2. Retro-fitting Existing Structures

Structures can be modified to allow debris to be directed through the structure with a reduced risk of blockage. These modifications can include improved inlet performance through the use of debris deflection walls and/or sediment training walls (Figure 6.6.7) or an increase in the size of the structure.

## 6.6.3. Debris control structures

Debris control structures or traps are structural measures provided in a watercourse upstream of critical structures to collect debris before it reaches the structure and causes problems. These can be (a) fences, posts or rails providing a much larger ‘interception area’ for debris than a pipe or culvert entrance, (b) storages or dry basins in which boulders or

other debris can collect, or (c) diversion structures designed to provide safe bypass of debris or water. Such structures can occasionally be incorporated into a water quality management plan for a catchment.

Where debris control structures or at-source control measures have been implemented, these should be incorporated into the assessment of the drainage system, which could mean a reduction in the allowance that needs to be made for blockage. Ongoing maintenance is however fundamental to the successful operation of these measures. Unless a deliberate maintenance program is in place and has been demonstrated to work, it would not be prudent to lower design blockage levels.as a consequence of such works.

Care should also be taken to ensure that the hydraulic impact of the debris control structure does not itself aggravate flooding in the system.

## 6.7. Conclusion

The inclusion of blockage in the analysis of hydraulic structures in drainage systems is an important consideration in the realistic simulation of flood behaviour. The impact of blockage is however a complex and difficult problem to analyse. It is important to ensure that the estimate of blockage used in analysis is probability neutral and not over or under-estimated as this can influence the performance of the total system. This chapter has presented an approach to the assessment of design blockage that has been developed in consultation with Australian experts and provides a consistent and logical approach to assist in the effective planning and design of drainage systems. Future investigation will refine this approach.

For further information on the background to this chapter, readers are referred to the following bibliography.

## 6.8. References

Parola, A.C. (2000), Debris Forces on Highway Bridge Issue 445, Prepared by the U.S. Transport Research Board of the National Research Council Queensland Department of Natural Resources and Water (2008).

Pilgrim, DH (ed) (1987) Australian Rainfall and Runoff - A Guide to Flood Estimation, Institution of Engineers, Australia, Barton, ACT, 1987.

Sundborg, A. (1956), The River Klarålven: Chapter 2. The morphological activity of flowing water-erosion of the stream bed: Geografiska Annaler, 38: 165-221.

U.S. Department of Transportation Federal Highway Administration (US DOTFHA), (2005), Debris Control Structures - Evaluation and Countermeasures. (DOTFHA) Hydraulic Engineering Circular No.9 Third Edition, 2005. Publication No. FHWA-IF-04-016.

U.S. Geological Survey (USGS) (2013), Potential Drift Accumulation at Bridges. URL: http:// tn.water.usgs.gov /pubs/FHWA-RD-97-028/accumwid.htm.

Weeks, W., Barthelmess, A., Rigby, T., Witheridge, G. and Adamson, R. (2009),'Blockage in Drainage Structures', Hydrology and Water Resources Symposium, Engineers Australia, Newcastle.

# Chapter 7. Safety Design Criteria

Grantley Smith, Ron Cox

| Chapter Status | Final |
|---|---|
| Date last updated | 14/5/2019 |

## 7.1. Introduction

The safety of people in floods is of major concern in floodplain management for both rural and urban areas. Consideration of the circumstances for individual flood fatalities, both in Australia and internationally, indicates that flood fatalities occur most commonly when people enter floodwaters either on foot or in a vehicle (French et al., 1983; Coates and Haynes, 2008; Haynes et al., 2016). However, where floodwaters rise rapidly and unexpectedly in flash flood areas, people may also perish trapped inside buildings as occurred in the Lockyer Valley QLD in 2010 (Rogencamp and Barton, 2012) and in Dungog, NSW in 2015. Further, recent analysis of the Queensland floods in 2011 by the Queensland Commission for Children, Young People, and Child Guardian (CCYPCG, 2012) and the Queensland Fire and Rescue Service, 2012 has reinforced the conclusion that floodwaters are extremely dangerous to both people trapped inside building or wading or driving vehicles of all types in floods. While floodplain management activities aim to reduce the risk arising from flooding events, ongoing human interaction with floodwaters during flood events is largely unavoidable, as significant areas of existing development and transport infrastructure in Australia remain within flood prone regions.

Records for past floods show that exposure of the community to flooding can result in significant death tolls and 1859 flood fatalities have occurred nationally between 1900 and 2015 (Haynes et al., 2016). Flood fatalities are significantly higher in flash flood events with rapidly rising violent flood flows than in comparably slower rising and moving riverine flooding. Two hundred and six (206) flash flood fatalities occurred in Australia between 1950 and March 2008 (Coates and Haynes, 2008). The cause of death for the majority of these cases was drowning. Other fatalities were a result of heart attacks or overexertion, or indirect causes such as electrocution or fallen trees (Coates and Haynes, 2008). Similarities have been observed in the United States, where 93 % of flash flood deaths can be attributed to drowning (French et al., 1983). Details about the activity of flash flood victims immediately prior to death are available for just under 50 % of the victims. Of these, almost 53 % perished attempting to cross a watercourse, either by wading/swimming, or by using a bridge or ford (Coates and Haynes, 2008). These values include those in vehicles. The motivation behind the activity leading to the death was known for 47 % of the study group. Of these, almost 22 % were undertaking business as usual, either attempting to reach a destination, ignoring the flood warnings or unaware of the flood intensity (Coates and Haynes, 2008).

The majority (31 %) of the Australian flash flood fatalities, for which the mode of transport is known, were inside a vehicle at the time of death. Similar results have been observed around the world, 42 % of the 93 % US flash flood drowning fatalities were vehicle-related (French et al., 1983) and 63 % of US riverine and flash flood fatalities were found to be vehicle-related (Ashley and Ashley, 2008). Jonkman and Kelman (2005) noted that vehicle-related fatalities occurred most frequently (33 %) in European and US floods.

The Lockyer Valley floods of January 2011 dramatically demonstrated that sheltering in a residential building was also not a safe option where flood flows have high force and

damage potential. Of the nineteen people who perished in the Lockyer Valley floods, thirteen were sheltering in buildings that were either completely inundated or collapsed under the force of the flood flows (Rogencamp and Barton, 2012).

Regardless, the high numbers of people that die in vehicles or on foot highlights the considerable risk in fleeing flash flood events. In many cases, people become exposed to greater risk when attempting to flee a flood affected area (Ashley and Ashley, 2008; Coates, 1999; Drobot and Parker, 2007; Jonkman and Kelman, 2005). The risks to those fleeing are not just the floodwaters themselves, but also include poor driving conditions, the danger of being hit by falling debris, electrocution from fallen power lines, lightning and mudslides (Haynes et al., 2016).

Whilst evacuation is generally considered the safest of emergency management options during flood events, it is not always possible. Subsequently, it is an important aspect of emergency planning to ensure that in flood prone locations where timely evacuation may not be possible people will not be in greater danger remaining in their homes.

Jonkman and Kelman (2005) highlighted that in most floods, people are more likely to be killed or injured if they are outside of their home or in their cars during the flood. Subsequently, undertaking evacuation at inappropriate times, such as when the floodwaters have risen in depth and velocity, is likely to increase chance of death (Cave et al., 2009).

Sound floodplain management and emergency planning requires identification of the location, timing and duration of potentially hazardous floodplain areas for design flood conditions and the careful assessment of the most suitable mitigation options taking into consideration the specifics of each floodplain location. The intention of this chapter of Australian Rainfall and Runoff is to provide background information and guidance on the application of approaches for prediction of flood hazard in those locations; additional background information can be obtained from Cox et al. (2010), Shand et al. (2011) and Smith et al. (2014). Note that while guidance is provided on predicting the flood hazard and flood risk, it is the role of the relevant floodplain management authority to define the acceptability or otherwise of the predicted risk.

A detailed discussion of risk with respect to floodplain management is presented in Book 1, Chapter 5 of Australian Rainfall and Runoff.

# 7.2. Flood Hazard

## 7.2.1. General Introduction

In terms of floodplain management, hazard can be defined as a source of potential harm or a situation with potential to result in loss. Hence, the primary hazard is the result of a flood event that has the potential to cause damage or harm to the community. Associated with the hazard is the probability of its occurrence.

There are a number of factors to be considered where assessing the hazard associated with floods. The usual starting point is to predict the flood characteristics and particularly the flow characteristics of the inundated areas of the floodplain. The main characteristics of interest typically are the flow depth and the flow velocity. In addition, the assessment of the flood hazard needs to consider a range of other social, economic and environmental factors, though these are often more difficult to quantify.

The magnitude of flood hazard can be variously influenced by the following factors:

- Velocity of Floodwaters;
- Depth of Floodwaters;
- Combination of Velocity and Depth of Floodwaters;
- Isolation During a Flood;
- Effective Warning Time; and
- Rate of Rise of Floodwater;

When quantifying and classifying flood hazard, it is important to understand the underlying causes of the hazard level. For example, if the hazard level is classified as ‘high’ then it is important to understand the key reason that it is high e.g. high depth, high velocity, high velocity and depth in combination, isolation issues, short warning time? If the core reasons that the hazard is high are not well understood, then attempts to modify and lower the hazard level may not be successful.

## 7.2.2. Flood Hazard Assessment

The base data that underpins assessment of floodplain risk typically comprises the flow characteristics (the flow depth and velocity) in the flood-affected areas of the catchment. A common approach to obtaining this information is the analysis of predictions obtained from catchment numerical modelling systems although physical models of the flood affected area may be used. More information on the application of catchment modelling systems is presented in Book 4 to Book 7 of Australian Rainfall and Runoff.

The data used for assessment of the floodplain hazard are presented commonly as maps of flood depth (see Figure 6.7.1) and flood velocity (speed and direction). Typically, these maps are shown as an envelope of maxima; a time series of flow behaviour, however, is an alternative presentation format.

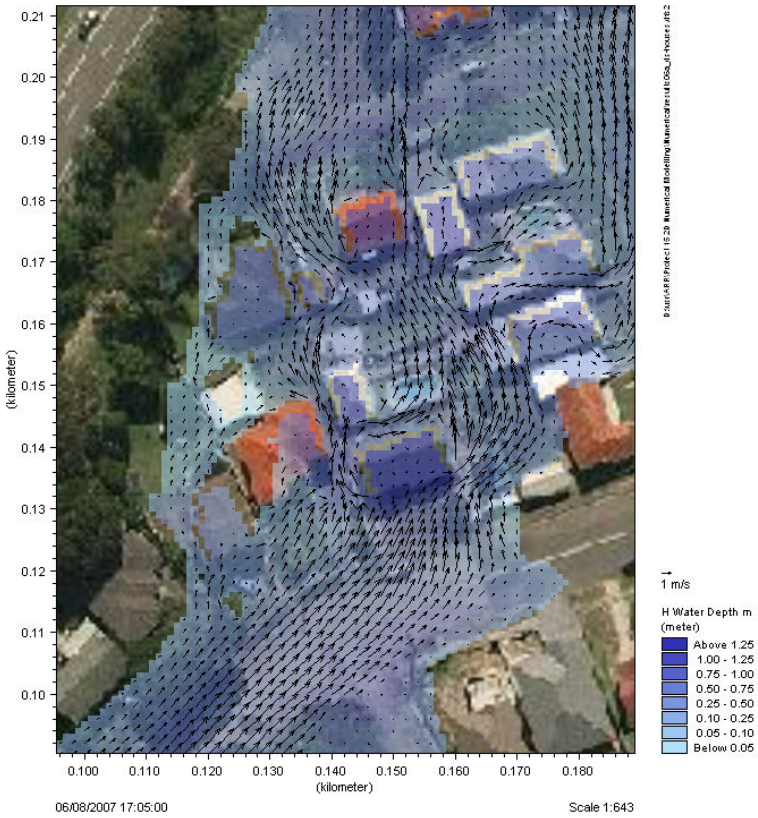


Figure 6.7.1. Example of a Flood Study Depth Map (Smith andWasko (2012))

Smith andWasko (2012) investigated the effects of alternative grid resolutions on prediction of the flood hazard. The predicted flood hazard (computed as D.V – flood depth times flood velocity) for two model grid resolutions, namely 1m and 10m, for the 2007 flood event at Merewether, NSW are shown in Figure 6.7.2. Comparing the predicted flood hazard estimates, it can be seen that those derived using the 1m grid are higher than those obtained with the 10m grid. Furthermore, Smith andWasko (2012) report that the predicted velocity and depth characteristics for the 1m grid more closely replicated those obtained from a physical model of the same area.

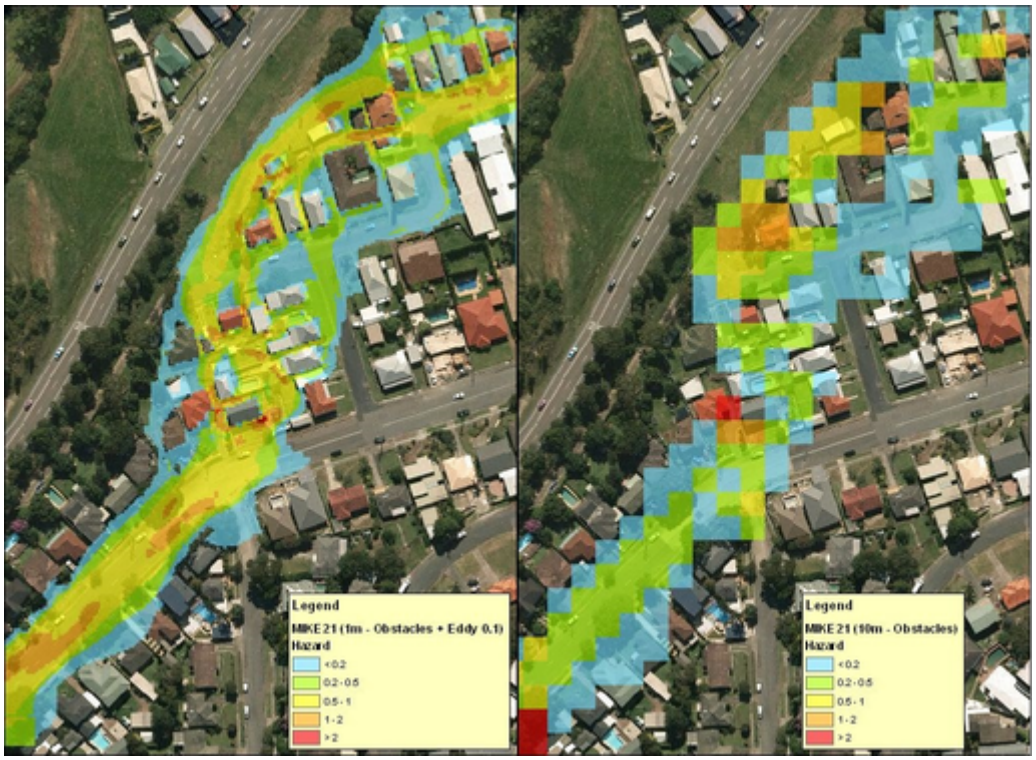


Figure 6.7.2. Comparison of Provisional Flood Hazard Estimates from Numerical Models at Differing Grid Resolutions (after Smith and Wasko, 2012)

a) 1 m grid resolution b) 10 m grid resolution

An important conclusion of Smith andWasko (2012) was that predictions from 2D numerical hydrodynamic models require further interpretation in order to ensure that suitable, representative flood behaviour information was obtained for application, especially in emergency planning and management decisions.

As described in the introduction to this chapter, people tend to be at risk in one of three main categories; on foot, in vehicles or in buildings. Subsequently, in order to further assess the vulnerability of a flood under the predicted conditions, flood hazard assessment can be divided into three categories; people stability, vehicle stability and structural stability.

## 7.2.3. People Stability

The two recognised hydrodynamic mechanisms by which people may lose stability in flood flows are *moment instability* and *friction instability* (Figure 6.7.3). A summary description of these mechanisms is provided here based on the comprehensive discussion of the topic presented in Cox et al. (2010).

In brief, moment (toppling) instability occurs when a moment induced by the oncoming flow exceeds the resisting moment generated by the weight of the body (Abt et al., 1989). This stability parameter is sensitive to the buoyancy of a person within the flow and to body positioning and weight distribution.

Frictional (sliding) instability occurs when the drag force induced by the horizontal flow impacting on a person's legs and torso is larger than the frictional resistance between a person's feet and the ground surface. This stability parameter is sensitive to weight and buoyancy, clothing type, footwear type and ground surface conditions.

Additionally, loss of stability may also be triggered by adverse conditions, which should be taken into account when assessing safety such as:

- **Bottom conditions:** uneven, slippery, obstacles;
- **Flow conditions:** floating debris, low temperature, poor visibility, unsteady flow and flow aeration;
- **Human subject:** standing or moving, experience and training, clothing and footwear, physical attributes additional to height and mass including muscular development and/or other disability, psychological factors;
- **Other issues:** strong wind, poor lighting, etc.

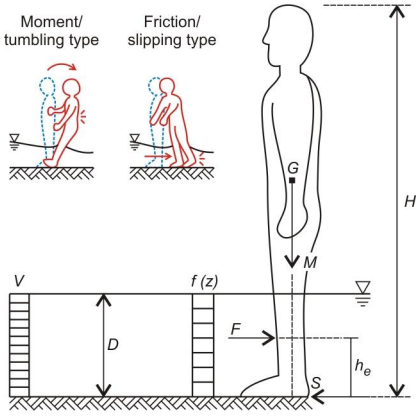


Figure 6.7.3. Typical Modes of Human Instability in Floods (Cox et al., 2010)

Determining safety criteria for people requires an understanding of the physical characteristics of the subjects along with the nature of the flow. The best measure of physical attributes for human stability is the parameter H.M (mkg), the product of subject height (H; m) and mass (M; kg) (Cox et al., 2010). The measure of flow attributes is the parameter D.V ($m^2s^{-1}$), the product of flow depth (D, m) and flow velocity (V, $ms^{-1}$)

While distinct relationships exist between a subject's height and mass and the tolerable flow value, definition of general flood flow safety guidelines according to this relationship is not considered practical given the wide range in such characteristics within the population.

In order to define safety limits, which are applicable for all persons, hazard regimes are defined based on H.M for representative population demographics. Each classification is based on laboratory testing of subject stability within floodwaters. The following suggested classifications, after Cox et al. (2010) are:

- Adults, where H.M > 50 mkg;
- Children, where H.M is between 25 and 50 mkg; and
- Infants and very young children, where H.M < 25 mkg.

Several hazard regimes are recommended based on D.V flow values for each H.M classification. The hazard regimes, as suggested from laboratory testing of subject stability and response within variable flow conditions, are:

- Low hazard zones where D.V < 0.4 $m^2s^{-1}$ for children and D.V < 0.6 $m^2s^{-1}$ for adults;

- A Significant hazard zone for children exists where flow conditions are dangerous to most between D.V = 0.4 to 0.6 $m^2s^{-1}$;

- Moderate hazard zone where conditions are dangerous for some adults and all children is defined between D.V = 0.6 to 0.8 $m^2s^{-1}$ for adults. This is inferred to define the limiting working flow for experienced personnel such as trained rescue workers;

- Significant hazard zone where flow conditions are dangerous to most adults and extremely dangerous for all children is suggested between flow values of D.V = 0.8 to 1.2 $m^2s^{-1}$; and

- Extreme hazard where flow conditions are dangerous to all people is suggested for D.V > 1.2 $m^2s^{-1}$.

Cox et al. (2010) concluded that self-evacuation of the most vulnerable people in the community (typically small children, and the elderly) is limited to relatively placid flow conditions. Furthermore, a D.V as low as 0.4 $m^2s^{-1}$ would prove problematic for people in this category, i.e. the more vulnerable in the community.

These hazard regimes for tolerable flow conditions (D.V) as related to the individual's physical characteristics (H.M) are presented in Figure 6.7.4 and Table 6.7.1.

Table 6.7.1. Flow Hazard Regimes for People (Cox et al., 2010)

| DV ($m^2s^{-1}$) | Children (H.M = 25 to 50)[1] | Adults (H.M > 50) |
|---|---|---|
| 0 | Safe | Safe |
| 0 - 0.4 | Low Hazard if depth < 0.5m and velocity < 3m/s otherwise Extreme Hazard | Low Hazard if depth < 1.2m and velocity < 3m/s otherwise Extreme Hazard |
| 0.4 - 0.6 | Significant Hazard; Dangerous to most if depth < 0.5m and velocity < 3m/s otherwise Extreme Hazard | |
| 0.6 - 0.8 | Extreme Hazard; Dangerous to all | Moderate Hazard; Dangerous to some[2] if depth < 1.2m and velocity < 3m/s otherwise Extreme Hazard |
| 0.8 - 1.2 | | Significant Hazard; Dangerous to most[3] if depth < 1.2m and velocity < 3m/s otherwise Extreme Hazard |
| > 1.2 | | Extreme Hazard; Dangerous to all |

**Maximum depth stability limit of 0.5 m for children and 1.2 m** for adults under good condition. **Maximum velocity stability limit of 3.0 $ms^{-1}$** for both adults and children.

[1]More vulnerable community members such as infants and the elderly should avoid exposure to floodwater. Flood flows are considered extremely hazardous to these community members under all conditions

[2]Working limit for trained safety workers or experienced and well equipped persons (D.V < 0.8 $m^2s^{-1}$)

[3]Upper limit of stability observed during most investigations (D.V > 1.2 $m^2s^{-1}$)

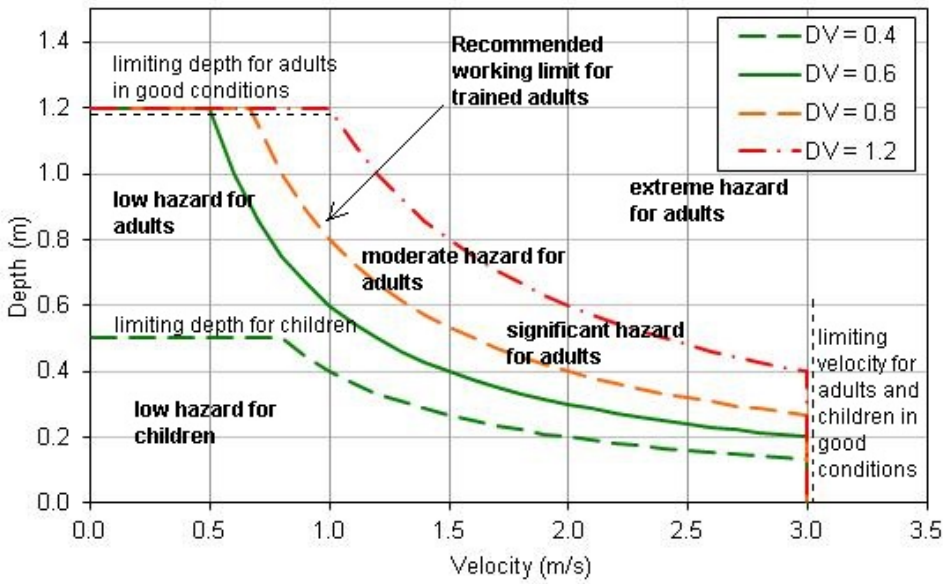


Figure 6.7.4. Safety Criteria for People in Variable Flow Conditions Cox et al. (2010)

## 7.2.3.1. Physical considerations

There is a lack of test data for infants and very young children as well as frail/older persons (Cox et al., 2004). These populations are unlikely to be safe in any flow regimes and as such, care is required in locating aged care and retirement villages as well as childcare centres and kindergartens.

For physically and/or mentally disabled people, similar intolerance criteria to the very young children and frail/older persons should be applied as subjects are considered vulnerable to all flow values. This is because while the H.M values may be similar to regular adults, they are clearly at a physical (e.g. muscular development, control of limbs) and/or psychological disadvantage (e.g. cognisant of the real/perceived danger, inability to cope with external stimulus).

Emergency personnel tasked with carrying evacuees should be aware that the additional H.M gained by carrying a person is not necessarily a benefit to their stability. This was demonstrated in a particular laboratory test of human stability criteria, Jonkman and Penning-Roswell (2008), who note that their test subject (a trained stuntman) considered balancing in the flowing water more difficult when carrying extra weight such as a child or elderly person.

It should also be noted that while these criteria are based on experimental data for loss of stability for persons wading in floodwaters, it is also inherently dangerous to swim through floodwaters. Swimming through floodwaters should not be attempted.

## 7.2.3.2. Psychological/behavioural considerations

A person's ability to withstand flood flows is affected by their mental disposition, perception, specific training and experience.

Where specific training has been undertaken or a subject has recent and relevant experience, personnel are able to tolerate situations of high D.V (Jonkman and Penning-

Roswell, 2008). A limiting working flow of D.V = 0.8 $m^2s^{-1}$ is suggested for experienced personnel such as trained rescue workers. These personnel should, where possible, be equipped for dangerous flow conditions with safety restraints, floatation aids and other safety apparatus, and be trained to cope with high D.V situations. It is trained emergency personnel who are likely to be instructing, driving and guiding evacuation paths, and consequently to whom the upper limit of safety design criteria is directed.

## 7.2.4. Vehicle stability

The two recognised hydrodynamic mechanisms by which stability of vehicles is lost include *buoyancy* or *floating* and *friction instability or sliding instability* (refer Figure 6.7.5). More comprehensive discussion is presented within Shand et al. (2011) but briefly, vehicle floating instability occurs when the upward buoyancy force exceeds the downward force exerted by the vehicle mass. This instability is dominant in low velocity, high depth flows. Frictional or sliding instability occurs when the horizontal force exerted on one or more car panels is greater than the vertical restoring force, which is dependent on the vehicle mass, buoyancy and the friction between the car tyres and road surface.

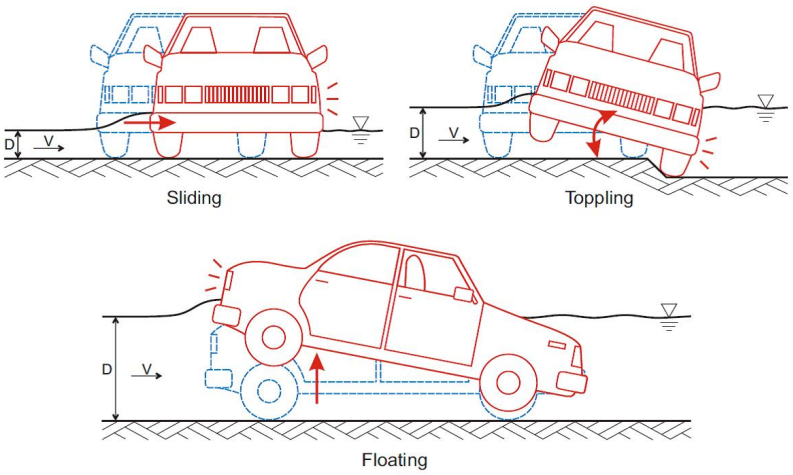


Figure 6.7.5. Typical Modes of Vehicle Instability (Shand et al., 2011)

Note that in the context of this discussion *friction instability* is associated with slow moving or stationary cars as distinct to *hydroplaning*, which occurs when a vehicle at high speed encounters very shallow, evenly distributed water covering a road, typically a highway or freeway. Hydroplaning is not considered further within this report.

Determining safety criteria for vehicles requires an understanding of the physical characteristics of the vehicle along with the nature of the flow.

The measure of physical attributes for vehicle stability analysis is the vehicle classification as based on length (L, m), kerb weight (W, kg) and ground clearance (GC, m). Three vehicle classifications are suggested:

- Small passenger: L < 4.3 m, W < 1250 kg, GC < 0.12 m
- Large passenger: L > 4.3 m, W > 1250 kg, GC > 0.12 m
- Large 4WD: L > 4.5 m, W > 2000 kg, GC > 0.22 m

The measure of flow attributes for vehicle stability analysis is D.V $m^2s^{-1}$, determined as the product of flow depth (D, m) and flow velocity (V, $ms^{-1}$)

Limiting conditions exist for each classification based on limited laboratory testing of characteristic vehicles. The upper tolerable velocity for moving water is defined based on the frictional limits, and is a constant 3.0 $ms^{-1}$ for all vehicle classifications.

The upper tolerable depths within still water are defined by the floating limits:

- Small passenger vehicles: 0.3 m
- Large passenger vehicles: 0.4 m
- Large 4WD vehicles: 0.5 m

The upper tolerable depths within high velocity water (at 3.0 $ms^{-1}$) are defined by the frictional limits:

- Small passenger vehicles: 0.1 m
- Large passenger vehicles: 0.15 m
- Large 4WD vehicles: 0.2 m

While specifically equipped vehicles may remain stable in water of greater depths, the intention of the presented criteria is to focus on the more vulnerable of typical vehicle types in common use.

Note that for all flow conditions in all vehicle classes, *the proposed vehicle safety criteria remain below the moderate hazard criteria for adults* (Cox et al., 2010). This ensures that adults occupying vehicles are, in principle, safe if exiting a vehicle in floodwaters with attributes within the specified hazard ranges.

During flood events, the majority of flood deaths are vehicle related, more than half of all deaths during floods in the United States are vehicular-related (Gruntfest and Ripps, 2000). Regardless of how often people see the power of water in flash floods or are notified through community advertising that driving through high water is dangerous, there remain sections of the community who will continue with ‘business as usual’ irrespective of the flooding conditions (Gruntfest and Ripps, 2000).

## 7.2.4.1. Vehicle Modernisation and Scale

A limiting aspect of the advice provided in this report is that vehicle stability data sets are limited to dated laboratory data (Shand et al., 2011). The properties of contemporary vehicles have significantly changed vehicle stability criteria through modified buoyancy properties (e.g. improve dust sealing), weight and ground clearance. These changes apply to all scales of vehicles from small passenger to large commercial vehicles.

As a result, the hazard criteria provided in this report are identified as interim recommended limits based on interpretation of existing information. The criteria presented here are subject to change once acceptable data for modern vehicles becomes available.

## 7.2.4.2. Stability Criteria for Vehicles

Stability criteria based on the best available information for stationary small passenger cars, large passenger cars and large 4WD vehicles in various flow situations are presented in Figure 6.7.6 and Table 6.7.2.

Table 6.7.2. Interim Flow Hazard Regimes for Vehicles (Shand et al., 2011)

| Class of vehicle | Length (m) | Kerb Weight (kg) | Ground clearance (m) | Limiting still water depth[1] | Limiting high velocity flow depth[2] | Limiting velocity[3] | Equation of stability |
|---|---|---|---|---|---|---|---|
| Small passenger | < 4.3 | < 1250 | < 0.12 | 0.3 | 0.1 | 3.0 | $DV \leq 0.3$ |
| Large passenger | > 4.3 | > 1250 | > 0.12 | 0.4 | 0.15 | 3.0 | $DV \leq 0.45$ |
| Large 4WD | > 4.5 | > 2000 | > 0.22 | 0.5 | 0.2 | 3.0 | $DV \leq 0.6$ |

[1]At velocity = 0 $ms^{-1}$; [2]At velocity = 3.0 $ms^{-1}$; [3]At low depth

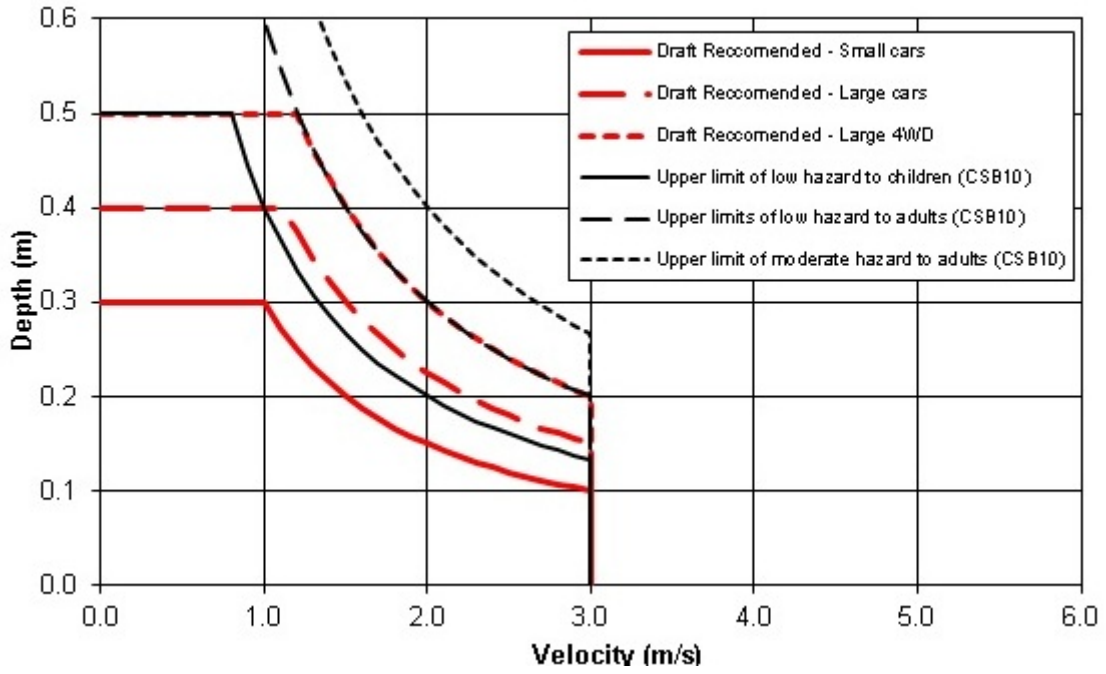


Figure 6.7.6. Interim Safety Criteria for Vehicles in Variable Flow Conditions (Shand et al., 2011)

Shand et al. (2011) concludes that the available datasets do not adequately account for the following factors and that more research is needed in these areas:

- Friction coefficients for contemporary vehicle tyres in flood flows;
- Buoyancy changes in modern cars;
- The effect of vehicle orientation to flow direction (including vehicle movement);
- Information for additional categories including small and large commercial vehicles and emergency service vehicles

## 7.2.5. Building Stability

A comprehensive summary of available literature describing the stability of buildings in floodwaters is provided in Smith et al. (2014). Numerous hazard threshold curves for building were collated from international literature and are compared in Figure 6.7.6. The collated curves have a variety of origins. As discussed by (Leigh, 2008), it can be difficult to synthesise the different building stability curves and associated data, as they are derived by various means of analysis. Subsequently, comparison between theory based curves, (e.g. Black (1975); Dale (2004)) field derived curves (e.g. Clausen and Clark (1990)) and curves derived from modelling and analysis (e.g. Becker *et al.*, 2011) is difficult. Further, different damage thresholds may apply for each of these curves e.g. some threshold curves presented represent the initiation of structural damage, while others represent the flood conditions for complete destruction of the building. The spread of curves in Figure 6.7.6 highlights the overall uncertainty surrounding building stability during flood events.

Investigation and review of the available information concerning the failure of building structures under flood loads has also been conducted by Kelman and Spence (2004) and (Leigh, 2008). Amongst a range of relevant conclusions, these reviews noted that while a series of studies had theoretically analysed incident flood forces compared to the resisting strength of various building structures, most of these studies had considered components of flood forces in isolation or in limited combinations e.g. hydrostatic and simplified hydrodynamic (velocity head) or buoyancy and drag forces.

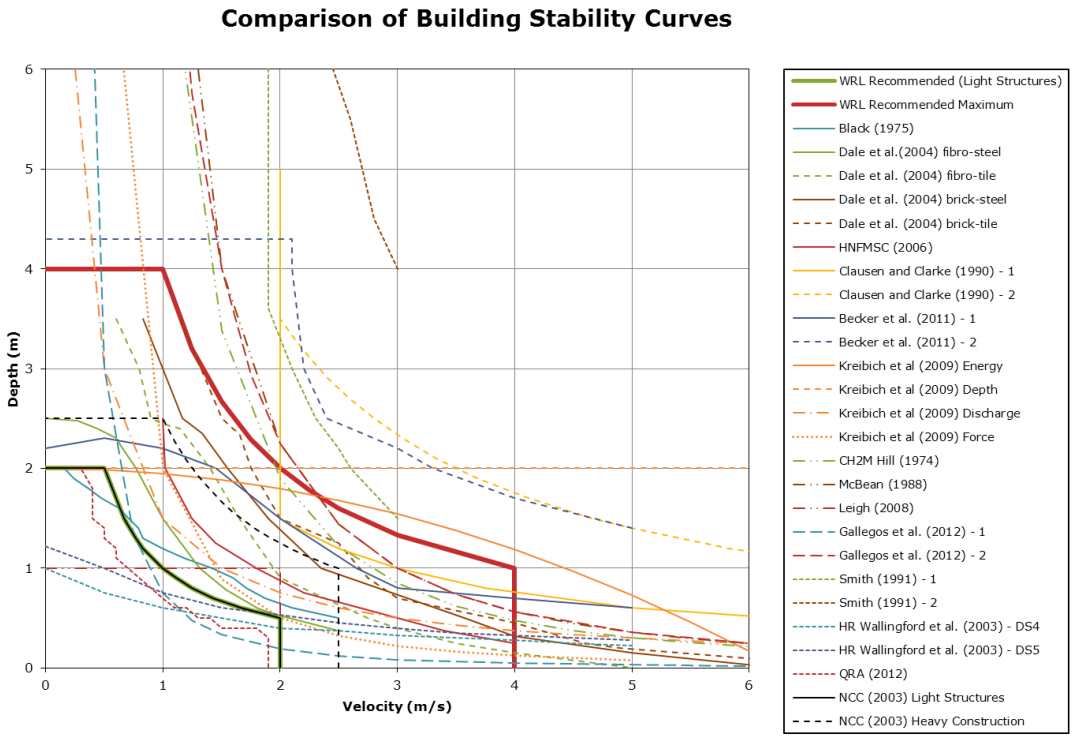


Figure 6.7.7. Comparison of Building Stability Curves

While the considerable variability in building construction is acknowledged, the analysis of building damage leading to collapse reported by Mason *et al.*, (2012) for the Lockyer Valley floods in January 2010 is compelling. This analysis shows that buildings constructed for Australian conditions are vulnerable to damage and collapse under flood hazard conditions at the lower end of the scale presented in Figure 6.7.6.

On this basis, the green curve in Figure 6.7.6 is proposed as a lower threshold for residential homes, built without consideration of flood forces. This curve can be used as a minimum criterion for building stability in existing flood affected areas.

The hazard zone between the green curve and the upper limit red curve in Figure 6.7.6 identifies flood hazard conditions where it is considered, if required, possible to construct a purpose built structure that is an appropriately engineered structure specifically designed to withstand the full range of anticipated flood forces including:

- **Hydrostatic forces**

  resulting from standing water or slow moving flow around the structure;

- **Buoyant forces**

  due to displaced volume of water;

- **Hydrodynamic forces**

  arising from moderate-to-high-velocity water flow around the structure;

- **Impulsive Forces**

  caused by the leading edge of the water impacting the structure;

- **Uplift forces**

  on elevated floors of a structure that are submerged during a flood event;

- **Debris Impact Forces**

  generated by floating debris colliding with the structure;

- **Damming of Waterborne Debris**

  due to the accumulation of debris on the upstream side of the structure, which results in an increase in the hydrodynamic force.

- **Wave actions**

  from wind and wakes; and

- **Erosion and Scour**

  due to flood actions.

In locations where timely evacuation is not possible, such purpose built structures may be required for vertical evacuation, not dissimilar to the process used in Japan for tsunamis. However, it would be important to ensure the structure was purpose built for the conditions it would be likely to encounter, up to and including the PMF or a similar extreme flood event. The bottom floor of such structures may need to be somewhat sacrificial during a flood event, for example, the windows and doors may ‘blow out’ under high flow conditions, however the building’s structural members will be required to remain intact.

The red curve in Figure 6.7.6 is a suggested upper limit for all buildings. Buildings in areas classified with flood hazard above this threshold are considered vulnerable to collapse under these extreme flood conditions.

## 7.2.6.

Previous hazard classification curves (e.g. SCARM (2000);HNFMSC (2006)) provided a single set of hazard curves that divide flood hazard levels into generic classifications of low, medium, high etc. While the thresholds between these classifications had some basis in data collected for stability/vulnerability of people and risk to life, in practice, such threshold curves have been widely interpreted (sometimes mis-interpreted) and applied in myriad ways.

It is interesting to compare the curves summarised for people, vehicle and building stability compiled for this report. Figure 6.7.7 provides a direct comparison of these three sets of curves. The first observation to be made is that for slow moving floodwaters at depths greater than 0.5 m, adults wading through floodwater are generally considered more stable than vehicles i.e. in most cases, vehicles are equally unstable or more unstable than adults wading through the same flow conditions. Secondly, the stability limit for an untrained adult walking through floodwater (D x V = 0.8) is almost the same level as the lower threshold limit for building stability (D x V = 1.0). Also, that for shallow fast moving flows, building stability (through foundation erosion/scour) may be less than the stability of a person walking through the same flow conditions. In some situations, this means that you would be safer to walk out through the prevailing floodwaters rather than sheltering in a poorly constructed building.

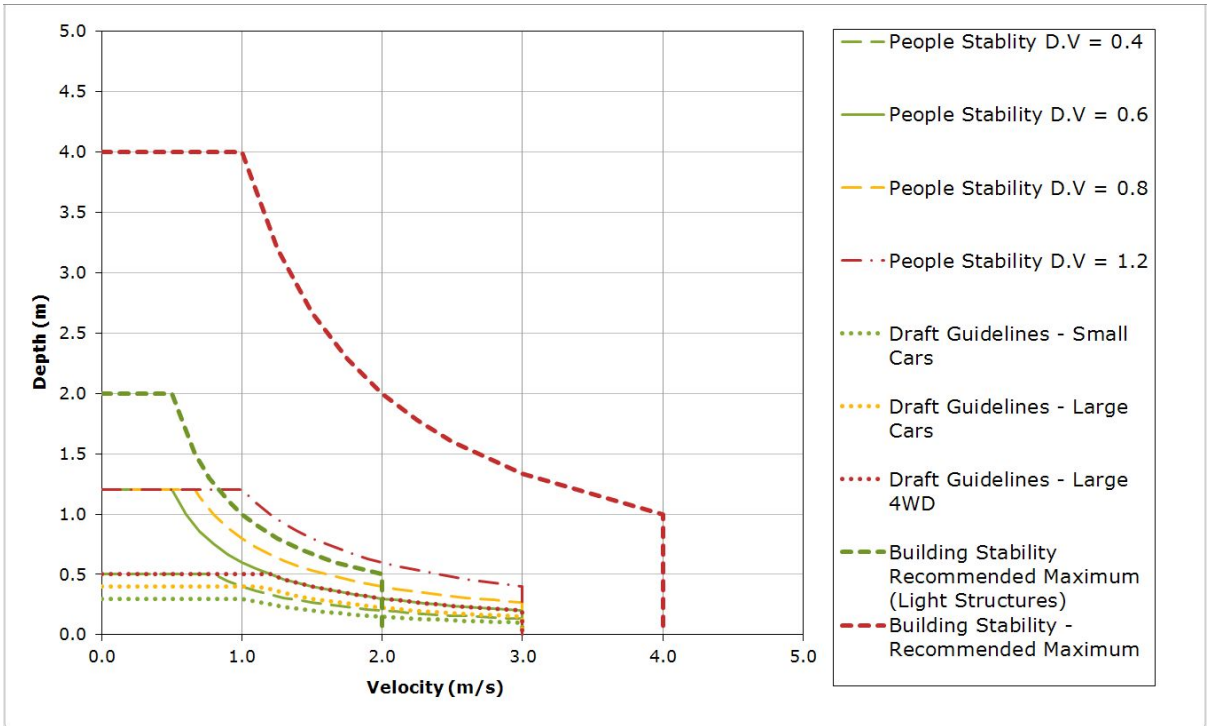


Figure 6.7.8. Comparison of Updated Hazard Curves (after Smith et al. 2014)

The third observation is that the flood water level that is used as the basis of a hazard depth varies between people and vehicle stability, where the flood depth is referenced to the ground level and building stability where the flood depth is nominally referenced to the floor level.

On a practical level, this would mean that once physical flood behaviour has been quantified in terms of flood depth and velocity, flood hazard could be classified individually for people,

vehicles or building thresholds separately. In many instances, this will suit the requirements of specific analyses. For example, if the required assessment is to determine whether a road evacuation route is trafficable for a given flood event, then the vehicle stability threshold curves should be applied. Likewise, if the assessment is to determine which buildings would be suitable for shelter in place during a PMF event, then the building stability thresholds for flood hazard should be used in the analysis.

## 7.2.7. General Flood Hazard Curves

When dealing with specific floodplain management or emergency management analysis there may be a clear need to use specific thresholds as described above. However, particularly in a preliminary assessment of risks or as part of a constraints analysis such as might be applied as part of a strategic floodplain management assessment, there is also an acknowledged need for a combined set of hazard vulnerability curves, which can be used as a general classification of flood hazard on a floodplain. A suggested set of curves based on the referenced thresholds presented above is provided in Figure 6.7.9.

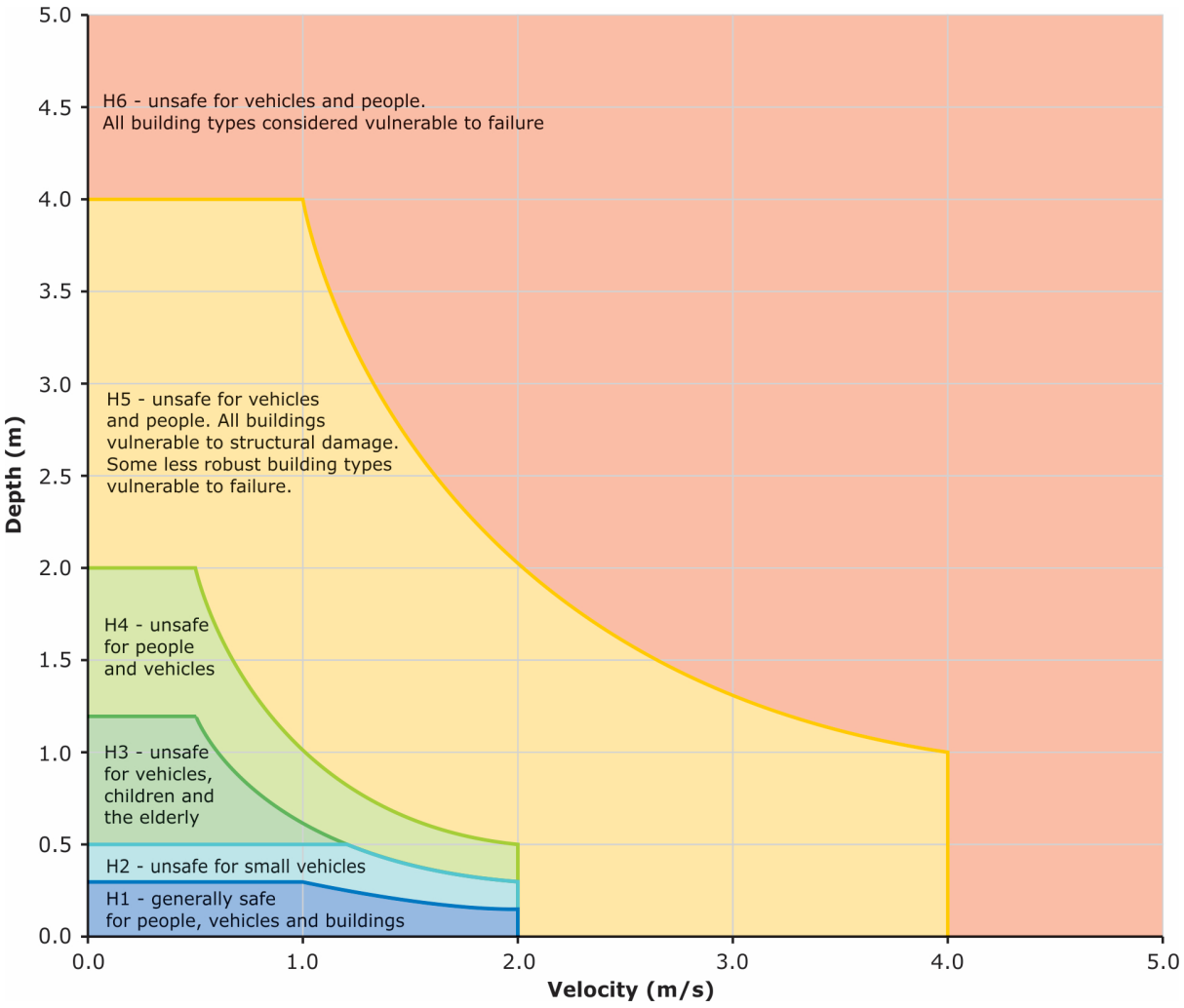


Figure 6.7.9. Combined Flood Hazard Curves (Smith et al., 2014)

The combined flood hazard curves presented in Figure 6.7.9 set hazard thresholds that relate to the vulnerability of the community when interacting with floodwaters. The combined curves are divided into hazard classifications that relate to specific vulnerability thresholds as described in Table 6.7.3. Table 6.7.4 provides the limits for the classifications in Table 6.7.3

Table 6.7.3. Combined Hazard Curves - Vulnerability Thresholds (Smith et al., 2014)

| Hazard Vulnerability Classification | Description |
|---|---|
| H1 | Generally safe for vehicles, people and buildings. |
| H2 | Unsafe for small vehicles. |
| H3 | Unsafe for vehicles. children and the elderly. |
| H4 | Unsafe for vehicles and people. |
| H5 | Unsafe for vehicles and people. All buildings vulnerable to structural damage. Some less robust buildings subject to failure. |
| H6 | Unsafe for vehicles and people. All building types considered vulnerable to failure. |

Table 6.7.4. Combined Hazard Curves - Vulnerability Thresholds Classification Limits (Smith et al., 2014)

| Hazard Vulnerability Classification | Classification Limit (D and V in combination) | Limiting Still Water Depth (D) | Limiting Velocity (V) |
|---|---|---|---|
| H1 | D*V ≤ 0.3 | 0.3 | 2.0 |
| H2 | D*V ≤ 0.6 | 0.5 | 2.0 |
| H3 | D*V ≤ 0.6 | 1.2 | 2.0 |
| H4 | D*V ≤ 1.0 | 2.0 | 2.0 |
| H5 | D*V ≤ 4.0 | 4.0 | 4.0 |
| H6 | D*V > 4.0 | - | - |

Importantly, the vulnerability thresholds identified in the flood hazard curves described above can be applied to the best description of flood behaviour available for a subject site. In this regard, the hazard curves can be applied equally to flood behaviour estimates from measured data, simpler 1D numerical modelling approaches, through to complex 2D model estimates with the level of accuracy and uncertainty of the flood hazard estimate linked to the method used to derive the flood behaviour estimate.

## 7.2.8. Isolation, Effective Warning Time, Rate of Rise and Time of Day

The effective warning time available to respond to a flood event, the rate of rise of floodwaters, the time of day a flood occurs, and isolation from safety by floodwaters and impassable terrain are all factors that may increase the potential for people to be exposed to hazardous flood situations. These factors are important considerations that influence the vulnerability of communities to flooding and are important considerations in managing flood risk.

### 7.2.8.1. Isolation

As outlined in AEM Handbook 7 (AEMI, 2014), flooding can isolate parts of the landscape and cut-off evacuation routes to flood-free land. This can result in dangerous situations,

because people may see the need to cross floodwaters to access services, employment or family members. Many flood fatalities result from the interactions of people, often in vehicles, with floodwaters. Any situation that increases people's need to cross floodwaters increases the likelihood of an injury or fatality.

AEM Handbook 7 recommends that the floodplain be classified by precinct or community based on flood emergency response categories. This classification is separate to the quantification of hazard outlined in this guideline and is addressed in the complementary *Technical Flood Risk Management Guideline on Flood Emergency Response Classification of the Floodplain*.

### 7.2.8.2. Effective Warning Time

As outlined in of AEM Handbook 7, effective warning time is the time available for people to undertake appropriate actions, such as lifting or transporting belongings and evacuating.

Lack of effective warning time can increase the potential for the exposure of people to hazardous flood situations. In contrast, having plenty of effective warning time provides the opportunity to reduce the exposure of people and their property to hazardous flood situations.

### 7.2.8.3. Rate of Rise

Rate of rise of floodwaters is discussed in AEM Handbook 7. A rapid rate of rise can lead to people evacuating being overtaken or cut off by rising floodwaters. It is often associated with high velocities but it can be an issue if access routes are affected by flooding.

### 7.2.8.4. Time of Day

The time of day influences where people are and what they are doing. This can influence their ability to receive any flood warnings and respond to a flood threat. Inability to receive and respond to a warning can increase the potential for people to be exposed to hazardous flood situations.

## 7.3. Examples of Hazard Assessment

This section presents practical examples of the interpretation of flood hazard criteria in a floodplain management context. The examples are not intended to be a comprehensive analysis of all possible circumstances, but rather provide representative case studies, which illustrate practical interpretation of flood hazard criteria for floodplain planning and management.

### 7.3.1. Example - Warehouse Car Park

Flood behaviour quantification, including flood hazard analysis, is used to guide land use planning in floodplains (AEMI, 2014). Often, a general, first pass assessment of flood hazard is required to provide floodplain planners the opportunity to have a general overview of the magnitude of flood hazard and potential flood risks over a floodplain. This type of preliminary assessment of risks might also be used as part of a constraints analysis for a strategic floodplain management assessment.

Effective strategic land use planning is about responding to flood risks in a way that minimises future flood consequences. Consideration of flood hazard is therefore important

so that development of land is encouraged in areas of low or no flood risk wherever possible. A clear understanding of flood risks early in the strategic land use planning process can help steer development away from areas that are not sustainable due to the likely impacts of the development on flood behaviour and guide land use zonings and development controls that support sustainable development on the floodplain in consideration of the flood risk

The following figures provide both a broad-scale example of the base data (variation in velocity and depth across a floodplain) and hazard mapping that can be developed as a first pass using standard two dimensional numerical model outputs from a flood study analysis. The flood hazard mapping presented in Figure 6.7.1 was developed by classifying the numerical flood model results shown in Figure 6.7.10 using the flood hazard thresholds listed in Table 6.7.4.

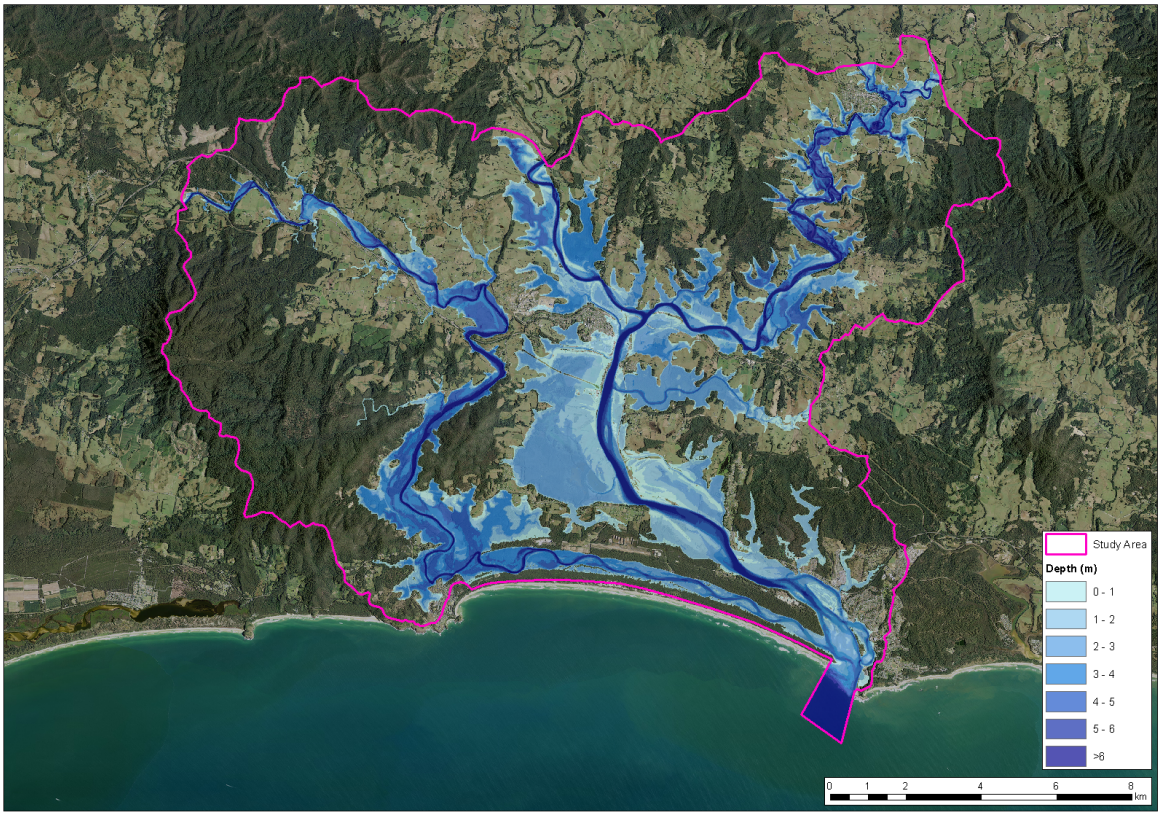


Figure 6.7.10. Flood Depth Map From Numerical Model Output (Courtesy WMAwater Pty Ltd)

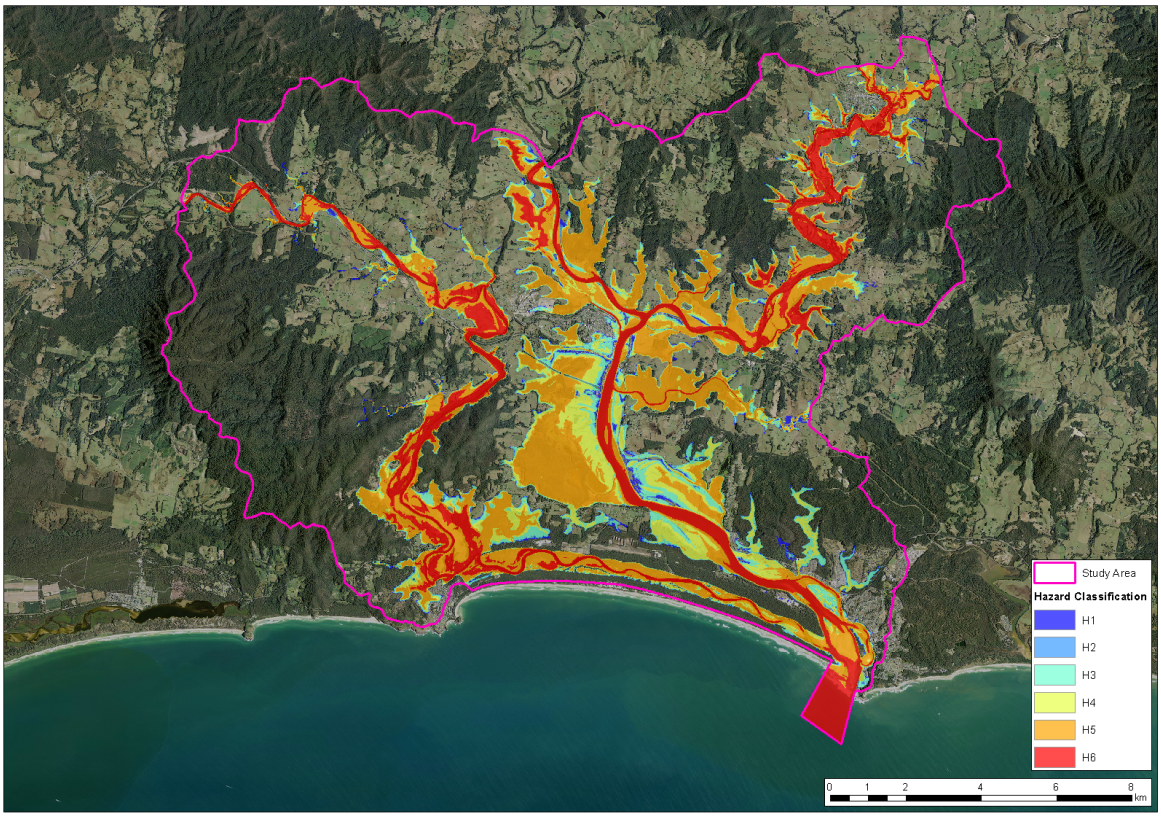


Figure 6.7.11. Flood Hazard Classification From Numerical Model Output (Courtesy WMAwater Pty Ltd)

## 7.3.2. Flood Mitigation - Warehouse Car Park

A large multinational retailer has identified an existing industrial area in an inner city suburb as a suitable site for re-development as a warehouse-style retail outlet. The site is gently sloping from the northwest to the southeast and, having been previously prepared for development, is clear of vegetation. An aging, concrete-lined channel runs along the eastern side of the site.

The retailer has submitted a development application, illustrated in Figure 6.7.12, “Schematic of Proposed Warehouse Development”, which conceptually has a warehouse building situated in the northwest corner of the site with the area between the building and the concrete-lined channel earmarked as a car park.

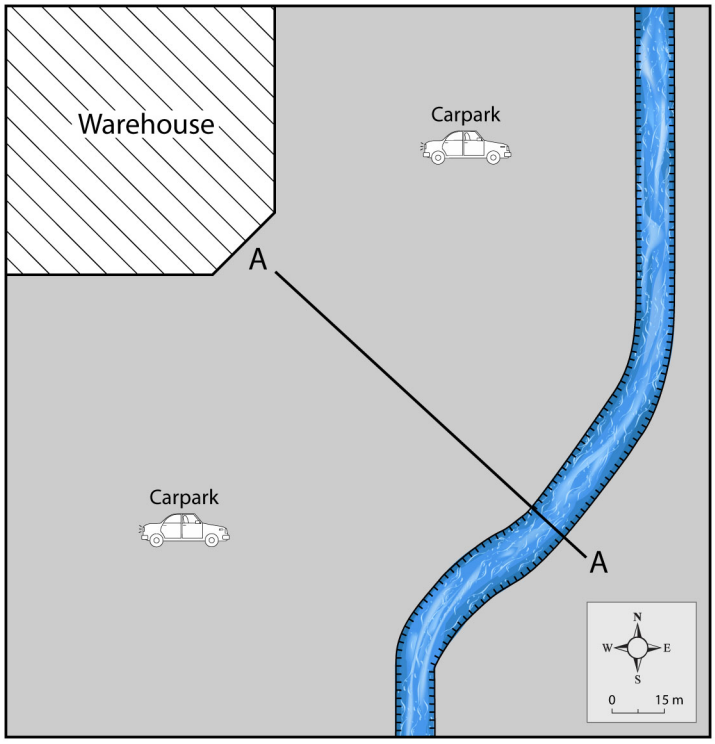


Figure 6.7.12. Schematic of Proposed Warehouse Development

The local council as the consent authority has identified a series of development constraints including flooding criteria. Amongst other criteria, the development must have:

- All retail floor space above the designated flood planning level defined as the 1% Annual Exceedance Probability (AEP) flood surface plus 500 mm freeboard;
- A flood free evacuation route for floods above the flood planning level; and
- All car park areas compliant with ARR flood hazard criteria for vehicle stability;

As there was no existing flood study, following consultation with Council, the developer engaged an experienced flood consultant to undertake flood modelling of the site to estimate 1% AEP flood behaviour. Flood modelling of the site for the 1% AEP event completed using industry best practice guidance as provided by ARR reference “Two Dimensional Modelling in Urban and Rural Floodplains” (Engineers Australia, 2012) predicted that while the warehouse building met the flood planning criteria, the car park was inundated by floodwaters. Figure 6.7.13 illustrates the extent of flood inundation for the existing site.

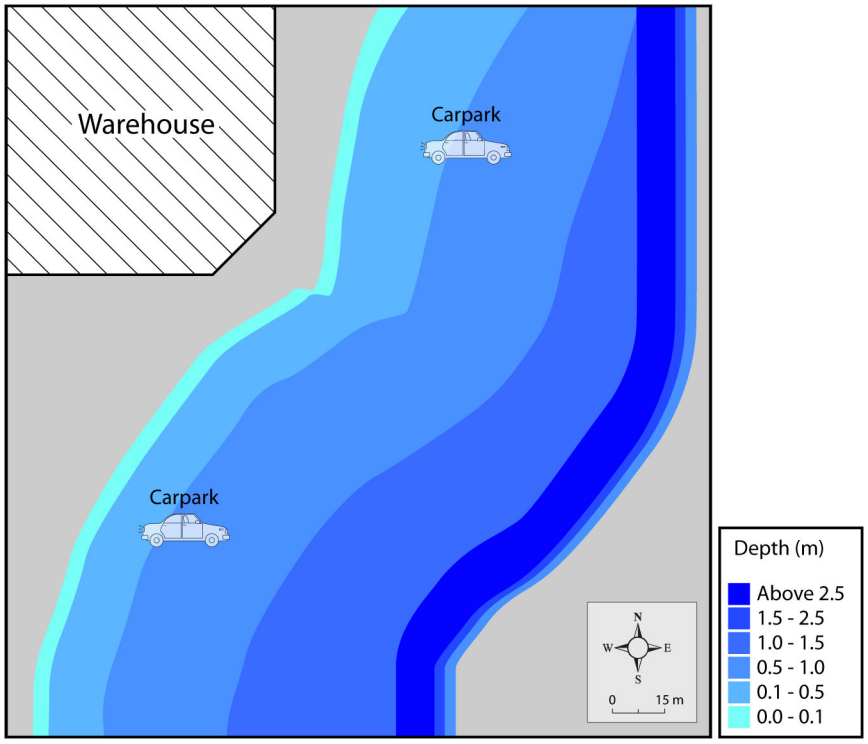


Figure 6.7.13. 1% AEP Flood Depth Map – Existing Site

Interrogation of the flood model results to determine provisional flood hazard as the product of flood depth (D) multiplied by flood velocity (V) showed that the peak flood hazard (D.V) corresponded with the maximum inundation of the site at the peak of the flood hydrograph. Provisional flood hazard for the 1% AEP flood on the existing site as illustrated by Figure 6.7.14 showed that flooding in most of the area identified for car parking exceeds the ARR stability criteria for small cars defined in Table 6.7.2 and illustrated in Figure 6.7.6. In Figure 6.7.14, areas coloured blue (D.V <0.3 $m^2s^{-1}$) indicate locations where small cars are likely to resist being moved by flood flows, whereas areas coloured green through red indicate areas where small cars are very likely to be pushed across the floodplain by floodwaters, with the flow having the potential to move larger cars closer to the creek channel. Based on this information, Council's preliminary advice to the developer was that the existing flood hazard conditions for the designated car parking area were incompatible with the nominated use.


Figure 6.7.14. 1% AEP Provisional Flood Hazard Map – Existing Car Park

As the concrete lined channel had low environmental value, Council was not opposed to the developer's proposed adjustment of the channel flow conveyance capacity to reduce the proportion of overbank flow at the site. The developer, in consultation with the flood consultant ran a range of cut and fill scenarios through the flood model aimed at expanding the channel capacity while raising the relative ground level of the car park to the flood peak. Figure 6.7.15 shows the adjustment of the channel and overbank area through the car park on the longitudinal section identified as 'A-A' in Figure 6.7.12.

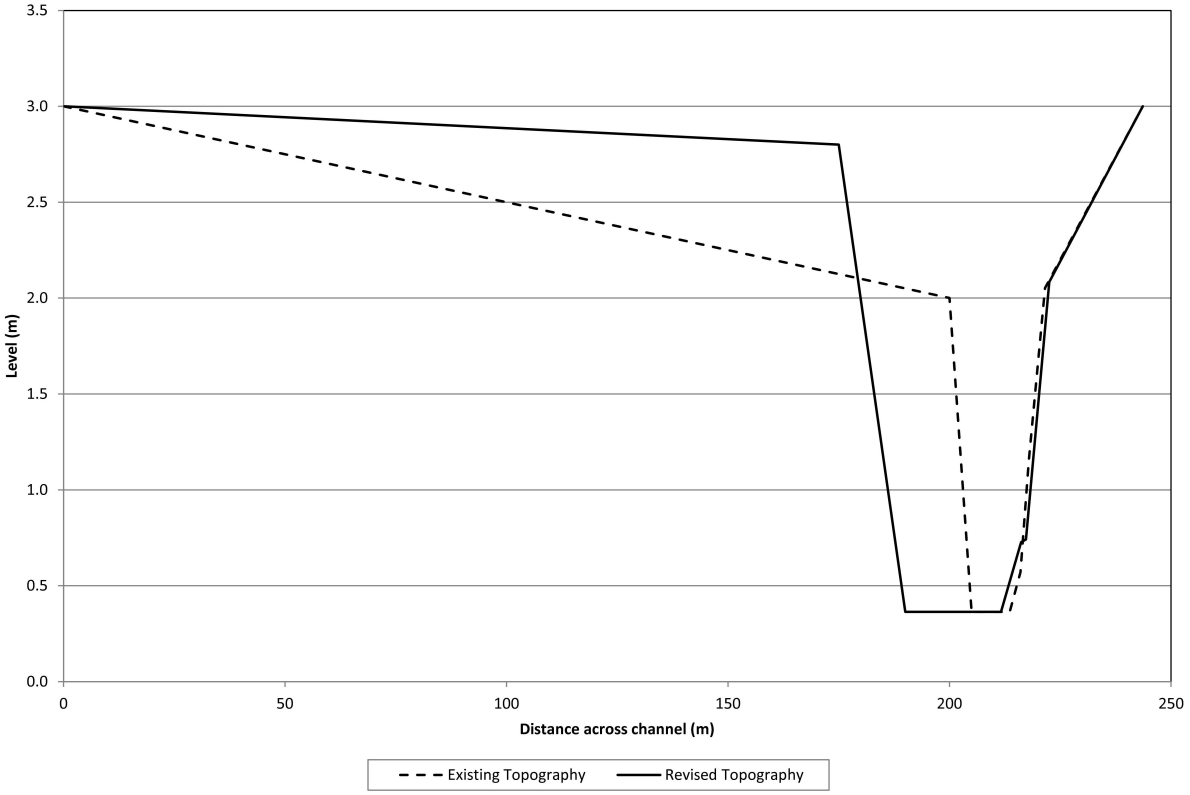


Figure 6.7.15. Comparison of Car Park Cross Sections (A-A)

This section is representative of a balance between the minimum volume of earthworks to meet the car parking capacity criteria for the development. The car park area adjacent to section A-A was graded to meet the natural surface areas outside of the development site.

Flood modelling for the revised site including the proposed earthworks is presented in Figure 6.7.16. The flood model results show that the site flood inundation area is significantly reduced with the works in place.

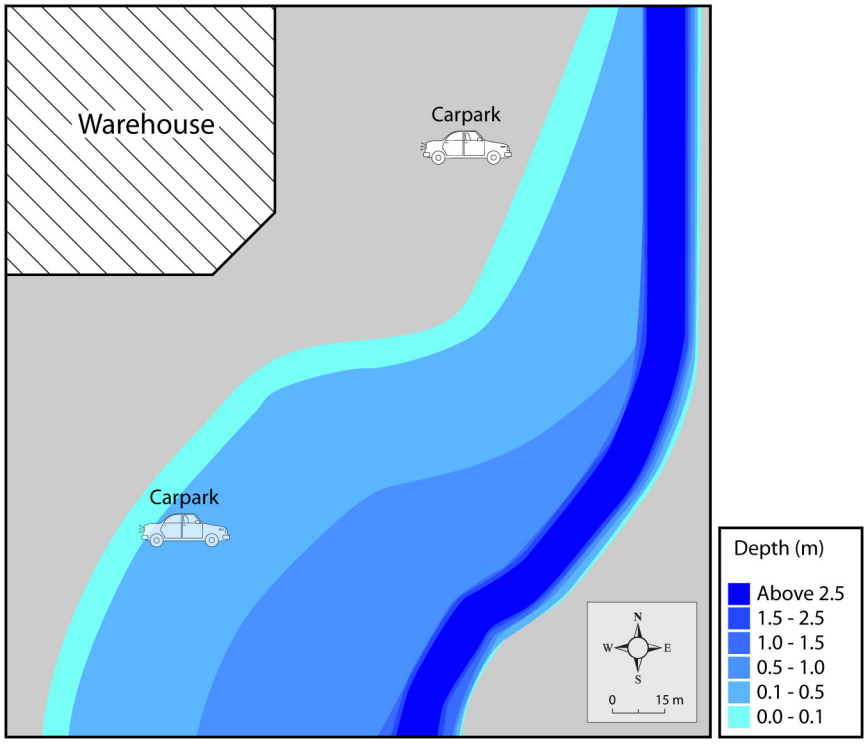


Figure 6.7.16. 1% AEP Flood Depth Map – Revised Car Park

Importantly, analysis of the provisional flood hazard as presented in Figure 6.7.17 shows that flood hazard for the area designated as car park in the conceptual site design now meets the ARR flood stability criteria for small vehicles. The nominated car park area has a D.V product of less than 0.3 $m^2s^{-1}$ as indicated by the blue shaded area of Figure 6.7.17. This indicates that it is now unlikely that cars inundated by floodwaters in the 1% AEP flood will be pushed across the floodplain and potentially into the channel creating a possible downstream blockage hazard.

Council's planners also suggested to the developer that the yellow zone of Figure 6.7.17 could be landscaped as gardens providing clear separation of the car park from the channel. From a floodplain management perspective, this suggested change would provide a significant further reduction in exposure risk with little impact on available car parking space.

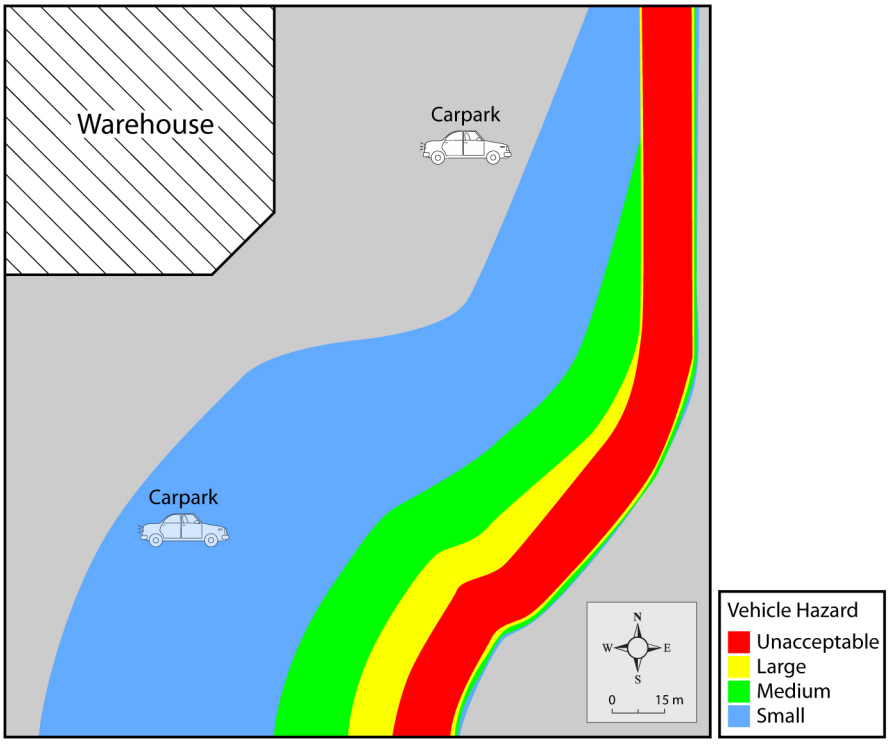


Figure 6.7.17. 1% AEP Provisional Flood Hazard Map – Revised Car Park

## 7.3.3. Example - Detention Basin

Council's conditions of consent for a proposed retirement village development require that on-site detention be provided so that peak flows from the site in floods up to the 1% AEP event remain similar to existing local runoff conditions.

The developer considers that a centralised detention basin on the site can be designed to have a dual use and integrated into the site grounds as a bowling green when not operating as a detention basin. Figure 6.7.18 illustrates the proposed design.

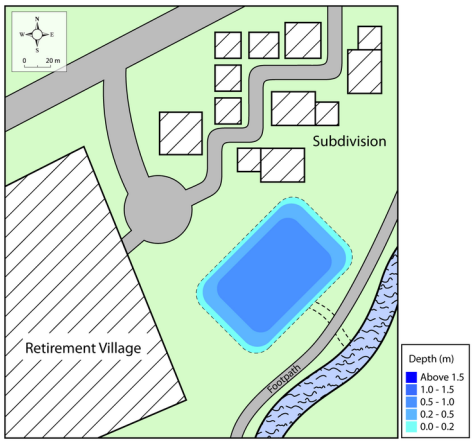


Figure 6.7.18. 1% AEP Flood Depth - Proposed Flood Detention Basin

As the catchment contributing runoff to the site is steep, Council's flood expert considers that there is some risk in a dual purpose design for the basin due to flash flooding in prevailing thunderstorms. Council's advice is that the developer engage a qualified flood expert to determine whether the basin meets the ARR hazard criteria for people safety.

The basin design philosophy is that the local catchment stormwater will collect both overland flows and also surcharge from the pit and pipe stormwater system. If the basin capacity is exceeded, flows spill at a designated location and flow overland to the adjacent creek channel. Flows that remain in the basin discharge through a grated pit in the lowest location in the basin floor.

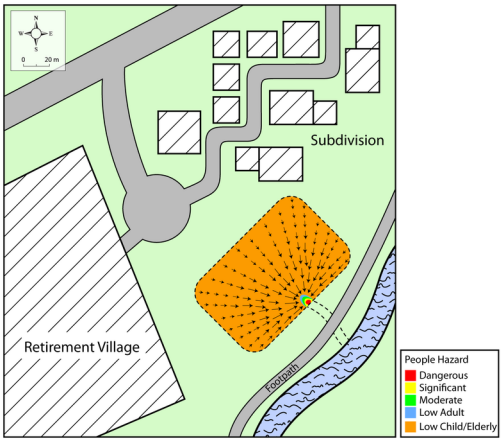


Figure 6.7.19. 1% AEP Provisional Flood Hazard Map - Proposed Flood Detention Basin

An assessment of the provisional flood hazard (flood depth multiplied by the flood velocity) is presented in Figure 6.7.19. When compared to flood hazard criteria presented in Table 6.7.1 and Figure 6.7.4, the provisional hazard meets the safety criteria for the elderly in most areas of the basin. This is because at full capacity, the basin is no greater than 0.5m deep. Analysis shows that a dangerous flood hazard is likely to occur near to the basin's outlet pit when the basin begins to drain at full capacity.

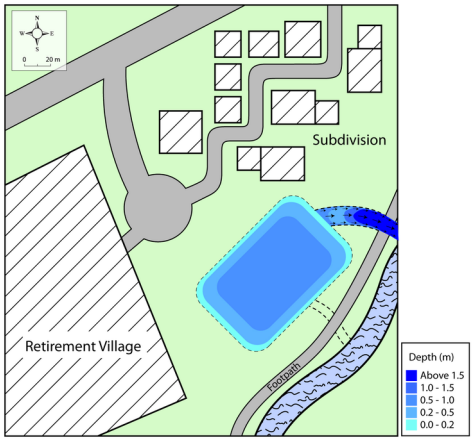


Figure 6.7.20. Basin Overflow Spillway – Flood Depth

Further analysis of the full design presented in Figure 6.7.20 shows that when the basin capacity is exceeded overflows will cross a public footpath adjacent the creek reserve. Provisional flood hazard analysis of the overflow path presented in Figure 6.7.21 shows that the flood hazard in the flow path will exceed the people stability criteria for adults and be a dangerous hazard to passing pedestrians.

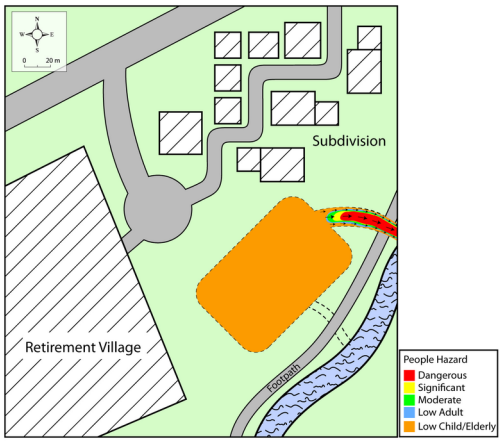


Figure 6.7.21. Provisional Flood Hazard Map – Basin Overflow Spillway

As a result of the analysis, Council consent criteria require signage to be placed in appropriate locations informing residents of the retirement village and the public passing the site on the public footpath of the dual purpose use of the basin and the danger of entering floodwaters when the basin is inundated. Further, Council's consent criteria require that the developer upgrade the footpath to include a bridge of suitable span over the basin spillway flow path so that safe thoroughfare of the footpath can be maintained during flood conditions.

## 7.4. Conclusions and Recommendations

Recent flood events on the east coast of Australia in 2010 and 2011 have highlighted that people continue to be exposed to dangerous and life threatening flow conditions in urban and rural floodplains. While floodplain management activities are continuing to mitigate problems associated the community's exposure to floodwaters, ongoing human activity in floods is largely unavoidable while significant areas of existing development and transport infrastructure in Australia remain flood prone.

This chapter of Australian Rainfall and Runoff presents a summary with an explanation of the limitations of recent analysis of flood stability thresholds for pedestrians and vehicles in floodwaters. Recommended flood hazard criteria for use within Australia based on the stability of people and vehicles in flood flows has also been presented.

Finally, the presented examples illustrate practical applications of these flood hazard criteria. While not exhaustive of all cases, the examples show how the criteria can be pragmatically applied to reduce the community's exposure to flood danger.

## 7.5. References

AEMI, Australian Emergency Management Institute. (2014). Technical flood risk management guideline: Flood Hazard. Australian Emergency Management Institute Barton, ACT.

Abt, S.R, Wittler, R.J, Taylor, A and Love, DJ. (1989). Human Stability in a High Flood Hazard Zone, Water Resources Bulletin, American Water Resources Association, 25 (4), pp 881-890.

Ashley, S.T. and Ashley, W.S. (2008), Flood Fatalities in the united States, Meteorology Program, Department of Geography, Northen Illinois University, DeKalb, Illinois, DOI: http://dx.doi.org/10.1175/2007JAMC1611.1.

Black, R.D. (1975), Flood proofing rural residences. Department of Agricultural Engineering, Cornell University.

Queensland Commission for Children, Young People, and Child Guardian (CCYPCG) (2012), https://www.fire.qld.gov.au/communitysafety/swiftwater/default.asp - accessed 11 August 2012

Cave, B., Cragg, L., Gray, J., Parker, D., Pygott, K. and Tapsell, S. (2009), Understanding of and response to severe flash flooding. Environment Agency, Bristol. Science Report No. SC070021.

Clausen, L. and Clark, P.B. (1990), The development of criteria for predicting dam break flood damages using modelling of historical dam failures. International conference on river flood hydraulics. John Wiley and Sons Ltd. Hydraulics Research Limited, Wallingford, England.

Coates, L. (1999), Flood Fatalities in Australia, 1788-1996, Australian Geographer, 30(3).

Coates, L. and Haynes, K. (2008), Flash flood shelter-in-place vs. evacuation research: Flash flood fatalities within Australia, 1950 - 2008. Report prepared for the New South Wales State Emergency Service.

Cox, R.J., Shand, T.D. and Blacka, M.J. (2010), Appropriate Safety Criteria for People in Floods, WRL Research Report 240. Report for Institution of Engineers Australia, Australian Rainfall and Runoff Guidelines: Project 10. 22 p.

Cox, R.J., Yee, M. and Ball, J.E. (2004), Safety of People in Flooded Streets and Floodways. 8th National Conference on Hydraulics in Water Engineering, Gold Coast. The Institution of Engineers, Australia.

Dale K.W., Edwards M.R., Middelmann M.H. and Zoppou C. (2004), Structural vulnerability and the Australianisation of Black's curves, in RISK 2004: Proceedings of a National Conference, Melbourne, 8-10 November, 2004.

Drobot, R. and Parker, D.J. (2007), Advances and Challenges in Flash Flood Warnings, Envrionmental Hazards, 7(3), 173-178, DOI:10.1016/j.envhaz.2007.09.001.

Engineers Australia (2012), Two Dimensional Modelling in Urban and Rural Floodplains. Project 15, Mark Babister, editor.

French J., Ing, R., Von Allmen, S. and Wood, R. (1983), Mortality from Flash Floods: a Review of National Weather Service Reports, 1969-81. Public Health Reports: Nov-Dec 1983, 98(6), 584-588.

Gruntfest, E. and Ripps, A. (2000), Flash floods: warning and mitigation efforts and prospects. In: Parker, D.J. (Ed.), Floods, vol. 1. Routledge, London, pp: 377-390.

HNFMSC (2006), Reducing Vulnerability of Buildings to Flood Damage, Hawkesbury-Nepean Floodplain Management Steering Committee, Parramatta.

Haynes, K. Coates, L., de Olivera, F.D., Gissing, A., Bird, D., van den Honert, R., Radford, D., D'Arcy, R. and Smith, C. (2016), An analysis of human fatalities from flood hazards in

Australia, 1900-2015. Proceedings 2016 Floodplain Management Association National Conference, Nowra, 2016.

Jonkman, S.N. and Kelman, I. (2005), An Analysis of the Causes and Circumstances of Flood Disaster Deaths. Disasters, 29: 75-97, doi: 10.1111/j.0361-3666.2005.00275.x.

Jonkman, S.N. and Penning-Rowsell, E. (2008), Human Instability in Flood Flows. Journal of the American Water Resources Association, 44(4), 1-11.

Kelman, I. and Spence, R. (2004), An overview of flood actions on buildings. Engineering Geology, 73(3), 97-309.

Leigh, R. (2008), Flash flood shelter-in-place vs. evacuation research: review of literature on building stability. Report prepared for NSW State Emergency Service.

Rogencamp, G. and Barton, J. (2012), The Lockyer Creek flood of January 2011: what happened and how should we manage hazard for rare floods, 52nd Annual Floodplain Management Association Conference. available at http://www.floodplainconference.com/papers2012.php., Vol.10.

SCARM (Standing Committee on Agriculture and Resource Management) (2000), Floodplain management in Australia: Best practice principles and guidelines, SCARM Report 73, CSIRO Publishing, Melbourne.

Shand, T.D., Cox, R.J., Blacka, M.J. and Smith, G.P. (2011), Appropriate Safety Criteria for Vehicles - Literature Review. ARR Report Number: P10/S2/020. Report for Institution of Engineers Australia, Australian Rainfall and Runoff Guidelines: Project 10. ISBN 978-0-85825-948-5.

Smith, G.P. and Wasko, C.D, (2012), Two Dimensional Simulations in Urban Areas: Representation of Buildings In 2d Numerical Flood Models. Australian Rainfall and Runoff Revision Project 15. Final Report, February 2012.

Smith, G.P., Davey, E.K. and Cox, R.J. (2014), Flood Hazard UNSW Australia Water Research Laboratory Technical Report 2014/07 30 September 2014.

Australian Rainfall & Runoff

ENGINEERS
AUSTRALIA

11 national Circuit
BARTON ACT 2600

**www.arr.org.au**

9 781925 848366